THE IMPACT OF AMPK SIGNALLING AND CLINICAL THERAPEUTICS ON CANCER METABOLISM

by

David Papadopoli

A thesis submitted to McGill University in partial fulfillment of the requirements of the degree of Doctor of Philosophy

Faculty of Medicine

Department of Biochemistry

McGill University

Montreal, Quebec, Canada

TABLE OF CONTENTS

CHAPTER 2: THE PGC-1α/ERRα AXIS REPRESSES ONE-CARBON METABOLISM AND PROMOTES SENSITIVITY TO ANTI-FOLATE THERAPY IN BREAST CANCER

ABSTRACT

Cancer metabolism is intricately re-wired to support tumour growth. Despite the initial discovery that cancers depend on aerobic glycolysis, it is well appreciated that cancer cells exploit numerous metabolic pathways, including those linked to mitochondrial metabolism, to help fuel tumorigenesis. Metabolic gene programs are controlled by transcriptional complexes, such as the peroxisome proliferator-activated gamma coactivator 1 (PGC-1) / estrogen-related receptor alpha (ERR) axis, which act as master orchestrators of metabolism. The activity of the PGC-1α/ERRα axis is upregulated by the AMP-activated protein kinase (AMPK), a central metabolic regulator that is triggered in response to energetic stress. The work in this thesis demonstrates that the AMPK/PGC-1α/ERRα axis increases the bioenergetic functions of cancer cells, but inhibits one-carbon metabolism and purine biosynthesis, resulting in improved sensitivity to methotrexate (MTX), a chemotherapeutic drug widely used in the clinic. MTX treatment promotes bioenergetic functions and has antiproliferative effects that are dependent on AMPK. As a result, the combination of MTX with AMPK activators can improve chemotherapeutic response. Recently, there is increased interest in repurposing metabolic drugs to treat cancer. We show that the antidiabetic drug canagliflozin decreases cancer cell proliferation and reduces the activity of the citric acid cycle through perturbation of glutamine metabolism. The work in this thesis unravels the role of the AMPK/PGC-1α/ERRα pathway in controlling antifolate response and reinforces the premise of pharmacologically targeting cancer metabolism to impede tumourigenesis.

RÉSUMÉ

Le métabolisme du cancer s'adapte de manière complexe pour soutenir la croissance tumorale. Outre leur dépendance à la glycolyse aérobie, tel que découvert initialement, les cellules cancéreuses exploitent de nombreuses autres voies métaboliques, incluant celle du métabolisme mitochondrial, afin d'alimenter la tumorigenèse. Les gènes métaboliques sont contrôlés par des complexes transcriptionnels tels que l'axe du peroxisome proliferator-activated gamma coactivator 1 (PGC-1) / estrogen-related receptor alpha (ERR), des facteurs de transcription bien connus dans l'orchestration du métabolisme. La régulation de cet axe est activée par l'AMPK, un acteur métabolique central qui est induit en réponse à un stress énergétique. Les travaux présentés dans cette thèse montrent que l'activation de l'axe AMPK/PGC-1α/ERRα augmente la fonction bioénergétique tout en diminuant le métabolisme du folate et la biosynthèse des purines, rendant ainsi ces cellules cancéreuses sensibles au méthotrexate (MTX), un agent chimiotherapeutique communément utilisé chez des patients atteints de cancer. Les mécanismes d'action du MTX se traduisent par une promotion des fonctions bioénergétiques tout en ayant des effets antiprolifératifs dépendants de l'AMPK. Par conséquent, la combinaison du MTX et d'un activateur de l'AMPK pourrait améliorer la réponse chimiothérapeutique, rendant ainsi le traitement plus efficace. L'utilisation de médicaments métaboliques suscite de plus en plus un grand intérêt dans le traitement du cancer. En effet, nous avons mis en évidence que la canagliflozine, un médicament anti-diabétique, induit une diminution de la prolifération des cellules cancéreuses et une réduction de l'activité du cycle de Krebs, due à la perturbation du métabolisme de la glutamine. Ainsi les travaux présentés dans cette thèse mettent en lumière le rôle de la voie AMPK/PGC-1α/ERRα dans le contrôle de la

réponse anti-folate et le potentiel de la thérapie pharmacologique ciblant le métabolisme du cancer comme stratégie pour bloquer la tumorigenèse.

ACKNOWLEDGEMENTS

Completing a Ph.D. would not have been possible without an effective support system. It is a process that requires many years of work, and more often than not, it is the people behind the scene that help secure one's success.

It is with sincere gratitude that I thank my mother, father, and my sister Sabrina, for all their continual support throughout my entire studies in life. I truly appreciate all your encouragement, assistance, and your belief in me. I truly appreciate all the sacrifices you have made to see me get to this point. To my loving wife, Loulou, I am extremely grateful your dedication and presence by my side. I can't even begin to express how thankful I am to for your patience and support. I truly appreciate you believing in me and for facing the challenges alongside me. I love you and I dedicate this dissertation to you.

I sincerely want to thank my supervisor, Dr. Julie St-Pierre, for challenging me to think critically about science and giving me the opportunity to strengthen my research and communication skills. I appreciate the independence I was given to develop my own ideas to fruition. I would also like thank members of the St-Pierre lab, whom have made my doctoral experience that much more enjoyable, whether it be working late nights and weekends, collaborating research, or celebrating achievements. Special thanks to Shawn, Sylvia, Ouafa, Simon-Pierre, Joe, Valerie, Katrina, Anna, Eva, and Shane. I am also very grateful to Elizabeth Kovacs and Carlo Ouellet for helping me with in vivo experiments and extracting tissue for mitochondrial preparations.

I would like to express appreciation to my co-supervisor Dr. Vincent Giguère, who provided many important insights that were instrumental to my success during my Ph.D. studies. I would like to thank everyone in the Giguère laboratory, including Carlo, Mathieu, Majid, Cathy, Ming, Summer, Yonghong. Special thanks to Étienne who shared a lot of his technical expertise in helping me with experiments. I would also like to thank Maxime Caron and Guillaume Bourque for their contributions.

I would like to reserve my gratitude to the members of the Metabolomics Core, including Daina, Gaëlle, Luc, Thierry, and Mariana. They have provided me with fundamental training of the metabolomics platforms and offered me helpful guidance in preparing experiments and analyzing data. My metabolomic achievements could not have been done without their kind help.

Furthermore, I would also like the thank Dr. Russell Jones for his helpful insights and discussions, including members from his lab, including Eric and Dominic, who helped me with in vivo experiments, as well as Said, Takla, Rebecca, and Ali for helpful discussions and reagents.

In addition, I would like to thank my RAC committee, which includes Dr. Julie St-Pierre, Dr. Vincent Giguère, and Dr. Nicole Beauchemin, who have provided counselling throughout my graduate studies. Also, I would like thank Dr. Michael Pollak and Dr. Ivan Topisirovic who have provided important guidance and feedback during my studies and in the writing of this dissertation.

Finally, I would like to thank the funding agencies that have supported me throughout my graduate studies, including the MICRTP (summer, masters, doctoral), (doctoral), Michael D'Avirro, and the Fonds de recherche du Québec – Santé (FRQS).

PUBLICATIONS ARISING FROM THIS WORK

Chapter 2 was published as an original research article:

Audet-Walsh É*, **Papadopoli DJ***, Gravel S-P, Yee T, Bridon G, Caron M, Bourque G, Giguère V, St-Pierre J. (2016) The PGC-1α/ERRα Axis Represses One-Carbon Metabolism and Promotes Sensitivity to Anti-folate Therapy in Breast Cancer. *Cell Reports* 14, (4) 920-931

https://doi.org/10.1016/j.celrep.2015.12.086 ***co-first authors**

Chapter 3 is in preparation for submission:

Papadopoli DJ, Ma E, Roy D, Bridon G, Avizonis D, Jones RG, St-Pierre J. (2018) Methotrexate mediates an AMPK-dependent metabolic response in cancer cells. Manuscript in preparation for submission.

Chapter 4 is in preparation for submission:

Papadopoli DJ, Uchenunu O, Hulea L, Topisirovic I, Pollak M, and St-Pierre J. (2018) Perturbations of cancer cell metabolism by the anti-diabetic drug canagliflozin. Manuscript in preparation for submission.

The following publications arose during my doctoral studies, but were not included in this thesis:

Vernier M, McGuirk S, **Papadopoli DJ**, Bourmeau G, Audet- Walsh É, St- Pierre J, Giguère V. "The estrogen- related receptor ERRα is a ROS sensor and protects against oxidative stress" *Manuscript in preparation for submission*.

Andrzejewski S, Klimcakova E, Tabariès S, Annis MG, Johnson R, McGuirk S, Northey JJ, Chénard V, Sriram U, **Papadopoli DJ**, Siegel PM, St- Pierre J. (2017) "PGC-1α promotes lung metastasis and confers bioenergetic flexibility against metabolic drugs" *Cell Metabolism* 26(5):778-87

McGuirk S, Gravel SP, Deblois G, **Papadopoli DJ**, Faubert B, Wegner A, Hiller K, Avizonis D, Akavia UD, Jones RG, Giguère V, St- Pierre J. (2013) "PGC-1α supports glutamine metabolism in breast cancer" *Cancer and Metabolism* 1:22

CONTRIBUTION OF AUTHORS

I wrote the abstract of this thesis, while the résumé was written by Dr. Ouafa Najyb.

Chapters 1 and 5: I wrote and created all figures. Reviewing and final editing were performed by Dr. Ivan Topisirovic, Dr. Vincent Giguère, and Dr. Julie St-Pierre.

Chapter 2: The conceptualization of experiments and methodology were performed under the guidance of Dr. Julie St-Pierre, as well as Dr. Étienne Audet-Walsh and Vincent Giguère. I performed western blots, qRT-PCR, oxygen consumption, RNAi, microarray, BrdU incorporation, cell proliferation, steady-state metabolomics by LC-MS and GC-MS, ^{13}C-^{15}N serine stable isotope tracing by LC-MS, formate quantification, and xenograft experiments. I also analyzed and interpreted data, as well as contributing to writing the manuscript. Specifically, I contributed to Figure 2.1 (all panels A-F), Figure 2.3 (A, B, C, F, G), Figure 2.4 (A-E, I ,K-O), Figure 2.5 (all panels A-H), Figure S2.1 (B-I), Figure S2.4 (all panels A-D), Figure S2.5 (all panels A-B). Dr. Étienne Audet-Walsh and Tracey Yee performed all ChIP and ChIP-qPCR, as well as western blot, qRT-PCR, and RNAi experiments. Specifically, their contribution consists of Figure 2.2 (all panels A-C), Figure 2.3 (A,B,D,E), Figure 2.4 (F,G,H), Figure 2.5 (C), Figure S2.2 (all panels A-G), and Figure S2.3 (A). Dr. Simon-Pierre Gravel and Dr. Gaëlle Bridon assisted in the execution and analysis of ^{13}C-^{15}N serine stable isotope tracing data, which consists of Figure 2.4 (J-O) and Figure S2.5 (B). Maxime Caron and Dr. Guillaume Bourque contributed to Figure 2.2 (all panels A-C). The summary Figure 2.6 was designed by Dr. Vincent Giguère. The manuscript also written and edited by Dr. Étienne Audet-Walsh, Dr. Gaëlle Bridon, Dr. Vincent Giguère, and Dr. Julie St-Pierre. The authors are grateful to Carlo Ouellet for mouse husbandry, as well as Daina Avizonis and Thierry Ntimbane of the Metabolomics Core Facility

for technical assistance. Chapter 2 is a co-first authorship between David Papadopoli and Dr. Étienne Audet-Walsh, and this data is not used in any other dissertation than this one.

Chapter 3: I conceptualized/designed experiments and developed methodology under the guidance of Dr. Julie St-Pierre and Dr. Vincent Giguère. I performed steady-state metabolomics using LC-MS and GC-MS, western blots, qRT-PCR, oxygen consumption using multiple bioenergetic platforms, formate quantification, metabolite quantification using NOVA Bioanalyser and cell proliferation assays. I analyzed and interpreted data and contributed to writing the manuscript. I contributed to all panels of this chapter (Figures 3.1-3.4 and Figure S3.1). Dr. Gaëlle Bridon developed methodology and analyzed data from Figure 3.1 (A) and Figure S3.1(A). Eric Ma and Dr. Dominic Roy performed in vivo mouse experiments.

Chapter 4: I conceptualized/designed experiments and developed methodology under the guidance of Dr. Julie St-Pierre, Dr. Michael Pollak, and Dr. Ivan Topisirovic. I performed cell proliferation, oxygen consumption assays on whole cells, steady-state metabolomics using GC-MS, ^{13}C glutamine stable isotope tracing analysis using GC-MS, metabolite quantification using NOVA Bioanalyser, and glutamine dehydrogenase assays. I also isolated mitochondria from murine skeletal muscle and performed oxygen consumption assays on the isolated mitochondria. I analyzed and interpreted data and contributed to writing the manuscript. I contributed to all panels of this chapter (Figures 4.1-4.4). Oro Uchenunu and Dr. Laura Hulea performed proliferation experiments for Figure 4.1 (C.) The manuscript was edited by Dr. Michael Pollak and Dr. Julie St-Pierre. The authors are also grateful to Elizabeth Kovacs and Carlo Ouellet for mouse husbandry.

ORIGINAL CONTRIBUTIONS OF KNOWLEDGE

1) We demonstrated that the PGC-1α/ERRα axis acts as a key downstream effector of AMPK reprogramming in HER2+ breast cancer cells. Activation of AMPK induces the PGC-1α/ERRα axis and increases cellular respiration, especially uncoupled respiration, which is indicative of increased PGC-1α activity. We show that the AMPK-mediated increase of cellular respiration is dependent on PGC-1α/ERRα axis. Furthermore, we show that AMPK activation induces the binding of ERRα to chromatin.

2) Through the intersection of transcriptomic and binding-event datasets, we elucidate that the PGC-1α/ERRα axis negatively controls folate cycle metabolism, thereby introducing a novel function of PGC-1α/ERRα signalling. PGC-1α/ERRα inhibits the transformation of folate intermediates, which are governed by the *MTHFD* family, and includes isoforms used in both the cytosolic and mitochondrial one-carbon metabolism pathways.

3) We identified that the PGC-1α/ERRα axis also inhibits genes involve de novo purine biosynthesis, which is a major output of one-carbon metabolism. We decipher that PGC-1α/ERRα signalling decreases the tracing of labelled serine into purine nucleotides, thus depicting that PGC-1α/ERRα inhibits the construction of de novo nucleotides.

4) Given its role in controlling one-carbon metabolism, we discovered that the PGC-1α/ERRα sensitises cells and tumours to antifolate therapy. These data demonstrate that the PGC-1α/ERRα axis acts as a modulator of methotrexate response in HER2+ breast cancer.

5) We demonstrate that methotrexate treatment induces AICAR levels, which activates AMPK/ PGC-1α/ERRα signalling along with reduced expression of one-carbon metabolism genes.

6) We show that methotrexate upregulates cellular respiration in an AMPK-dependent manner. Furthermore, we demonstrate that methotrexate increases the bioenergetic capacity of cells, predominantly by inducing oxidative metabolism.

7) In addition to cellular respiration, we also identify AMPK as an important determinant of the antiproliferative response of methotrexate. In support of this point, we uncovered that AMPK activators such as phenformin can improve the antiproliferative response of methotrexate.

8) We established that the SGLT2 inhibitor canagliflozin has antineoplastic effects in HER2+ breast cancer cell lines in the presence and absence of glucose, suggesting that the effects are unrelated to glucose transport.

9) We demonstrate that canagliflozin, but not dapagliflozin, decreases cellular respiration and bioenergetic capacity. Using isolated mitochondria, we show that both canagliflozin and dapagliflozin do not affect complex I-mediated respiration, but canagliflozin perturbs complex II-mediated respiration to a similar extent as the established complex II inhibitor, malonate.

10) We identify canagliflozin as an inhibitor of glutamine-mediated anapleurosis as canagliflozin inhibits the activity of glutamate dehydrogenase and reduces the tracing of labelled glutamine into the citric acid cycle. In support of this point, the antirespiratory and antiproliferative response of canagliflozin are greatly reduced when cells are grown under glutamine deprivation. Canagliflozin also increases the uptake of glutamine, but strongly the efflux of glutamate in the media, which may act as an indicator of diminished glutamate utilization. Taken together, these data describe the metabolic effects incurred by canagliflozin treatment, which are associated with reduced complex II-mediated respiration and reduced glutamine metabolism.

PREFACE

This is a manuscript-based thesis. Chapter 2 is published, while Chapters 3 and 4 are being prepared for submission.

The thesis is divided into five chapters:

Chapter 1: Introduction

Chapter 2: The PGC-1α/ERRα axis represses one-carbon metabolism and promotes sensitivity to anti-folate therapy in breast cancer

Chapter 3: Methotrexate mediates an AMPK-dependent metabolic response in cancer cells

Chapter 4: Perturbations of cancer cell metabolism by the ant-diabetic drug canagliflozin

Chapter 5: Discussion

LIST OF FIGURES AND TABLES

CHAPTER 1: INTRODUCTION

CHAPTER 2: THE PGC-1α/ERRα AXIS REPRESSES ONE-CARBON METABOLISM AND PROMOTES SENSITIVITY TO ANTI-FOLATE THERAPY IN BREAST CANCER

LIST OF ABBREVIATIONS

1,3-BPG: 1,3-bisphosphoglycerate
1C: one-carbon unit
2-HG: 2-hydroxyglutarate
2-PG: 2-phosphoglycerate
3-PG: 3-phosphoglycerate
4EBP: eukaryotic initiation factor 4E binding protein
5-FU: 5-fluorouracil
ACC: acetyl-CoA carboxylase
ACL: ATP-citrate lyase
ADP: adenosine diphosphate
AICAR: 5-aminoimidazole-4-carboxamide ribonucleotide
AIF1: allograft inflammatory factor 1
Akt: Protein kinase B
ALL: acute lymphoblastic leukemia
alpha-KG: alpha-ketoglutarate
ALT: alanine transaminase
AML; acute myeloid leukemia
AMP: adenosine monophosphate
AMPK: AMP-activated protein kinase
AP-1/2: activator protein 1 or 2
AST: aspartate transaminase
ATF4: activating transcription factor 4
ATIC : 5-aminoimidazole-4-carboxamide ribonucleotide formyltransferase
ATP: adenosine triphosphate
BRAF: B-Raf proto-oncogene, serine/threonine kinase
CAC: citric acid cycle
CAD : carbamoyl-phopshate synthetase 2, aspartate transcarbamylase, dihydroorotase
CAMKKβ: calmodulin-dependent protein kinase kinase β
ccRCC: clear cell renal carcinoma
CDK: cyclin dependent kinase
ChIP: chromatin immunoprecipitation
CLK2: CDC like kinase 2
COX1: cytochrome c oxidase 1
CPT: carnitine palmitoyltransferase
CS: citrate synthase
CTP: cytosine triphosphate
DBD: DNA-binding domain
DHAP: dihydroxyacetone phosphate
DHF: dihydrofolate
DHFR: dihydrofolate reductase
DHO : dihydroorotate
DHODH : dihydroorotate dehydrogenase
DMEM: dulbecco modified eagle medium
DMSO: dimethyl sulfoxide
dTMP: deoxythymidine monophosphate
ECAR; extracellular acidification rate
EGFR: epidermal growth factor receptor
EIF4E: eukaryotic translation initiation factor 4E
EMT: epithelial-to-mesenchymal transition
ER: estrogen receptor
ErbB2: erythoblastic oncogene B
ERR: estrogen related receptor
ERRE: estrogen related receptor response element
ETC: electron transport chain
F1,6BP: fructose 1,6 bisphosphate
F6P: fructose 6-phosphate
$FADH_2$: flavin adenine dinucleotide
FASN : fatty acid synthase
FBS: fetal bovine serum
FCCP: trifluoromethoxyphenylhydrazone
FDG-PET: ^{18}F-deoxyglucose positron emission tomography
Fe-S: iron/sulphur clusters
FH: fumarate hydratase
FLCN: folliculin
FMN: flavin mononucleotide
FOXA1: forkhead box A1
FPGS: folylpolyglutamate synthetase
G3P: glyceraldehyde 3-phosphate
G6P: glucose 6-phosphate
G6PDH: glucose 6-phosphate dehydrogenase
GABPA/B: GA repeat-binding protein α or β
GART : phosphoribosylglycinamide formyltransferase
GC-MS: gas chromatography – mass spectrometry
GCN5: histone acetyltransferase
GCS/GLDC: glycine cleavage system
GDH: glutamate dehydrogenase
GLS: glutaminase
Glut1: glucose transporter 1
GMP: guanine monophosphate
GS: glycogen synthase
GSDM1: glutathione-S-transferase
GSK3β: glycogen synthase kinase 3 β
GTP: guanine triphosphate
HEPES: 4-2-hydroxyethyl-1-piperazineethanesulfonic acid
HER2: epidermal growth factor receptor 2
HIF-1α: hypoxia-inducible factor 1 α
HK: hexokinase
HPLC: high pressure liquid chromatography
IDH: isocitrate dehydrogenase
IMP : inosine monophosphate
IMPDH : inosine monophosphate dehydrogenase
IPA: Ingenuity pathway analysis
J ATPglyc: glycolytic ATP production
J ATPox: oxidative ATP production
LBD: ligand binding domain
LC-MS: liquid chromatography – mass spectrometry

LDH: lactate dehydrogenase
LKB1: liver kinase B1
MAPK: mitogen activated protein kinase
MEF: mouse embryonic fibroblast
MID: mass isotopomer distribution
MITF: microphthalmia associated transcription factor
MPC: mitochondrial pyruvate carrier
MTBSTFA: N-tert-butyldimethylsilyl-N-methyltrifluoroacetamide
MTHFD1: methylenetetrahydrofolate dehydrogenase, cyclohydrolase, formyltetrahydrofolate synthetase 1
MTHFD1L: methylenetetrahydrofolate formyltetrahydrofolate synthetase 1 like
MTHFD2: methylenetetrahydrofolate dehydrogenase, cyclohydrolase 2
MTHFD2L: methylenetetrahydrofolate dehydrogenase, cyclohydrolase 2 like
MTHFR: methylenetetrahydrofolate reductase
mTOR: mammalian target of rapamycin
mTORC1: mammalian target of rapamycin complex 1
MTR: methionine synthase
MTX: methotrexate
NAD/NADH: nicotinamide adenine dinucleotide
NADP/NADPH: nicotinamide adenine dinucleotide phosphate
NRF1/2: nuclear respiratory factor 1 or 2
NSCLC: non-small cell lung cancer
NTD: nonconserved amino terminal domain
OAA: oxaloacetate
OCR: oxygen consumption rate
Oct1: organic cation transporter 1
OMP: orotate monophosphate
OXPHOS: oxidative phosphorylation
PC: pyruvate carboxylase
PDH: pyruvate dehydrogenase
PDK: pyruvate dehydrogenase kinase
PEP: phosphoenolpyruvate
PEPCK: phosphoenolpyruvate carboxykinase
PFK: phosphofructokinase
PGC-1: peroxisome proliferator-activated receptor gamma coactivator 1
PHD: prolyl-hydroxylase
PHGDH: 3-phosphoglycerate dehydrogenase
PI3K: phosphoinositide 3-kinase
PK: pyruvate kinase
PPARγ: peroxisome proliferator-activated receptor gamma
PPAT : phosphoribosyl pyrophosphate amidotransferase
PR: progesterone receptor
PRC: PGC related coactivator
PRKAA: Protein kinase AMP-activated catalytic subunit α
PRKAB: Protein kinase AMP-activated non-catalytic subunit β
PRKAG: Protein kinase AMP-activated non-catalytic subunit γ
PRMT1: protein arginine-N-methyltransferase 1
PRPP: 5-phosphoribosyl-1-pyrophosphate
PRPS2: phosphoribosyl pyrophosphate synthetase 2
PSAT: phosphoserine aminotransferase
PSPH: phosphoserine phosphatase
PTEN: phosphatase and tensin homolog
PUMA: p53 upregulated modulator of apoptosis
RAPTOR: Regulatory-associated protein of mTOR
RCR: respiratory control ratio
RICTOR: rapamycin-insensitive companion of mammalian target of rapamycin
RNR: ribonucleotide reductase
ROS: reactive oxygen species
RPMI: Roswell Park Memorial Institute medium
RRM2: ribonucleotide reductase regulatory subunit M2
RTK: receptor tyrosine kinase
S6K: S6 kinase
SAH: S-adenosylhomocysteine
SAM: S-adenosylmethionine
SCO2: cytochrome c oxidase assembly protein
SDH: succinate dehydrogenase
SGLT: sodium glucose transporter
SHMT: serine hydroxymethyltransferase
SIRT1: sirtuin 1
SITA: stable isotope tracing analysis
SOD: superoxide dismutase
SREBP : sterol response element binding protein
SUMO1: small ubiquitin-related modifier 1
TAK-1: TGF-β-activated kinase 1
TCA: tricarboxylic acid cycle
TET: Ten-Eleven translocation proteins
TFAM: transcription factor A
THF: tetrahydrofolate
TIGAR: p53 inducible regulator of glycolysis and apoptosis
TPI: triose phosphate isomerase
TSC2: tuberous sclerosis complex 2
TYMS: thymidine synthase
ULK1: Unc-51 like autophagy activating kinase 1
UMP: uracil monophosphate
UPP: uridine phosphorylase
UTP: uracil triphosphate
VEGF: vascular endothelial growth factor
VHL: Von-Hippl-Lindau
YYI: ying-yang 1

CHAPTER 1: INTRODUCTION

1.1 CANCER: A MALIGNANCY OF DERAILED CELLULAR GROWTH

Mammalian cells normally follow a set of instructions to perform their destined cellular processes. As instructions are coded in genetic material, genetic alterations can perturb cellular functions, which can impact cell survival and even dysregulate processes linked to cell growth and proliferation. Cancer is characterized by neoplastic growth which comprises alterations in cell cycle, differentiation and survival with the capacity of spreading throughout the body (Kleinsmith, 2006). Nearly 1 in 2 Canadians will be diagnosed with cancer at some point in their lives, and 1 in 4 will die from a form of the disease (Canadian Cancer Statistics Advisory Committee, 2018).

Cancer or neoplasia can be caused by the lesions in the genome such as mutations, amplifications, and gene re-arrangements (Hanahan and Weinberg, 2000). Some of these alterations affect regions of the genome occupied by oncogenes, which can drive tumourigenesis, and tumour suppressors, which prevent aberrant cell growth (Kleinsmith, 2006). Although cancer cells can originate from different tissues, they correspond to a group of diseases that possess similar characteristics that propel transformation. Originally termed by Hanahan and Weinberg in 2000, cancer cells have six hallmarks including invasion and metastasis, enabling replicative immortality, inducing angiogenesis, resisting cell death, sustaining proliferative signalling, and evading growth suppressors (Hanahan and Weinberg, 2000). More recently, four emerging hallmarks were added to this list including genome instability, tumour-promoting inflammation, avoiding immune destruction, and especially modulating cellular energetics (Hanahan and

Weinberg, 2011). Given that uncontrolled cell growth and proliferation requires meeting high bioenergetic and biosynthetic demands, cellular metabolism plays an important role in fuelling transformation, especially as several metabolic enzymes also act as oncogenes and tumour suppressors (Jones and Thompson, 2009).

1.2 CANCER METABOLISM: HOTWIRING THE CIRCUITRY TO DRIVE TUMORIGENESIS

In general, differentiated mammalian cells only take up nutrients from their environment when they are stimulated to do so by growth factors. In contrast, cancer cells overcome this dependency due to the acquisition of oncogenic mutations that perturb signalling pathways to drive cell-autonomous nutrient uptake and metabolism (Hsu and Sabatini, 2008) (Deberardinis et al., 2008) (Vander Heiden et al., 2009). Dr. Otto Warburg has observed that cancer cells prefer to catabolize glucose to lactate, even in the presence of ample oxygen to support oxidative phosphorylation (OXPHOS) (Warburg, 1956). In fact, these observations have been exploited clinically through the use ^{18}F-deoxyglucose positron emission tomography (FDG-PET) (Ben-Haim and Ell, 2009). Warburg hypothesized that the preference for glycolysis arose from mitochondrial defects in cancer cells that prevented the use of OXPHOS for ATP generation (Vander Heiden et al., 2009). However, evidence from the past decade had elucidated that not only do cancer cells derive a significant portion of their ATP from OXPHOS, but that mitochondria play a pivotal role in carrying out the biosynthetic reactions required for cancer growth (Ward and Thompson, 2012).

The following sections will be devoted to summarizing the metabolic pathways used by cancer cells to fuel growth. In brief, cells metabolize glucose to pyruvate, which can be reduced

to lactate or completely oxidized to CO_2 in mitochondria through the citric acid cycle / tricarboxylic acid cycle (CAC or TCA). Other fuel sources such as amino acids and fatty acids are also catabolized through the CAC. The CAC generates reducing equivalents that feed the electron transport chain (ETC), where oxygen acts as the final acceptor, and an electrochemical gradient is generated to facilitate ATP production. In contrast, cells also metabolize glucose and other fuels to provide building blocks for constructing nucleotides, fatty acids, and amino acids, as well as reducing power to fuel those anabolic processes. Through this end, cells wield their metabolic potential to supply themselves with the tools needed to promote survival and proliferation.

1.2.1 GLYCOLYSIS: FUELING CANCER'S SWEET TOOTH

Carbohydrates are first digested by the body and broken down to glucose molecules. Glucose is actively transported from intestinal lumen into brush border cells, using the glucose/sodium transport SGLT1 (also known as SGLUT1) (Appling et al., 2019). Glucose is then passively diffused through a glucose uniport into the blood, where it is taken up by members of the GLUT family of glucose transporters. Most cells, including cancer cells, express and transport glucose with high affinity using GLUT1 (Ancey et al., 2018).

The oxidation of glucose occurs through a series of ten reactions in the cytosol, referred to as glycolysis, in which the 6-carbon glucose is oxidised to produce two 3-carbon pyruvate molecules. Glycolysis is useful for generating ATP, for building intermediates for the construction of building blocks, and intermediates for further metabolism. The first three steps involve preparing for the catabolism of glucose, which involves a cellular investment of two

ATP molecules per molecule of glucose (referred to as the energy investment phase). Specifically, glucose is first phosphorylated by hexokinase (HK) to generate glucose 6-phosphate (G6P), to retain the metabolite in the cell (Appling et al., 2019). Hexokinase exhibits product inhibition in as much as the accumulation of G6P inhibits the enzyme to prevent further phosphorylation of glucose. Several cancer cells express high levels of the *HK2* isoform relative to non-transformed cells, especially in KRas-driven non-small cell lung cancer and ErbB2-driven breast cancer (Patra et al., 2013).

The next step involves the isomerization of G6P into fructose 6-phosphate (F6P), which is subsequently phosphorylated by phosphofructokinase 1 (PFK1), producing fructose 1,6 bisphosphate (F1,6BP) (Appling et al., 2019). The PFK1 reaction is the rate-limiting step of glycolysis, while PFK2 converts F6P to fructose 2,6 bisphosphate (F2,6BP), which acts as an activator of PFK1 (Appling et al., 2019). PFK1 is also sensitive to the energy status of the cell, whereby high levels of ATP inhibit the enzyme, while AMP acts as an activator. Parallel to HK isoforms, cancer cells express the *PFKFB3* isoform, which produces elevated levels F2,6BP to maintain high glycolytic activity (Kessler et al., 2008) (Minchenko et al., 2002) (Atsumi et al., 2002) (Clem et al., 2013).

F1,6BP is then cleaved by aldolase, yielding glyceraldehyde 3 phosphate (G3P) and dihydroxyacetone phosphate (DHAP) (Appling et al., 2019). DHAP can be converted back into G3P, through the reaction of triose phosphate isomerase (TPI), to produce a second molecule of G3P (Appling et al., 2019). Once two G3P molecules are produced, glycolysis enters the return on energy investment phase, in which the oxidation of both G3P molecules through series of reactions yields a total of four ATP and two NADH. Specifically, G3P is oxidized by

glyceraldehyde-3-phosphate dehydrogenase, producing the short-lived 1,3-bisphosphoglycerate, which is then converted to 3-phosphoglycerate by phosphoglycerate kinase (Appling et al., 2019) The next two reactions involve an isomerization reaction by phosphoglyceromutase to 2-phosphoglycerate, then a dehydration reaction by enolase to phosphoenolpyruvate (PEP) (Appling et al., 2019). The final step of glycolysis involves the conversion of PEP into pyruvate, generated by pyruvate kinase (PK) (Appling et al., 2019). PK is allosterically activated by F1,6BP and inhibited by ATP (Appling et al., 2019). PK exist in two isoforms, with PKM2 being less active than PKM1 (Israelsen and Vander Heiden, 2015). Unexpectedly, some cancers express the less active *PKM2* isoform (Christofk et al., 2008), as it allows for the accumulation of glycolytic intermediates that can divert into biosynthetic pathways, such as the biosynthesis of serine for one-carbon metabolism (Ye et al., 2012).

Given that two molecules of ATP were used to prepare glucose for catabolism, the breakdown of glucose to pyruvate generates net of two ATP and two NADH. The fate of pyruvate is subsequently dependent on the needs of the cell. Pyruvate can be converted into lactate through lactate dehydrogenase (LDH), regenerating NAD+ to be used for the next round of glycolysis. The second option is to metabolize pyruvate in mitochondria through the citric acid cycle (CAC) for generating ATP mainly through oxidative phosphorylation (OXPHOS). In most cancer cells, most of the pyruvate is converted to lactate through LDHA, where lactate is excreted into the extracellular media, which is thought to promote tumour invasion (Estrella et al., 2013). In addition, the excreted lactate may be used as a fuel source for aerobic human cervix squamous cells (Sonveaux et al., 2008) and human non-small cell lung cancer (NSCLC) tumours *in vivo* (Faubert et al., 2017). Despite the lower energetic yield per glucose molecule in glycolysis relative to OXPHOS, most cancer cells still preferentially use glycolysis even in the

presence of oxygen, a term defined as aerobic glycolysis also commonly referred to as the Warburg effect. Arguably, when glucose is highly accessible and is quickly processed, glycolysis has the potential to generate a high quantity of ATP at a fast rate (Guppy et al., 1993). In addition, glycolysis can be used in hypoxia to allow for quick regeneration of NAD+ for further glucose catabolism (Samanta and Semenza, 2018). Lastly, glycolysis provides many of the building blocks for anabolic processes such as nucleotide, lipid, and amino acid biosynthesis (Vander Heiden et al., 2009).

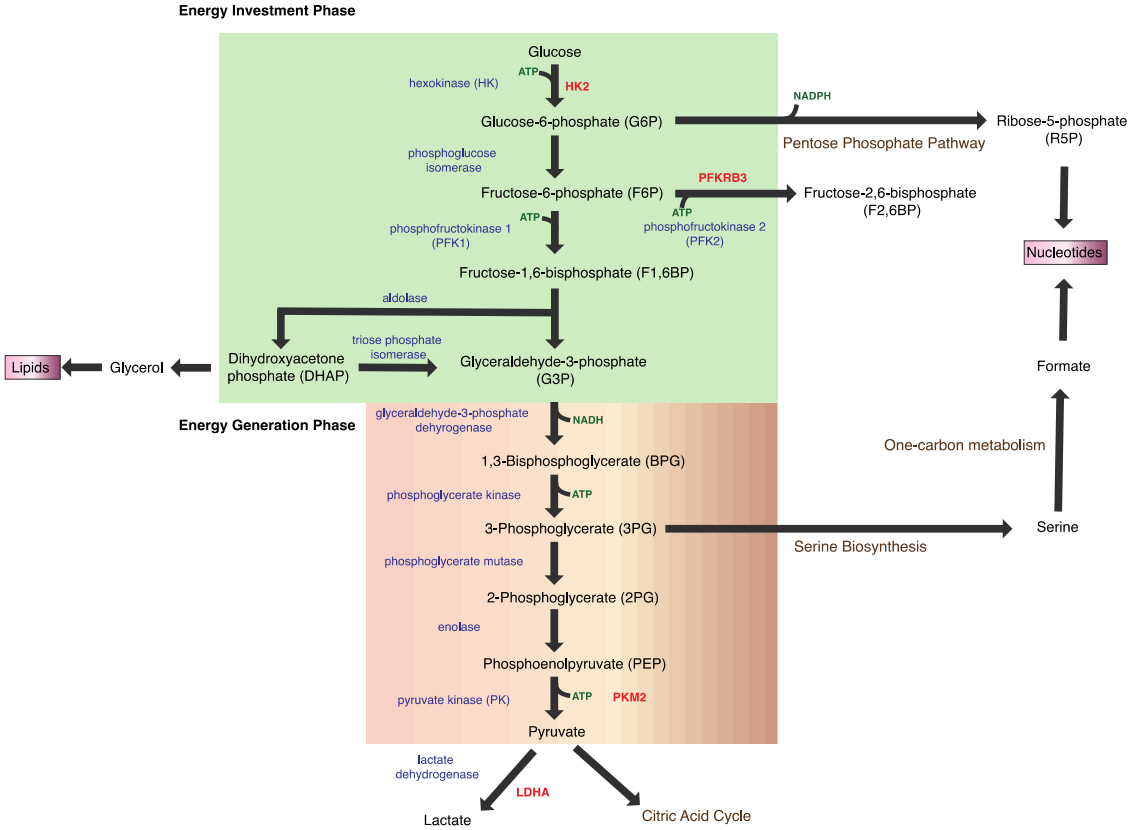

Figure 1.1: Glycolysis is central to the bioenergetic and biosynthetic needs of cancer cells. Glucose is broken down in a series of enzymatic reactions (enzymes in blue) to pyruvate, which can be reduced to lactate or further oxidized in the citric acid cycle. Glycolysis is divided in two phases, including the energy investment phase (green box), which utilizes ATP to prepare glucose for its oxidation, and the energy generation phase (orange box), which generates ATP and NADH. Branching pathways include the pentose phosphate pathway for NADPH and ribose-5-phosphate generation, glycerol production for lipid biosynthesis and serine biosynthesis for one-carbon reactions. Enzymes upregulated in cancer are in red.

1.2.2 MITOCHONDRIA: HARNESSING THE CELLULAR FURNACE AND FACTORY

The oxidation of pyruvate, as well as lipids and amino acids occur in specialized organelles called mitochondria. These organelles originating from bacteria (Sagan. L. 1967) are the bioenergetic hub of the cell. They host the citric acid cycle (CAC) and the components of the electron transport chain (ETC), which conduct oxidative phosphorylation (OXPHOS). They contain a permeable outer membrane to allow communication of metabolites with the cytosol, and an impermeable inner membrane to permit the establishment of an electrochemical gradient. Mitochondria also contain a matrix that host a variety of enzymes and the mitochondrial genome. Aside from its bioenergetic capabilities, mitochondria play various biosynthetic roles which are exploited for cancer proliferation.

1.2.2.1 CITRIC ACID CYCLE: CANCER'S METABOLIC STEERING WHEEL

To complete its full oxidation, the pyruvate generated from glycolysis is transported into mitochondria using the mitochondrial pyruvate carrier (MPC) and interacts with pyruvate dehydrogenase (PDH) complex (Appling et al., 2019). This irreversible reaction converts pyruvate into acetyl CoA and yields another NADH (Appling et al., 2019). The pyruvate dehydrogenase kinase (PDK) can inhibit this reaction by phosphorylating and inactivating PDH. This is thought to prevent further pyruvate utilization in mitochondria thereby supporting the Warburg effect in cancer cells (Sradhanjali and Reddy, 2018).

Acetyl-CoA can enter the CAC by reacting with oxaloacetate to generate citrate which is catalyzed by citrate synthase (CS) (Appling et al., 2019). This enzyme is inhibited by citrate, NADH, and succinyl-CoA (Appling et al., 2019). Citrate can be further processed through the citric acid cycle or can be exported into the cytosol for fatty acid biosynthesis. In the CAC,

citrate is isomerized by aconitase to produce isocitrate (Appling et al., 2019). Non-transformed prostate cells accumulate zinc, which inhibits aconitase, causing the accumulation and export of citrate to the extracellular environment (Costello and Franklin, 2016). In contrast, prostate cancer cells prevent the accumulation of zinc, thereby alleviating the inhibition of aconitase to bolster CAC activity and sustain mitochondrial metabolism (Costello and Franklin, 2016). As a result, prostate cancer is an example of a disease that does not exhibit the Warburg effect, thereby diversifying the complexity of metabolic perturbations in neoplasia.

Furthermore, isocitrate is decarboxylated by isocitrate dehydrogenase (IDH), producing α-ketoglutarate and an NADH molecule (Appling et al., 2019). There are three IDH isoforms, with IDH3 isoform being the most abundant. IDH1 and IDH2 both use NADP+ as an oxidizing agent, but IDH1 is cytosolic and IDH2 is mitochondrial (Al-Khallaf, 2017). Similar to CS, IDH3 is inhibited by NADH (Al-Khallaf, 2017). Mutations in IDH1 and IDH2 have been discovered in gliomas, acute myeloid leukemias, sarcomas, and renal cell carcinomas (Parsons et al., 2008) (Lu et al., 2013; Shim et al., 2014), resulting in the production of the oncometabolite 2-hydroxyglutarate (2-HG) (Dang et al., 2009). In contrast to α-ketoglutarate, 2-HG competitively inhibits dioxygenase enzymes (Figueroa et al., 2010) (Turcan et al., 2012)(Turcan S. et al. 2012), which are used to demethylate histones .The repression of dioxygenases, such as members of the Ten-Eleven translocation proteins (TET) family, leads to histone hypermethylation which may stimulate neoplastic growth and cancer progression (Losman et al., 2013) (Sullivan et al., 2016). 2-HG can also inhibit the prolyl-hydroxylase 2 and 3 (PHD2 and PHD3), which are involved in the degradation of HIF-1α, resulting in its stabilization under normoxia (Wong et al., 2013).

In addition, α-ketoglutarate can be decarboxylated by α-ketoglutarate dehydrogenase, producing succinyl-CoA and NADH (Appling et al., 2019). Succinyl-CoA synthetase converts succinyl-CoA to succinate and produces a GTP molecule (Appling et al., 2019). Succinate is further oxidized by succinate dehydrogenase (SDH), producing fumarate and a molecule of $FADH_2$ (Appling et al., 2019). SDH (also known as complex II) is found in both the CAC and the ETC (Appling et al., 2019). Mutations in SDH have been found in several cancers including paraganglioma and pheochromocytoma (Hao et al., 2009), renal carcinoma (Ricketts et al., 2008), breast cancer (Kim et al., 2013), and gastrointestinal cancer (Janeway et al., 2011). Cells harbouring an SDH mutation accumulate succinate, which also acts as a competitive inhibitor of α-ketoglutarate dioxygenases (Sciacovelli and Frezza, 2016). Similar to 2-HG, succinate inhibits TET proteins, which can cause histone hypermethylation (Xiao et al., 2012) and cause the prolyl hydroxylation of HIF-1α (Selak et al., 2005). Given succinate accumulation also increase the potential for tumorigenesis, succinate is also considered as an oncometabolite (Ward and Thompson, 2012).

In addition, fumarate undergoes a hydration reaction through fumarate hydratase (FH), yielding malate (Appling et al., 2019) Mutations in FH have been found in renal cancer (Tomlinson et al., 2002), paraganglioma and pheochromocytoma (Castro-Vega et al., 2014) and neuroblastoma (Fieuw et al., 2012). Cells with the FH mutation accumulate fumarate, which also acts as an oncometabolite by inhibiting PHD2 (Isaacs et al., 2005). Once malate is produced, it is ultimately oxidized to oxaloacetate through malate dehydrogenase, generating NADH (Appling D.R. et al. 2019). Alternatively, oxaloacetate can be produced from pyruvate through pyruvate carboxylase (PC) (Lao-On et al., 2018) to ensure the availability of substrates for the next round of CAC. The re-synthesis of oxaloacetate completes the CAC. In summary, one round of the

CAC generates 3 NADH, 1 $FADH_2$, and 1 GTP molecule. The accumulation of reducing agents NADH and $FADH_2$ act as substrates for the electron transport chain to harvest ATP through OXPHOS.

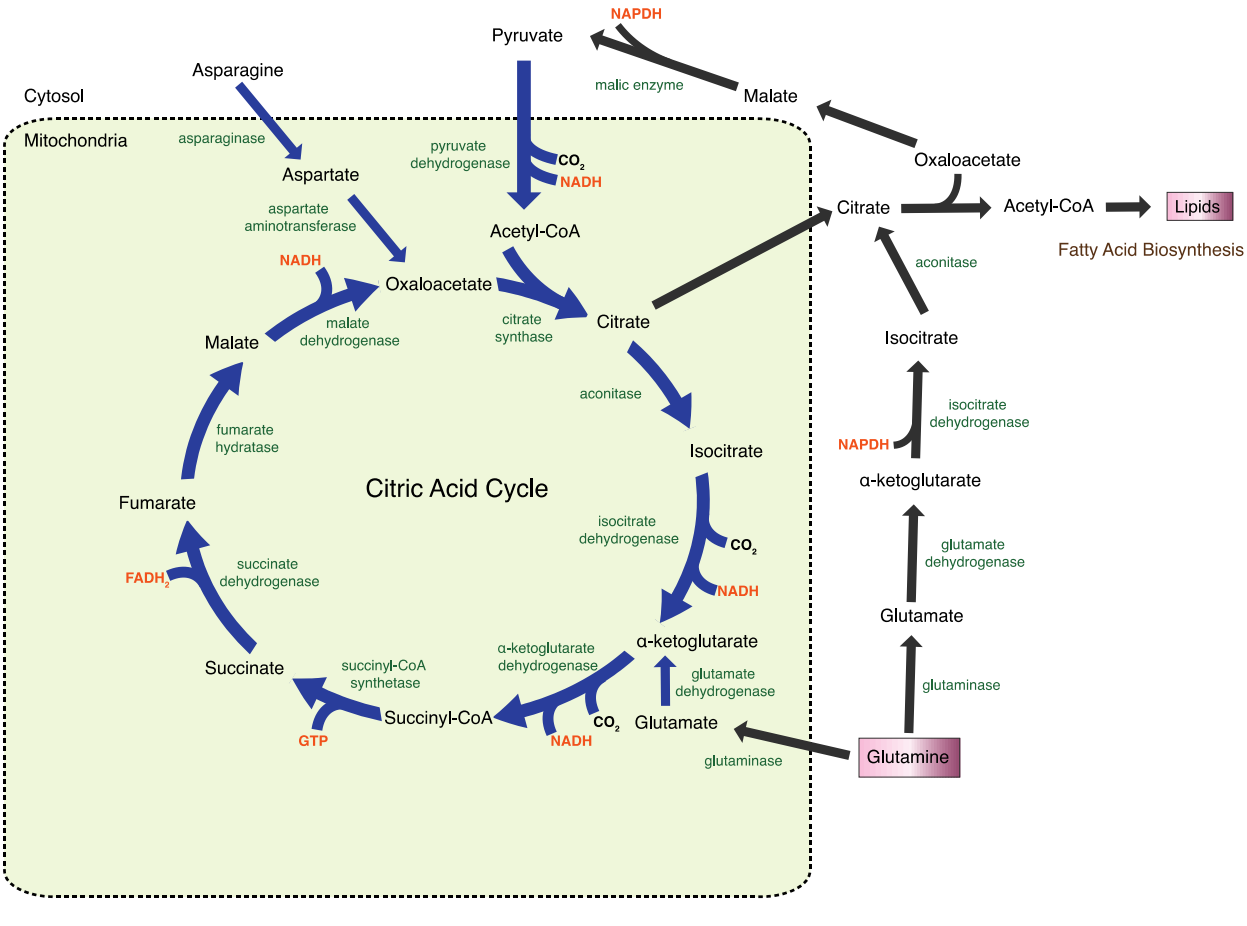

Figure 1.2: The citric acid cycle fuels oxidative and reductive activities of cancer cells. Pyruvate is converted to acetyl-CoA, which enters the citric acid cycle (CAC) following the condensation with oxaloacetate to form citrate. Citrate is metabolized through the CAC to CO_2, forming reducing agents NADH and $FADH_2$ that supply OXPHOS. Citrate can also be exported to the cytosol for fatty acid biosynthesis. Amino acids such as glutamine can replenish the CAC and is used for both oxidative and reductive processes. Enzymes are in green.

1.2.2.2 OXPHOS: THE AEROBIC RETURN ON INVESTMENT

Oxidative phosphorylation (OXPHOS) is the process by which ATP is generated through the oxidation of NADH and FADH2 through an electron transport chain (ETC) to reduce molecular O_2 to H_2O. Electrons are transferred through a series of complexes (Complex I, Complex III, Complex IV) or (Complex II, Complex III, and Complex IV), which permit the pumping of electrons from the matrix into the intermembrane space to establish an electrochemical gradient, which drives the synthesis of ATP (Appling D.R. et al. 2019).

Complex I (NADH dehydrogenase) is the final destination for NADH. NADH is oxidized to NAD+, releasing two high-powered electrons that are transferred to a flavin mononucleotide (FMN), a sequence of iron/sulphur clusters (Fe-S), then accepted by ubiquinone (coenzyme Q) (Appling D.R. et al. 2019). The series of reduction-oxidation (redox) reactions causes a conformational change within the complex that pumps four protons into the intermembrane space (Appling D.R. et al. 2019). Similarly, complex II (succinate dehydrogenase) also oxidizes $FADH_2$ and releases electrons through a series of Fe-S to ubiquinone, although no protons are pumped into the intermembrane space (Appling D.R. et al. 2019). The reduced ubiquinone molecules (called ubiquinol) from complex I and II are oxidized at complex III (coenzyme Q-cytochrome c reductase) (Appling D.R. et al. 2019). Electrons are transferred through cytochromes b, c, and Fe-S, within the complex and donated to the cytochrome c carrier (Appling D.R. et al. 2019). This series of reactions in complex III also pumps four protons (Appling D.R. et al. 2019). The cytochrome c carrier transports the electrons to complex IV (cytochrome c oxidase), where the electrons are transferred to two heme groups, three copper ions, then ultimately reducing molecular oxygen to water (Appling D.R. et al. 2019). Similarly,

these reactions in complex IV also pump two protons (Appling D.R. et al. 2019). The accumulation of protons in the intermembrane space causes an electrochemical gradient. Protons pass through the F_0 subunit of ATP synthase (Complex V) causing a conformational change in the F_1 subunit, allowing the binding of ADP and Pi to catalyze ATP synthesis (Mitchell, 1961).

The transfer of electrons through the ETC is an important for maintaining cell survival. However, the incomplete reduction of oxygen can lead to the production of reactive oxygen species (ROS) (Appling D.R. et al. 2019). Cells can detoxify ROS using enzymes such as glutathione peroxidase, catalase, and superoxide dismutase (Berg et al., 2007).

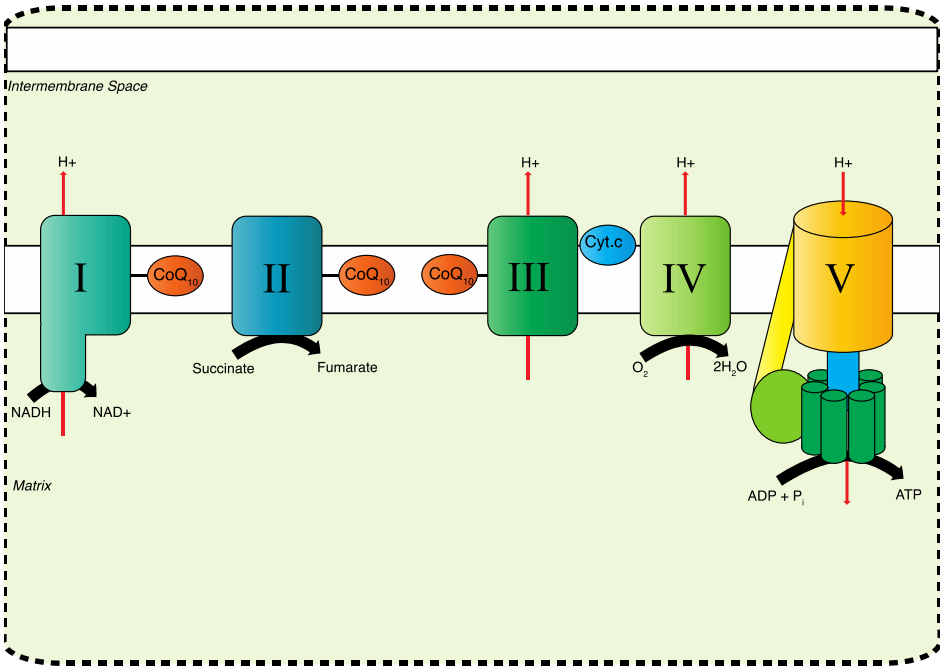

Figure 1.3: The electron transport chain generates an electrochemical gradient that facilitates ATP production. Reducing agents NADH and $FADH_2$ are oxidized and high-energy electrons are transported through a series of complexes (I-III-IV or II-III-IV) that reduces molecular oxygen to water. The electron transport chain pumps protons into the intermembrane space, creating an electrochemical gradient that drives ATP synthesis through complex V or ATP synthase.

1.2.3 AMINO ACID METABOLISM: CANCER BULKING UP ON GLUTAMINE

Amino acids serve as an important source of fuel for propelling both catabolic and anabolic processes. Glutamine is the most abundant free amino acid in the body (Dang, 2010) and is an important source of fuel for many cancer types (DeBerardinis and Cheng, 2010). Indeed, glutamine transport has been shown to be upregulated in many cancers (Bhutia and Ganapathy, 2016). The catabolism of glutamine, known as glutaminolysis, involves the conversion of glutamine to glutamate, catalyzed by glutaminase (GLS) (DeBerardinis RJ, Cheng T. 2010). The carbons of glutamate enter the CAC by first being directly transformed into α-ketoglutarate through the enzyme glutamate dehydrogenase (GDH) (DeBerardinis RJ, Cheng T. 2010). Glutamine-mediated anapleurosis is used to replenish intermediates of the CAC, which are being used up for macromolecular synthesis (Romero-Garcia et al., 2011). Consequently, the oxidation of glutamine in the CAC acts as an important contributor to bioenergetic functions in proliferating cells and cancer (DeBerardinis RJ, Cheng T. 2010). Glutamine is also used to build the glutathione, which is used to combat ROS (DeBerardinis RJ, Cheng T. 2010).

In addition, glutamine plays a pivotal role in anabolic processes. Both glutamate and α-ketoglutarate are involved in transaminase reactions used to produce other amino acids. For example, glutamate reacts with pyruvate through alanine transaminase (ALT) to generate alanine and α-ketoglutarate, whereas with oxaloacetate it is used by aspartate transaminase (AST or GOT) to generate aspartate and α-ketoglutarate (DeBerardinis RJ, Cheng T. 2010). Glutamate is also a substrate for the phosphoserine aminotransferase (PSAT) reaction of serine biosynthesis, in which glutamate is used to facilitate generation of a precursor to serine (Kim and Park, 2018).

In addition, the export of glutamine allows for increased import of essential amino acids, which activates mTORC1 signalling (Nicklin et al., 2009).

Moreover, glutamine can also fuel fatty acid synthesis through a set of reactions called reductive carboxylation (Metallo et al., 2011). The α-ketoglutarate generated from glutamine in mitochondria can be converted to isocitrate by the *IDH2* isoform, thereby running the CAC in the reverse direction than the *IDH3* reaction (Filipp et al., 2012). Isocitrate can be converted to citrate, which is exported to the cytosol for fatty acid biosynthesis (Filipp et al. 2012). Glutamine can also be converted to citrate through a series of reactions exclusively in the cytosol, governed by the *IDH1* isoform (Filipp et al. 2012). Both IDH1 and IDH2 reductive carboxylation reactions consume NADPH (Bell and Baron, 1968). Glutamine is also used for *de novo* nucleotide biosynthesis (DeBerardinis and Cheng, 2010). Lastly, glutamine transport and metabolism are strongly upregulated at the transcriptional level through oncogenic Myc signalling (Dejure and Eilers, 2017).

1.2.4 FATTY ACID METABOLISM: BUTTERING UP TUMOURIGENESIS

Fatty acids represent another important fuel source and contributor to maintaining the integrity of cancer cells. Cells store lipids in the cytoplasm as lipid droplets to be used for catabolic or anabolic reactions upon demand. In fact, colon cancers have increased abundance of lipid droplets (Accioly et al., 2008). During periods of limited glucose availability, triglycerides are catabolized to glycerol and fatty acids. Glycerol is converted to DHAP through the actions of glycerol kinase and glycerol-3-phosphate dehydrogenase and can enter glycolysis (Berg JM. et al. 2007). Fatty acids, such as palmitate, are activated and bound to carnitine, producing acyl-

carnitine through the rate-limiting reaction of carnitine palmitoyltransferase 1 (CPT1) and is processed to palmitoyl-CoA by CPT2 (Berg JM. et al. 2007). In the matrix, fatty acids are broken down through a series of oxidation and hydration reactions called β-oxidation, which generates reducing agents NADH and $FADH_2$ and acetyl-CoA (Berg JM. et al. 2007). Human lung cancers express *CPT1C*, an isoform of CPT1 that is normally only found in neurons, which increases fatty acid oxidation to prevent metabolic stress and promote tumour growth (Zaugg et al., 2011).

Fatty acids are also a key constituent of membranes needed for cell growth and proliferation. To undergo lipogenesis, citrate from the CAC is exported to the cytosol and hydrolyzed by ATP-citrate lyase (ACL) into oxaloacetate and acetyl CoA (Berg JM. et al. 2007). Oxaloacetate is returned to the mitochondria through a set of reactions that include cytosolic malate dehydrogenase, malic enzyme (an NADPH-generating reaction), and pyruvate carboxylase (Berg JM. et al. 2007). The cytosolic pool of acetyl-coA is converted to malonyl CoA, through the rate-limiting enzyme acetyl-CoA carboxylase (ACC). The following steps are driven by fatty acid synthase (FASN), involving condensation, dehydration and reduction reactions that consume NADPH to yield palmitate (Berg JM. et al. 2007).

Given the high demand for anabolic processes, cancer cells conduct higher lipogenesis relative to normal cells (Swinnen et al., 2006). *FASN* has been found to be upregulated in prostate cancer (Shah et al., 2006) pancreatic ductal adenocarcinoma (Witkiewicz et al., 2008), ovarian cancer (Cai et al., 2015), and colorectal patients (Long et al., 2014) among others. In addition, ACC (Chajes et al., 2006) and ACLY (Migita et al., 2008) are also important for tumour growth. Furthermore, the sterol response element binding protein (SREBP), a major transcription factor that activates fatty acid synthesis, is also upregulated in glioblastoma (Guo et

al., 2009) (Cheng et al., 2018). Lipids are also used for signal transduction pathways, by lipid messengers or by lipid modification (palmitoylation, myristoylation, and isoprenylation) of oncogenes such as WNTs, RAS and Akt. As a result, targeting fatty acid metabolism has emerged as an exciting strategy to limit tumourigenesis (Cheng C. et al. 2018).

1.2.5 PENTOSE PHOSPHATE PATHWAY: FROM RIBOSE TO REDUCING POWER

One of the main offshoots of glycolysis, known as the pentose phosphate pathway, is critical to the synthesis of nucleotides and the generation of reducing power in the form of NADPH. The first set of reactions, called the oxidative arm, involves the oxidation of glucose 6-phosphate (G6P) to ribulose 5-phosphate, which generates two molecules of NADPH (Berg JM. et al. 2007). Importantly, the rate-limiting step is the irreversible glucose 6-phosphate dehydrogenase (G6PDH) reaction that yields NADPH and is in turn strongly inhibited by NADPH (Berg JM. et al. 2007). The second part of the pathway, termed the non-oxidative arm, involves the production of ribose 5-phosphate for nucleotide biosynthesis through the recycling of sugar intermediates, which can ultimately feed back into glycolysis as fructose 6-phosphate and glyceraldehyde-3-phosphate (Berg JM. et al. 2007)..

G6PDH is important for cell growth as severe G6PDH deficiency is lethal in embryos (Longo et al., 2002). In fact, *G6PDH* is overexpressed in many cancers including diffuse large B cell lymphoma (Compagno et al., 2009), lung cancer (Stearman et al., 2005), and breast cancer (Pu et al., 2015), among others. Given that the pentose phosphate pathway provides both building blocks for growth and reducing power to support antioxidant defences, it is not surprising that this pathway is exploited for tumour growth (Cho et al., 2018). As a result, recent

work even suggests that G6PDH can act as an unfavourable prognostic marker in renal cancer (Zhang et al., 2014a).

1.2.6 NUCLEOTIDE BIOSYNTHESIS: TO PROLIFERATE, CANCER "BETTER PUT A RING ON IT"

One of the requirements for proliferating cells is to upregulate nucleotide biosynthesis to pass into S phase of the cell cycle (Lane and Fan, 2015). In fact, the expression of genes of nucleotide biosynthesis are increased in late G1 phase to meet this requirement (Sigoillot et al., 2003) (Fridman et al., 2013). As aforementioned, ribose 5-phosphate from the pentose phosphate pathway acts as the starting point for both purine and pyrimidine biosynthesis. Ribose 5-phosphate is phosphorylated to 5-phosphoribosyl-1-pyrophosphate (PRPP) by phosphoribosyl pyrophosphate synthetase (*PRPS2*) (Appling D.R. et al. 2019). Given its importance for nucleotide biosynthesis, PRPS2 is upregulated in several cancers, and is important for Myc-driven tumourigenesis (Cunningham et al., 2014).

The synthesis of purine nucleotides occurs in the cytosol and involves building the purine ring piece by piece while being attached to its sugar group. Upon production of PRPP, the next reaction involves the incorporation of ammonia group (NH_3) from glutamine in the phosphoribosyl pyrophosphate amidotransferase (*PPAT*) reaction, generating 5-phosphoribosylamine, which is the rate-limiting step of purine biosynthesis (Appling D.R. et al. 2019). The following steps involve an incorporation of glycine, NH_3 from glutamine, CO_2, aspartate, and two one-carbons units as formate to yield the inosine monophosphate (IMP), the precursor to AMP and GMP (Appling D.R. et al. 2019). Importantly, the

phosphoribosylglycinamide formyltransferase (GART) and 5-aminoimidazole-4-carboxamide ribonucleotide formyltransferase (ATIC) reactions both incorporate formate from formyl-THF of one-carbon metabolism into building the purine ring. The addition of another aspartate group, and removal of fumarate from IMP yields adenosine monophosphate (AMP) (Appling D.R. et al. 2019). The addition of a NH_3 group from glutamine generates GMP from IMP through the enzyme IMP dehydrogenase (IMPDH) (Appling D.R. et al. 2019). Recently, it was shown that small cell lung cancers are dependent on IMPDH as inhibition of the enzyme inhibits tumour growth (Huang et al., 2018).

In contrast to purines, pyrimidine biosynthesis involves first constructing the pyrimidine ring prior to linking to the sugar group. The ring in constructed from the synthesis of carbamoyl phosphate from glutamine and bicarbonate, followed by the addition of aspartate, dephosphorylation and dehydration reactions, yielding dihydroorotate (DHO) (Appling D.R. et al. 2019). This reaction is catalyzed by trifunctional enzyme carbamoyl-phosphate synthetase 2, aspartate transcarbamylase, and dihydroorotase (CAD), (Garavito et al., 2015). The next step involves the oxidation of dihydroorotate to orotate by orotate dehydrogenase, the only step that occurs in mitochondria (Appling D.R. et al. 2019). The pyrimidine ring as orotate is added to PRPP, generating orotate monophosphate (OMP), which is decarboxylated to uracil monophosphate (UMP) (Appling D.R. et al. 2019). UMP undergoes two phosphorylation reactions to generate UTP, which acts as the substrate for CTP synthase, to build CTP (Appling D.R. et al. 2019). To generate deoxyribonucleotides, ribonucleotides are reduced through the reaction with ribonucleotide reductase (*RNR*), which is an NADPH-dependent reaction. dUMP can be converted to dTMP through (TYMS) (Appling D.R. et al. 2019).

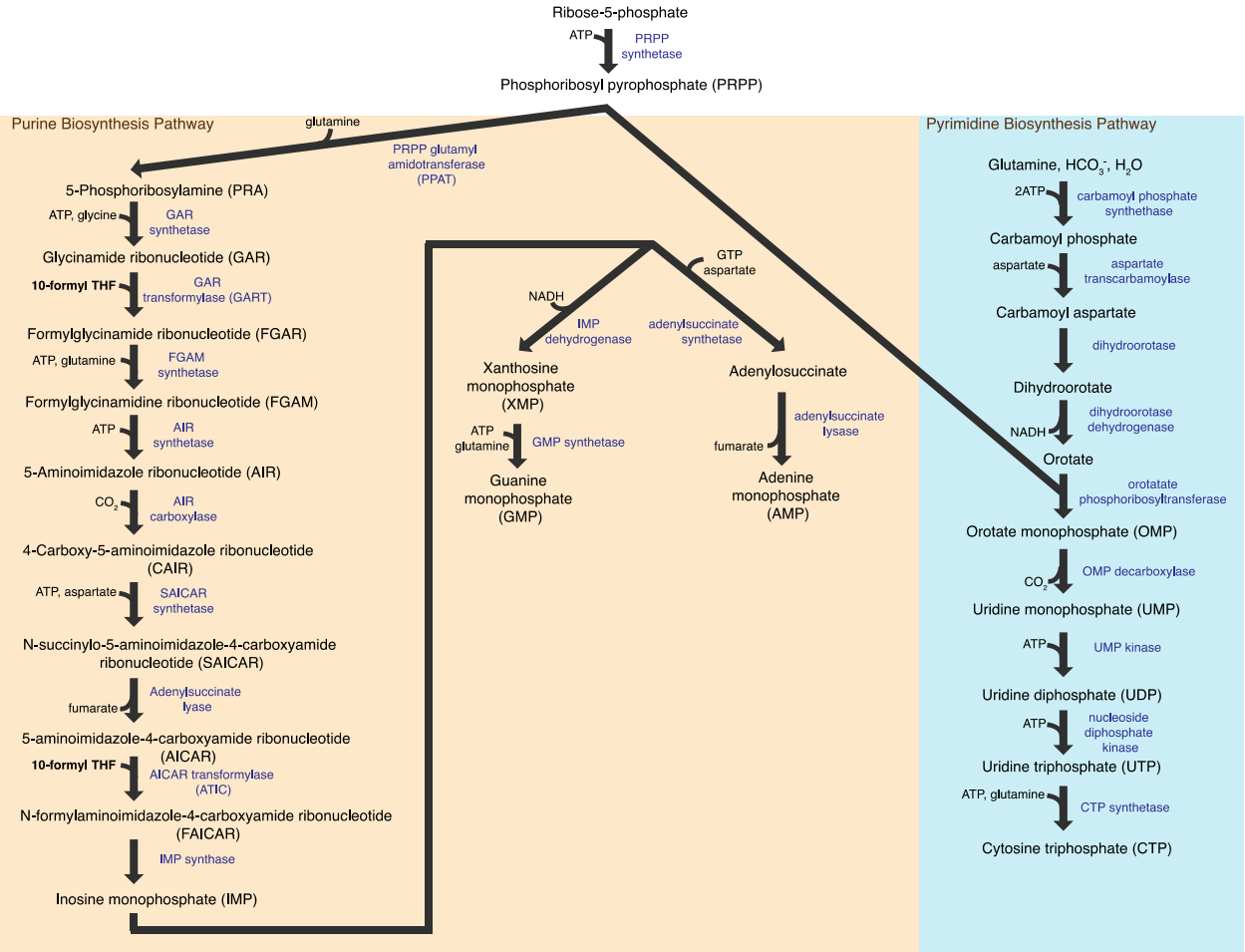

Figure 1.4: The purine and pyrimidine biosynthetic pathways. Ribose-5-phosphate from the pentose phosphate pathway is converted to PRPP, which acts as the sugar base for both purines and pyrimidines. The purine ring is generated from amino acids glutamine, glycine, and aspartate, as well as from 10-formyl THF from one-carbon metabolism, which enters at the GART and ATIC reactions (blue). The pyrimidine ring is constructed from glutamine, bicarbonate, and aspartate. Enzymes are in blue.

1.2.7 ONE-CARBON METABOLISM: PROLIFERATION COMES FULL CIRCLE

One-carbon metabolism encompasses a complex metabolic network that plays various roles in maintaining redox metabolism and proliferation. Specifically, it involves the transfer of a one-carbon (1C) unit through a set of reactions involving several folate coenzymes called the

folate cycle, and reactions involving the generation of methylation substrates, called the methionine cycle. This pathway integrates several nutrients, including amino acids, glucose, and vitamins, to generate biological outputs such as the biosynthesis of nucleotides, the maintenance of redox state, and the construction of substrates for methylation reactions.

The folate carrier tetrahydrofolate (THF) is used as the acceptor of 1C units through one-carbon metabolism and its availability is essential for one-carbon reactions (Newman and Maddocks, 2017). THF is produced by dihydrofolate (DHF), an intermediate transformed from folic acid, using the enzyme dihydrofolate reductase (*DHFR*) (Newman and Maddocks, 2017). Given the importance of THF availability for maintaining the pathway, several chemotherapeutic drugs such as methotrexate target *DHFR* (Newman and Maddocks, 2017).

One-carbon metabolism is primarily fueled by the amino acid serine, which is accessed via uptake or produced *de novo* from glycolysis. The glycolytic intermediate 3-phosphoglycerate (3-PG) is converted to 3-phosphopyruvate by phosphoglycerate dehydrogenase (PHGDH*)*, the rate-limiting step of serine biosynthesis (Locasale, 2013). Furthermore, 3-phosphopyruvate is a substrate for phosphoserine aminotransferase (PSAT) to generate 3-phosphoserine, which is dephosphorylated to form serine by the phosphoserine phosphatase (PSPH) (Locasale, 2013). Serine reacts with THF, through the serine hydroxymethyltransferase (SHMT; SHMT1 in cytosol*)* reaction to yield the 1C unit 5,10- methylene THF and the amino acid glycine (Locasale, 2013). 5,10-methylene THF enters the one-carbon pathway at a branch point, and its further processing is dependent on the needs of the cell. Firstly, if the cell requires purines, 5,10-methylene THF is converted to 10-formyl THF through a set of reactions in the cytosol governed by methylenetetrahydrofolate dehydrogenase, cyclohydrolase, formyltetrahydrofolate synthetase

1 (*MTHFD1)* (Newman and Maddocks, 2017). 10-formyl THF is the substrate for the purine biosynthetic reactions *GART* and *ATIC*, where the 1C unit releases its active carbon as formate to help build the purine ring (Lane and Fan, 2015). Importantly, the oxidation of 5,10-methylene THF to 10-formyl THF also generates NADPH, and this reaction was recently shown to be an important source of NADPH in proliferating cells (Fan et al., 2014). Furthermore, if the cell requires dTMP, 5,10-methylene THF can convert dUMP to dTMP, through the reaction thymidine synthase (TYMS) (Lane and Fan, 2015).

Secondly, 5,10-methylene THF can also be converted by the enzyme methylenetetrahydrofolate reductase (*MTHFR)* to produce 5-methyl THF, which can react with homocysteine to produce methionine through methionine synthase (*MTR*) (Newman and Maddocks, 2017). Methionine is subsequently used to generate S-adenosyl methionine (SAM), a broadly used methyl donor for methyltransferase reactions, such as DNA methylation (Newman and Maddocks, 2017). As a result, the production of SAM links one-carbon metabolism to the genetic and epigenetic processes of cells. The by-product of methylation reactions, S-adenosyl homocysteine (SAH) can be converted back to homocysteine for a second round of the methionine cycle (Newman and Maddocks, 2017). Another use of the methionine cycle is to produce cysteine, which is used in combination with glycine and glutamate to make glutathione, which is critical for cellular redox balance (Locasale, 2013).

1.2.7.1 ONE-CARBON METABOLISM IN MITOCHONDRIA

While the cytoplasmic pathway has one trifunctional MTHFD1 enzyme with dehydrogenase, cyclohydrolase, and formyl synthetase domains, the mitochondrial counterpart has three enzymes: formyltetrahydrofolate synthetase (MTHFD1L), bifunctional

methylenetetrahydrofolate dehydrogenase/cyclohydrolase (MTHFD2), bifunctional methylenetetrahydrofolate dehydrogenase/cyclohydrolase 2 like (MTHFD2L) (Tibbetts and Appling, 2010). MTHFD2 is essential during early embryonic development, but then declines as the fetus approaches birth (Di Pietro et al., 2002) (Di Pietro et al., 2004). Conversely, MTHFD2L is turned on late during embryogenesis, while MTHFD1L is expressed continuously from fetus to adulthood (Tibbetts and Appling, 2010). The diversity of MTHFD isoforms in mitochondria relative to cytoplasm is still unclear.

One distinctive feature of mitochondrial one-carbon metabolism is that this pathway supplies the cytoplasm with the largest source of formate for purine biosynthesis in rapidly dividing cells. As a result, maintenance of the mitochondrial one-carbon metabolism pathway is important feature of proliferating cells, including cancer cells. One-carbon fuels such as serine and glycine can enter the mitochondrial pathway through *SHMT2* reaction (Tibbetts and Appling, 2010). In addition, glycine can be catabolized in the mitochondria using the glycine cleavage system (*GCS*), to yield a second 1C unit of 5,10-methylene THF (Tibbetts and Appling, 2010). The mitochondrial pathway in liver mitochondria can remethylate homocysteine through choline metabolism, in which choline is converted to betaine, which enters the methionine synthase reaction to generate methionine and dimethylglycine, another precursor to glycine (Tibbetts and Appling, 2010). Given its link to choline metabolism, the methionine cycle is used to create phosphatidylcholine, a major contributor of the lipid membranes (Locasale, 2013). Mitochondrial 10-formylTHF is also used as a substrate for methionyl-tRNA formyltranferase to produce fMet-TRNA, the initiator tRNA for mitochondrial protein synthesis (Li et al., 2000).

1.2.7.2 ONE-CARBON METABOLISM IN CANCER

Many emerging genetic and functional studies have established the importance of one-carbon metabolism as well as the serine/glycine biosynthesis in driving tumourigenesis (DeBerardinis, 2011). Genes such as *DHFR* and *TYMS* are frequently overexpressed in cancer and are targets of several chemotherapeutic drugs (Huennekens, 1994) (Longley et al., 2003). Enzymes of mitochondrial one-carbon metabolism, such as MTHFD2, which are normally low or absent in normal adult tissues, are highly upregulated in cancer, such as breast, colon, and AML cancers, and are negatively correlated with survival in patients (Nilsson et al., 2014) (Lehtinen et al., 2013) (Miyo et al., 2017) (Pikman et al., 2016). A recent report showed that patients with high expression of mitochondrial one-carbon metabolism genes have shorter overall survival rate compared to patients with low expression of these genes (Koseki et al., 2018) Interestingly, the production of serine is also frequently upregulated in cancer, as *PHGDH* has found to upregulated in triple-negative breast cancer and melanoma (Locasale et al, 2011) (Possemato et al., 2011). Similarly, SHMT2 has been shown to be essential for tumour survival (Lee et al., 2014), and both SHMT2 and the consumption of glycine also correlate with cancer cell proliferation and poor prognosis (Jain et al, 2012) (Kim et al, 2015). The glycine cleavage system (GLDC) is also increased in cancer (Woo et al., 2018). In addition, expression of both serine biosynthesis and the mitochondrial one-carbon metabolism pathway can be driven by ATF4, which is activated by the mTORC1 signalling (Ben-Sahra et al., 2016). As the mitochondrial one-carbon metabolism pathway produces the bulk of formate for nucleotide biosynthesis (Ducker et al., 2016), upregulation of this pathway is important to meet the proliferative demands of cancer cells.

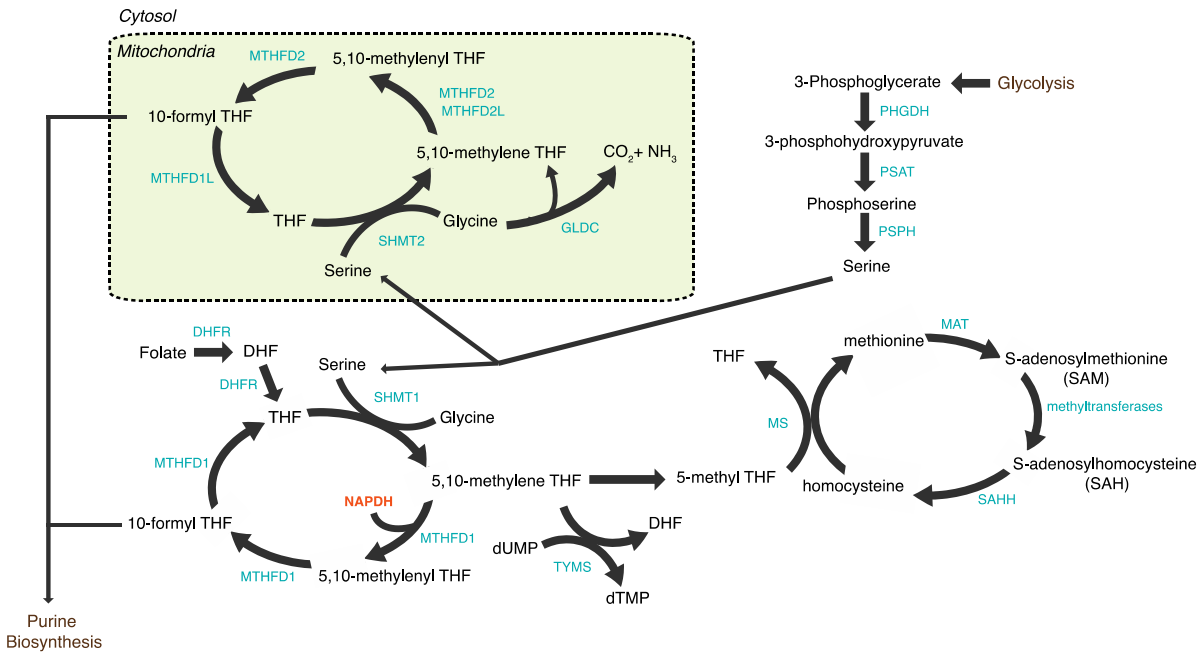

Figure 1.5: One-carbon metabolism directs nutrients for numerous cellular processes. The serine generated from glycolysis drives folate-based reactions that deliver one-carbon units for purine biosynthesis, methylation reactions, and NADPH production. One-carbon metabolism is compartmentalized in the cytosol and mitochondria, where the mitochondrial pathway is responsible for providing one-carbon units from the catabolism of both serine and glycine. Enzymes are in green.

1.2.8 THERAPEUTIC APPROACHES TO TARGET ONE-CARBON METABOLISM

The importance of one-carbon metabolism in cancer was initially recognized over 60 years ago. Sydney Farber had noted that folic acid could induce the proliferation of acute lymphoblastic leukemia (ALL) cells, and investigated whether perturbation of its metabolism could inhibit cancer proliferation (Farber et al., 1947). In a landmark paper in 1948, Sydney Farber and colleagues discovered that treatment of patients with a folic acid antagonist, aminopterin, produced temporary remission in children with acute lymphoblastic leukemia (ALL) (Farber and Diamond, 1948). This finding is among the first that spearheaded the development of the first class of chemotherapeutics to treat cancer, called antimetabolites (or

antifolates). This class of therapeutics is similar in structure to natural folates and thus competes with them for binding enzymes of the folate cycle and nucleotide biosynthesis (Shuvalov et al, 2017). Following the landmark study, aminopterin was replaced with a structural analog called methotrexate (MTX) (also known as amethopterin), which was more effective and less toxic. MTX is still being used as frontline chemotherapy for a diverse set of cancers, including acute lymphoblastic leukemia, breast cancer, bladder cancer, lymphomas, among others (Chabner and Roberts, 2005).

The sensitivity of MTX is dependent on its bioavailability in cells and expression of its target genes. MTX is uptaken by the low affinity reduced folate carrier (RFC) which also transports natural folates into the cell (Wong et al., 1995). Upon entry, polyglutamate chains are added to methotrexate, as well as natural folates, via the enzyme folypolyglutamyl synthetase (FPGS) (Chabner et al, 1985). The addition of these groups increases the half-life of methotrexate to improve its retention in cells (Chabner et al, 1985). The main enzymatic target of MTX is dihydrofolate reductase (DHFR), an enzyme required to produce tetrahydrofolate (THF) for one-carbon reactions (Hitchings and Burchall, 1965). MTX also inhibits ATIC and TYMS, which are enzymes of the purine and pyrimidine biosynthesis pathways respectively (Chabner et al, 1985). Inhibition of ATIC blocks the production of de novo purines, leading to an accumulation of AICAR, while inhibition of TYMS results in reduced thymine production, which is toxic to actively dividing cells (Genestier et al., 2000). Thus, MTX can inhibit cell proliferation by targeting one-carbon mediated nucleotide biosynthesis.

Furthermore, the development of resistance remains as one of the greatest challenges facing oncology. Resistance to MTX can occur through several mechanisms including increased

efflux of the drug through the P-glycoprotein (Pearce et al., 1989), decreased ability of cells to add polyglutamate groups to MTX (Chabner et al, 1985), and alteration or overproduction of DHFR (Dicker et al., 1993). The expression of other genes including TYMS (Sorich et al., 2008), and the mitochondrial one-carbon metabolism genes MTHFD2 and SHTM2 also correlate with efficacy of MTX (Vazquez et al, 2013). The development of therapies that alter the function of these targets may help improve the response to methotrexate.

In addition, 5-flurouracil (5-FU) is an antimetabolite that is the standard of care for many cancers, including late stage colorectal cancer and breast cancer (Spears et al., 1982). 5-FU acts as a structural mimic of uracil and inhibits TYMS, thereby preventing the methylation of dTMP from dUMP (Spears et al, 1982). In addition, gemcitabine is an antifolate that is used to treat pancreatic cancer patients, by inhibiting the biosynthesis of cytidine and disrupting ribonucleotide reductase (RNR), preventing the production of deoxynucleotides (Heinemann et al, 1995). Although antifolates can be used as a solo agent, such as MTX to treat choriocarcinoma (Hertz and Spencer, 1956), most are used in combination. One such example is the combination of methotrexate with cyclophosphamide and 5-fluorouracil as part of the CMF regime to treat breast cancer (Munzone et al., 2012. Despite its wide use as cancer therapeutics, antifolates can have high toxicity by targeting metabolic enzymes found in both transformed and non-transformed cells, which reduces its therapeutic index (Howard et al, 2016) (Tennant et al, 2010). As a result, the identification of cancer-specific metabolic activity, as well as determining the global metabolic effects caused by antifolates are required to provide molecular basis for designing more effective therapeutic strategies to treat cancer.

1.3 BREAST CANCER: MOST COMMON CANCER AMONG CANADIAN WOMEN

Breast cancers are the third most commonly diagnosed malignancy in Canada, accounting for 13% of all cancers, and is also the most commonly diagnosed cancer among women (Canadian Cancer Statistics Advisory Committee, 2018). Breast cancer is classified based on the expression of hormone receptors such as the estrogen receptor (ER), progesterone receptor (PR), and the human epidermal growth factor receptor 2 (HER2). Through the use of gene expression profiling, breast cancers have been divided into 5 subtypes: luminal A, luminal B, basal, claudin low, and HER2 amplified.

Luminal breast cancers display gene expression profiles similar to those of normal luminal cells, and is subdivided into luminal A, which typically is positive for ER and PR, but negative for HER2 (ER+, PR+, HER2-) and luminal B, which is typically positive for ER and PR, but can vary for HER2 (ER+, PR+, HER2-/+) (Eroles et al. 2012). Luminal breast cancers are the most common subtype and are considered to be relatively well-responsive to treatment, as they respond to targeted receptor-targeted hormonal therapy (Eroles et al. 2012). The basal-like subtype displays gene expression profiles similar to normal basal cells, and includes triple negative breast cancers (ER-, PR-, HER2-) (Eroles et al. 2012). Due to the absence of these markers, these cancers do not respond to targeted therapy, limiting their treatment options to chemotherapy, and generally have the worse prognosis (Eroles et al. 2012). The claudin-low subtype is also generally triple negative for ER, PR, and HER2, but express E-Cadherin, Claudin, which are used for junction formation and adhesion (Dias et al. 2017) and genes involved in epithelial-to-mesenchymal transition (EMT) (Eroles et al. 2012) Like the basal

subtype, these cancers have limited treatment options and have very poor prognosis (Prat et al. 2010).

The HER2 subtype include cancers that are ER-, PR-, HER2+ (Eroles et al., 2012). HER2 or ErbB2 belongs to the epidermal growth factor receptor (EGFR) family of receptor tyrosine kinases (Dittrich et al., 2014). Activation of HER2 involves the activation of its kinase domain by either dimerization or interaction with another EGFR family member, causing autophosphorylation on its C-terminal (Lemmon, 2009)(Dittrich et al., 2014). The phosphorylated C-terminal acts as a docking site for ligands such as PI3K and Ras/MAPK, which activate signalling cascades important for cellular proliferation and survival (Dittrich A. et al., 2014). As such, *HER2* is classified as an oncogene, and HER2 cancers are known to be aggressive, but can be treated using targeted therapy, such as the inhibitory monoclonal antibody Trastuzumab (Herceptin) which impedes HER2 activity (Tong et al., 2018).

One characteristic of HER2/ErbB2 is that it activates PI3K/Akt signalling, which upregulates glycolysis (Menendez, 2010). ErbB2 expression enhances glucose uptake, the pentose phosphate pathway, and fatty acid oxidation (Deblois et al., 2010)(Schafer et al., 2009), and ErbB2 levels are regulated by glucose availability (Klimcakova et al., 2012).

1.4 SIGNALLING PATHWAYS IN CANCER

1.4.1 PI3K/Akt/mTOR SIGNALLING

PI3K/Akt/mTOR pathway is a major signalling cascade normally involved in cell proliferation and growth in response to hormones or growth factors. As such, cancer exploits this pathway to fulfill its proliferative demands as mutations in this pathway are found in many cancers (Thorpe et al., 2015). The phosphoinisitide 3 kinase (PI3K) is activated by receptor tyrosine kinases (RTK) on the cell surface in response to the binding of a hormone or growth factor (Vivanco and Sawyers, 2002). PI3K also responds to the constitutive activation of HER2 as is found in breast cancer. Upon activation, PI3K phosphorylates PIP2 to PIP3, which activates a signalling cascade that activates the protein kinase B (Akt) (Vivanco and Sawyers, 2002). The tumour suppressor PTEN is a lipid phosphatase that converts PIP3 to PIP2 and inhibits Akt (Chen et al., 2018). Akt controls a signalling axis that promote cell survival and proliferation and activate several glycolytic enzymes (Elstrom et al., 2004) (Plas and Thompson, 2005)(Jones and Thompson, 2009).

In addition, Akt is linked to the mammalian target of rapamycin (mTOR), a signalling cascade involved in several biological functions, including anabolic pathways such as protein synthesis, to drive growth and proliferation (Laplante and Sabatini, 2012) (Morita et al., 2015). Akt activates mTOR by inhibiting its negative regulator, the tuberous sclerosis complex 2 (TSC2) (Inoki et al., 2002). mTOR exists as two complexes: mTORC1(which includes the binding partner RAPTOR) (Hara et al., 2002) and mTORC2 (which includes the binding partner RICTOR) (Sarbassov et al., 2004). mTORC1 induces protein synthesis in large part by activating the ribosomal protein S6 kinase (S6K) and inhibiting the eukaryotic initation factor 4E binding

protein (4EBP), an inhibitor of eukaryotic translation initiation factor 4E (EIF4E) (Roux and Topisirovic, 2012). In addition, mTORC1 can activate lipogenesis through SREBP (Duvel et al., 2010; Zhu et al., 2013). mTORC1 can also increase pyrimidine biosynthesis through the phosphorylation of CAD by S6K (Ben-Sahra et al., 2013) and purine biosynthesis though the activation of MTHFD2 expression through ATF4 (Ben-Sahra et al., 2016). In terms of catabolic pathways, mTORC1 can activate glycolysis through HIF-1α (Dodd et al., 2015), and glutaminolysis by inhibiting SIRT4 to promote the activity of glutamate dehydrogenase (Csibi et al., 2013). mTORC1 controls mitochondrial functions by promoting the translation of nuclear-encoded mitochondrial genes through inhibition of 4EBP (Morita et al., 2013). As a result, the PI3K/Akt/mTOR signalling pathway can modulate several metabolic pathways needed by cancer cells to meet their high proliferative demands.

1.4.2 HIF-1α

The hypoxia-inducible factor 1 (HIF-1α) is a transcription factor that activates gene expression pertinent to enhancing cell survival under hypoxic conditions (Semenza, 2011). HIF-1α activates several glycolytic genes, notably *HK2* and *LDHA*, and increases glucose uptake by activating *GLUT1* (Semenza, 2011). HIF-1α also increases pyruvate dehydrogenase kinase 1 (*PDK1)*, to prevent pyruvate processing in the mitochondria, and as such is an inducer of the Warburg effect (Kim et al., 2006). In addition, HIF-1α activates angiogenesis through the induction of vascular endothelial growth factor (*VEGF*) (Brahimi-Horn et al., 2007). HIF-1α protein levels are stabilized under hypoxic conditions. Under normoxia, the prolyl hydroxylase enzyme (PHD) hydroxylates HIF-1α, which is subsequently ubiquinated by the Von Hippl-

Lindau (VHL) complex to which commit HIF-1α for proteasomal degradation (Courtnay et al., 2015). However, once oxygen levels drop to hypoxic conditions, the PHD enzyme is inhibited, which prevents the degradation of HIF-1α, allowing it to be translocated to the nucleus to transcribe genes important for the hypoxic response (Courtnay et al., 2015). Cancers, such as clear cell renal carcinomas (ccRCC) with loss-of-function mutations in VHL have increased HIF-1α activity even in oxygenated conditions (Cockman et al., 2000; Zhang and Zhang, 2018).

1.4.3 MYC SIGNALLING:

Myc is a transcription factor that regulates many cellular processes from cell cycle progression, apoptosis, and metabolism. Myc activates *GLUT1* (Osthus et al., 2000) and promotes glycolysis by activating the transcription of glycolytic genes such as *HK2, PKM2,* and *LDHA*, which are widely used by cancer cells to enact aerobic glycolysis (Goetzman and Prochownik, 2018). Myc is also a strong modulator of glutamine metabolism, by increasing the expression of glutamine transporters (Wise et al., 2008) and *GLS1* (Shroff et al., 2015). In addition, Myc also increases fatty acid synthesis by targeting *ACLY* and *FASN* (Morrish et al., 2010) (Edmunds et al., 2014), and increasing nucleotide biosynthesis by targeting *CAD*, *PRPS2*, *IMPDH2*, and *RRM2* (Mannava et al., 2008). Myc also promotes the expression of *SHMT2*, which converts serine to glycine in the mitochondrial one-carbon metabolism pathway (Ye et al., 2014). In addition, Myc controls mitochondrial gene expression and biogenesis (Morrish and Hockenbery, 2014). Lastly, Myc also upregulates protein synthesis (Pourdehnad et al., 2013). Consequently, Myc activates several metabolic pathways needed to fuel tumourigenesis.

1.4.4 p53 SIGNALLING

p53 is a well characterised tumour suppressor, which is mutated in almost half of all cancers (Hainaut and Pfeifer, 2016). When cells are exposed to DNA damage, p53 is activated by the ATM kinase and modulates cell cycle arrest, through the activation of p21, which blocks the activity of CDK-cyclin complex (Kleinsmith, 2006). Concurrently, p53 activates DNA repair enzymes to mend damaged DNA (Kleinsmith, 2006). During energetic arrest, p53 is phosphorylated and activated by AMPK leading to cell cycle arrest (Jones et al., 2005). If the DNA damage could not be repaired, p53 causes apoptosis, by activating the p53 upregulated modulator of apoptosis (PUMA), which represses Bcl-2, the inhibitor of apoptosis, leading to programmed cell death (Kleinsmith, 2006). Given its role in mediating DNA repair, mutations in p53 cause cells to accumulate damaged DNA, which can unleash tumorigenesis (Courtnay et al., 2015).

In addition, p53 controls many aspects of cellular metabolism. p53 represses the expression of *GLUT1* to block glucose uptake (Kawauchi et al., 2008), and induces *TIGAR* to inhibit glycolysis (Bensaad et al., 2006). p53 also promotes the catabolism of pyruvate and glutamate into the mitochondria by regulating *PDK2* and *GLS2* (Hu et al., 2010; Suzuki et al., 2010). In addition, p53 promotes OXPHOS through the regulation of *SCO2* and *AIF1* (Matoba et al., 2006). As a result, p53 signalling also opposes the Warburg Effect in cancer cells to limit tumorigenesis (Labuschagne et al., 2018).

1.4.5 AMPK: THE GATEKEEPER OF ENERGY BALANCE

The AMP-activated protein kinase (AMPK) is an evolutionary-conserved, heterotrimeric serine/threonine kinase that is instrumental in controlling the energy-sensing of the cell. The AMPK complex includes an α catalytic subunit, and a β submit and γ subunit used for regulatory functions (Hardie, 2018). AMPK is activated in a response to metabolic stress and is inhibited when cellular energy is plentiful. Specifically, AMPK is sensitive to adenylate charge, which is determined by the levels of AMP, ADP, and ATP (Hardie et al., 2011). When cellular ATP levels are high, ATP binds to the γ subunit, thereby inhibiting the enzyme (Hardie et al., 2011). In contrast, when the cell undergoes metabolic stress and must maintain ATP levels, the levels of ADP as a by-product of ATP-consuming processes rise along with the levels of AMP from adenylate kinase reactions (Hardie, 2018). Both AMP and ADP can bind the γ subunit, activating the signalling cascade that is coordinated towards promoting and preserving ATP levels (Hardie, 2011). The activation of AMPK also requires phosphorylation by an upstream kinase, which includes LKB1, calmodulin-dependent protein kinase kinase β (CAMKKβ), and TGF-β-activated kinase 1 (TAK-1) (Hardie et al., 2012).

Recently, it has been shown that AMPK can sense glucose availability using mechanisms independent of adenylate charge. In the presence of glucose, the glycolytic intermediate F1,6BP prevents AMPK activation by binding to aldolase/V-ATPase/Ragulator complex, which dissociates from the AXIN-LKB1 complex in lysosomes (Zhang et al., 2017). Upon glucose deprivation, the absence of F1,6BP causes the aldolase/V-ATPase/Ragulator complex to bind the Axin-LKB1 complex, allowing for LKB1-mediated activation of AMPK (Zhang et al., 2017). The importance of F1,6BP is that it is the rate-limiting product of the PFK1 reaction and an

allosteric activator of PK. Thus, the presence of F1,6BP indicates glucose flux is committed through glycolysis, and a shortage may reduce PK activity (Hardie, 2018). AMPK can also sense mitochondrial ROS and trigger a PGC-1α-dependent antioxidant response (Rabinovitch et al., 2017).

In addition, AMPK promotes energy homeostasis by inhibiting ATP-consuming processes, such as lipid and protein synthesis. AMPK phosphorylates and inhibits the ACC1/ACC2, the rate-limiting step of fatty acid biosynthesis (Davies et al., 1990) (Merrill et al., 1997)and inhibits SREBP-1 (Yang et al., 2009), an activator of lipogenesis genes like FASN. AMPK also inhibits the mTORC1 regulatory subunit Raptor (Gwinn et al., 2008) and activates the Tuberous Sclerosis Complex 2 (TSC2) (Inoki et al., 2003), which inhibits mTOR signalling, leading to decreased protein synthesis. In addition, AMPK maintains ATP levels by promoting catabolic reactions such as lipid oxidation, glycolysis, autophagy and cellular respiration. Given the repression of ACC, the decreased production of malonyl-CoA alleviates repression of CPT1, allowing for increased fatty acid oxidation (Merrill et al. ,1997). AMPK can also phosphorylate PFK2 in heart tissue to increase glycolysis (Marsin et al., 2002). Furthermore, AMPK phosphorylates and activates PGC-1α, a master orchestrator of mitochondrial metabolism and mitochondrial biogenesis, which increases cellular respiration (Jager S. et al. 2007)(Canto et al., 2009). AMPK also regulates autophagy through the phosphorylation of Unc-51 like (ULK) kinases, to remove damaged organelles such as mitochondria (Egan et al., 2011). Thus, AMPK coordinates signalling cascades to preserve ATP levels.

1.4.5.1 AMPK IN CANCER

Given its ability to combat metabolic stress, the activity of AMPK has been a subject of interest in cancer research. AMPK is situated within a pathway of tumour suppressors, including its upstream kinase LKB1, and its downstream target TSC2 (Faubert et al., 2015). LKB1 or liver kinase B1 is a serine/threonine kinase acts as a regulator of cell growth and metabolism, in which AMPK acts as its important effector (Alessi et al., 2006; Shaw et al., 2004). LKBI mutations are found in 30-40% of non-small cell lung cancers (Sanchez-Cespedes et al., 2002) and in 20% of cervical cancers (Wingo et al., 2009). Mutations in LKB1 causes Peutz-Jegers syndrome, which is an inherited cancer predisposition syndrome that leads to the development of hamartomatous polyps in the intestine (Hemminki, 1999). TSC2 is a tumour suppressor, whose inactivation leads to tuberous sclerosis, and blocks protein synthesis by inhibiting mTOR (Brugarolas et al., 2003). AMPK also phosphorylates and stabilizes the tumour suppressor p53 causing cell cycle arrest (Jones et al., 2005) In view of its proximity to several tumour suppressors, AMPK signalling appears to act as a metabolic tumour suppressor (Faubert et al., 2013) (Rehman et al., 2014). However, in contrast to these signalling partners, there is little evidence of AMPK mutations, which can partly be due to the redundancy of AMPK isoforms. AMPK can have either of two α subunits (*PRKAA1*, *PRKAA2*), two β subunits (*PRKAB1, PRKAB2*) and three γ subunits (*PRKAG1, PRKAG2, PRKAG3*), but the expression of these subunits varies between tissue types (Ross et al., 2016). Thus, AMPK complexes can be formed using 12 different combinations (Ross et al., 2016). Nevertheless, the mutation rate of AMPK is so low and there is no evidence of AMPK mutations predisposing tumour growth (Liang et al., 2013). This is in line with reports demonstrating that AMPK loss alone does not cause tumorigenesis, although AMPK loss can assist growth of Myc-induced lymphomas (Faubert et al., 2013).

AMPK activity is decreased in several cancers, including breast cancer (Hadad et al., 2008), hepatocellular carcinoma (Lee et al., 2012). In melanoma, mutant B-RAF V600E can promote an ERK-dependent inhibition of LKB1, which decreases AMPK activity (Zheng et al., 2009). AMPK is also inhibited in PTEN-deficient thyroid cancer (Antico Arciuch et al., 2013). In addition to p53, AMPK also regulates cyclin dependent kinase (CDK) inhibitors p21WAF1 and p27CIP1 to stabilize p27 to inhibit proliferation (Liang et al., 2007). Due to the inhibition of metabolic and signalling pathways involved in modulating cell growth, proliferation, and stress responses, AMPK appears to play an anti-tumorigenic role (Rehman et al. 2014). This is supported by studies showing loss or reduced AMPK activity promotes a HIF-1α-dependent aerobic glycolytic shift that fuels tumourigenesis (Faubert et al. 2013). In addition, several studies using AMPK agonists such as AICAR and A769662 show decreased cell proliferation in vitro (Cool et al., 2006; El-Masry et al., 2012; Swinnen et al., 2005; Theodoropoulou et al., 2010) and reduced tumour growth in vivo (Huang et al., 2008).

Conversely, the ability to respond to metabolic stress is important for promoting cell survival. By rewiring cellular metabolism to maintain energy homeostasis, AMPK provides metabolic flexibility to cope with energetic pressure, such as the promoting fatty acid oxidation, generating NADPH through the pentose phosphate pathway to combat reactive oxygen species (ROS) (Jeon et al., 2012; Jeon and Hay, 2012), and inducing autophagy (Kim et al., 2011). Thus, AMPK activation may also provide a selective advantage to tumour cells seeking to survive under stressful conditions, such as glucose limitations. Indeed, several studies indicate that AMPK promotes prostate cancer and glioblastoma survival and growth (Frigo et al., 2011; Godlewski et al., 2010; Park et al., 2009; Tennakoon et al., 2014). Consequently, AMPK can provide the tools needed to produce pro- and anti-tumorigenic effects. Whether AMPK produces

positive or negative effects could be dependent on cell type, the presence and activity of oncogenes and tumour suppressors, as well as extracellular environmental conditions.

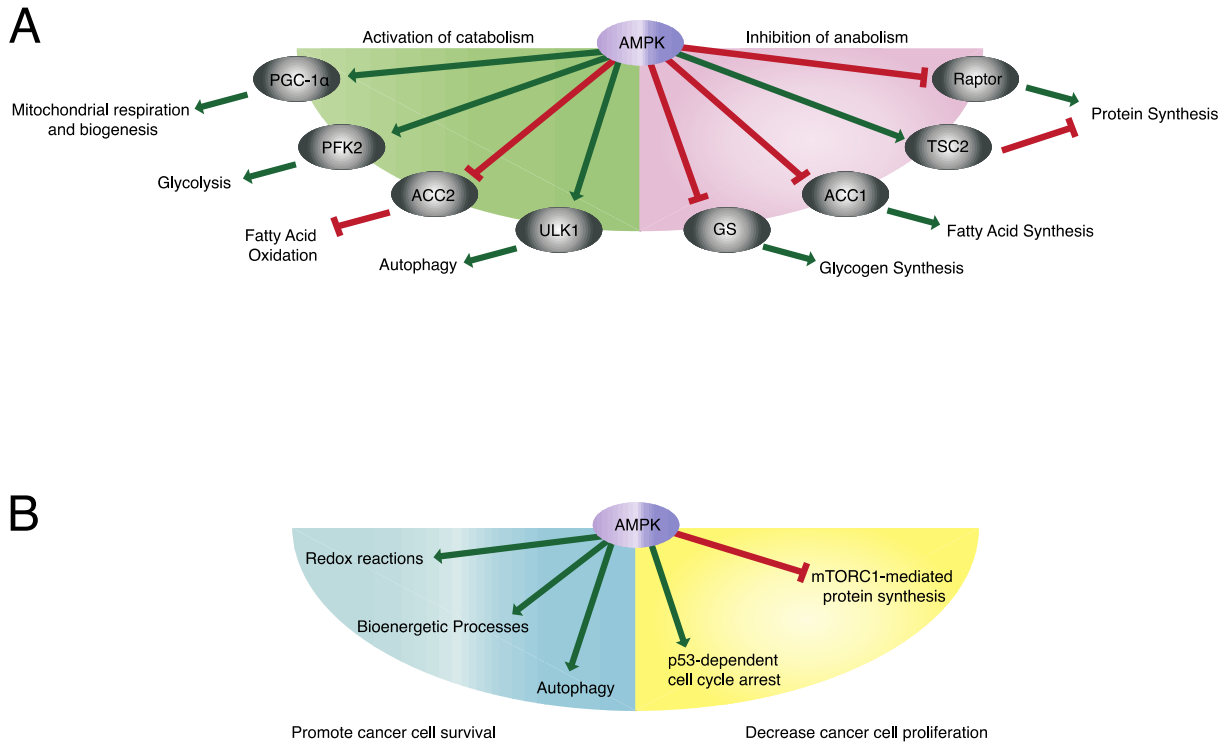

Figure 1.6: AMPK regulates cellular and bioenergetics processes to control energy homeostasis. A. AMPK activates catabolic pathways (green box) and inhibits anabolic pathways (red box). AMPK can acts an activator (green arrow) or inhibitor (red line) of downstream effectors. B. AMPK has both pro-growth (blue box) and anti-growth (yellow) properties in cancer. The balance between factors will ultimately determine the outcome of AMPK activation in cancer.

1.4.6 PGC-1s: TRANSCRIPTIONAL ORCHESTRATORS OF METABOLISM

Cells need to coordinate metabolic programs to maintain energy homeostasis. The peroxisome proliferator-activated receptor gamma coactivator 1 (PGC-1s) are a family of transcriptional coactivators that act as central regulators of metabolism. The family consists of PGC-1α, PGC-1β, and the PGC related coactivator (PRC). The most studied member, PGC-1α, was originally discovered during a screening experiment for proteins that interact with PPARγ (Puigserver et al., 1998). PGC-1α was initially identified in brown fat tissue as a transcriptional coactivator driving mitochondrial function and adaptive thermogenesis (Puigserver et al. 1998). The other two members of the family, PGC-1β and PRC were discovered based on sequence homology (Kressler et al., 2002; Lin et al., 2002). PGC-1β activates mitochondrial biogenesis and respiration (Lin et al., 2003; St-Pierre et al., 2003), as well as lipogenesis in liver (Lin et al., 2005) and activates the formation of oxidative type IIX fibres in muscle (Arany et al., 2007). Furthermore, PRC regulates the expression of the respiratory chain (Vercauteren et al., 2009) and is involved in cell cycle progression (Andersson and Scarpulla, 2001). Collectively, the PGC-1 family is involved in regulating mitochondrial metabolism.

PGC-1α controls a wide network of metabolic functions. PGC-1α is instrumental in controlling cellular bioenergetics, through the activation of glycolysis, the CAC, and OXPHOS, leading to biological functions such as increased cellular respiration and mitochondrial biogenesis (Handschin and Spiegelman, 2006). In particular, PGC-1α is uniquely involved in increasing the contribution of respiration to proton leak reactions, known as uncoupled respiration (St-Pierre et al. 2003). In relation to increased OXPHOS, PGC-1α coordinates ROS detoxification response through superoxide dismutase 2 (SOD2) and glutathione S-transferase

(GSDM1) regulation in neurogenerative disease (St-Pierre et al., 2006). In addition, PGC-1α appears to play a dual role based on its nutrient conditions. Under nutrient deprivation, PGC-1α can promote the catabolism of other fuels, such as β-oxidation (Tabata et al., 2014). However, conditions of abundant nutrients, PGC-1α can promote lipogenesis (Lin et al. 2005) (Bhalla et al., 2011). PGC-1α can also support gluconeogenesis in liver (Cao et al., 2005; Lustig et al., 2011) and can promote angiogenesis through VEGF (Arany et al., 2008). Furthermore, PGC-1α can regulate purine biosynthesis through inhibition of one-carbon metabolism (Audet-Walsh et al., 2016). Importantly, glucose also increases the uptake of glucose (Michael et al., 2001) and glutamine (McGuirk et al., 2013). As a result, PGC-1α controls both catabolic and anabolic functions to maintain energy homeostasis.

The PGCs are a family of transcriptional coactivators. To induce transcription, the N terminal half of the PGCs contain a several LXXLL motifs, that are used to dock transcription factors. PGC-1 can interact with several transcription, including PPARγ, NRF-1/2, GABP/A, YYI, among others (Luo et al., 2016). PGC-1α works with NRF-1 and NRF2 to regulate the mitochondrial transcription factor A (TFAM) to regulate mitochondrial biogenesis (Wu et al., 1999). However, the most well characterized transcription factors that interact with the PGC-1s are the estrogen-related receptors (ERRs) (Huss et al., 2002)(Deblois et al., 2012). Several studies show a functional codependency between the PGC-1s and the ERRs for the ability to control the expression of metabolic genes (Deblois et al, 2012) (Sonoda et al., 2007). Together, the PGC-1s and ERRs orchestrate the programming of cellular metabolism to support growth of cells and to direct metabolic programs necessary for cell differentiation and to maintain cellular energy homeostasis (Deblois et al. 2012).

The activity of the PGC-1/ERR signalling are subject to various physiological and pathological stresses. The activity of the PGC-1α/ERRα transcriptional axis is controlled by modulating its own expression (Mootha et al., 2003) as well as by posttranslational modifications which can modify both of its expression and nature of its interactions (Fernandez-Marcos and Auwerx, 2011)(Lustig et al., 2011) (Adamovich et al., 2013) (Gravel, 2018). The energy-sensor AMPK phosphorylates PGC-1α and modulates the expression of PGC-1α/ERRα signalling (Jäger et al., 2007)(Audet-Walsh et al., 2016). PGC-1α can also be modified by other factors, which either increase or decrease its activity (Austin and St-Pierre, 2012). Phosphorylation by p38MAPK increases its activity towards mitochondrial genes (Puigserver et al., 2001), while deacetylation by SIRT1 increases expression of gluconeogenesis genes (Rodgers et al., 2005), and methylation by PRMT1 increases the expression genes involved in mitochondrial biogenesis (Teyssier et al., 2005). Conversely, PGC-1α activity is decreased upon phosphorylation by CLK2 (Rodgers et al. 2010) and Akt (Li et al., 2007), which inhibit gluconeogenesis. Phosphorylation by S6 kinase also decreases gluconeogenetic gene expression, but maintains mitochondrial gene expression (Lustig et al., 2011). Acetylation by GCN5 (Lerin et al., 2006) and SUMOylation by SUMO1 (Rytinki and Palvimo, 2009) both inhibit the transcriptional activity of PGC-1α, while GSK3B phosphorylation designates PGC-1α for proteasomal degradation (Olson et al., 2008). As a result, the activity of PGC-1α is subject to tight regulation through post-transcriptional regulation. This thesis will explore the metabolic functions governed by PGC-1α/ERRα signalling and their role in cancer, with an emphasis on their regulation by AMPK signalling.

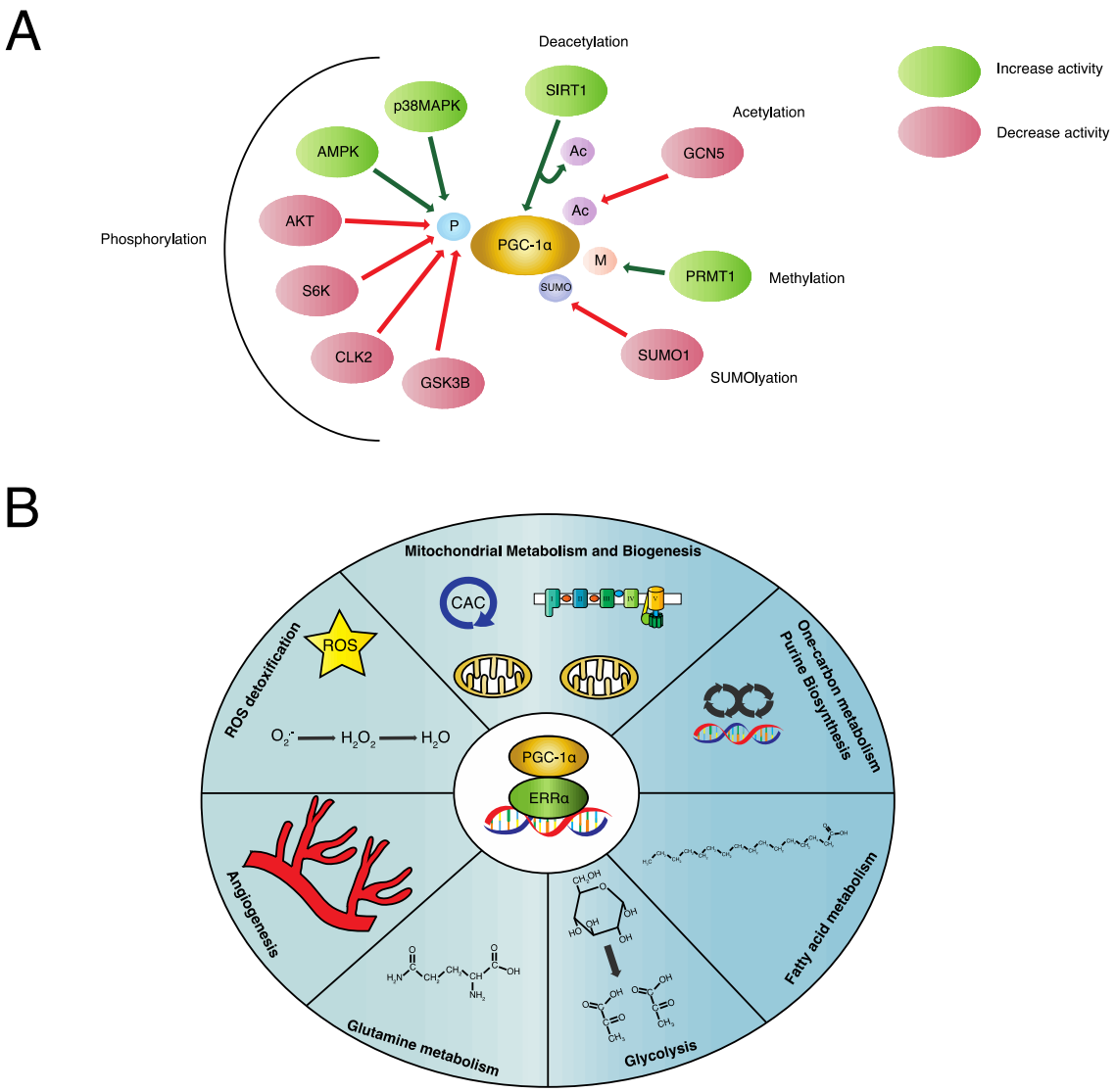

Figure 1.7: PGC-1α orchestrates cellular metabolism and responds to environmental cues. A. The activity of PGC-1α is regulated by post-translational modifications such as phosphorylation, deacetylation, acetylation, methylation, and SUMOylation at different sites. Regulators in green activate PGC-1α activity, while those in red inhibit its activity. B. The PGC-1α/ERRα axis controls the expression of genes involved in metabolic pathways such as glycolysis, mitochondrial metabolism (CAC, OXPHOS, biogenesis), glutamine metabolism, fatty acid metabolism and one-carbon metabolism, and regulates genes involved in ROS detoxification and angiogenesis.

1.4.6.1 PGC-1α IN CANCER

Metabolic perturbations in cancer cells are required to meet their bioenergetic and biosynthetic demands. In accordance with the role of PGC-1 in controlling the metabolic networks that fuel bioenergetics, as well as catabolic and anabolic metabolism, it is not surprising that this family of transcriptional coactivators is linked to tumorigenesis. However, given its dynamic nature, its regulation by transcriptional and posttranscriptional mechanisms, and the nutrient conditions of the tumour microenvironment, PGC-1α plays an intricate role in cancer. Accordingly, the expression profile of PGC-1α in cancer is variable. PGC-1α expression is decreased in breast cancer (Jiang et al., 2003) (Watkins et al., 2004), colon cancer (Feilchenfeldt et al., 2004), ovarian cancer (Zhang et al., 2007), and liver cancer (Ba et al., 2008). Conversely, PGC-1α expression is increased in endometrial (Cormio et al., 2009), renal cancers (Klomp et al., 2010), and prostate cancer (Shiota et al., 2010). In addition, the link between PGC-1α and prognosis is also variable. Low levels of PGC-1 are associated with poor outcome in breast, prostate and VHL-deficient clear renal cell carcinoma (Jiang et al., 2003) (LaGory et al., 2015) (Torrano et al., 2016). High levels are associated with poor outcome in melanoma, breast and prostate cancer (Haq et al., 2013) (Vazquez et al., 2013) (LeBleu et al., 2014) (Li et al., 2016). These heterogeneous effects of PGC-1α in cancer are due to the execution of metabolic programs, which under different oncogenic and nutrient environments, can produce pro and anti-tumorigenic effects.

In cancer, the PGC-1/ERR axis is influenced by oncogenic signals and is exploited for the coordination of metabolic programs that fuel cell growth and proliferation. Although it is reported that PGC-1α is reduced in most breast cancers, PGC-1α is highly expressed in HER2+

and triple-negative breast cancer subtypes (McGuirk et al. 2013). In accordance, PGC-1α can promote ErbB2 tumour growth and angiogenesis (Klimcakova et al. 2012). PGC-1α, along with ERRα, can also regulate glutamine metabolism and promote reductive carboxylation of glutamine to lipogenesis in HER2+ breast cancer (McGuirk et al. 2013). Given the multitude of bioenergetic options conveyed through PGC-1α signalling, PGC-1α can induce bioenergetic capacity and fuel flexibility, providing a bioenergetic advantage which supports breast cancer metastasis (Andrzejewski et al., 2017).

The heterogeneous nature of PGC-1α is also observed in melanoma, prostate cancer, colorectal cancer, and renal cancer. Reports show that the melanocyte lineage specification transcription factor (MITF) a transcription factor that is upregulated in 30% of melanomas (Garraway et al., 2005), activates PGC-1α signalling including increased mitochondrial biogenesis, respiration, and ROS detoxification among others (Haq et al. 2013). However, another subset of melanoma activates BRAF, which suppresses MITF/PGC-1α signalling, promoting a shift to glycolysis (Vazquez et al., 2013). In prostate cancer, PGC-1α promotes OXPHOS and mitochondrial biogenesis in androgen-dependent cancers through AMPK signalling and is overexpressed in a subset of patients (Tennakoon et al. 2014). However, other reports show that PGC-1α/ERRα axis can suppresses prostate cancer metastasis (Torrano et al., 2016). Furthermore, PGC-1α can support colon cancer growth through increased lipogenesis (Bhalla K et al., 2011), yet it also has protective effects in colorectal cancer cells by activating apoptosis (D'Errico et al., 2011a; D'Errico et al., 2011b). In renal cancers, some reports have witnessed an increase in PGC-1α expression (Klomp et al., 2010) yet others show that it is suppressed (LaGory et al., 2015). In addition while an oxidative phenotype is usually linked to decreased EMT (Sciacovelli and Frezza, 2017) (Gaude and Frezza, 2016) (Luo et al., 2016),

PGC-1α can still provide a growth advantage in vivo by modulating other pathways and offering bioenergetic flexibility. Thus, the expression and activity of PGC-1α is heterogenous in cancer. Other factors such as tumour heterogeneity and context-specific transcriptional programs are needed to determine the impact of PGC-1α in cancer (Gravel, 2018).

1.4.7 ESTROGEN-RELATED RECEPTORS (ERRs): ORPHANS LINKED TO ONCOGENESIS

The estrogen-related receptor (ERR or NR3B) is family of orphan nuclear receptors that play a critical role in regulating energy homeostasis. The ERRs were originally discovered during a cloning experiment designed at identifying receptors of steroid hormones that are structurally similar to the estrogen receptor (ERα) (Giguère et al., 1988). It includes ERRα, ERRβ, ERRγ (Tremblay and Giguère, 2007) and they are distinct from estrogen receptor as in they do not bind estrogens. Instead, ERR isoforms are needed for regulating the expression of metabolic genes (Giguère, 2008). They rely on the presence of coregulatory proteins such as the PGC-1s to help control metabolic gene expression (Schreiber et al., 2003) (Laganiere et al., 2004) (Kamei et al., 2003) (Sonoda et al., 2007).

The structure of the ERRs includes nonconserved amino terminal (NTD), a DNA-binding domain (DBD), and a ligand-binding domain (LBD) with docking sites for coregulators (Giguère V, 2008). The NTD can be controlled through post-translational modifications such as phosphorylation and SUMOylation (Giguère V, 2008). In addition, the ERRs recognize a consensus sequence TCAAGGTCA, known as the ERR response element (ERRE), and bind to this sequence as a monomer, homodimer, or heterodimer complex (Giguère V, 2008). Indeed, most ERR binding sites contain this motif (Dufour et al., 2007). The ERRs also contain

functional LBD, which can interact with coactivators such as the PGC-1s. The ERRs interact directly with PGC-1s through a sequence-specific leucine-rich nuclear receptor interacting motifs (LxxLL) found in the PGC-1 proteins (Huss et al., 2002) (Laganiere et al., 2004)(Schreiber et al., 2003). The PGC-1s have three LxxLL motifs, with motif 2 recognized by a large number of receptors, and motif 3 (LLKYL, a reverse LXXLL) interacting exclusively with the ERRs (Huss et al., 2002) (Schreiber et al. 2003).

The ERRs are widely distributed in several embryonic and adult tissues (Tremblay and Giguère, 2007), but are highly expressed in tissues of high energy demands such as heart, kidney, and skeletal muscle (Bookout et al., 2006; Dufour et al., 2011; Horard et al., 2004). The expression of ERRα is stimulated by physiological cues, such as fasting or cold induction, and is upregulated by PGC-1α (Schreiber et al., 2003)(Ichida et al., 2002)(Giguère, 2008). Most of the targets of PGC-1/ERR signalling are linked to energy metabolism. ERRα binds to the promotors of most genes involved in glycolysis, pyruvate metabolism, CAC, the components of OXPHOS, lipid, glutamine, amino acid metabolism, one-carbon metabolism, and the induction of mitochondrial biogenesis (Mootha et al., 2004)(Audet-Walsh et al., 2016)(Dufour et al., 2011)(Dufour et al., 2007) (Alaynick et al., 2007) (Sonoda et al., 2007) (Charest-Marcotte et al., 2010)(Deblois et al. 2013). In addition, mTOR can also control the transcription of ERRα target genes involved in energy metabolism such as the CAC and lipogenesis (Chaveroux et al., 2013).

1.4.7.1 ERR IN CANCER

The ERR isoforms ERRα and ERRγ also have polarizing roles in cancer, particularly in breast cancer where they have been the most studied. ERRα activity is highly expressed in breast cancer (Ariazi et al., 2002; Fradet et al., 2011; Heck et al., 2009; Jarzabek et al., 2009), colorectal

cancer (Cavallini et al., 2005), ovarian cancer (Fujimoto et al., 2007), and prostate cancer (Stein and McDonnell, 2006). The expression of ERRα is inversely correlated with good prognostic markers ER and PR, but is positively correlated with ErbB2 (Ariazi et al., 2002). ERRα is also associated with markers of recurrence, such as the Myc oncogene and the proliferation marker Ki-67 (Jarzabek et al., 2009) (Chang et al., 2011). Thus, ERRα acts as an unfavourable marker in breast cancer.

In contrast, ERRγ also shows high expression in some breast cancers, but is positively correlated with good prognostic markers, ER and ERBB4, as well as lymph-node negative status (Ariazi et al. 2002) (Ijichi et al., 2011). Consequently, ERRγ is considered a favourable marker in breast cancer. ERRγ can also be found in ovarian cancers, but its expression is linked to increased survival in patients (Sun et al., 2005), and is downregulated in prostate cancer (Audet-Walsh E. et al. 2017)(Cheung et al., 2005) and medulloblastoma (Lucon et al., 2013).

In cancer, ERRα binds to metabolic genes linked to cancer development such as *LDHA*, *PGM1*, *PFKM* of glycolysis, mitochondrial metabolism (*SDHB, IDH1, IDH2*), OXPHOS (*COX1*), amino acid metabolism (*PHGDH, GLS2*), lipid synthesis (*ACLY, FASN*), and one-carbon metabolism/purine biosynthesis (Deblois et al., 2009) (Cervera et al., 2008)(Audet-Walsh et al., 2016)(Deblois et al., 2012). Genes regulated by PGC-1/ERR are associated with shorter disease-free survival in patients (Chang et al. 2011). Indeed, PGC-1β correlates with ERRα expression in breast cancer (Chang et al. 2011). Conversely, ERRγ enhances OXPHOS and inhibits the growth of xenografts (Tiraby et al., 2011). Inhibition of ERRγ by the mi378* reduces CAC gene expression and increases lactate production and cell proliferation, shifting toward the Warburg effect (Eichner et al., 2010).

Furthermore, the activity of the ERRs are linked to oncogenic signals. The PGC-1β/ERRα axis binds to the promoters of genes of the ErbB2 amplicon, which includes *ErbB2* and other genes involved in promoting mammary tumourigenesis (Deblois et al. 2011). In addition, ErbB2 signalling regulates the activity of ERRα (Ariazi et al. 2007)(Barry and Giguère, 2005). Activation of the ErbB2-Myc-PGC-1β axis triggers the expression of miR-378* which inhibits ERRγ to promote the Warburg effect (Eichner L. et al. 2010).

In addition to tumour growth, the ERRs also play a role in metastasis. ERRα, in concert with PGC-1α, activate VEGF, a factor in angiogenesis and invasion. ERRα also activates genes involved in migration and invasion, such as FGF and CXCR4 (Deblois et al. 2010). PGC-1α also increases metastasis in breast cancer (Andrzejewski et al., 2017)(LeBleu et al. 2016). In contrast, ERRγ regulates the expression of E-cadherin to promote a mesenchymal-to-epithelial transition (Tiraby et al. 2011).

Lastly, the ERRs are also linked to therapeutic resistance as ERRα promotes the survival of lapatinib-resistant cancers, hinting that inhibition of ERRα may be helpful in treating lapatininb-resistant breast cancer (Deblois et al., 2016).

1.5 REPURPOSING METABOLIC DRUGS TO TREAT CANCER: MYTH OR REALITY?

1.5.1 BIGUANIDES IN CANCER:

The anti-diabetic class of medications, known as biguanides, have received much attention as potential anti-neoplastic agents. Metformin is the most commonly prescribed medication for treating type II diabetes (Mallik and Chowdhury, 2018). The biguanide phenformin was also used to treat diabetes, but was removed from the clinic in 1994 due to side-effects of lactic acidosis (Bailey, 1993) (Heckman-Stoddard et al., 2017). Contrary to phenformin, metformin is a safe medication with a few mild side effects such as indigestion and diarrhea (Bouchoucha et al., 2011).

Biguanides are used to treat diabetes by decreasing hepatic gluconeogenesis (DeFronzo et al., 1991), and increasing insulin-mediated glucose uptake (Bailey, 1993)(Liu et al., 2016). Metformin blocks hepatic gluconeogenesis through the inhibition of mitochondrial glycerophosphate dehydrogenase, which raises cytosolic NADH and blocks incorporation of lactate into glucose (Madiraju et al., 2014). In cultured cells, metformin inhibits complex I of the electron transport chain, leading to an increase in the AMP/ATP ratio, which activates AMPK (Andrzejewski et al., 2014a; Wheaton et al., 2014). Metformin triggers many of the metabolic effects of AMPK, including increased glucose uptake, increased fatty acid oxidation, decreased hepatic glucose production, and induction of PGC-1α signalling (Suwa et al., 2006)(Audet-Walsh et al., 2016) (Dowling et al., 2007). Metformin also has AMPK-independent effects, such as the suppression of mitochondrial-dependent biosynthesis (Griss et al., 2015) and can even inhibit mTORC1 through a RAG-GTPase-dependent manner (Kalender et al., 2010).

The first indication of potential antineoplastic activity arose from epidemiological studies in diabetic patients that showed that metformin treatment was associated with reduced cancer risk (Evans et al., 2005) (Libby et al., 2009) (Decensi et al., 2010; Landman et al., 2010). These observations inspired the investigations on whether metformin has antineoplastic effects. Indeed, metformin has been shown to inhibit proliferation in vitro in breast, prostate, colon, and ovarian cell lines (Cantrell et al., 2010) (Fendt et al., 2013) (Hadad et al., 2014) (Song et al., 2012). Metformin reduces tumor incidence (Anisimov et al., 2005) and may delay tumour growth (Buzzai et al., 2007) (Wu et al., 2011) (Ben Sahra et al., 2008). Given these antineoplastic properties, metformin is being investigated in more than 150 ongoing individual clinical trials (ClinincalTrial.gov., 2018)

Phenformin has also shown antineoplastic effects in breast cancer (Guo et al., 2017), ovarian cancer (Jackson et al., 2017), hepatocellular carcinoma (Veiga et al., 2018), Pancreatic cancer (Rajeshkumar et al., 2017) and melanoma (Trousil et al., 2017). Phenformin can act as a single agent to promote tumour cell apoptosis in vivo using a K-Ras driven LKB1null lung cancer (Shackelford et al., 2013). In response to this subtype, phenformin has a larger effect than metformin on AMPK activation, apoptosis, and reduction in tumour burden (Hardie, 2013b). One explanation is that biguanides accumulate in mitochondria due to the charge gradient across the inner membrane of mitochondria (Owen et al., 2000). Although metformin enters mitochondria using the organic cation transporter (Oct1) (Fogarty and Hardie, 2010), phenformin is less dependent on Oct1 due to its greater hydrophobicity (Fogarty and Hardie, 2010).

1.5.2 SGLT2 INHIBITORS: NEW KIDS ON THE BLOCK

Most cancers rely on glycolysis and import more glucose than normal cells, a phenomenon that serves as the basis of FDG-PET scanning for cancer imaging (Ben-Haim and Ell, 2009). Most cells, including neoplasms, depend on GLUT family of glucose transporters for glucose uptake (Ancey et al., 2018), such as GLUT1(Ganapathy et al., 2009). Although most cancers cells have increased glucose uptake, normal proliferating cells such as immune cells, also greatly dependent on glucose (Chang et al. 2013). Indeed, prior attempts to develop cancer therapies that inhibit GLUT-mediated glucose uptake were not successful (Koepsell, 2017).

Recently, a new class of oral therapeutics that inhibit the sodium-glucose transporter 2 (SGLT2) was approved for treating Type II diabetes (Rosenwasser et al., 2013). Unlike biguanides which inhibit hepatic glucose production (Foretz et al., 2014)(Madiraju et al., 2018), SGLT2 inhibitors block glucose reabsorption in the renal proximal tubules, decreases blood glucose levels and increases glucose in the urine (glucosuria) (Chao et al, 2010). The SGLTs are a family of glucose transporters belonging to the solute carrier 5 A gene family, which utilize a sodium ion gradient to drive glucose transport across apical membranes of epithelial cells. The most well-known members are SGLT1 (*SLC5A1*) and SGLT2 (*SLC5A2*), which facilitate glucose transport mainly in the small intestine and kidneys respectively (Wright et al. 2017). Nearly 90% of glucose is reabsorbed in the kidney by SGLT2, and 10% by SGLT1 (Cangoz et al., 2013; Rieg et al., 2014), suggesting SGLT2 as a good target for blocking glucose reabsorption.

Phlorizin was developed as the first SGLT inhibitor, which was effective at lowering blood glucose, but caused gastrointestinal side-effects through the inhibition of intestinal SGLT1

(Bays, 2013). As a result, several SGLT2-specific inhibitors have been successfully developed and received approval for treatment of type II diabetes in several countries (Lin and Tseng, 2014). In Canada, inhibitors canagliflozin, dapagliflozin, and empagliflozin have been approved and are in wide use (Government of Canada, 2016). SGLT2 inhibitors are used as a monotherapy (DeFronzo et al., 2016)or a combinatorial therapy with other antidiabetic drugs such as metformin (Lavalle-Gonzalez et al., 2013; Nauck et al., 2011)

Although SGLT2 expression had been regarded as restricted to normal kidney, recent studies have indicated the presence of SGLT2 in brain, pancreas, liver, and prostate tumours (Scafoglio et al., 2015)(Wright et al., 2017)(Kaji et al., 2018). Unlike GLUT1 which is ubiquitously expressed, the limited expression of SGLT2 in the body has sparked interest for targeting SGLT2 for treating cancer. Indeed, there is early evidence that canagliflozin and dapagliflozin inhibit the growth of pancreatic and prostate adenocarcinomas in vivo (Scafoglio et al., 2015) and dapagliflozin inhibits the growth of colon tumours (Saito Tsugumichi, 2015). Interestingly, Kaji et al. have reported that canagliflozin can inhibit hepatocellular carcinoma cell proliferation and tumour growth by inhibiting glucose uptake (Kaji et al. 2018). Although SGLT2 expression was similar between lung carcinoma and normal lung cells, its expression was also upregulated in liver metastases from the lung (Ishikawa et al., 2001), suggesting that SGLT2 activation could provide a metabolic adaptation of cancer cells in that environment.

However, recent studies have shown that canagliflozin can still perturb proliferation of cancer cells in the absence of glucose, hinting to the possibility of alternative mechanisms to blocking glucose uptake, such as the inhibition of the electron transport chain (Hawley Simon, 2016)(Villiani et al., 2016). Recently, a report showed that SGLT2 inhibitors can also target

glutamate dehydrogenase in the kidney, which can partially explain the adverse nephrotoxic effects of these drugs in treating kidney disease (Secker et al. 2018). However, the mechanisms of action of SGLT2 inhibitors on cancer cells remain unclear. Nevertheless, given the importance of glucose transporters for cancer metabolism, targeting SGLT2 may provide an innovative strategy to blocking antineoplastic growth.

1.6 METHODOLOGY IN CANCER METABOLISM

The study of cancer metabolism involves an arsenal of tools designed to monitor and perturb metabolic pathways used by cancer cells. In addition to various genomic, transcriptomic, and proteomic methodologies, metabolic research includes the use of various metabolomic technologies to screen for individual metabolites and their tracing throughout pathways, in addition to platforms used to assess bioenergetic status. Below is a summary of some of the common methodologies used by researchers to study cancer metabolism.

1.6.1 METABOLOMICS TECHNOLOGIES

Several metabolomic technologies are used to detect metabolites in cells and tissues. Gas chromatography - mass spectrometry (GC-MS) and liquid chromatography - mass spectrometry (LC-MS) provide methods to reliably detect many classes of metabolites including amino acids, organic acids, and fatty acids. These techniques involve identifying molecules based on their elution time, mass spectra of fragmented pieces, and their specific mass-to-charge (m/z) ratios.

1.6.1.1 GC-MS: GAS CHROMATOGRAPHY – MASS SPECTROMETRY

GC-MS is a robust method that allows for the detection of many metabolites in a relatively economical manner. Compared to other methods, GC-MS requires derivatization of analytes to allow separation in the gas chromatography column (Grimm et al., 2016). Briefly, cells are quenched, processed then derivatized to make analytes more volatile (Grimm F. et al. 2016). The sample is vaporized to separate the analytes, which are pushed through a heated column by an inert gas, acting as the mobile phase (Grimm et al., 2016). The analytes are then allowed to interact with the stationary phase, with molecules eluting off the column at different retention times due to the differential interaction of each analyte with the stationary phase (Grimm et al., 2016). Upon elution, analytes are ionized by electron ionization and fragmented to specific mass to charge (m/z) ratios (Grimm et al., 2016). This method is useful for detecting amino acids and organic acids, including CAC intermediates.

1.6.1.2 LC-MS: LIQUID CHROMATOGRAPHY – MASS SPECTROMETRY

The LC-MS method involves the analysis of larger, more polar compounds. The basis of this metabolomic technique is similar to GC-MS, but uses a liquid mobile phase based on high pressure liquid chromatography (HPLC) separation (Lu et al., 2008). Although no derivatization is needed for LC-MS, polar and non-polar compounds need to be run on different columns. This method is useful for detecting larger compounds such as nucleotides, NAD+/NADH, NADP+/NADPH. Methods to detect the presence of small molecule drugs in cells can also be used using LC-MS.

1.6.1.3 SITA: STABLE ISOTOPE TRACER ANALYSIS

Although it is useful to detect metabolites of a certain pathway, changes in metabolite concentration alone are not always informative about the activity of a pathway (Grimm et al. 2016). For example, a reduction in a metabolite level can occur due to decreased production of the metabolite or increased consumption of the metabolite (Buescher JM. et al. 2015). An informative technique to properly determine the activity of a metabolic pathway is stable isotope tracing analysis (SITA). This technique involves the use of a metabolite with at least one heavy stable isotopomer (ex. ^{13}C, ^{15}N, ^{2}H) that is used as a tracer (ex. ^{13}C-glucose or ^{13}C-glutamine) (Buescher et al., 2015). The fate of these atoms can be traced through the intermediates of a metabolic pathway by a mass shift that is measured by the mass spectrometer. Cells are incubated in media containing the labelled metabolite to replace the natural metabolite pool. Upon measuring these metabolites, the heavier m/z ratio of the labelled atom (^{13}C) relative to the natural carbon (^{12}C) allows for the unique identification of the fate of the labelled metabolite within the metabolome.

Due to dynamic nature of metabolites and the convoluted networks of which they can flow through, metabolites can have different m/z ratios. The quantification of the proportion of different m/z ratios of a metabolite is called the mass isotopomer distribution (MID) (Buescher et al., 2015). The occurrence of different m/z ratios can provide an indication of the flow of the metabolites through a pathway. For example, a fully labelled ^{13}C-glutamine can be metabolized to citrate using the oxidative/conventional direction of the CAC, yielding m+4 citrate. Conversely, the metabolism of glutamine can run in the reverse direction through the reductive carboxylation of glutamine, yielding m+5 citrate. In addition, SITA allows researchers to

observe the metabolic pathways used by cells when exposed to different environmental stresses, such as nutrient starvation, hypoxia, or a drug treatment. Thus. SITA is useful in discovering how cancers adapt to metabolic stresses to fuel their uncontrolled growth.

1.6.2 RESPIROMETRY

The bioenergetic activity of cells is an important indicator of metabolic health. As mitochondria are important sites of ATP generation, measuring the oxygen consumption through respirometry provides quantitative measures to indicate the throughput of metabolic pathways to fuel ATP generation. Respirometry can be performed manually using a Clark-type electrode apparatus or using an automated system using Seahorse XF analysers.

1.6.2.1 Clark-type Electrode

The Clark-type oxygen electrode (Rank Brothers) is designed for following the uptake of oxygen mainly by cell suspensions and isolated mitochondria. Briefly, a silver electrode (anode) is suspended in a potassium chloride solution, where silver is oxidized, and oxygen is reduced at a platinum cathode (Rank Brothers Ltd, 2002). Oxygen can be transferred from media through the permeable Teflon membrane to saturate the platinum electrode (Rank Brothers Ltd, 2002). Once cells or mitochondria are added to the chamber, the percent of oxygen saturation decreases a function of the oxygen being consumed.

1.6.2.2 Seahorse XF Analyser

The Seahorse XF Analyser is an 8,24, or 96-well microplate-based system that enables the real-time measurement of cellular bioenergetics in a user-friendly platform (Agilent, 2018).

In contrast to the Clark-type system, the Seahorse can measure oxygen consumption rate (OCR) and has a pH electrode to measure the extracellular acidification (ECAR) of the media, which acts a crude estimate of lactate secretion (Agilent, 2018). Briefly, cells or isolated mitochondria are adhered to microplates and cartridges are lined with fluorescent probes to measure OCR and ECAR and contain ports to inject drugs (Agilent, 2018).

To study the bioenergetics of whole cells, different drugs are treated to test for certain bioenergetic parameters. To determine the contribution of oxygen consumption linked to ATP synthesis (known as coupled respiration), the ATP synthase inhibitor oligomycin is used (Gnaiger E, 2007). Following injection of oligomycin, the resulting respiration is the contribution linked to proton leak (known as uncoupled respiration) (Gnaiger E, 2007), while the coupled respiration is calculated as the difference between basal respiration and uncoupled respiration. To determine the maximal respiration potential, carboyl cyanide-p-trifluoromethoxyphenylhydrazone (FCCP) is used, which uncouples the inner mitochondrial membrane to dissipate the electrochemical gradient (Gnaiger E, 2007). Lastly, the complex III inhibitor myxothiazol is used to block mitochondrial respiration (Gnaiger E, 2007). Alternatively, rotenone and antimycin A are also used to block complex I and complex III-based respiration (Gnaiger E, 2007). Any resulting oxygen consumption is referred to as non-mitochondrial respiration.

Furthermore, to study the bioenergetics of isolated mitochondria, cells or tissues are fractioned into mitochondrial fractions, which are tested directly for respirometry. As the metabolism of many nutrients occur within mitochondria, different substrates can be added to assess the functionality of these pathways within isolated mitochondria. To assess the

functionality of complex I, substrates such as pyruvate, glutamate or palmitoyl-carnitine, along with malate are added to fuel NADH production from the CAC (Gnaiger, 2014). In addition, the functionality of complex II can be assessed using succinate, the substrate for complex II-mediated FADH2, coupled to rotenone, which blocks complex I-mediated respiration (Gnaiger, 2014). The respiration following the addition of substrates is referred to as state 2 respiration (Gnaiger, 2014). The measurement of respiration linked to ATP synthesis, known as state 3 respiration is determined following addition of ADP (Gnaiger, 2014). State 4 respiration refers to the respiration produced from proton leak, which is determined following addition of oligomycin (Gnaiger, 2014). Lastly, FCCP is added to determine the maximum respiratory capacity (Gnaiger, 2014). The degree of mitochondrial integrity is an important determinant when studying respirometry of isolated mitochondria. High quality, functional mitochondria produce high ATP-synthesis with minimal proton leak. As such, the criterion for mitochondrial quality can be calculated using the respiratory control ratio (RCR), which is measured as the quotient of state 3 respiration on state 4 respiration (RCR= State3/State4) (Gnaiger, 2014). Mitochondrial suspensions with an RCR of 3 or greater are considered appropriate for studying mitochondrial bioenergetics (Brand and Nicholls, 2011).

1.7 RATIONALE:

In this thesis, we reinforce the notion of the PGC-1/ERR transcriptional complex acting as a downstream effector of AMPK signalling in cancer. This work supports the role of the AMPK/PGC-1/ERR axis as an activator of catabolic processes, such as cellular respiration, and an inhibitor of anabolic reactions, such as one-carbon metabolism and purine biosynthesis. Given its role in modulating one-carbon reactions, activation of the PGC-1/ERR axis can improve sensitivity to the antifolate drug, methotrexate. Furthermore, we demonstrate the importance of AMPK in regulating the response to methotrexate and suggest the use of AMPK activators to improve the antiproliferative effects of methotrexate. Lastly, we also shed light on the use of the SGLT2 inhibitor, canagliflozin, in oncology. We demonstrate that canagliflozin displays antineoplastic effects and perturbs the citric acid cycle by inhibiting glutamate dehydrogenase and complex II-mediated respiration. Given its metabolic and antineoplastic effects in cancer, we propose the notion of repurposing SGLT2 inhibitors such as canagliflozin for treating cancer. We also discuss the opportunity of combining several metabolic treatments, which may produce therapeutic responses that are clinically relevant.

CHAPTER 2:

The PGC-1α/ERRα Axis Represses One-Carbon Metabolism and Promotes Sensitivity to Anti-Folate Therapy in Breast Cancer

Étienne Audet-Walsh[1,6], **David J. Papadopoli** [1,2,6], Simon-Pierre Gravel[1], Tracey Yee[1,2], Gaëlle Bridon[1], Maxime Caron[3], Guillaume Bourque[3,4], Vincent Giguère[1,2,5,7], Julie St-Pierre[1,2,7]

[1]Goodman Cancer Research Centre, McGill University, Montréal, QC H3A 1A3, Canada

[2]Department of Biochemistry, McGill University, Montréal, QC H3G 1Y6, Canada

[3]McGill University and Génome Québec Innovation Centre, Montréal, QC H3A 0G1, Canada

[4]Department of Human Genetics, McGill University, Montréal, QC H3G 1Y6, Canada

[5]Departments of Medicine and Oncology, McGill University, Montréal, QC H3G 1Y6, Canada

[6]Co-first author

[7]Co-senior author

*Correspondence: vincent.giguère@mcgill.ca (V.G.), julie.st-pierre@mcgill.ca (J.S.-P.)
http://dx.doi.org/10.1016/j.celrep.2015.12.086

Received 22 June 2015, Revised 2 November 2015, Accepted 18 December 2015,

Available online 21 January 2016.Published: January 21, 2016

2.1 OBJECTIVES OF THIS CHAPTER:

1) Elucidate the role of the PGC-1α/ERRα axis as a downstream effector of AMPK signalling
2) Identify how AMPK modulates the binding of ERRα to chromatin
3) Determine the impact of PGC-1α/ERRα signalling on one-carbon metabolism
4) Uncover the effect of PGC-1α/ERRα on methotrexate sensitivity

2.2 SUMMARY

Reprogramming of cellular metabolism plays a central role in fueling malignant transformation, and AMPK and the PGC-1α/ERRα axis are key regulators of this process. The intersection of gene-expression and binding-event datasets for breast cancer cells shows that activation of AMPK significantly increases the expression of PGC-1α/ERRα and promotes the binding of ERRα to its cognate sites. Unexpectedly, the data also reveal that ERRα, in concert with PGC-1α, negatively regulates the expression of several one-carbon metabolism genes, resulting in substantial perturbations in purine biosynthesis. This PGC-1α/ERRα-mediated repression of one-carbon metabolism promotes the sensitivity of breast cancer cells and tumors to the anti-folate drug methotrexate. These data implicate the PGC-1α/ERRα axis as a core regulatory node of folate cycle metabolism and further suggest that activators of AMPK could be used to modulate this pathway in cancer.

2.3 INTRODUCTION

The orphan nuclear receptor known as estrogen-related receptor a (ERRα, NR3B1) and the peroxisome proliferator-activated receptor g co-activator 1a (PGC-1α) act together as a transcriptional regulatory node important for the expression of metabolic genes (Deblois et al., 2013; Giguère, 2008; Mootha et al., 2004; Villena and Kralli, 2008). Indeed, the PGC-1α/ERRα axis is now well established as a central regulator of energy metabolism that induces the global expression of genes involved in mitochondrial biogenesis and functions (Eichner and Giguère, 2011; Giguère, 2008; Handschin and Spiegelman, 2006). Specifically, gene expression and genome-wide binding analyses demonstrated that PGC-1α and ERRα share a functional

relationship in controlling the expression of vast metabolic gene networks in numerous tissues (Chang et al., 2011; Deblois et al., 2010; Laganière et al., 2004; Schreiber et al., 2004; Wende et al., 2005). ERRα binds to the promoters of all genes encoding enzymes of glycolysis and many nuclear-encoded mitochondrial genes involved in energy metabolism (Charest-Marcotte et al., 2010; Dufour et al., 2007; Eichner and Giguère, 2011). Moreover, PGC-1α and ERRα exploit auto-regulatory feedforward loops to promote the expression of metabolic genes and mitochondrial activity (Handschin et al., 2003; Laganière et al., 2004; Mootha et al., 2004; Schreiber et al., 2004).

The expression and activity of ERRα and PGC-1α are highly adaptable and can respond to various physiological and pathological cues. In support of this point, PGC-1α is a key effector of the energy-sensing signalling cascade orchestrated by AMP-activated protein kinase (AMPK) (Jäger et al., 2007). AMPK occupies a central position in the reprogramming of cells to adapt to metabolic stress by promoting catabolism and inhibiting anabolism in order to restore the pool of cellular ATP (Hardie et al., 2012). Specifically, AMPK promotes catabolic reactions, such as lipid oxidation and cellular respiration, and inhibits anabolic processes, such as lipid and protein synthesis (Hardie et al., 2012). AMPK activation induces the expression of PGC-1α, and the AMPK-mediated increase in mitochondrial respiration has been shown to be dependent on PGC-1α in muscle cells (Jäger et al., 2007). In addition, AMPK phosphorylates PGC-1α, which potentiates its activity (Jäger et al., 2007). Clearly, PGC-1α is a significant downstream effector of AMPK- dependent metabolic effects, but which specific pathways are regulated by the AMPK/PGC-1α/ERRα partnership are yet to be identified.

The PGC-1α/ERRα axis is a central regulator of metabolism in cancer, notably breast cancer (Deblois and Giguère, 2013; Deblois et al., 2013). The expression of PGC-1α is reduced in breast tumors compared with normal tissues (Deblois et al., 2013). However, within the various breast cancer subtypes, the levels of PGC-1α, along with that of ERRα, are highest in HER2+ and triple-negative breast tumors, the two breast cancer subtypes associated with the poorest prognosis (Ariazi et al., 2002; Deblois et al., 2009; McGuirk et al., 2013). Functional studies have shown that PGC-1α promotes the growth of HER2+ tumors by regulating intra-tumoral nutrient availability (Klimcakova et al., 2012). ERRα also promotes the growth of HER2+ breast tumors by promoting the expression of the HER2 amplicon (Deblois et al., 2010), and the ERRα signalling axis is downstream of HER2 (Ariazi et al., 2007; Barry and Giguère, 2005; Chang et al., 2011). In addition, a recent study has shown that the PGC-1α/ERRα axis is a positive regulator of glutamine metabolism in HER2+ breast tumors and that elevated expression of glutamine enzymes is associated with poor clinical outcome in breast cancer patients (McGuirk et al., 2013). Overall, increasing experimental evidence supports a role for the PGC-1α /ERRα axis in fueling breast tumor growth.

Histological analyses of phospho-AMPK in breast tumors showed that AMPK signalling is reduced in breast cancer compared with normal tissues (Hadad et al., 2008). Furthermore, reduced AMPK signalling in breast tumors is associated with poor clinical outcome (Hadad et al., 2008). However, functional studies have shown both pro- and anti-growth effects of AMPK in breast cancer (Fox et al., 2013; Laderoute et al., 2014). The impact of AMPK on breast cancer growth is associated with metabolic changes (Laderoute et al., 2014), and metabolic effectors, such as PGC-1α, likely play a central role in mediating the AMPK-dependent metabolic effects. Indeed, recent studies revealed that the AMPK/PGC-1α signalling cascade in various cancers

causes metabolic perturbations and promotes growth (Huang et al., 2014; Tennakoon et al., 2014; Yan et al., 2014). Most of the metabolic perturbations associated with the AMPK/PGC-1α signalling cascade relate to mitochondrial metabolism. However, little is known regarding the global impact of the AMPK/PGC-1α axis on cancer metabolism.

In this study, we uncovered a role for the AMPK/PGC-1α/ ERRα signalling cascade in repressing one-carbon metabolism by using a combination of functional genomics and metabolomics approaches. One-carbon metabolism plays a central role in dividing cells by participating in the synthesis of nucleotides, and hyperactivation of this metabolic pathway is linked to onco- genesis (Locasale, 2013). The clinical relevance of our data is highlighted by the fact that the AMPK/PGC-1α/ERRα-dependent regulation of one-carbon metabolism promotes sensitivity to anti-folate therapy in the context of breast cancer.

2.4 RESULTS

2.4.1 AMPK Activation Promotes PGC-1α/ERRα-Dependent Metabolic Reprogramming

To study the interplay between the metabolic regulators AMPK, PGC-1α, and ERRα in breast cancer, we used two human cell lines of HER2+ breast cancer, namely, BT474 and SKBR3. Both of these cell lines display high ERRα activity, overexpress HER2, and are dependent on aerobic glycolysis (Chang et al., 2011; Deblois et al., 2009). To activate AMPK, we used three different compounds, namely, AICAR (5-aminoimidazole-4- carboxamide 1-b-ribofuranoside) (Figure 2.1A; Figures S2.1A and S2.1B), A769662 (Figure S2.1C), and metformin (Figure S2.1D) (Cool et al., 2006; Corton et al., 1995). AMPK activation increased the expression of PPARGC1A (PGC-1α) and ESRRA (ERRα), but not that of PPARCG1B

(PGC-1β) or ESRRG (ERRγ), suggesting that AMPK specifically modulates the PGC-1α/ERRα axis (Figure 2.1B; Figures S2.1A, S1E, and S1F). This is in line with published results in a non-transformed cell line showing that AMPK phosphorylates PGC-1α increasing its level and activity (Jäger et al., 2007) and that PGC-1α promotes ERRα expression resulting in a positive feedback loop in which ERRα stimulates its own expression (Laganière et al., 2004; Mootha et al., 2004). AMPK activation stimulated the expression of known targets of the PGC-1α/ERRα axis, such as genes encoding enzymes of the citric acid cycle (CS, FH, MDH2) and a component of the electron transport chain (NDUFB5) (Figure 2.1B; Figure S2.1E). To validate the biological significance of these changes in expression of metabolic genes, we assessed the bioenergetics status of these two cell lines by measuring their glycolytic and mitochondrial respiration capacities. AMPK activation decreased aerobic glycolysis as illustrated by reduced lactate production (Figure S2.1G), increased cellular respiration (Figure 2.1C; Figure S2.1H), and altered the balance between coupled and uncoupled respiration (Figure 2.1D; Figure S2.1I). This pattern of mitochondrial respiration is typical of cells with elevated PGC-1α expression (St-Pierre et al., 2003). To test whether the metabolic changes seen upon AMPK activation were dependent on the PGC1α/ERRα axis, we used siRNA targeting PGC-1α or ERRα. Knockdown of either PGC-1α or ERRα nearly completely abolished the AMPK-mediated increase in ERRα expression and in respiration (Figures 2.1E and 2.1F). Collectively, these data show that AMPK activation in breast cancer cells increases the activity of the PGC-1α/ERRα axis and that this transcriptional node plays a central role in promoting AMPK-dependent increase in cellular respiration.

2.4.2 AMPK Activation Induces ERRα Binding Events on a Genome-wide Scale

To gain a global understanding of the PGC-1α/ERRα-dependent transcriptional events downstream of AMPK, we first performed chromatin immunoprecipitation coupled with deep sequencing (ChIP-seq) experiments for ERRα following AICAR treatment in BT474 cells (Figure 2.2; Figure S2.2). Under basal conditions, ERRα was bound to more than 22,000 genomic regions and the binding was enriched near genes involved in metabolic pathways, most notably, mitochondrial functions (Figures S2.2A–S2D). AMPK activation increased the total number of binding sites for ERRα by more than 50% (Figure 2.2A). Heatmaps of ChIP-seq data showed that the sites strongly bound by ERRα in basal conditions tended to stay bound during AMPK activation (Figure 2.2B), including the ERRα binding site localized at its own promoter (Figure S2.2C). It is important to note that significant binding events for ERRα following AICAR treatment also seemed to be present under basal conditions, although below the threshold for peak calling. These data thus indicate that AMPK activation does not significantly change the global ERRα binding site distribution, but rather, it modulates ERRα binding to sites displaying lower affinity for ERRα in the absence of a stimulus (Figure 2B). Validation of ChIP-seq data using standard ChIP-qPCR showed loci to which ERRα binding is either unregulated or regulated in a positive or negative manner in the presence of AICAR (Figure 2.2C). Pathway and motif enrichment analyses comprising all bound genes identified by ChIP-seq did not reveal major differences between basal or AMPK-activated conditions. In fact, the most enriched pathways in both conditions were related to cellular metabolism, notably, mitochondrial functions (Figure S2.2D). Also, the ERR response element (ERRE) motif was the most significantly enriched motif in both conditions, with no major change observed in other significantly co-enriched motifs such as FOXA1, AP-1, and AP-2 (Figure S2.2E).

These results were confirmed in SKBR3 cells (Figure S2.2F). In addition, we validated that AMPK activation induces ERRα binding near the transcriptional start site of known ERRα metabolic targets in mouse embryonic fibroblasts (MEFs) (Figure S2.2G). Importantly, this AICAR-mediated induction of ERRα binding was impaired in MEFs null for PRKAA1 and PRKAA2, encoding the two α subunits of AMPK (Figure S2.2G), illustrating that the induction of ERRα binding upon AICAR treatment is dependent on AMPK. Together, these results show that ERRα binding is increased following AMPK activation in human and mouse cells.

2.4.3 The PGC-1α/ERRα Axis Negatively Controls the Expression of Folate Cycle Genes

To reveal the main pathways targeted by increased ERRα binding following AMPK activation, we first looked at the interconnection between microarray and ChIP-seq datasets. Specifically, we looked for genes that displayed changes in expression and that were associated with an ERRα binding event following AMPK activation (Figure 2.3A). The most significantly enriched pathways connected with these 413 genes were linked to folate metabolism such as histidine degradation, folate transformation, and tetrahydrofolate salvage (Figures 2.3B and 2.3C). These results were validated using qPCR showing that the expression of several folate cycle genes was reduced following AMPK activation (Figure 2.3D, yellow bars). The observed downregulation in the expression of folate cycle genes was ERRα-dependent because ERRα knockdown attenuated the reduction in folate cycle gene expression upon AMPK activation (Figure 3D, compare the orange and red bars).

These results were validated with a separate AMPK activator, A769662 (Figure S2.3). Furthermore, the AMPK activator metformin also led to elevated levels of PGC-1α and ERRα

along with repression of the folate cycle gene MTHFD1 (Figure S2.1F). ChIP- qPCR validation experiments confirmed that ERRα binding was increased at several folate cycle gene promoters upon AMPK activation (Figure 2.3E). In addition, the data revealed that ERRα knockdown, in the absence of AMPK activation in BT474 cells, significantly increased the expression of several folate cycle genes (Figures 2.3D, blue bars, and 2.3F) indicating that under basal conditions ERRα negatively regulates the expression of folate cycle genes. PGC-1α knockdown also significantly increased the level of MTHFD1L in these cells (Figure 2.3F), whereas overexpression of PGC-1α in murine cells expressing activated ERBB2 (NT2196 cells) led to a sharp decrease in the level of MTHFD1L (Figure 2.3G). Altogether, these results reveal that the PGC-1α/ ERRα axis negatively controls the expression of several folate cycle genes under basal conditions and in response to AMPK activation in HER2+ breast cancer cells.

2.4.4 The PGC1α/ERRα Axis Represses Folate Metabolism and Purine Biosynthesis

Folate intermediates play a central role in one-carbon metabolism reactions. They are used as messengers of one-carbon units for the de novo production of purines and the formation of thymidylate, both of which are important for nucleotide synthesis and cell proliferation (Locasale, 2013). Folate intermediates also play a central role in the replenishment of S-adenosyl-methionine (SAM) for methylation reactions (Locasale, 2013). Given the modest, but concerted, repression of the expression of several folate cycle genes by the PGC-1α/ERRα axis, we evaluated its impact on one-carbon metabolism. To do so, we first assessed the impact of the PGC-1α/ERRα axis on nucleotide synthesis by quantifying DNA synthesis and cell proliferation. Knockdown of either PGC-1α or ERRα increased DNA synthesis and cell proliferation in BT474

cells (Figures 2.4A and 2.4B). Conversely, AMPK activation, which activates the PGC-1α/ERRα axis (Figure 1), decreased DNA synthesis (Figure 2.4C) and cell proliferation (Figure 2.4D; Figure S2.4A). Taken together, these results indicate that the PGC-1α/ERRα axis acts as a repressor of nucleotide synthesis and cell proliferation. In order to substantiate these results, we quantified the impact of the PGC-1α/ERRα axis on the expression of key purine biosynthesis enzymes, namely, phosphoribosyl pyrophosphate amidotransferase (PPAT), phosphoribosylglycinamide formyltransferase, phosphoribosylglycinamide synthetase, phosphoribosylaminoimidazole synthetase (GART), and 5-aminoimidazole-4-carboxamide ribonucleotide formyltransferase/IMP cyclohydrolase (ATIC). PPAT is the enzyme catalyzing the rate-limiting step in de novo purine synthesis, and GART and ATIC receive the one-carbon unit from the folate cycle. Knockdown of either PGC-1α or ERRα in BT474 cells increased the expression of PPAT, GART, and ATIC (Figure 2.4E). ChIP-qPCR analysis confirmed binding of ERRα to the promoter of PPAT, GART, and ATIC and positive regulation of ERRα binding at these loci following AMPK activation (Figure 2.4F). AMPK activation in BT474 cells, which activates the PGC-1α/ERRα axis, decreased the expression of PPAT, GART, and ATIC, but it only reached statistical significance for GART. Importantly, the AMPK-mediated repression of all three genes was reversed upon treatment with siERRα (Figure 4G, compare the orange and red bars). Additionally, both ATIC and GART were increased at the protein level upon ERRα repression (Figure 2.4H). On the other hand, PGC-1α overexpression in NT2196 cells, which was paralleled by increased ERRα expression (Figure S4B), decreased the expression of PPAT, GART, and ATIC (Figure 2.4I). Together, these data demonstrate that the PGC-1α/ERRα axis acts as a repressor of the expression of purine biosynthesis enzymes.

To directly assess whether these changes in the expression of purine biosynthesis genes had an impact on purine biosynthesis, we established a stable isotope tracer analysis methodology to follow the incorporation of labeled serine (13C3-15N-serine) into AMP, ATP, and S-adenosyl methionine (SAM), which is a component of the methionine cycle that is directly linked to the folate cycle (Figure 2.4J). Knockdown of ERRα in BT474 cells, which was paralleled by reduced PGC-1α expression (Figure S2.4C), increased the fraction of labeled AMP (m+1–5), ATP (m+1–5) and SAM (m+1–5) (Figures 2.4K–4M). Conversely, overexpression of PGC-1α decreased the fraction of labeled ATP (m+1–5) (Figure 2.4N). This was accompanied by decreased formate levels, a one-carbon unit that links folate metabolism to purine biosynthesis (Figure 2.4O). Overall, these results demonstrate that the PGC-1α/ERRα axis represses folate metabolism and purine biosynthesis.

2.4.5 The PGC-1α/ERRα Axis Sensitizes Cells and Tumors to Methotrexate

Given that the PGC-1α/ERRα axis is a negative regulator of folate metabolism, we assessed whether this regulatory complex influences sensitivity to anti-folate therapy. Anti-folates are common chemotherapeutic drugs used to treat several cancers, including breast cancer (Munzone et al., 2012). Indeed, cells that are rapidly dividing and require high levels of nucleotides are particularly sensitive to these drugs. We used the anti-folate drug methotrexate (MTX) to study whether the PGC-1α/ERRα axis influences the sensitivity of breast cancer cells to this drug. MTX treatment decreased cell numbers significantly more in murine NT2196 cells overexpressing PGC-1α relative to controls (Figure 2.5A). Conversely, reduction of both PGC-1α and ERRα using siRNA in human BT474 cells led to higher cell counts after MTX treatment

compared with cells transfected with control siRNA (Figure 2.5B). This result was paralleled with lower levels of cleaved caspase 3 in cells depleted of PGC-1α and ERRα upon MTX treatment (Figure 2.5C). Furthermore, AICAR treatment, which induces the expression and activity of PGC-1α/ ERRα and causes a decrease in cell proliferation (Figures 2.1 and 2.4D; Figure S2.4A), potentiated the effect of MTX on proliferation, as illustrated by lower cell counts when cells were treated with both AICAR and MTX compared with either treatment alone (Figure S2.4D). Together, these data show that the PGC-1α/ERRα axis sensitizes cells to anti-folate therapy in vitro.

Next, we wanted to validate the role of PGC-1α/ERRα in response to anti-folate therapy in vivo. To do so, we performed xenograft experiments where NT2196 cells overexpressing PGC-1α were injected on the right flank of the animal, and control cells were injected on the left flank. Once tumors reached a volume of 0.1 cm3, MTX treatment was started for 21 days using a suboptimal dosage that allows for the sustained growth of control cells during the course of the experiment, as determined in a pilot study. This experimental design, in which the cells overexpressing PGC-1α and controls are injected in the same animal, also limits the confounding effect of inter-individual variation in response to MTX treatment that could have arisen if the PGC-1α and control cells had been injected in different animals (Figure 2.5D). As previously reported (Klimcakova et al., 2012), cells overexpressing PGC-1α generated endpoint tumors much faster than controls (Figures 2.5E, compare the red and blue lines, and 2.5F), even though they displayed reduced expression of MTHFD1 and GART and had reduced formate levels (Figures 5G and 5H, blue bars), indicating reduced one-carbon metabolism. Indeed, even though cells overexpressing PGC-1α have reduced one-carbon metabolism (Figures 2.3 and 2.4) and proliferate less in vitro, they form larger tumors in xenograft experiments, mainly due to their

increased angiogenesis and intratumoral nutrient levels compared to control cells, as previously described (Klimcakova et al., 2012; McGuirk et al., 2013; Figure S2.5). Clearly, the elevated nutrient levels in PGC-1α overexpressing tumors overcome their baseline reduction in one-carbon metabolism. This is particularly relevant in the context that PGC-1α/ERRα limit one-carbon metabolism but do not block it completely (Figures 2.3 and 2.4) and that these cells are particularly sensitive to nutrient deprivation (McGuirk et al., 2013).

Importantly, MTX treatment significantly decreased the growth of PGC-1α overexpressing tumors compared to vehicle treated mice (Figures 2.5E, compare the green and blue lines, and 2.5F), whereas it had little effect on that of control tumors at the suboptimal dosage used in the experiment (Figures 2.5E, compare the yellow and red lines, and 2.5F). Indeed, after MTX treatment, the PGC-1α overexpressing tumors were similar in size to the controls (Figures 2.5E and 2.5F). The fact that cells overexpressing PGC-1α proliferate less and are more sensitive to MTX in vitro (Figure 2.5A) while they formed larger tumors that are also more sensitive to MTX in vivo (Figures 2.5E and 2.5F) highlights that the relative growth status of these cells does not dictate their MTX sensitivity. Taken together, our results indicate that the PGC-1α/ERRα axis is a central modulator of the response of HER2+ mammary tumors to MTX treatment.

2.5 FIGURES

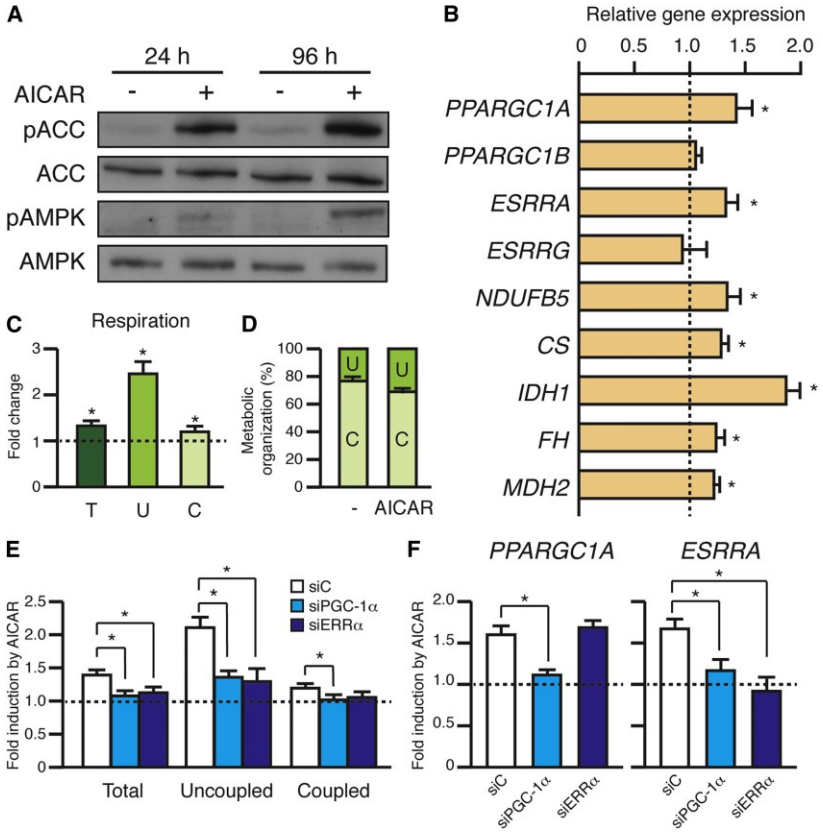

Figure 2.1. AMPK Increases Mitochondrial Metabolism in Human Breast Cancer Cells in a PGC-1α/ERRα-Dependent Manner

(A) Immunoblots of phosphorylated-ACC (S79), total ACC, phosphorylated-AMPKα (T172), and total AMPKα in BT474 cells upon 0.5 mM AICAR or vehicle treatment for 24 hr or 96 hr.

(B) Expression of PPARGC1 and ESRR family members and their metabolic target genes in BT474 cells in the presence of 0.5 mM AICAR for 96 hr, normalized to that of BT474 cells treated with vehicle (n = 5) (dashed line).

(C) Total (T), uncoupled (U), and coupled (C) respiration of BT474 cells treated with 0.5 mM AICAR for 96 hr, normalized to that of BT474 cells treated with vehicle (n = 6) (dashed line).

(D) Percentage of mitochondrial respiration that is coupled and uncoupled, calculated from (C) (n = 6).

(E) Total, uncoupled, and coupled respiration of BT474 cells transfected with siC, siPGC-1α, or siERRα, and treated with 0.5 mM AICAR for 96 hr, normalized to that of transfected BT474 cells treated with vehicle (n = 7) (dashed line).

(F) Expression of *PPARGC1A* and *ESRRA* in BT474 cells transfected with siC, siPGC-1α, or siERRα and treated with 0.5 mM AICAR for 96 hr, normalized to that of transfected BT474 cells

treated with vehicle (n = 7) (dashed line).All data are presented as means + SEM, *p < 0.05, Student's t test. See also Figure S1.

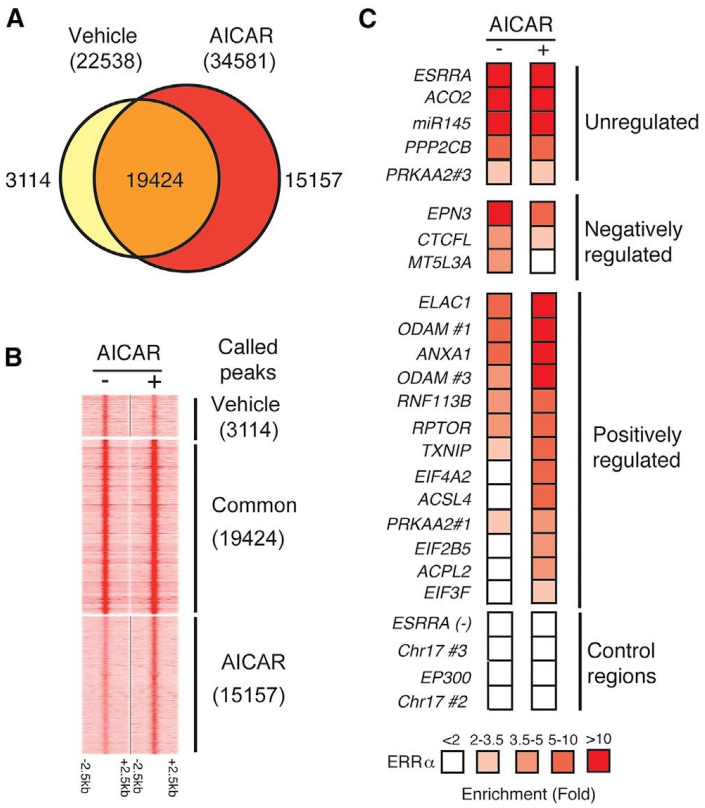

Figure 2.2. AMPK Activation Induces Genomic ERRα Binding in Breast Cancer Cells

(A) Venn diagrams representing number of ERRα-bound segments obtained by ChIP-seq in BT474 cells upon 90 min stimulation with 0.5mM AICAR or vehicle.

(B) Heatmaps showing signal intensities of ERRα binding by ChIP-seq in BT474 cells upon 0.5 mM AICAR or vehicle treatment and clustered according to overlapping peaks. The window represents a region covering ± 2.5 kb around the center of the binding event.

(C) Standard ChIP-qPCR validation of ERRα binding in BT474 cells at several target genes upon treatment with 0.5 mM AICAR or vehicle for 90 min. Results are presented as the average of at least three independent experiments. See also Fig. S2

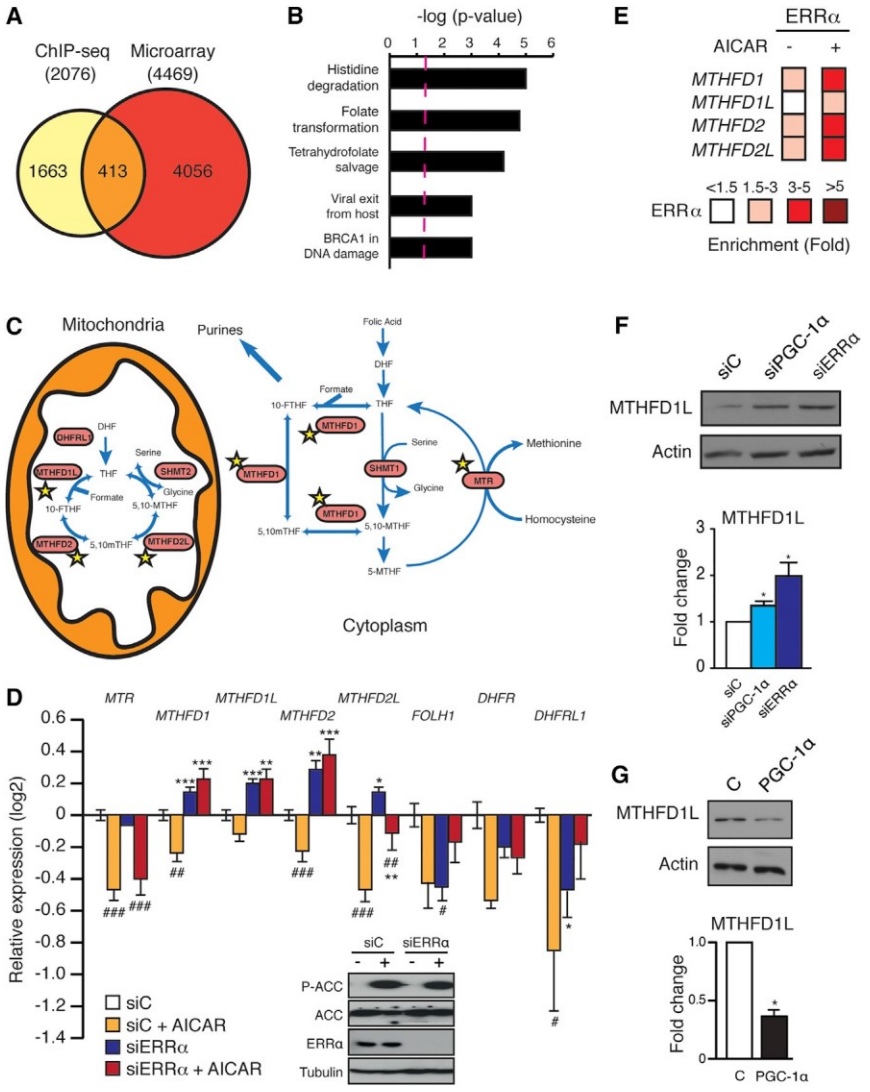

Figure 2.3. The PGC-1α/ERRα Axis Represses Folate Metabolism Gene Expression

(A) Venn diagrams representing the overlap between ERRα peaks unique to BT474 cells treated with 0.5 mM AICAR (ChIP-seq) and the genes whose expression is significantly altered upon 0.5 mM AICAR treatment (microarray). The number of genes in each group is shown.

(B) Pathways enriched in the overlap of the Venn diagrams in (A). Values greater than 1.3 (red dashed line) indicate statistical significance ($p < 0.05$).

(C) Schematic representation of the folate metabolic pathways in the cytoplasm and mitochondria. Upon AICAR treatment, the expression of enzymes boxed in pink are downregulated and the genes encoding the enzymes marked with a yellow star are associated with an ERRα binding event. DHF: dihydrofolate; THF: tetrahydrofolate; 10-

formylTHF; 5,10-MTHF: 5,10-methyleneTHF; 5,10-mTHF: 5,10-methenylTHF; 5-MTHF: 5-methylTHF.

(D) Relative expression of folate metabolism genes in BT474 cells transfected with siC or siERRα, and treated with 0.5 mM AICAR or vehicle for 24 hr, normalized to that of siC cells treated with vehicle (n = 3). Data are shown as means and SEM, # $p < 0.05$; ## $p < 0.01$; ### $p < 0.001$ indicate that AICAR induces a significant change in expression compared with vehicle treatment; $^{*}p < 0.05$; $^{**}p < 0.01$; $^{***}p < 0.001$ indicate that siERRα induces a significant change compared with siC (Student's t test). Immunoblots of phosphorylated-ACC (S79), total ACC, and ERRα in BT474 cells transfected with siC or siERRα and treated with 0.5 mM AICAR or vehicle for 24 hr are shown in the inset. Tubulin represents the loading control.

(E) Standard ChIP-qPCR validation of ERRα binding to several MTHFD family genes in BT474 cells treated with AICAR or vehicle for 90 min (n = 3).

(F) Immunoblots of MTHFD1L in BT474 cells transfected with either siC, siPGC-1α, or siERRα. Fold changes are normalized to actin levels (n = 3).

(G) Immunoblots of MTHFD1L levels in control NT2196 cells (C) and NT2196 cells overexpressing PGC-1α (PGC-1α). Fold changes are normalized to actin levels (n = 3).

For (F) and (G), data are presented as means + SEM, $^{*}p < 0.05$, Student's t test. See also Fig S3.

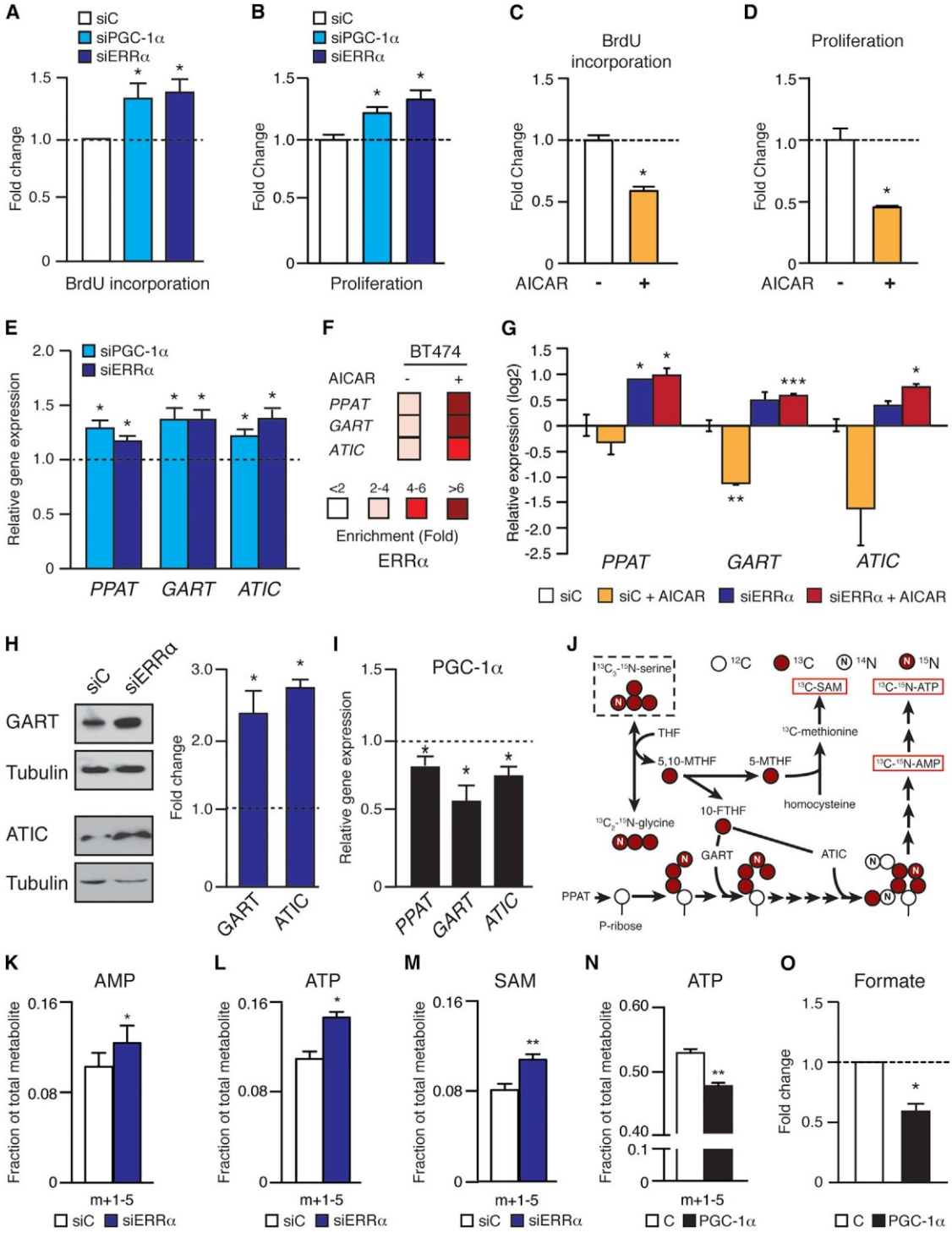
A
siC
siPGC-1α
siERRα
Fold change
BrdU incorporation
B
Proliferation
C
BrdU incorporation
AICAR
D
Proliferation
E
Relative gene expression
PPAT
GART
ATIC
F
BT474
AICAR
Enrichment (Fold)
ERRα
G
Relative expression (log2)
siC + AICAR
siERRα + AICAR
H
GART
Tubulin
ATIC
I
PGC-1α
J
THF
5,10-MTHF
5-MTHF
10-FTHF
homocysteine
PPAT
P-ribose
K
AMP
Fraction ot total metabolite
m+1-5
L
ATP
M
SAM
N
ATP
O
Formate
Fold change
C
PGC-1α

Figure 2.4. The PGC-1α/ERRα Axis Inhibits de Novo Purine Biosynthesis

(A) BrdU incorporation assay for BT474 cells transfected with siC, siPGC-1α, or siERRα. Data are normalized to siC (n = 6) (dashed line). Data are presented as means + SEM, $^{*}p < 0.05$, Student's t test.

(B) BT474 cell counts following siRNA transfection with either siC, siPGC-1α, or siERRα. Data are normalized to siC (n = 6) (dashed line). Data are presented as means + SEM, $^{*}p < 0.05$, Student's t test.

(C) BrdU incorporation assay for BT474 treated with 0.5 mM AICAR or vehicle for 96 hr (n = 7). Data are presented as means + SEM, $^{*}p < 0.05$, Student's t test.

(D) BT474 cell counts following treatment with 0.5 mM AICAR or vehicle for 96 hr. Data are normalized to vehicle (n = 6) (dashed line). Data are presented as means + SEM, $^{*}p < 0.05$, Student's t test.

(E) Expression of de novo purine biosynthesis genes in BT474 cells transfected with siC, siPGC-1α, or siERRα. Data are normalized to siC (n = 3–4). Data are presented as means + SEM, $^{*}p < 0.05$, Student's t test.

(F) Standard ChIP-qPCR of ERRα binding to *PPAT*, *GART*, and *ATIC* in BT474 cells treated with 0.5 mM AICAR or vehicle for 90 min (n = 3).

(G) Relative expression of *GART*, *ATIC*, and *PPAT* in BT474 cells transfected with siC or siERRα and treated with 0.5 mM AICAR or vehicle for 24 hr, normalized to that of siC cells treated with vehicle. One representative experiment of two independent experiments performed in triplicate is shown. Data are presented as means and SEM, $^{*}p < 0.05$; $^{**}p < 0.01$; $^{***}p < 0.001$ indicate that siERRα induces a significant change compared with the respective siC condition (Student's t test).

(H) Immunoblots of GART and ATIC in BT474 cells transfected siC or siERRα. Fold changes are normalized to tubulin levels (n = 3). Data are presented as means + SEM, $^{*}p < 0.05$, Student's t test.

(I) Expression of de novo purine biosynthesis genes in NT2196 cells overexpressing PGC-1α (PGC-1α) normalized to that of controls (n = 3). Data are presented as means + SEM, $^{*}p < 0.05$, Student's t test.

(J) Stable isotope tracer analysis experiment. Labeled serine ($^{13}C_3$-^{15}N-serine) was added to cultured cells, and incorporation of labeling into downstream metabolites linked to the folate cycle activity was monitored. AMP and ATP come from the purine synthesis pathway, whereas S-adenosyl methionine (SAM) is a metabolite from the methionine cycle that is linked to the folate cycle. 5,10-MTHF: 5,10-methyleneTHF, 5-MTHF: 5-methylTHF, 10-FTHF: 10-formylTHF. Red boxes depict the metabolites that were analyzed in (K)–(N).

(K) Mass isotopomer enrichment of AMP in BT474 cells transfected with either siC or siERRα and pulsed with $^{13}C_3$-^{15}N-serine for 8 hr (n = 3). Data are presented as means + SEM, $^{*}p < 0.05$, Student's t test.

(L) Mass isotopomer enrichment of ATP in BT474 cells transfected with either siC or siERRα and pulsed with $^{13}C_3$-^{15}N-serine for 8 hr. One representative experiment performed in triplicate of three independent experiments is shown. Data are presented as means + SEM, $^{*}p < 0.05$, Student's t test.

(M) Mass isotopomer enrichment of SAM in BT474 cells transfected with either siC or siERRα and pulsed with $^{13}C_3$-^{15}N-serine for 8 hr (n = 3). Data are presented as means + SEM, $^{*}p < 0.05$, Student's t test.

(N) Mass isotopomer enrichment of ATP in control NT2196 cells (C) and NT2196 cells overexpressing PGC-1α (PGC-1α) pulsed with $^{13}C_3$-^{15}N-serine for 8 hr (n = 3). Data are presented as means + SEM, $^{*}p < 0.05$, Student's t test.

(O) Formate levels in control NT2196 cells (C) and NT2196 cells overexpressing PGC-1α (PGC-1α) (n = 3). Data are presented as means + SEM, $^{*}p < 0.05$, Student's t test. See also Fig. S4.

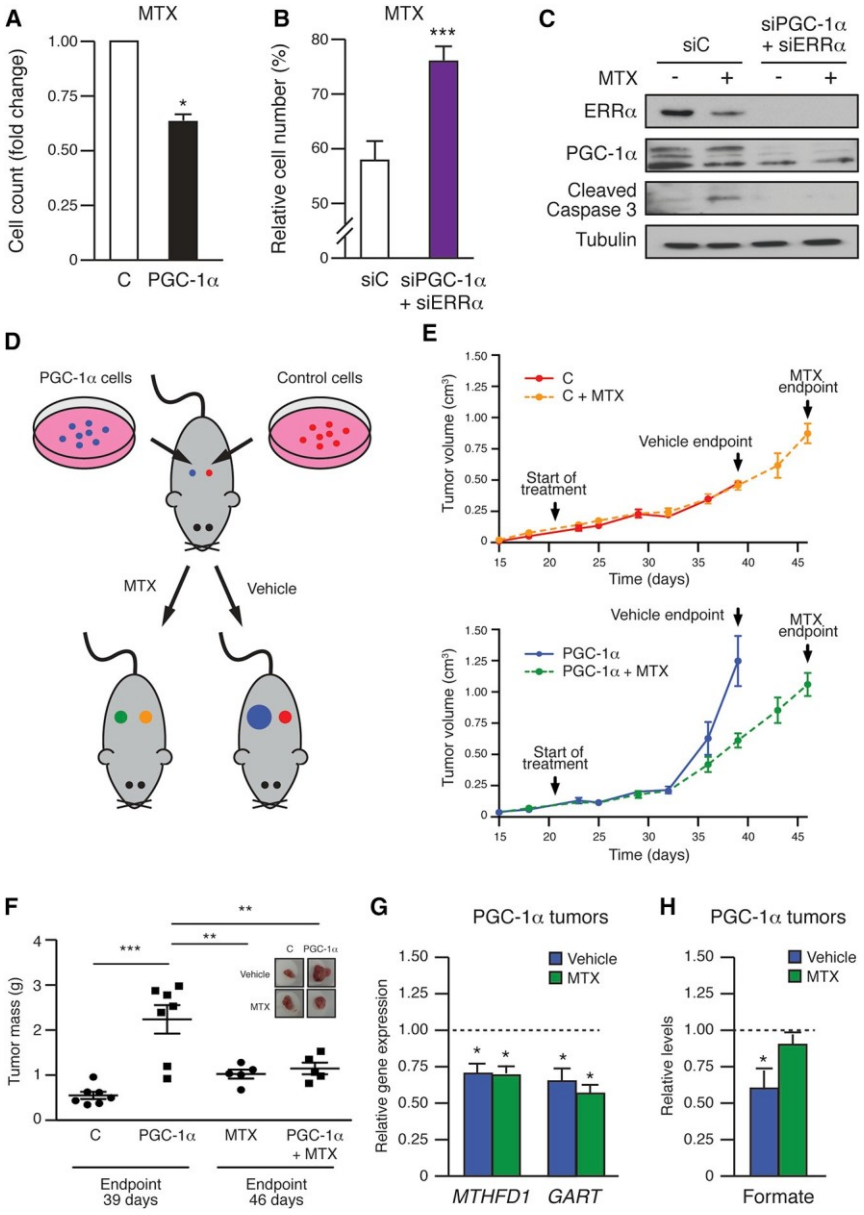

Figure 2.5. The PGC-1α/ERRα Axis Sensitizes Breast Cancer Cells to MTX Treatment In Vitro and In Vivo

(A) Cell counts of control NT2196 cells (C) and NT2196 cells overexpressing PGC-1α (PGC-1α) treated with 0.1 μM MTX for 96 hr, normalized to control cells (C) treated with MTX (n = 3). Data are presented as means + SEM, $^{*}p < 0.05$, Student's t test.

(B) Cell counts for BT474 cells transfected with siC or both siPGC-1α and siERRα and treated with 100 μM MTX for 72 hr, normalized to cells treated with vehicle. Data are presented as means + SEM, $^{***}p < 0.001$, Student's t test.

(C) Immunoblots of ERRα, PGC-1α, and cleaved caspase 3 in BT474 cells treated as described for (B).

(D) Control or PGC-1α overexpressing NT2196 cells were injected into mammary fat pads of SCID/BEIGE mice. Control cells were injected in the left flank, whereas PGC-1α overexpressing cells were injected in the right flank of each mouse. Once tumors reached approximately 0.1 cm^3 (18–23 days post-injection), mice were treated with 5.56 mg/kg of MTX or vehicle twice weekly until the tumors reached approximately 1.5 cm^3.

(E) Tumor growth curves. Top panel, control tumors; bottom panel, PGC-1α overexpressing tumors.

(F) Tumor masses and images of tumors at endpoint from each group (n = 5–7). Data are presented as means ± SEM, $^{**}p < 0.01$; $^{***}p < 0.001$, Student's t test.

(G) Expression of *MTHFD1* and *GART* in PGC-1α overexpressing tumors treated with vehicle or MTX, normalized to control tumors treated with vehicle or MTX (n = 5–7). Data are presented as means + SEM, $^{*}p < 0.05$, Student's t test.

(H) Formate levels in PGC-1α overexpressing tumors treated with vehicle or MTX, normalized to control tumors treated with vehicle or MTX (n = 5). Data are presented as means + SEM, $^{*}p < 0.05$, Student's t test. See also Fig S5.

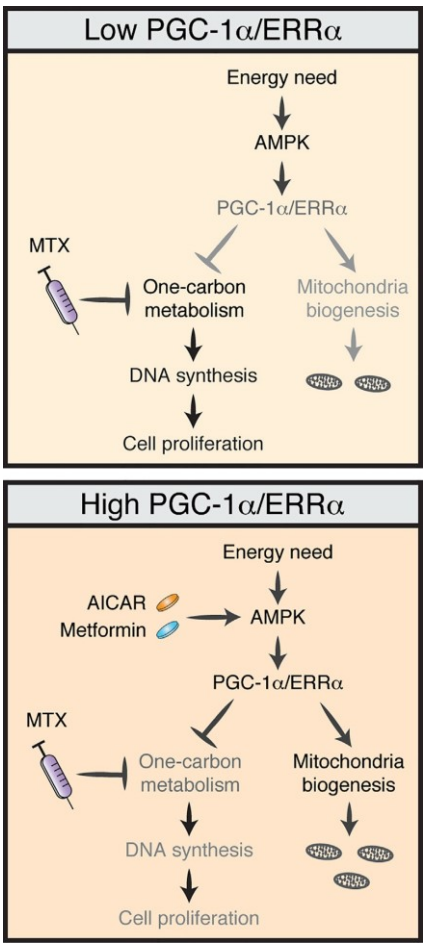

Figure 2.6. The PGC-1α/ERRα Axis Modulates One-Carbon Metabolism and MTX Sensitivity Schematic representation of the impact of the relative levels of PGC-1α/ERRα (top panel, low; bottom panel, high) on catabolic and anabolic metabolism in cancer cells. Our model indicates that cancer cells with higher levels of PGC-1α/ERRα have a greater sensitivity to MTX and that AMPK activators, such as AICAR and metformin, could further enhance PGC-1α/ERRα activity and therapeutic response.

2.6 DISCUSSION

In this study, we report functional interactions between the energy sensor AMPK and the PGC-1α/ERRα transcriptional partners in breast cancer cells. PGC-1α/ERRα were shown to be important for the increased mitochondrial activities of breast cancer cells after AMPK activation. We also uncovered that one-carbon metabolism was a key metabolic pathway targeted by the AMPK/PGC-1α/ERRα axis. Indeed, the expression of several folate cycle genes was negatively regulated by PGC-1α/ERRα under basal conditions, and it was further repressed in a PGC-1α/ERRα-dependent manner upon activation of AMPK. This transcriptional regulation of folate cycle genes led to decreased purine biosynthesis and SAM replenishment, which are key end metabolites of one-carbon metabolism. Hence, we show that PGC-1α/ERRα are central effectors of both catabolic (increased mitochondrial respiration) and anabolic (inhibition of purine biosynthesis) metabolic pathways. The clinical relevance of our data is illustrated by the fact that breast cancer cells with elevated levels of PGC-1α/ERRα display reduced folate metabolism and increased sensitivity to anti- folate therapy.

Folate intermediates play diverse roles in cellular metabolism. Notably, through their integration into one-carbon metabolism, folates are important for transfer of one-carbon units for the biosynthesis of nucleotides (Locasale, 2013). Serine donates a one-carbon unit to tetrahydrofolate (THF), generating 5,10-methylene-THF, a folate intermediate that can ultimately produce purines (Locasale, 2013). A recent study showed that a significant amount of NADPH in cells is generated through the conversion of 5,10-methylene-THF to 10-formyl-THF (Fan et al., 2014), identifying this pathway as a major contributor to the NADP/NADPH ratio. Given the central role of the folate pathway and one-carbon metabolism in the generation of key metabolites sustaining cell growth, it is perhaps not surprising that when examining for altered

metabolic pathways across numerous cancer types, mitochondrial one-carbon metabolism, notably MTHFD2, emerged as the most significant (Nilsson et al., 2014). Furthermore, several studies have shown that cancer cells are highly dependent on serine, a key substrate for one-carbon metabolism, for their growth (Labuschagne et al., 2014; Locasale and Cantley, 2011a, 2011b; Maddocks et al., 2013; Tedeschi et al., 2013), and serine deprivation augments the antineoplastic activity of the metabolic drug metformin (Gravel et al., 2014). The dominant role of folate and one-carbon metabolism in sustaining cell proliferation is further highlighted by the fact that numerous cancer drugs target key enzymes in these pathways and that several biomarkers of one-carbon metabolism exist to detect cancer or predict therapeutic response (Locasale, 2013).

Despite the central role of folate metabolism in cancer, little is known regarding the regulation of the expression of folate cycle enzymes. In this study, we demonstrate that PGC-1α/ERRα control the expression of numerous folate cycle genes, leading to changes in purine biosynthesis and modulation of sensitivity to anti-folate therapy. One interesting feature of the transcriptional regulation of folate cycle genes by PGC-1α/ERRα is that they act as repressors of their expression. Most studies on PGC-1α/ ERRα have revealed that they promote the expression of numerous enzymes involved in metabolism (Giguère, 2008). Indeed, PGC-1α/ERRα coordinately regulate the expression of numerous citric acid cycle enzymes and electron transport chain components resulting in elevated mitochondrial bioenergetics capacity (Eichner and Giguère, 2011). Similarly, we have recently shown that PGC-1α/ERRα work together to increase the expression of many enzymes involved in glutamine metabolism and promoting glutamine usage (McGuirk et al., 2013). However, PGC-1α/ERRα have also been shown to function as repressors of the expression of specific targets. Indeed, PGC-1α represses the

expression of LDHA in muscle (Summermatter et al., 2013) and β-secretase/BACE1 in brain (Wang et al., 2013). ERRα also negatively regulates the expression of PEPCK, one of the key enzymes in hepatic gluconeogenesis (Herzog et al., 2006). Our data now highlight that PGC-1α and ERRα can also work together to repress numerous enzymes in a metabolic pathway causing suppression of its activity. PGC-1α/ERRα cause small and coordinated changes in the expression of numerous enzymes involved in one-carbon metabolism. This is in agreement with numerous studies showing that PGC-1α/ERRα lead to small and coordinated changes in the expression of numerous genes that are metabolically related (St-Pierre et al., 2006; Mootha et al., 2003). For example, PGC-1α/ERRα regulate the expression of OXPHOS, ROS detoxification, and glutamine metabolism genes by eliciting small changes in their expression. Yet, the concerted biological impact of these modest changes in gene expression is profound (Wu et al., 1999; St-Pierre et al., 2006; McGuirk et al., 2013).

Both PGC-1α and ERRα play important roles in the metabolic reprogramming of cancer cells. Most studies investigating the role of the PGC-1α/ERRα transcriptional axis in breast cancer have associated PGC-1α and ERRα with increased tumor growth, notably by altering metabolism and promoting angiogenesis (recently reviewed in Bianco et al., 2012; Deblois and Giguère, 2013; Deblois et al., 2013). At first glance, this could seem to be in apparent contradiction with the results reported here, where the PGC-1α/ERRα axis promotes tumor growth and represses folate metabolism, which is one of the main metabolic pathways upregulated in cancer as it promotes nucleotide synthesis for DNA replication in rapidly dividing cells. However, PGC-1α/ERRα regulate numerous metabolic pathways that individually may have a different impact on cancer cell proliferation and survival. Hence, the net effect of PGC-1α/ERRα on tumor growth will represent the balance between the activity of all downstream

programs. High levels of PGC-1α/ERRα activity will confer an advantage to maximize energy production by promoting mitochondrial metabolism and angiogenesis to sustain the high metabolic needs of rapidly dividing cells, as well as increasing their stress resistance capacity (Arany et al., 2008; Klimcakova et al., 2012; St-Pierre et al., 2006). In this context, repression of folate cycle metabolism by the PGC-1α/ERRα axis is probably largely compensated for by these other PGC-1α/ERRα-dependent metabolic programs that fuel tumor growth and promote survival. In support of this point, cells overexpressing PGC-1α proliferate less in vitro, whereas they formed larger tumors in vivo. The main reason for their increased growth in vivo is their elevated levels of intratumoral nutrients (Klimcakova et al., 2012; Figure S5B), which clearly overcome the baseline reduction in one-carbon metabolism (Figures 2.3, 2.4, and 2.5). However, when examining the gain and loss of function experiments performed in vitro, where nutrient levels are abundant and identical, PGC-1α/ERRα levels are inversely correlated with one-carbon metabolism and cell proliferation. Indeed, cells overexpressing PGC-1α display a reduction in one-carbon metabolism and a reduction in proliferation, whereas cells with reduced levels of PGC-1α/ERRα display an increase in one-carbon metabolism and an increase in proliferation (Figure 2.4; Figure S2.5).

The sensitivity to anti-folate treatment was correlated with PGC-1α/ERRα expression levels rather than with proliferation capacities. Indeed, cells overexpressing PGC-1α proliferate less and are more sensitive to MTX in vitro (Figure 2.5A), although they form larger tumors that are also more sensitive to MTX in vivo (Figures 2.5E and 2.5F). Hence, the relative growth capacity of these cells does not determine their MTX sensitivity. Clearly, the PGC-1α/ERRα-dependent metabolic programs that confer a growth advantage to PGC-1α overexpressing tumors

can no longer counterbalance for the inhibition of folate cycle metabolism in the presence of MTX; hence, these tumors lose their growth advantage (Figure 2.6).

Overall, our results may have potentially significant clinical implications because they suggest that patients with tumors expressing high levels of PGC-1α/ERRα may be particularly sensitive to MTX treatment. Importantly, subsets of melanomas (Vazquez et al., 2013) and prostate tumors (Tennakoon et al., 2014) with elevated levels of PGC-1α have been defined, and our data suggest that these cancer patients may benefit from anti-folate therapy. In that context, it is also tempting to speculate that AMPK activators, such as AICAR or metformin, could be used to sensitize cancer patients to adjuvant treatments targeting the folate pathway.

2.7 CONCLUSION

This work elucidates the importance of the PGC-1α/ERRα partnership as key effectors of AMPK signalling. Firstly, the role of this transcriptional complex in regulating mitochondrial bioenergetics upon AMPK activation was validated in HER2+ breast cancer cells. Furthermore, activation of AMPK caused increased binding of ERRα to the promoters of several *MTHFD* genes, thereby triggering an inhibition of one-carbon metabolism. In addition, the PGC-1α/ERRα complex also decreases the activity of the de novo purine biosynthesis pathway. Perturbation of these metabolic pathways by the PGC-1α/ERRα axis promotes the sensitivity of breast cancer cells and tumours to methotrexate, implicating PGC-1α/ERRα as a key determinant of folate cycle metabolism.

2.8 EXPERIMENTAL PROCEDURES

2.8.1 Cell Lines and Reagents

BT474 and SKBR3 cell lines were purchased from ATCC and cultured as previously described (Deblois et al., 2009). NT2196-PGC-1α and control NT2196 stable cell lines were cultured and prepared as previously described (Ursini-Siegel et al., 2007; Klimcakova et al., 2012). AMPK null MEFs were a generous gift from Dr. Arnim Pause's laboratory (McGill University; Yan et al., 2014). AICAR, metformin, and MTX were purchased from Sigma. A769662 was purchased from Abcam.

2.8.2 siRNA Transfection

Cells were transfected immediately upon seeding with either control siRNA (siC) (Dharmacon), an siRNA pool targeting ESRRA (siERRα) (ON-TARGETplus siRNA pool, Dharmacon), an siRNA pool targeting PPARGC1A (siPGC-1α) (QIAGEN), or both siPGC-1α and siERRα (siPGC-1α/siERRα) using HiPerFect reagent (QIAGEN) or calcium phosphate. Cells were transfected for 36 hr, and then they were treated with AICAR, A769662, MTX, or the corresponding vehicle for 24 to 96 hr.

2.8.3 Microarray Analysis

BT474 cells were treated with 0.5 mM AICAR for 1 day or 4 days, and RNA was extracted and purified using an Aurum Total RNA Mini Kit (Bio-Rad). RNA was hybridized to GeneChip Human Genome U133 Plus 2.0 (Affymetrix) and quantified at Génome Québec Innovation Centre (McGill University). The expression data were analyzed using FlexArray10 software. Microarray data are available in the GEO database (GEO: GSE75877).

2.8.4 qRT-PCR

RNA was extracted and purified using the RNeasy Mini Kit (QIAGEN) or the Aurum Total RNA Mini Kit (Bio-Rad) following the manufacturers' protocols. Reverse transcriptase reactions were performed using SuperScript II (Invitro- gen) or iScript cDNA Synthesis Kit (Bio-Rad). Samples were then analyzed by qRT-PCR with SYBR-green-based qRT-PCR with a LightCycler 480 instrument (Roche) or a MyiQ2 Real-Time Detection System (Bio-Rad). Gene-specific primers are found in Table S2.1.

2.8.5 ChIP-Seq and ChIP-qPCR

BT474, SKBR3, or MEFs were plated 24 hr in complete media before being treated with fresh media containing 0.5 mM AICAR or vehicle for 90 min. Cells were then cross-linked with 1% formaldehyde, and ChIP-qPCR or ChIP-seq were performed as previously described (Chaveroux et al., 2013) with an anti-ERRα rabbit antibody (Abcam 2131) or a control anti-rabbit IgG antibody (Sigma-Aldrich 10500C). Pathway analyses were performed with Ingenuity Pathways Analysis software (Ingenuity Systems [IPA]) using genes with peaks found within ± 20 kb of the transcription start site to study significantly enriched pathways. Gene-specific primers are found in Table S2.2.

2.8.6 Western Blotting

Protein extracts were prepared using lysis buffer (50 mmol/L Tris-HCl [pH 7.4], 1% Triton X-100, 0.25% sodium deoxycholate, 150 mmol/L NaCl, 1 mmol/L EDTA) or buffer K (Chaveroux et al., 2013) supplemented with protease and phosphatase inhibitors. Immunoblots were incubated with the following primary antibodies from Cell Signalling Technology: pAMPK (2531), AMPK (2532), pACC (3661), ACC (3662), Caspase 3 (9662); from Santa Cruz: Actin

(sc-1616); from Abcam: MTHFD1 (ab103698), ERRα (ab2131), MTHFD1L (ab153840), PGC-1α (ab54481); from Bethyl Laboratories: ATIC (A304- 271A-T) and GART (A304-311A-T); and from Cedarlane: α-tubulin (CLT- 9002). The results were visualized with Western Lightning Plus-ECL (PerkinElmer) and analyzed with ImageJ software (NIH).

2.8.7 Respiration

Cellular respiration was determined as described previously (Fantin et al., 2006). BT474 and SKBR3 cells were treated for 96 hr with 0.5 mM and 0.25 mM AICAR, respectively.

2.8.8 Stable Isotope Tracing Experiments and Metabolite Quantification

Intratumoral glucose and glutamine levels, as well as stable isotope tracer analyses, were determined at the Metabolomics Core Facility of the Goodman Cancer Research Centre using standard protocols (see the Supplemental Experimental Procedures).

2.8.9 BrdU Assay

The BrdU assay was conducted using the 5-Bromo-20-deoxy-uridine labeling and detection kit III (Roche) according to the manufacturer's instructions.

2.8.10 Xenograft Assays

For in vivo xenograft experiments, $5x10^4$ cells re-suspended in 30 ml of sterile PBS were injected on each side of the mouse in the mammary gland fat pad of 5- to 7-week-old SCID/BEIGE mice (Taconic). Control or PGC-1α overexpressing cells (PGC-1α), derived from NT2196 as previously described (Klimcakova et al., 2012), were injected in the left or right mammary fat pad, respectively. Following cell injection, tumor growth was monitored twice a week with calipers. I.P. injections of MTX (5.56 mg/kg) were given twice a week when tumors

on both sides reached a volume of at least 0.1 cm3. Tumor monitoring was continued twice a week, and animals were sacrificed when the total tumor volume reached 1.5 cm3. Tumors were excised, weighed, and flash frozen in liquid nitrogen for subsequent analyses. All animal studies were approved by the McGill University Animal Care Committee.

2.9 SUPPLEMENTAL FIGURES

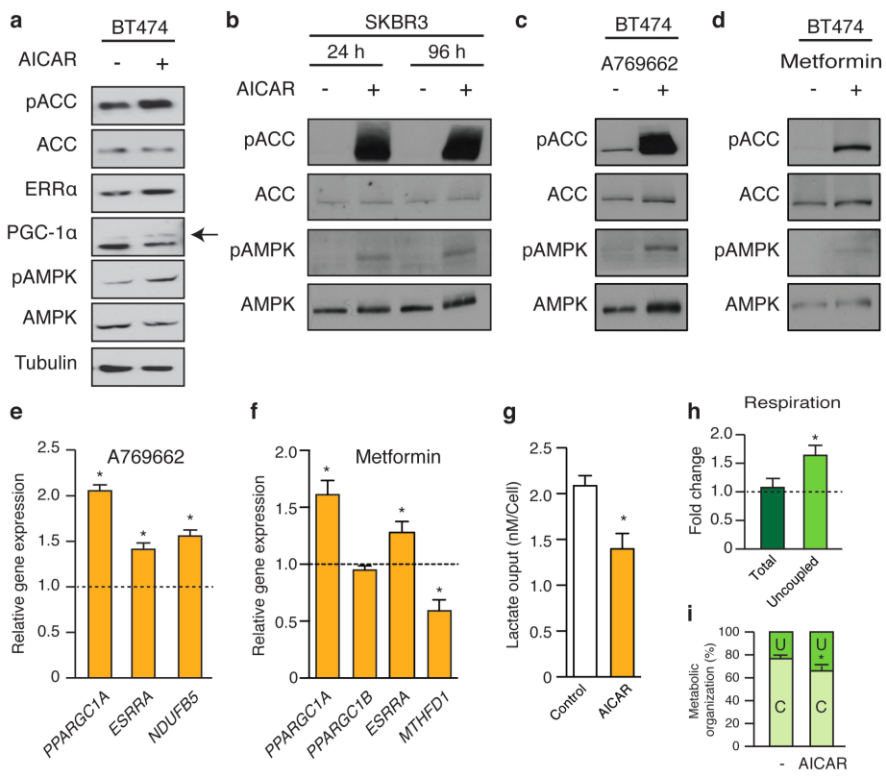

Figure S2.1. AMPK activation increases the expression of the PGC-1α/ERRα axis to promote mitochondrial activity and inhibit expression of folate cycle genes in breast cancer cells

(A) Immunoblots of phosphorylated-ACC (S79), total ACC, phosphorylated-AMPKα (T172), total AMPKα, PGC-1α (arrow), and ERRα in BT474 cells treated with AICAR or vehicle for 48h

(B) Immunoblots of phosphorylated-ACC (S79), total ACC, phosphorylated-AMPKα (T172), and total AMPKα in SKBR3 cells treated with 0.25 mM AICAR or vehicle for 24 h and 96 h.

(C-D) Immunoblots of phosphorylated-ACC (S79), total ACC, phosphorylated-AMPKα (T172), and total AMPKα in BT474 cells treated with 0.15 mM A769662 (C) or 2 mM metformin (D) for 96 h.

(E) Expression of PPARGC1A, ESRRA and NDUFB5 in BT474 cells treated with 0.15 mM A769662 for 96 h relative to vehicle (n=3) (dashed line).

(F) Expression of PPARGC1A, PPARGC1B, ESRRA, and MTHFD1 in BT474 cells treated with 2 mM metformin for 96 h relative to vehicle (n=3) (dashed line).

(G) Lactate production from BT474 cells treated with AICAR or vehicle for 96 h (n=5).

(H) Total (T) and uncoupled (U) respiration of SKBR3 cells treated with 0.25 mM AICAR for 96 h, normalized to that of SKBR3 cells treated with vehicle (n=5) (dashed line).

(I) Percentage of uncoupled and coupled respiration of the cells in (h) (n=5). Data from panels E-I are presented as means + SEM, * $p<0.05$, Student's t-test.

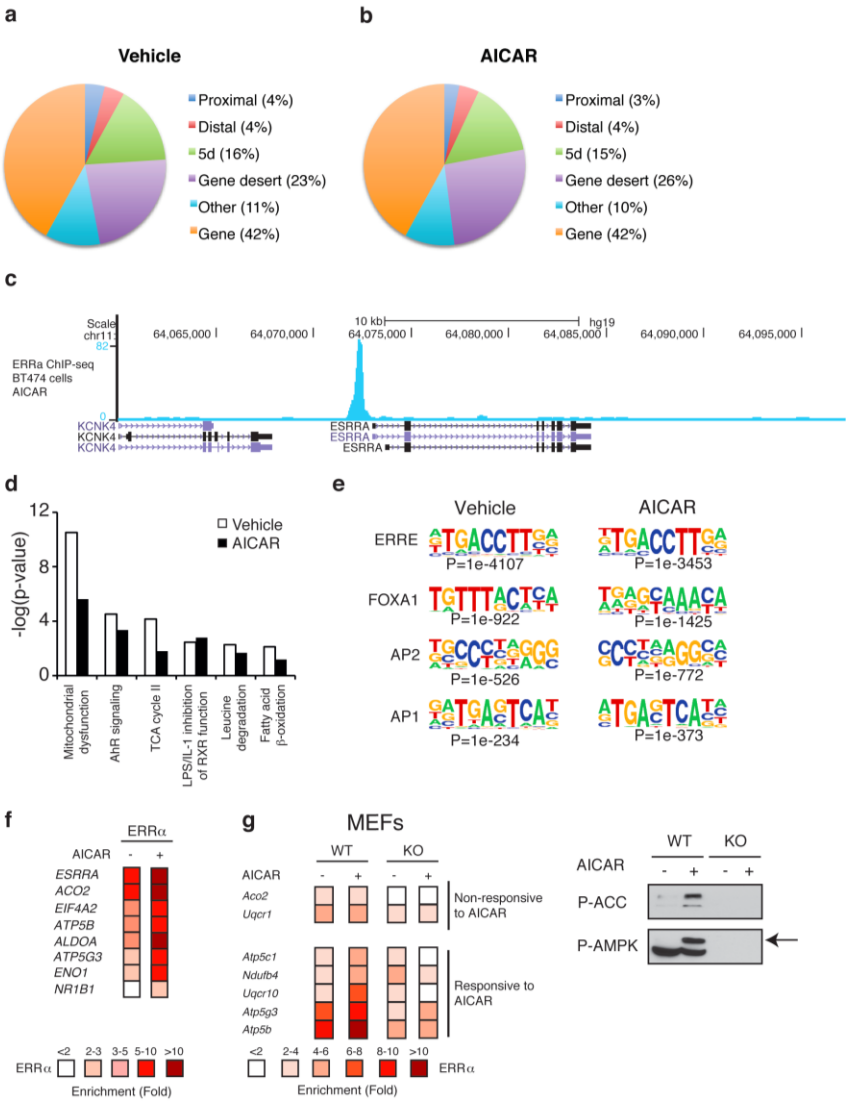

Figure S2.2. AMPK activation induces ERRα DNA binding

(A-B) Location analysis of binding sites identified in BT474 cells treated with vehicle (A) or

AICAR (B) for 90 min.

(C) UCSC browser view of ERRα binding at its own promoter (ESRRA) in BT474 cells treated with AICAR for 90 min.

(D) Major enriched canonical pathways identified by IPA analysis of ERRα targets found within ± 20 kb relative to the TSS of the nearest gene (a value over 1.3 indicates significance with $p<0.05$) as identified using Ingenuity Pathway Analysis.

(E) Top de novo enriched motifs in ERRα ChIP-seq in BT474 cells treated with AICAR or vehicle for 90 min.

(F) Standard ChIP-qPCR of ERRα binding at various ERRα target genes in SKBR3 cells treated with AICAR or vehicle for 90 min. Data are presented as the average of 2 independent experiments.

(G) ChIP-qPCR of ERRα binding at various ERRα metabolic target genes in wild-type (WT) or AMPK null (KO) MEFs treated with AICAR or vehicle for 90 min. Data are presented as the average of 3 independent experiments (left panel). Immunoblots of phosphorylated-ACC (S79) and phosphorylated-AMPKα (T172) for the WT and KO MEFs (right panel).

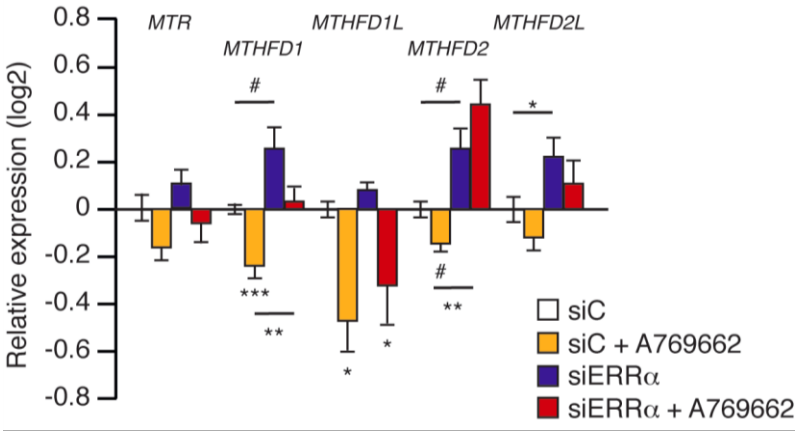

Figure S2.3. ERRα represses folate cycle and purine biosynthesis genes following AMPK activation.

Expression of MTR, MTHFD1, MTHFD1L, MTHFD2 and MTHFD2L in BT474 cells transfected with non-targeted siRNA (siC) or siERRα, then treated with 0.15 mM A769662 or vehicle for 24 h (n=3). Data are presented as means + SEM, # $p<0.10$; *$p<0.05$; ** $p<0.01$; *** $p<0.001$ compared with siC or as indicated (Student's t-test).

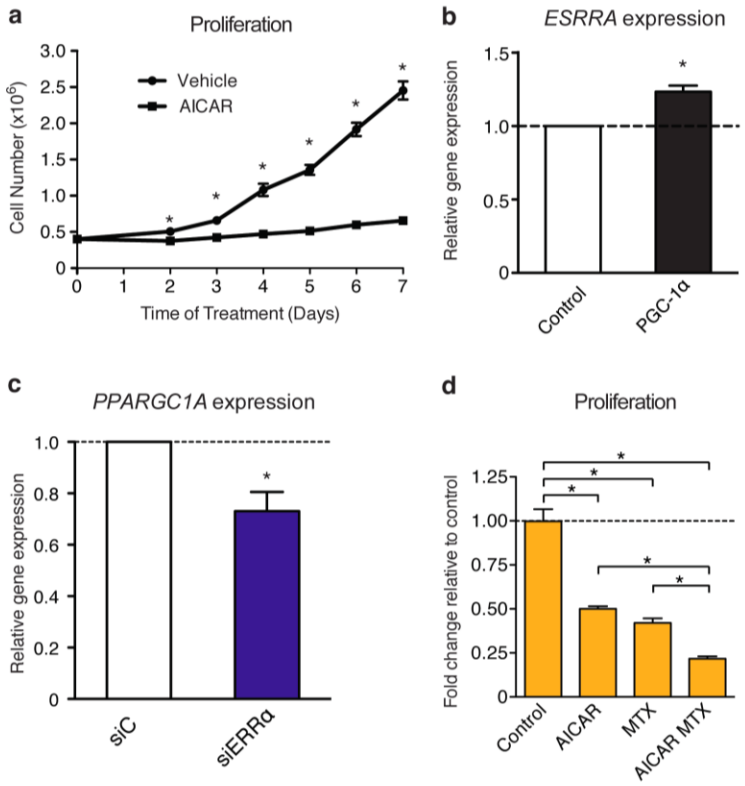

Figure S2.4. The AMPK/PGC-1α/ERRα axis inhibits de novo purine biosynthesis and sensitizes breast cancer cells to methotrexate

(A) Proliferation of BT474 cells treated with 0.5 mM AICAR or vehicle for up to 7 days (n=3). Data are presented as means ±SEM, * $p<0.05$, Student's t-test.

(B) ESRRA expression in NT2196 cells overexpressing PGC-1α, relative to control NT2196 cells (n=3). Data are presented as means + SEM * $p<0.05$, Student's t-test.

(C) PPARGC1A expression in BT474 cells transfected with siC or siERRα, relative to siC (n=3). Data are presented as means + SEM * $p<0.05$, Student's t-test.

(D) Cell counts for BT474 cells treated with AICAR, MTX, or a combination of both. 200 000 cells were plated at day 0 and treated with 0.5 mM AICAR or vehicle (control) for 96 h. Then, both control and AICAR treated cells were either treated with 2.5 uM MTX or vehicle for 72 h. Cells were counted after 7 days (n=4). Data are presented as means + SEM * $p<0.05$, Student's t-test.

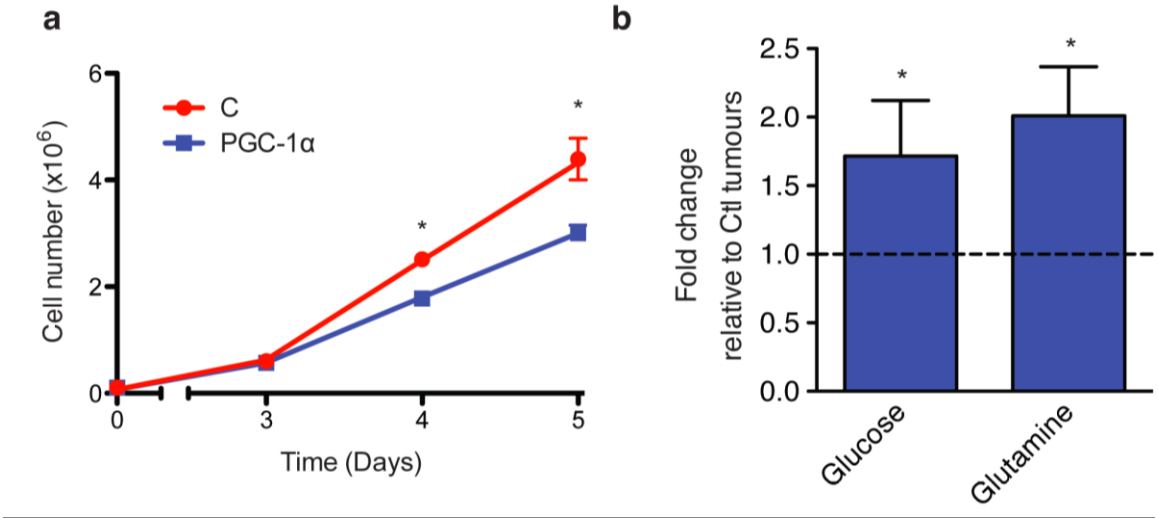

Figure S2.5. NT2196 cells overexpressing PGC-1α proliferate less in vitro, and generate tumors with elevated nutrient levels compared with controls

(A) Proliferation of NT2196 cells overexpressing PGC-1α compared with controls in vitro (n=3). 20 000 cells were plated at day 0. Data are presented as means +/- SEM *p<0.05, Student's t-test.

(B) Glucose and glutamine levels in PGC-1α overexpressing tumors relative to those in control tumors (dashed line) (n=5). Data are presented as means + SEM, * p<0.05, Student's t-test.

Table S1: List of Human and Mouse Primers used for qRT-PCR

Human Primers

Gene Symbol	Full Gene Name	Forward Primer	Reverse Primer	Reference
PPARGC1A	peroxisome proliferator-activated receptor gamma coactivator 1 alpha	CCTGTGATGCTTTTGCTGCTCTTG	AAACTATCAAAATCCAGAGAGTCA	(Eichner et al., 2010)
PPARGC1B	peroxisome proliferator-activated receptor gamma coactivator 1 beta	GTACATTCAAAATCTCTCCAGCGACATG	GAGGGCTCGTTGCGCTTCCTCAGGGCAG	(Eichner et al., 2010)
ESRRA	estrogen-related receptor alpha	GCTGCCCTGCTGCAACTAGTG	GCCGCCGCTCAGCACCCCCTC	(Eichner et al., 2010)
ESRRG	estrogen-related receptor gamma	CTGGTAAAGAAATACAAGAGCATGAAGC	CAGCATCTTGCCAGCTCGACGAGGGTCT	(Eichner et al., 2010)
UCP2	uncoupled protein 2	CTCGTAATGCCATTGTCAACTGTG	AGAAGGGAGCCTCTCGGGAAGTGC	(Eichner et al., 2010)
UCP3	uncoupled protein 3	ACAGATGTCGTCAAGGTCCGATTT	GGTAGTCCAGCAGCTTCTCCTTGA	(Eichner et al., 2010)
NDUFB5	NADH dehydrogenase (ubiquinone) 1 beta subcomplex, 5,	CCGAAGGCTGCTGCTCCTGT	TCCCAGTGTTCTGGGACATAGCCT	This study
CS	citrate synthase	CAACTCAGGACGGGTTGTTCCAGG	GTAGTAATTCATCTCCGTCATGCC	(Eichner et al., 2010)
IDH1	isocitrate dehydrogenase 1	ACCAATCCCATTGCTTCCATTTTT	TCAAGTTTTCTCCAAGTTTATCCA	(Eichner et al., 2010)
FH	fumarate hydratase	CCATGTTGCTGTCACTGTCGGAGG	CATACCCTATATGAGGATTGAGAG	(Eichner et al., 2010)
MDH2	mitochondrial malate dehydrogenase	GCTCTGCCACCCTCTCCATG	TTTGCCGATGCCCAGGTTCTTCTC	(Eichner et al., 2010)
MTHFD1	methylenetetrahydrofolate dehydrogenase (NADP+ dependent) 1, methenyltetrahydrofolate cyclohydrolase, formyltetrahydrofolate synthetase	TTGTTGGCCCAGAAGGGTTT	CTGACAGTGGCAACAAGCAC	This study
MTHFD1L	methylenetetrahydrofolate dehydrogenase (NADP+ dependent) 1-like	AGGTGTCAACCTAGATGGAAAGA	GCTTTGAAGCTGGCGTGTTT	This study
MTHFD2	methylenetetrahydrofolate dehydrogenase (NADP+ dependent) 2, methenyltetrahydrofolate cyclohydrolase	TTCTGGAAGGAAACTGGCCC	TTCTCGCCAACCAGGATCAC	This study
MTHFD2L	methylenetetrahydrofolate dehydrogenase (NADP+ dependent) 2-like	CACCCCCAAAGAGCAACTGA	TCCTGTCACTGGATCGTGGA	This study
MTR	5-methyltetrahydrofolate-homocysteine methyltransferase	TCTCAAGCCCTGGCGATTTT	ATTGAGGCGGGGGTGTAAAG	This study
DHFR	dihydrofolate reductase	GGAGGAGGTGGATTTCAGGC	CATCCTTGCCCTGCCATGT	This study
DHFRL1	dihydrofolate reductase-like 1	CATTGTCCCGCTGAGAGCTT	GGGAGCTAAGCCTCTTCGAC	This study
PPAT	phosphoribosyl pyrophosphate amidotransferase	GATCACTCTGGGACTCGTG	TACAAGACCCATTCCCTTGTG	This study
ATIC	5-aminoimidazole-4-carboxamide ribonucleotide formyltransferase/IMP cyclohydrolase	CCATGCTGGAATCCTAGCTC	ACAGTTACACCTGGAGAAGC	This study
GART	phosphoribosylglycinamide formyltransferase, phosphoribosylglycinamide synthetase, phosphoribosylaminoimidazole synthetase	GAATGGGAGCCTATTGTCCA	TCCAGCATAGAGAATACCTGT	This study
Pum1	pumilio RNA-binding family member 1	ACGGATTCGAGGCCACGTCC	CATTAATTACCTGCTGGTCTGAAGGA	This study
TBP	TATA box binding protein	TGCCACGCCAGCTTCGGAGA	ACCGCAGCAAACCGCTTGGG	This study

Gene Symbol	Full Gene Name	Forward Primer	Reverse Primer	Reference
PPAT	phosphoribosyl pyrophosphate amidotransferase	ATGTGATCACTCTGGGACTC	CAAGACCCATTCCCTTATGC	This study
ATIC	5-aminoimidazole-4-carboxamide ribonucleotide formyltransferase/IMP cyclohydrolase	CAGAGAAGTGTCGGATGGTA	TCATCTGGTTTGTAGGACTGG	This study
GART	phosphoribosylglycinamide formyltransferase, phosphoribosylglycinamide synthetase, phosphoribosylaminoimidazole synthetase	GAAAGGACTCGCTGCTCTAA	AGTCCTTGTAAGTCAAGCCC	This study
TBP	TATA box binding protein	ACCTTATGCTCAGGGCTTGG	GCCATAAGGCATCATTGGAC	(Klimcakova, et al. 2012)
RPLP0	ribosomal protein, large, P0	TGATCATCCAGCAGGTGTTT	CATTGATGATGGAGTGTGGC	This study

Table S2.1: List of Human and Mouse Primers used for qRT-PCR

Table S2: List of Human and Mouse Primers used for ChIP

Human Primers				
Gene Symbol	Full Gene Name	Forward Primer	Reverse Primer	Reference
MTHFD1	methylenetetrahydrofolate dehydrogenase (NADP+ dependent) 1, methenyltetrahydrofolate cyclohydrolase, formyltetrahydrofolate synthetase	TGGGTATCGTTGCCAGCTTT	ACGGGTGATGTGAAAGGTCC	This study
MTHFD1L	methylenetetrahydrofolate dehydrogenase (NADP+ dependent) 1-like	TTAAGGGAAGGGCAGTGCAG	CCTATTCCAGCCCAAGGCAA	This study
MTHFD2	methylenetetrahydrofolate dehydrogenase (NADP+ dependent) 2, methenyltetrahydrofolate cyclohydrolase	ACTGCGGTTCAGTTGAGGTT	AGCCACAGAGAATACCAACCA	This study
MTHFD2L	methylenetetrahydrofolate dehydrogenase (NADP+ dependent) 2-like	GCAGATATTTTGCTTCCTCACCA	AGGAGCAAAACCTGGCTGAA	This study
ESRRA	estrogen-related receptor alpha	ATGCATGGTCCGTGAGTCAG	ATTGCGAGTCCCGGAAGGTA	This study
ACO2	aconitase 2, mitochondrial	CCAACTTCTCGTGTACCTGTCCCGGT	CAAAAAGAAGAAAGAGGTGCCTTCG	(Deblois et al., 2010)
Mir145	microRNA 145	CCCAGGCTGAATCCCAGTG	CCTGACAACAGTGAGGCTGA	This study
PPP2CB	protein phosphatase 2, catalytic subunit, beta isozyme	TTTTGGAGGCCGAGGCAG	CAGTCTCCTGAGTAGCTGAGAC	This study
PRKAA2 #1	protein kinase, AMP-activated, alpha 2 catalytic subunit	GGAGCATTTTAAAGCCCCACT	GCCATCTCTCATGAGTTTTTCCA	This study
PRKAA2 #3	protein kinase, AMP-activated, alpha 2 catalytic subunit	GGTGAGAAAACTAGGACCCCT	TGAAGGAATCTGGGGATGGC	This study
EPN3	epsin 3	GAAACCCTTGCTGGGGATGA	GGCACGGAGTATCAGCTCTC	This study
CTCFL	CCCTC-binding factor (zinc finger protein)-like	ATTGTGGACTTCTGGCCTCC	GGAATTTGCACACAGCCCAG	This study
NT5C3A	5'-nucleotidase, cytosolic IIIA	ACACCCTGAGTTCTTCTGTCC	GGCATCTCTGGGTAGTGCTT	This study
ELAC1	elaC ribonuclease Z 1	TTTACAAGCAGGAGCCACCG	AACCCCGGGGGCATATTAGA	This study
ODAM #1	odontogenic, ameloblast asssociated	CCCAGGGCAGATCTTCACAA	TTGCTTGGGTCCTTCACACA	This study
ODAM #3	odontogenic, ameloblast asssociated	GAAGGGCAGTCTGGGAACAG	CTGAAGAATGCTGCGTGCTC	This study
ANXA1	annexin A1	AGCACAATTGCTGGATTGCAT	AGTCAGCGAATGACTTGGTG	This study
RNF113B	ring finger protein 113B	GCCTCTCCTGGAGTCTTTGG	CCAGGCTGCAGTTAAGCAAC	This study
RPTOR	regulatory associated protein of MTOR, complex 1	GACCGCTCTGAGGAGGTTTG	CATCAGCCCATCAAGGAGGA	This study
TXNIP	thioredoxin interacting protein	AGCACTCTCCTCCCTCTCTT	CAACTGTGCACACAACCAGG	This study
EIF4A2	eukaryotic translation initiation factor 4A2	GGATCATGTCTGGTGGCTCC	CCTCCGTGCCATCCACTATC	This study
ACSL4	acyl-CoA synthetase long-chain family member 4	GCTATGTCCTGTCTGAGCCC	AGCCATGCACCTCTTTGTGT	This study
EIF2B5	eukaryotic translation initiation factor 2B, subunit 5 epsilon, 82kDa	TATGGGACCCCACTCCTACC	GGGGACAAAAAGGATCCAGC	This study
ACPL2	2-phosphoxylose phosphatase 1	CACTCCACCTCCATCCCCTA	AGCCTCCTTTGTCCCGTACT	This study
EIF3F	eukaryotic translation initiation factor 3, subunit F	CAGCAGGAGAAATCCAGCTAAG	CGGAGGTCGAAATTCGTGTT	This study

Negative regions	Forward Primer	Reverse Primer	Reference
ESRRA (negative)	GTGGCCCACAGGTGTCGCTCAAGTCTTC	GGATGCAGTGTCCTTCTCCCCAGATTG	(Deblois et al., 2010)
Chr17 #3	TGCTACTCCTGGGGTGCTGGACTGTC	AGTCAGAAGGCCTGGCTCCAGATCAG	(Deblois et al., 2010)
Chr 17#2	ACAAAGGGAATAAGCAATCTGGCATA	TCGGCTCCAACTCAACTCGTCTATGT	(Deblois et al., 2010)
EP300	AATGAATTGGCGAGAGGTTG	AAACCTCACTCCTGCCACAC	(Charos et al., 2012)

Mouse Primers				
Gene Symbol	Full Gene Name	Forward Primer	Reverse Primer	Reference
Uqcr1		TCTTGCAATGGTCGCCTTCT	CACTTACCGTGCAGGTAGCA	This study
Atp5c1		ACCCAGCAAAGAGTCGGATG	GGAGCACAGCTTGCAAAGTC	This study
Ndufb4		CAGTCCAGGGTGGGTTCTTC	GGGGCGTAGCTAGGGAAATG	This study
Uqcr10		TGGAGTGGTTCAGACCCGTA	AGGGAGGTAGGACGGAACTC	This study
Atp5g3		CAAGGGTGAAGGAGAGCCG	CTGTCACCTAGATCCACGCC	This study
Atp5b		TCTTCTCCCCGTGACCTTGA	AAATGGGACGCTGCTGGTTA	This study
Ep300 (negative)		TCCATACCGAACAAAGGCCC	CAATCCCCTTGCCATTCCCT	This study
p21 (negative)		GGGATCCAACTCCTGGCTTC	TCCGTTAATATAGCGCTTGCC	This study

Table S2.2: List of Human and Mouse Primers used for ChIP

2.10 SUPPLEMENTAL EXPERIMENTAL PROCEDURES

Stable isotope tracing experiments and metabolite quantification

BT474 and NT2196 cells were incubated for 16 h in full media containing 800 μM Lserine. The following day, media were replaced with full media containing 400 μM Lserine and 400 μM $_{13}C_{3}{}_{15}N$-L-serine (Sigma, 608130) for 8 h (dynamic labeling range for AMP, SAM and ATP). Cells were rinsed twice with cold 150 mM ammonium formate solution pH 7.4 and quenched

using dry ice cold 80 % methanol solution. Extracts were transferred in pre-chilled tubes on dry ice and kept at -80 $_{o}$C. Following equilibration at 4$_{o}$C, 3 ceramic beads (2.8 mm, VWR, 19-646-3) were added to each tube which werevortexed at maximal speed for 1 min and sonicated for 5 minutes at high setting using a cold sonicator (Biorupter, Diagenone), with 30 sec on and 30 sec off intervals. Samples were separated using dichloromethane phase extraction. The aqueous phase was preserved and allowed to dry entirely using a centrivap cold trap (Labconco).

Relative quantitation of metabolites was determined for m+0 and m+(1-5) isotopomers using an Agilent 6540 UHD Accurate-Mass Q-TOF mass spectrometer (Agilent Technologies, Santa Clara, CA, USA) equipped with a 1290 Infinity ultraperformance LC system (Agilent Technologies). Analyte ionization was accomplished using ESI in positive mode. The source operating conditions were set at 325 °C and 9l/min for gas temperature and flow respectively, nebulizer pressure was set at 40 psi and capillary voltage was set a 4.0 kV. Reference masses 121.0509 and 922.0099 were introduced into the source through a secondary spray nozzle to ensure accurate mass. MS data were acquired in full scan mode mass range: m/z 100-1000; scan time: 1.4 sec; data collection: centroid and profile modes. Retention times, accurate masses, and MS/MS (collision energies: 10, 20, 30, 40 V) for each compound were confirmed against authentic standards (Sigma-Aldrich Co., Oakville, Ontario, Canada), as well as matched unlabelled cell extracts. For ATP measurements, chromatographic separation was performed on a Scherzo SM-C18 column 3 μm, 3.0Å~150 mm (Imtakt Corp, JAPAN). The chromatographic gradient started at 100 % mobile phase A (5 mM ammonium acetate in water) with a 5 min gradient to 100 % mobile phase B (200 mM ammonium acetate in 20% ACN/80 % water) at a flow rate of 0.4 mL/min. This was followed by a 5 min hold time and a subsequent 6 min re-equilibration before next injection. AMP measurements were performed on a ZORBAX SB-Aq

column 1.8 µm, 2.1Å~50 mm (Agilent Technologies), starting with 100% mobile phase A (0.2 % formic acid in water) for 2 min followed by an 8 min linear gradient to 100 % mobile phase B (0.2 % formic acid in MeOH) followed by a 5 min washing time. SAM measurements were performed on an Intrada Amino Acid column 3 µm, 3.0Å~150 mm (Imtakt Corp, JAPAN). The chromatographic gradient started at 100 % mobile phase B (0.3 % formic acid in ACN) with a 3 min linear gradient up to 73 % mobile phase B, followed by a 20 min linear gradient to 100 % mobile phase A (100 mM ammonium formate in ACN/water (80/20)) at a flow rate of 0.6 mL/min, followed by a 6 min hold. Injection volume was 5 µL. The column temperatures were all maintained at 10 °C. Metabolite level were quantified by integrating the area under the curve of each compound (MRM transitions or accurate mass) using MassHunter Quant (Agilent Technologies, Santa Clara, CA, USA). Each metabolite's accurate mass ion and subsequent isotopic ions were extracted (EIC) using a 10 ppm window. Stable isotope tracer analyses were done as previously described (McGuirk et al., 2013). Abundances of naturally occurring stable isotopes were removed using in-house algorithm to generate correction matrices specific for the analyzed metabolites.

2.11 AUTHOR CONTRIBUTIONS

Conceptualization and design, E.A.-W., D.J.P., V.G., and J.St-P.; Development of methodology, E.A.-W., D.J.P., S.P.G., and G.B.; Acquisition of data, E.A.-W., D.J.P., T.Y., S.P.G., and G.B.; Analysis and interpretation of data, E.A.-W., D.J.P., S.P.G., M.C., G.B., V.G., and J.St-P.; Writing of the manuscript, E.A.-W., D.J.P., V.G., and J.St-P.;Study supervision, V.G. and J.St-P.

2.12 ACCESSION NUMBERS

The accession number for the microarray data reported in this paper is GEO: GSE75877.

2.13 ACKNOWLEDGMENTS

The authors wish to thank Geneviève Deblois and Catherine Dufour for discussions concerning ChIP-seq, Carlo Ouellet for mouse husbandry, and Ingrid Tam for helpful insights. The authors also thank the Goodman Cancer Research Centre Metabolomics Core Facility, particularly Thierry Ntimbane, and Daina Avizonis for technical assistance. D.J.P. is a recipient of doctoral scholarships from the Fonds de Recherche du Québec – Santé (FRQS), the McGill Integrated Cancer Research Training Program (MICRTP), and the Michael D'Avirro Fellowship in Molecular Oncology (McGill University). E.A.W. is a recipient of postdoctoral fellowships from the Canadian Institutes of Health Research (CIHR), FRQS, and MICRTP. T.Y. was a recipient of a summer MICRTP studentship. J.St-P. is an FRQS Research Scholar. This research was funded by grants from CIHR (MOP-273977 to G.B., MOP-64275 to V.G., and MOP-106603 to J.St-P.) and the Terry Fox Research Institute (TFF-116128 to J.St-P., V.G., and Metabolomics Core).

2.14 COPYRIGHT

Cell Reports Volume 14, Issue 4, 2 February 2016, Pages 920-931

doi: 10.1016/j.celrep.2015.12.086

2.15 REFERENCES

Arany, Z., Foo, S.Y., Ma, Y., Ruas, J.L., Bommi-Reddy, A., Girnun, G., Cooper, M., Laznik, D., Chinsomboon, J., Rangwala, S.M., et al. (2008). HIF-independent regulation of VEGF and angiogenesis by the transcriptional coactivator PGC-1α. Nature 451, 1008–1012.

Ariazi, E.A., Clark, G.M., and Mertz, J.E. (2002). Estrogen-related receptor α and estrogen-related receptor γ associate with unfavorable and favorable bio-markers, respectively, in human breast cancer. Cancer Res. 62, 6510–6518.

Ariazi, E.A., Kraus, R.J., Farrell, M.L., Jordan, V.C., and Mertz, J.E. (2007). Estrogen-related receptor α1 transcriptional activities are regulated in part via the ErbB2/HER2 signalling pathway. Mol. Cancer Res. 5, 71–85.

Barry, J.B., and Giguère, V. (2005). Epidermal growth factor-induced signalling in breast cancer cells results in selective target gene activation by orphan nuclear receptor estrogen-related receptor α. Cancer Res. 65, 6120–6129.

Bianco, S., Sailland, J., and Vanacker, J.M. (2012). ERRs and cancers: effects on metabolism and on proliferation and migration capacities. J. Steroid Bio- chem. Mol. Biol. 130, 180–185.

Chang, C.Y., Kazmin, D., Jasper, J.S., Kunder, R., Zuercher, W.J., and McDonnell, D.P. (2011). The metabolic regulator ERRα, a downstream target of HER2/IGF-1R, as a therapeutic target in breast cancer. Cancer Cell 20, 500–510.

Charest-Marcotte, A., Dufour, C.R., Wilson, B.J., Tremblay, A.M., Eichner, L.J., Arlow, D.H., Mootha, V.K., and Giguère, V. (2010). The homeobox protein Prox1 is a negative modulator of ERRα/PGC-1α bioenergetic functions. Genes Dev. 24, 537–542.

Charos, A.E., Reed, B.D., Raha, D., Szekely, A.M., Weissman, S.M., Snyder, M. (2012). A highly integrated and complex PPARGC1A transcription factor binding network in HepG2 cells. Genome Res. 22, 1668–1679

Chaveroux, C., Eichner, L.J., Dufour, C.R., Shatnawi, A., Khoutorsky, A., Bourque, G., Sonenberg, N., and Giguère, V. (2013). Molecular and genetic cross- talks between mTOR and ERRα are key determinants of rapamycin-induced nonalcoholic fatty liver. Cell Metab. 17, 586–598.

Cool, B., Zinker, B., Chiou, W., Kifle, L., Cao, N., Perham, M., Dickinson, R., Adler, A., Gagne, G., Iyengar, R., et al. (2006). Identification and characterization of a small molecule AMPK activator that treats key components of type 2 diabetes and the metabolic syndrome. Cell Metab. 3, 403–416.

Corton, J.M., Gillespie, J.G., Hawley, S.A., and Hardie, D.G. (1995). 5-amino-imidazole-4-carboxamide ribonucleoside. A specific method for activating AMP-activated protein kinase in intact cells? Eur. J. Biochem. 229, 558–565.

Deblois, G., and Giguère, V. (2013). Oestrogen-related receptors in breast cancer: control of cellular metabolism and beyond. Nat. Rev. Cancer 13, 27–36.

Deblois, G., Hall, J.A., Perry, M.C., Laganière, J., Ghahremani, M., Park, M., Hallett, M., and Giguère, V. (2009). Genome-wide identification of direct target genes implicates estrogen-related receptor α as a determinant of breast cancer heterogeneity. Cancer Res. 69, 6149–6157.

Deblois, G., Chahrour, G., Perry, M.C., Sylvain-Drolet, G., Muller, W.J., and Giguère, V. (2010). Transcriptional control of the ERBB2 amplicon by ERRα and PGC-1β promotes mammary gland tumorigenesis. Cancer Res. 70, 10277–10287.

Deblois, G., St-Pierre, J., and Giguère, V. (2013). The PGC-1/ERR signalling axis in cancer. Oncogene 32, 3483–3490.

Dufour, C.R., Wilson, B.J., Huss, J.M., Kelly, D.P., Alaynick, W.A., Downes, M., Evans, R.M., Blanchette, M., and Giguère, V. (2007). Genome-wide orchestration of cardiac functions by the orphan nuclear receptors ERRα and γ. Cell Metab. 5, 345–356.

Eichner, L.J., Perry, M.-C., Dufour, C.R., Bertos, N., Park, M., St-Pierre, J., Giguère, V. (2010). miR-378* Mediates Metabolic Shift in Breast Cancer Cells via the PGC-1β/ERRγ Transcriptional Pathway. Cell Metab. 12, 352-361.

Eichner, L.J., and Giguère, V. (2011). Estrogen related receptors (ERRs): a new dawn in transcriptional control of mitochondrial gene networks. Mitochondrion 11, 544–552.

Fan, J., Ye, J., Kamphorst, J.J., Shlomi, T., Thompson, C.B., and Rabinowitz, J.D. (2014). Quantitative flux analysis reveals folate-dependent NADPH production. Nature 510, 298–302.

Fantin, V.R., St-Pierre, J., and Leder, P. (2006). Attenuation of LDH-A expression uncovers a link between glycolysis, mitochondrial physiology, and tumor maintenance. Cancer Cell 9, 425–434.

Fox, M.M., Phoenix, K.N., Kopsiaftis, S.G., and Claffey, K.P. (2013). AMP-activated protein kinase α 2 isoform suppression in primary breast cancer alters AMPK growth control and apoptotic signalling. Genes Cancer 4, 3–14.

Giguère, V. (2008). Transcriptional control of energy homeostasis by the estrogen-related receptors. Endocr. Rev. 29, 677–696.

Gravel, S.P., Hulea, L., Toban, N., Birman, E., Blouin, M.J., Zakikhani, M., Zhao, Y., Topisirovic, I., St-Pierre, J., and Pollak, M. (2014). Serine deprivation enhances antineoplastic activity of biguanides. Cancer Res. 74, 7521–7533.

Hadad, S.M., Fleming, S., and Thompson, A.M. (2008). Targeting AMPK: a new therapeutic opportunity in breast cancer. Crit. Rev. Oncol. Hematol. 67, 1–7.

Handschin, C., and Spiegelman, B.M. (2006). Peroxisome proliferator-activated receptor gamma coactivator 1 coactivators, energy homeostasis, and metabolism. Endocr. Rev. 27, 728–735.

Handschin, C., Rhee, J., Lin, J., Tarr, P.T., and Spiegelman, B.M. (2003). An autoregulatory loop controls peroxisome proliferator-activated receptor gamma coactivator 1a expression in muscle. Proc. Natl. Acad. Sci. USA 100, 7111–7116.

Hardie, D.G., Ross, F.A., and Hawley, S.A. (2012). AMPK: a nutrient and energy sensor that maintains energy homeostasis. Nat. Rev. Mol. Cell Biol. 13, 251–262.

Herzog, B., Cardenas, J., Hall, R.K., Villena, J.A., Budge, P.J., Giguère, V., Granner, D.K., and Kralli, A. (2006). Estrogen-related receptor α is a repressor of phosphoenolpyruvate carboxykinase gene transcription. J. Biol. Chem. 281, 99–106.

Huang, B., Cheng, X., Wang, D., Peng, M., Xue, Z., Da, Y., Zhang, N., Yao, Z., Li, M., Xu, A., and Zhang, R. (2014). Adiponectin promotes pancreatic cancer progression by inhibiting apoptosis via the activation of AMPK/Sirt1/PGC-1α signalling. Oncotarget 5, 4732–4745.

Jäger, S., Handschin, C., St-Pierre, J., and Spiegelman, B.M. (2007). AMP-activated protein kinase (AMPK) action in skeletal muscle via direct phosphorylation of PGC-1α. Proc. Natl. Acad. Sci. USA 104, 12017–12022.

Klimcakova, E., Chénard, V., McGuirk, S., Germain, D., Avizonis, D., Muller, W.J., and St-Pierre, J. (2012). PGC-1α promotes the growth of ErbB2/Neu- induced mammary tumors by regulating nutrient supply. Cancer Res. 72, 1538–1546.

Labuschagne, C.F., van den Broek, N.J., Mackay, G.M., Vousden, K.H., and Maddocks, O.D. (2014). Serine, but not glycine, supports one-carbon metabolism and proliferation of cancer cells. Cell Rep. 7, 1248–1258.

Laderoute, K.R., Calaoagan, J.M., Chao, W.R., Dinh, D., Denko, N., Duellman, S., Kalra, J., Liu, X., Papandreou, I., Sambucetti, L., and Boros, L.G. (2014). 5`-AMP-activated protein kinase (AMPK) supports the growth of aggressive experimental human breast cancer tumors. J. Biol. Chem. 289, 22850–22864.

Laganie` re, J., Tremblay, G.B., Dufour, C.R., Giroux, S., Rousseau, F., and Giguère, V. (2004). A polymorphic autoregulatory hormone response element in the human estrogen related receptor a (ERRα) promoter dictates PGC-1α control of ERRα expression. J. Biol. Chem. 279, 18504–18510.

Locasale, J.W. (2013). Serine, glycine and one-carbon units: cancer metabolism in full circle. Nat. Rev. Cancer 13, 572–583.

Locasale, J.W., and Cantley, L.C. (2011a). Genetic selection for enhanced serine metabolism in cancer development. Cell Cycle 10, 3812–3813.

Locasale, J.W., and Cantley, L.C. (2011b). Metabolic flux and the regulation of mammalian cell growth. Cell Metab. 14, 443–451.

Maddocks, O.D., Berkers, C.R., Mason, S.M., Zheng, L., Blyth, K., Gottlieb, E., and Vousden, K.H. (2013). Serine starvation induces stress and p53-dependent metabolic remodelling in cancer cells. Nature 493, 542–546.

McGuirk, S., Gravel, S.-P., Deblois, G., Papadopoli, D.J., Faubert, B., Wegner, A., Hiller, K., Avizonis, D., Akavia, U.D., Jones, R.G., et al. (2013). PGC-1α supports glutamine metabolism in breast cancer. Cancer Metab. 1, 22.

Mootha, V.K., Lindgren, C.M., Eriksson, K.F., Subramanian, A., Sihag, S., Lehar, J., Puigserver, P., Carlsson, E., Ridderstråle, M., Laurila, E., et al. (2003). PGC-1 alpha-responsive genes involved in oxidative phosphorylation are coordinately downregulated in human diabetes. Nat. Genet. 34, 267–273.

Mootha, V.K., Handschin, C., Arlow, D., Xie, X., St Pierre, J., Sihag, S., Yang, W., Altshuler, D., Puigserver, P., Patterson, N., et al. (2004). ERRα and GABPAα/β specify PGC-1α-dependent oxidative phosphorylation gene expression that is altered in diabetic muscle. Proc. Natl. Acad. Sci. USA 101, 6570–6575.

Munzone, E., Curigliano, G., Burstein, H.J., Winer, E.P., and Goldhirsch, A. (2012). CMF revisited in the 21st century. Ann. Oncol. 23, 305–311.

Nilsson, R., Jain, M., Madhusudhan, N., Sheppard, N.G., Strittmatter, L., Kampf, C., Huang, J., Asplund, A., and Mootha, V.K. (2014). Metabolic enzyme expression highlights a key role for MTHFD2 and the mitochondrial folate pathway in cancer. Nat. Commun. 5, 3128.

Schreiber, S.N., Emter, R., Hock, M.B., Knutti, D., Cardenas, J., Podvinec, M., Oakeley, E.J., and Kralli, A. (2004). The estrogen-related receptor alpha (ERRα) functions in PPARγ coactivator 1a (PGC-1α)-induced mitochondrial biogenesis. Proc. Natl. Acad. Sci. USA 101, 6472–6477.

St-Pierre, J., Lin, J., Krauss, S., Tarr, P.T., Yang, R., Newgard, C.B., and Spiegelman, B.M. (2003). Bioenergetic analysis of peroxisome proliferator-activated receptor gamma coactivators 1 alpha and 1 beta (PGC-1 alpha and PGC-1 beta) in muscle cells. J. Biol. Chem. 278, 26597–26603.

St-Pierre, J., Drori, S., Uldry, M., Silvaggi, J.M., Rhee, J., Jäger, S., Handschin, C., Zheng, K., Lin, J., Yang, W., et al. (2006). Suppression of reactive oxygen species and neurodegeneration by the PGC-1 transcriptional coactivators. Cell 127, 397–408.

Summermatter, S., Santos, G., Pérez-Schindler, J., and Handschin, C. (2013). Skeletal muscle PGC-1α controls whole-body lactate homeostasis through estrogen-related receptor α-dependent activation of LDHB and repression of LDHA. Proc. Natl. Acad. Sci. USA 110, 8738–8743.

Tedeschi, P.M., Markert, E.K., Gounder, M., Lin, H., Dvorzhinski, D., Dolfi, S.C., Chan, L.L., Qiu, J., DiPaola, R.S., Hirshfield, K.M., et al. (2013). Contribution of serine, folate and glycine metabolism to the ATP, NADPH and purine requirements of cancer cells. Cell Death Dis. 4, e877.

Tennakoon, J.B., Shi, Y., Han, J.J., Tsouko, E., White, M.A., Burns, A.R., Zhang, A., Xia, X., Ilkayeva, O.R., Xin, L., et al. (2014). Androgens regulate prostate cancer cell growth via an AMPK-PGC-1α-mediated metabolic switch. Oncogene 33, 5251–5261.

Ursini-Siegel, J., Rajput, A.B., Lu, H., Sanguin-Gendreau, V., Zuo, D., Papava- siliou, V., Lavoie, C., Turpin, J., Cianflone, K., Huntsman, D.G., and Muller, W.J. (2007). Elevated expression of DecR1 impairs ErbB2/Neu-induced mammary tumor development. Mol. Cell. Biol. 27, 6361–6371.

Vazquez, F., Lim, J.H., Chim, H., Bhalla, K., Girnun, G., Pierce, K., Clish, C.B., Granter, S.R., Widlund, H.R., Spiegelman, B.M., and Puigserver, P. (2013). PGC1α expression defines a subset of human melanoma tumors with increased mitochondrial capacity and resistance to oxidative stress. Cancer Cell 23, 287–301.

Villena, J.A., and Kralli, A. (2008). ERRα: a metabolic function for the oldest orphan. Trends Endocrinol. Metab. 19, 269–276.

Wang, R., Li, J.J., Diao, S., Kwak, Y.D., Liu, L., Zhi, L., Buëler, H., Bhat, N.R., Williams, R.W., Park, E.A., and Liao, F.F. (2013). Metabolic stress modulates Alzheimer's β-secretase gene transcription via SIRT1-PPARg-PGC-1 in neurons. Cell Metab. 17, 685–694.

Wende, A.R., Huss, J.M., Schaeffer, P.J., Giguère, V., and Kelly, D.P. (2005). PGC-1α coactivates PDK4 gene expression via the orphan nuclear receptor ERRα: a mechanism for transcriptional control of muscle glucose metabolism. Mol. Cell. Biol. 25, 10684–10694.

Wu, Z., Puigserver, P., Andersson, U., Zhang, C., Adelmant, G., Mootha, V., Troy, A., Cinti, S., Lowell, B., Scarpulla, R.C., and Spiegelman, B.M. (1999). Mechanisms controlling mitochondrial biogenesis and respiration through the thermogenic coactivator PGC-1. Cell 98, 115–124.

Yan, M., Gingras, M.C., Dunlop, E.A., Nouët, Y., Dupuy, F., Jalali, Z., Possik, E., Coull, B.J., Kharitidi, D., Dydensborg, A.B., et al. (2014). The tumor suppressor folliculin regulates AMPK-dependent metabolic transformation. J. Clin. Invest. 124, 2640–2650.

CHAPTER 3:

Methotrexate mediates an AMPK-dependent metabolic response in cancer cells

David J. Papadopoli[1,2], Eric Ma[2,3], Dominic Roy[3], Gaëlle Bridon[3], Daina Avizonis[3], Russell G. Jones[2,3], and Julie St-Pierre[1,4,5]*

[1]Department of Biochemistry, McGill University, Montreal, QC, H3G 1Y6, Canada

[2]Goodman Cancer Centre, Montréal, QC, H3A 1A3, Canada

[3]Department of Physiology, McGill University, Montreal, QC, H3G 1Y6, Canada

[4]Departments of Biochemistry, Microbiology and Immunology, University of Ottawa, Ottawa, ON, K1H 8M5, Canada

[5]Ottawa Institute of Systems Biology, University of Ottawa, Ottawa, ON, K1H 8M5, Canada

*Correspondence: julie.st-pierre@mcgill.ca (J.S.-P.)

3.1 OBJECTIVES OF THIS CHAPTER:

1) Identify the metabolic determinants of methotrexate response
2) Elucidate how methotrexate affects metabolic processes
3) Determine how methotrexate response could be improved

3.2 SUMMARY

One-carbon metabolism fuels the high demand of cancer cells for nucleotides and other building blocks needed for increased proliferation. This metabolic pathway has been targeted in the clinic through the use of antifolate chemotherapy, such as methotrexate. Although antifolates are widely used to treat many cancer subtypes, our ability to predict response remains unclear. Here, we show that methotrexate treatment leads to increased intracellular concentration of the

metabolite AICAR, which activates AMPK. Methotrexate-induced AMPK activation leads to decreased one-carbon metabolism gene expression and proliferation and increased bioenergetic capacity. The antiproliferative and respiratory effects of methotrexate are AMPK-dependent, and as a result, cells with reduced AMPK activity are less sensitive to methotrexate treatment. Conversely, the combination of methotrexate with biguanides, which activate AMPK, improves the antiproliferative response of methotrexate in cancer cells. These data implicate AMPK activation as a metabolic determinant of methotrexate response, which can be exploited using clinical therapeutics, such as biguanides, to enhance the antineoplastic activity of methotrexate.

3.3 INTRODUCTION

Cell growth and proliferation requires the production of numerous macromolecules. One-carbon metabolism covers a complex metabolic network important for the production of many macromolecules including nucleotides, lipids, reducing power, and substrates for methylation reactions (Deberardinis et al., 2008; Locasale, 2013). Indeed, many genetic and functional studies have highlighted the importance of this pathway, along with hyperactivation of serine/glycine biosynthesis, in driving tumourigenesis (DeBerardinis, 2011; Ducker and Rabinowitz, 2017). Enzymes of the mitochondrial folate pathway, such as MTHFD2, which are normally low or absent in normal adult tissues, are highly upregulated in cancer and are negatively correlated with survival in breast cancer patients (Nilsson et al., 2014). Also, enzymes implicated in serine biosynthesis, such as PHGDH, are upregulated in triple-negative breast cancer and melanoma (Locasale et al., 2011; Possemato et al., 2011), and SHMT2 expression and glycine consumption correlate with cancer cell proliferation and poor prognosis (Jain et al., 2012; Kim et al., 2015; Lee et al., 2014). In support of this point, a recent report showed that

patients with high expression of mitochondrial one-carbon metabolism genes have shorter overall survival rate compared to patients with low expression of these genes (Koseki et al., 2018). As the mitochondrial one-carbon metabolism pathway produces most of the formate used to fuel nucleotide biosynthesis (Ducker et al., 2016), there is much interest in targeting this pathway as a potential route for improving cancer therapy.

The importance of one-carbon metabolism in cancer was initially recognized over 60 years ago. In 1948, Sydney Farber discovered that treatment of patients with a folic acid antagonist, aminopterin, produced temporary remission in children with acute lymphoblastic leukemia (ALL) (Farber and Diamond, 1948). This landmark paper led the way for the development of a class of drugs called antifolates, with methotrexate (MTX) being the most well known. MTX is still being used as frontline chemotherapy for various cancers, including acute lymphoblastic leukemia, breast cancer, bladder cancer, lymphomas, among others (Chabner and Roberts, 2005). Although MTX can be used as a single agent, such as to treat choriocarcinoma (Hertz et al., 1956), it is most often used in combination with cyclophosphamide and 5-fluorouracil as part of the CMF treatment for breast cancer (Munzone et al., 2012). MTX inhibits dihydrofolate reductase (DHFR), an enzyme required to produce tetrahydrofolate (THF), which is a cofactor for one-carbon units needed to build nucleotides (Hitchings and Burchall, 1965). MTX also inhibits 5-aminoimidazole-carboxyamide ribonucleotide formyltransferase (ATIC) and thymidylate synthetase (TYMS), which are enzymes of the purine and pyrimidine biosynthesis pathways respectively (Chabner et al., 1985). Despite its wide use as a cancer therapeutic, methotrexate can have high toxicity by targeting metabolic enzymes found in both transformed and non-transformed cells, which reduces its therapeutic index (Howard et al., 2016; Tennant et al., 2010). As a result, the identification of cancer-specific metabolic activity, as well as

determining the metabolic effects caused by methotrexate are both useful in designing new therapeutic strategies to treat cancer.

In this study, we uncovered the importance of AMP-activated protein kinase (AMPK) activation in controlling the metabolic and anti-proliferative effects of methotrexate. Recently, we linked AMPK activation to the PGC-1α/ERRα axis in the repression of one-carbon metabolism, specifically through inhibition of the expression of several folate and purine metabolism enzymes(Audet-Walsh et al., 2016). Here, we show that methotrexate treatment increases the intracellular concentration of the metabolite AICAR which activates AMPK, which elevates bioenergetic capacity and induces proliferation. The translational impact of this data is underlined by the fact that clinically used biguanides, which activate AMPK, enhance the antineoplastic activity of methotrexate, which we propose as an innovative strategy for improving cancer treatment.

3.4 RESULTS

3.4.1 Methotrexate induces AMPK signalling. To study the effect of methotrexate on metabolism, we used the human breast cancer cell line, BT-474, and murine embryonic fibroblasts (MEFs). Given that methotrexate inhibits purine biosynthesis, we first quantified the levels of metabolic intermediates in this pathway upon treatment. MTX caused a strong increase (~30 fold) in endogenous AICAR levels (Figure 3.1A) (Figure S3.1A), with little effect on the downstream metabolites IMP and AMP, indicating a blockage in de novo purine biosynthesis the ATIC step. AICAR is used as a compound to activate AMPK in various cell models (Audet-Walsh et al., 2016; Yan et al., 2014), hence we assessed whether the increase in AICAR levels

upon methotrexate treatment was sufficient to promote AMPK activation. MTX treatment increased the phosphorylation of Ser^{79} on acetyl-CoA carboxylase (pACC) (Hardie, 2013a), and the phosphorylation of Thr^{172} on AMPK, indicating that AMPK is activated. PGC-1α signalling is a known downstream effector of AMPK activation in both non-transformed and transformed cells (Audet-Walsh et al., 2016; Chaube et al., 2015; Jager et al., 2007). Accordingly, MTX treatment increased the expression of *PPARGC1A* and its partner *ESRRA*, indicating that MTX upregulates the PGC-1α/ERRα axis (Figure 3.1C). In addition, MTX also decreases the expression of *MTHFD1L* (Figure 3.1C), a folate cycle gene that is repressed by AMPK/PGC-1α/ERRα signalling (Audet-Walsh et al., 2016). Collectively, these data show that MTX treatment enhances AMPK signalling.

3.4.2 Methotrexate promotes AMPK-dependent oxidative metabolism. To test the biological implications of AMPK activation upon MTX treatment, we performed respirometry experiments. In accordance with the role of AMPK in promoting catabolic reactions, MTX increased cellular respiration, including the respiration linked to ATP synthesis (coupled respiration) and the respiration linked to proton leak (uncoupled respiration) (Figure 3.2A)(Figure S3.1B-G). To formally quantify the impact of MTX modulates on cellular bioenergetics, we performed Seahorse analyses using recently published algorithms (Mookerjee et al., 2017). MTX treatment increased total ATP production (J ATP total) largely due to increase in oxidative phosphorylation (J ATP ox), with a small contribution from glycolysis (J ATP glyc) (Figure 3.2B). In accordance with higher oxidative metabolism, MTX treatment also increased bioenergetic capacity (Figure 3.2C-D). To determine if the MTX-induced increase in oxidative metabolism was AMPK-dependent, MEF cells deficient for AMPKα1/2 and wild-type (WT)

controls were treated with MTX. Similar to BT-474 cells, WT MEF cells displayed increased total, uncoupled and coupled respiration upon methotrexate treatment (Figure 3.2 E, F-H blue bars). In contrast, AMPK null MEF cells showed no significant increase in oxidative metabolism (Figure 3.2E, F-H purple bars). Taken together, these results demonstrate that MTX promotes cellular respiration in an AMPK-dependent manner.

3.4.3 Methotrexate exerts antineoplastic effects in an AMPK-dependent manner. It is well established that MTX acts as an antifolate agent as a mean of inhibiting cellular proliferation (Shuvalov et al., 2017). Given that AMPK-mediated metabolic reprogramming has previously been shown to impact proliferation and tumour growth (Faubert et al., 2013; Faubert et al., 2015), we tested if the antiproliferative effect of methotrexate is reliant on AMPK. AMPK null MEF cells were less responsive to methotrexate treatment than WT controls (Figure 3.3A-C). To test if the antiproliferative effects could be observed in cancer cells, we used an AMPKα1/α2 hairpin construct (shAMPK) targeting AMPK in R5 lymphoma cells. Knockdown of AMPK decreased the anti-proliferative effects of MTX compared to controls (Figure 3.3D-F). Together, these results indicate that the growth inhibitory effects of MTX are partially dependent on AMPK.

3.4.4 Co-treatment with biguanides potentiates the antineoplastic effect of methotrexate. Cancer cells are dependent on one-carbon metabolism to help build de novo nucleotides (Locasale, 2013). Recently, we have shown that one-carbon metabolism is inhibited through activation of AMPK/PGC-1α/ERRα signalling, resulting in increased sensitivity to MTX (Audet-Walsh et al., 2016). In addition, the AMPK/PGC-1α/ERRα axis is activated by treatment with

biguanides (Figure S2.1 of this thesis, Corominas-Faja et al., 2012; Zakikhani et al., 2006; Zakikhani et al., 2008). To investigate whether co-treatment with biguanides can potentiate the anti-proliferative effects of MTX, cells were treated with phenformin for 24 hours then treated with MTX for 72 hours. Cells treated with both phenformin and methotrexate demonstrated lower cell counts than methotrexate alone (Figure 3.4A-B), suggesting that activation of AMPK pharmacologically can further boost methotrexate response in cancer cells.

3.5 FIGURES

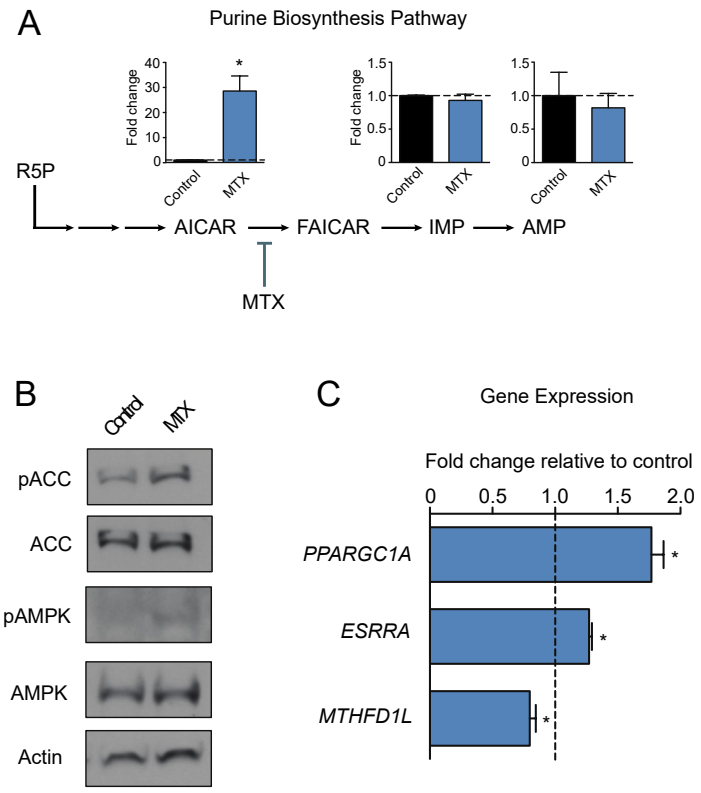

Figure 3.1: Methotrexate activates AMPK signalling through AICAR induction.

(A) Analysis of purine metabolites (AICAR, IMP, AMP) following treatment with 0.1µM MTX (blue) or control (black) for 72 hours in BT-474 cells, normalized to control treatment (dashed line) (n=3).

(B) Immunoblots of phosphorylated-ACC (Ser79), total ACC, phosphorylated-AMPKα, total AMPK, or Actin in BT-474 cells treated with 0.1µM MTX or control for 72 hours (n=4).

(C) Expression of *PPARGC1A*, *ESRRA* and *MTHFD1L* in BT-474 cells treated with 0.1µM MTX (blue) or control for 72 hours, normalized to control treatment (dashed line) (n=3). All data are presented as means + SEM, *p<0.05, Student's *t* test

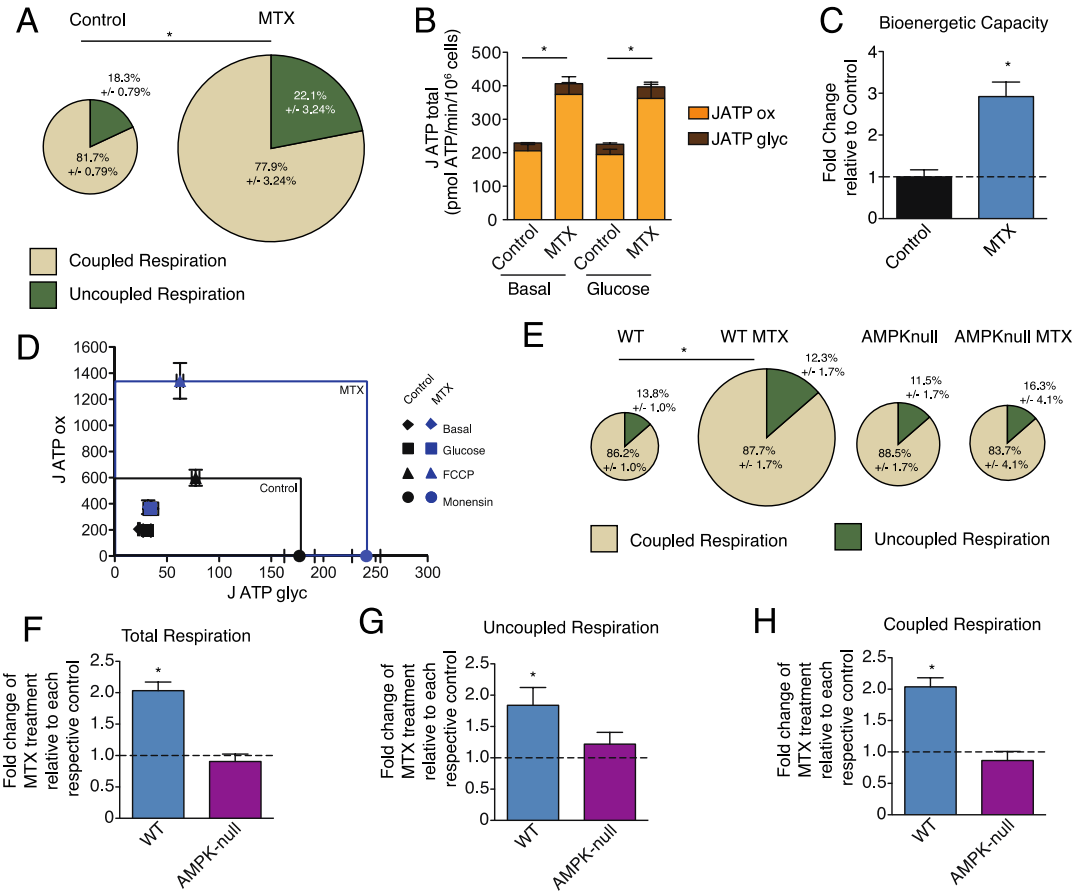

Figure 3.2: Methotrexate promotes cellular respiration and increases bioenergetic capacity in an AMPK-dependent manner.

(A) Respiration in BT-474 cells treated with 0.1µM MTX or control for 72 hours. Size of chart indicates fold change of total respiration, while % of coupled respiration (beige) and uncoupled respiration (green) are shown (n=4).

(B) Measurement of total ATP production (J ATP total) for BT-474 cells treated with 0.1µM MTX or control for 72 hours under basal conditions (minimal XF media) as well as after addition of 10mM glucose using Seahorse XF Extracellular Analyser. J ATP total is the sum of J ATP ox (oxidative phosphorylation) (orange) and J ATP glyc (glycolysis) (brown) (n=3).

(C) Measurement of bioenergetic capacity in BT-474 cells treated with 0.1µM MTX (blue) or control (black), compared to control treatment (dashed line) (n=3).

(D) Bioenergetic capacity of BT-474 cells treated with 0.1µM MTX (blue box/data points) or control (black box/data points). Data points represent J ATP values as a function of J ATP glyc (x-axis) and J ATP ox (y-axis) after the following additions: basal (diamond), glucose (square), FCCP (triangle), monensin (circle). Box signifies the size of theoretical bioenergetic space that can be occupied by each condition (n=3).

(E) Respiration of WT and AMPK-null MEFs treated with 0.02μM MTX or control for 72 hours. Size of chart indicates fold change of total respiration, while % of coupled respiration (beige) and uncoupled respiration (green) are shown (n=4).

(F-H) Total, uncoupled, and coupled respiration of WT MEF cells treated with MTX (blue) and AMPK null MEF cells treated with MTX (purple) compared to each respective control (dashed line) (n=4). All data are presented as means + SEM, *p<0.05, Student's *t* test for (A-C) and (F-H), two-way ANOVA for (E).

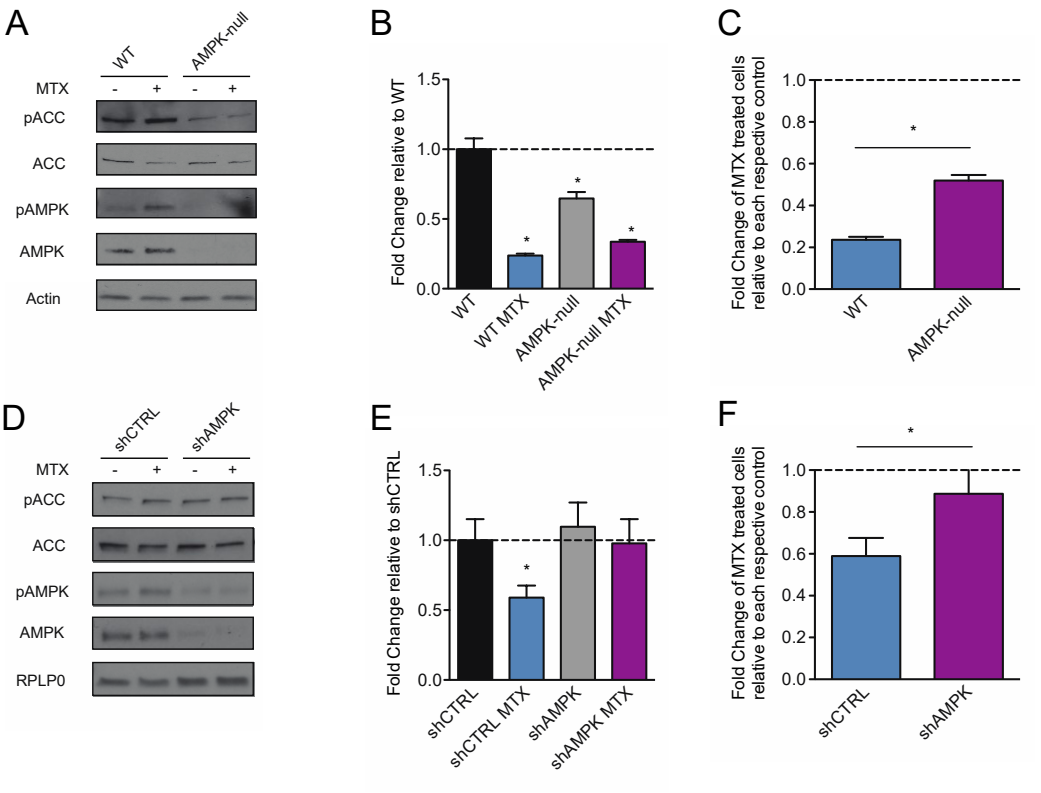

Figure 3.3: Methotrexate decreases cellular proliferation in an AMPK-dependent manner.

(A) Immunoblots of phosphorylated-ACC (Ser79), total ACC, phosphorylated-AMPKα (T172), total AMPK, or Actin in WT and AMPK-null MEF cells treated with 0.05uM MTX or control for 72 hours (n=3).

(B) Cell proliferation of WT and AMPK-null MEF cells treated with 0.05uM MTX (blue for WT, purple for AMPK-null) or control (black for WT, grey for AMPK-null) for 72 hours compared to WT control (dashed line) (n=3).

(C) Cell proliferation of WT and AMPK-null MEF cells treated with MTX compared to each respective control (dashed line) (n=3).

(D) Immunoblots of phosphorylated-ACC (Ser79), total ACC, phosphorylated-AMPKα (T172), total AMPK, or RPLP0 in R5 lymphoma cells transfected with shCTRL or shAMPK and treated with 2nM MTX or control for 72 hours (n=3).

(E) Cell proliferation of R5 lymphoma cells transfected with shCTRL or shAMPK treated with 2nM MTX (blue for shCTRL, purple for shAMPK) or control (black for shCTRL, grey for shAMPK) for 72 hours compared to shCTRL control (dashed line) (n=4).

(F) Cell proliferation of R5 lymphoma cells transfected with shCTRL (blue) or shAMPK (purple) and treated with MTX compared to each respective control (dashed line) (n=4). All data are presented as means + SEM, *p<0.05, two-way ANOVA for (B,E).

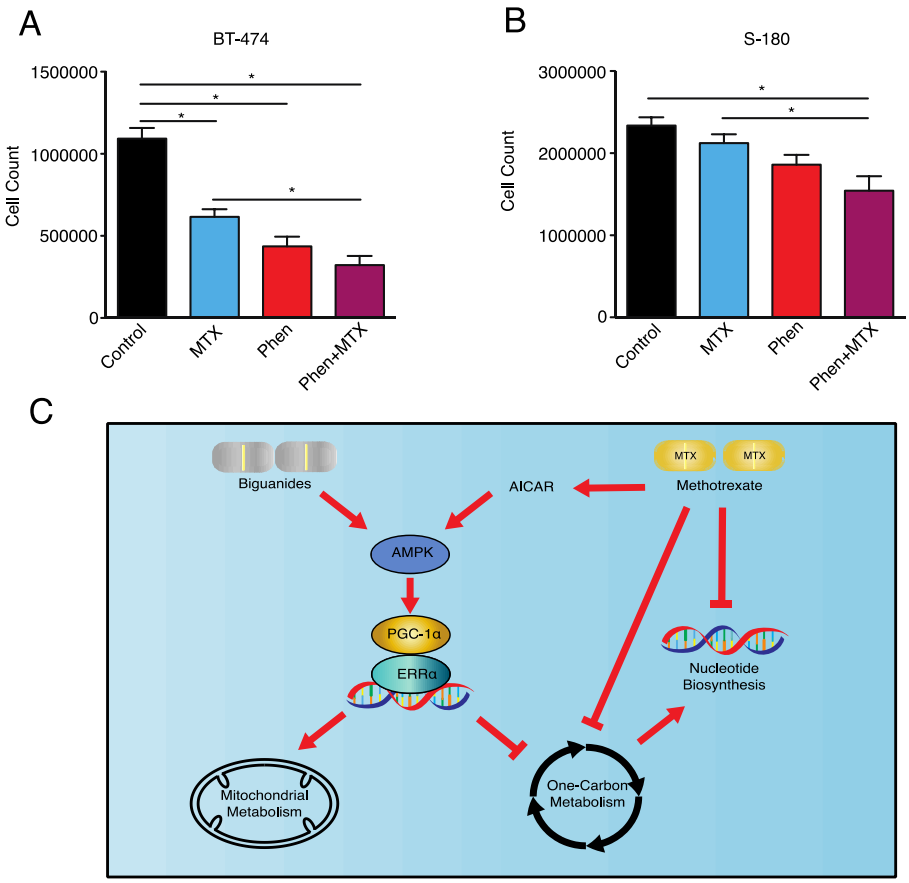

Figure 3.4: Phenformin treatment improves MTX response.

(A) Cell proliferation of BT-474 cells treated with 0.02mM phenformin for 24 hours, then treated with 0.02mM phenformin and 0.1µM MTX for 72 hours (n=5).

(B) Cell proliferation of sarcoma-180 (S-180) cells treated with 0.01mM phenformin for 24 hours, then treated with 0.01mM phenformin and 0.01µM MTX for 72 hours (n=7).

(C) Schematic indicating AMPK signalling plays a functional role upon biguanide and methotrexate treatments. All data are presented as means + SEM, *p<0.05, one-way ANOVA.

3.6 DISCUSSION

In this study, we report that AMPK plays a critical role in regulating MTX response. MTX treatment induces an AICAR-mediated increase in AMPK signalling, which decreased one-carbon metabolism gene expression (Figure 3.4C). The biological significance of MTX-mediated induction of AMPK signalling entailed the activation of bioenergetic functions including elevated cellular respiration and boosted bioenergetic capacity. The clinical relevance of these data is illustrated by the fact that phenformin improves the antiproliferative response of methotrexate, signifying the importance of regulating cancer metabolism to improve chemotherapeutic action.

MTX is a potent inhibitor of one-carbon metabolism and nucleotide biosynthesis. Consequently, MTX treatment causes an accumulation of AICAR, due to the diminished availability of one-carbon units for further de novo purine biosynthesis (Cronstein et al., 1993). The buildup of AICAR is sufficient to activate AMPK (Beckers et al., 2006; Fodor et al., 2016; Pirkmajer et al., 2015; Tedeschi et al., 2015). The MTX-induced AMPK promotes glucose uptake and lipid oxidation (Pirkmajer et al., 2015), as well as the inhibition of protein synthesis (Tedeschi et al., 2015). Here, we show that MTX not only increases cellular respiration, but also elevates bioenergetic capacity, mainly due to an increase in ATP generation from oxidative phosphorylation (J ATP ox). Thus, MTX increases mitochondrial functions, which is a characteristic of reverting Warburg metabolism.

AMPK can have both anti-Warburg and antiproliferative effects (Faubert et al., 2013). MTX increased cellular bioenergetics and decreased proliferation, both of which were dependent on AMPK. Recently, our group showed that the AMPK/PGC-1α/ERRα complex can inhibit one-

carbon metabolism and purine biosynthesis, resulting in decreased proliferation (Audet-Walsh et al., 2016). Seeing that the antiproliferative effects of MTX are linked to AMPK activity, we show in this study that phenformin treatment can improve the antiproliferative response of MTX. This is line with reports that show that pharmacological AMPK activation with AICAR is synergetic with MTX treatment (Beckers et al., 2006). However, given that AICAR has poor bioavailability (Dixon et al., 1991) and the main effector is AMPK, combining MTX with AMPK activators that have higher bioavailability, such as biguanides, may prove to be an effective option in the clinic.

There has been increased interest in repurposing biguanides for cancer treatment. Indeed, both phenformin and metformin display antineoplastic effects in several cancer subtypes including breast, prostate, and colorectal cancers, of which include both AMPK-dependent and AMPK-independent effects (Griss et al., 2015; Mallik and Chowdhury, 2018). Despite these successes, clinical trials regarding biguanide treatment in cancer have been inconclusive so far (Mallik and Chowdhury, 2018). Seeing that biguanides and MTX both share a common effector in AMPK, the combination of both drugs may have strong clinical implications in improving AMPK-dependent antineoplastic response.

Overall, our results highlight the importance of AMPK in mediating chemosensitivity. Importantly, the data suggest that AMPK activators should be encouraged as neoadjuvant therapy to improve chemotherapeutic response. Future work regarding the impact of AMPK activators on other antifolate/antimetabolite-based therapy is warranted.

3.7 CONCLUSION

This chapter underlies the significance of AMPK in modulating methotrexate response. Firstly, this work links methotrexate to the transcriptional regulation of one-carbon metabolism genes, as methotrexate induces the intracellular concentration of the metabolite AICAR, which increases AMPK/PGC-1α/ERRα signalling. Furthermore, AMPK is responsible for increasing the bioenergetic capacity of cells following methotrexate treatment. AMPK is also important for the antiproliferative response of methotrexate on cancer cells and is supported by the fact that AMPK activators such as phenformin can further potentiate the antineoplastic effects of methotrexate.

3.8 EXPERIMENTAL PROCEDURES

3.8.1 Cell Lines and Reagents. BT474, S-180, MCF10A, MCF7, and NMUMG cell lines were purchased from ATCC and cultured as previously described(Andrzejewski et al., 2014a; Audet-Walsh et al., 2016). NT2196 is a stable cell line corresponding to immortalized NMuMG cells that were transformed with an oncogenic form of Neu (rat ErbB2), which was cultured as previously described (Ursini-Siegel et al., 2007). AMPKnull MEFs, R5 lymphoma shCTRL/shAMPK, HCT-116 shCTRL/shAMPK, and H1299 shCTRL/shAMPK cell lines were generous gifts from Dr. Russell Jones' laboratory, and were cultured as previously described(Griss et al., 2015; Yan et al., 2014). Methotrexate (MTX) (dissolved in DMSO) and phenformin (dissolved in water) was purchased from Sigma. All LC/MS grade solvents and salts were purchased from Fisher (Ottawa, Ontario Canada: water, acetonitrile (ACN), Methanol

(MeOH), formic acid, and ammonium acetate. The authentic metabolite standards were purchase from Sigma-Aldrich Co. (Oakville, Ontario, Canada).

3.8.2 Western Blotting. Protein extracts were prepared using lysis buffer (50 mmol/L Tris-HCl [pH 7.4], 1% Triton X-100, 0.25% sodium deoxycholate, 150 mmol/L NaCl, 1 mmol/L EDTA) supplemented with protease inhibitors (cOmplete Mini EDTA-free Protease Inhibitor Cocktail, cat# 4693159001) and phosphatase inhibitors (PhosphoStop cat# 4906837001). Immunoblots were incubated with the following primary antibodies from Cell Signalling: pAMPK (2531), AMPK (2532), pACC (3661), ACC (3662); from Santa Cruz: Actin (sc-1616); RPLP0 (11290-AP) The results were visualized with Western Lightning Plus-ECL (PerkinElmer) and analyzed with ImageJ software (NIH).

3.8.3 Gene Expression. RNA was extracted and purified using the Aurum Total RNA Mini Kit (Bio-Rad) following the manufacturers' protocols. Reverse transcriptase reactions were performed using iScript cDNA Synthesis Kit (Bio-Rad). Samples were then analyzed by qRT-PCR with SYBR-green-based qRT-PCR with a MyiQ2 Real-Time Detection System (Bio-Rad). Gene-specific primers are found in Table S3.1. Values were normalized to Pum1 in BT474 cells, and RPLP0 in MEF cells.

3.8.4 Respiration. Cellular respiration was determined using a Digital Model 10 Clark Electrode (Rank Brothers) as previously described (Fantin et al., 2006). $1x10^6$ cells (BT474, MCF10A, MCF7) or $1.5x10^6$ (NMuMG, NT2196) cells were treated with methotrexate for 72 hours and used for respiration measurements. Oligomycin (2.5 mg/mL/$1x10^6$ cells) was added to inhibit the ATP synthase, which allows for the calculation of respiration coupled to ATP synthesis (coupled respiration) and respiration linked to proton leak (uncoupled respiration). Myxothiazol (0.5

mM/1x10^6 cells) was added to inhibit complex III, and is used to determine the contribution of non-mitochondrial respiration, which was not observed.

3.8.5 Seahorse Bioenergetic Analysis. Oxygen Consumption Rate (OCR) and Extracellular Acidification Rate (ECAR) were measured using the XF24 Extracellular Flux Analyzer (Seahorse Bioscience) according to the manufacturer's protocol. BT474 cells were treated for 72 hours with methotrexate, then trypisizinzed and 50,000 cells per well were plated overnight in Seahorse cell culture plate (Seahorse Bioscience). The next day, cells were washed with XF media (Seahorse Bioscience) without glucose and incubated in a CO_2-free incubator for 2 hours to establish equilibrium. During the assay, injections included glucose (10mM), oligomycin (1mM), FCCP (1.5mM), rotenone/myxothiazol (0.5mM), and monensin (20uM). FCCP uncouples the inner mitochondrial membrane, thereby allowing for maximal oxygen consumption. The combination of rotenone (complex I inhibitor) and myxothiazol (complex III inhibitor) is used to maximally perturb mitochondrial respiration. Monensin is used to calculate maximum glycolytic capacity of cells, by driving the increased ATP demand by the Na^+/K^+–ATPase, which stimulates the ATP-requiring Na^+ cycling across the plasma membrane. In addition, HCl (hydrochloric acid) was injected into wells containing media with no cells (four injections of 0.25mM each) in order to calculate the buffer capacity of the XF media. OCR, ECAR, and PPR (proton production rate) measurements were taken before and after each injection, and were used to calculate J ATP production and bioenergetic capacity as previously described(Mookerjee et al., 2017). Briefly, bioenergetics capacity is the product of the maximal J ATP glycolysis (J ATP glyc) and J ATP oxidative phosphorylation (J ATP ox). Values were normalized to cell counts.

3.8.6 Cell Proliferation. Cell counts were quantified using an automated TC10 cell counter (Bio-Rad) and viability was determined using trypan blue exclusion.

3.8.7 Formate assay. Formate activity was assessed using an assay kit according to the manufacturer's instructions (Sigma). Briefly, $1x10^6$ cells were homogenized and 20µl of the homogenates of each condition was used.

3.8.8 Metabolomics. Nucleotide detection and analysis was performed using LC-MS at the Metabolomics Core Facility of the Goodman Cancer Research Centre. Cultured cells were treated with methotrexate for 72 hours. Cells were washed in ammonium formate three times, then quenched in 50% methanol (v/v) and acetonitrile. Cells were lysed following bead beating at 30Hz for 2 minutes. Cellular extracts were partitioned into aqueous and organic layers following dicholomethane treatment and centrifugation. Aqueous supernatants were dried down using a speed-vac. Dried samples were subsequently resuspended with 50µl of water. 5µl of sample was injected onto an Agilent 6430 Triple Quadrupole (QQQ)-LC-MS/MS for targeted metabolite analysis of nucleotides (AICAR, IMP, AMP). The liquid chromatography was performed using a 1290 Infinity ultra-performance binary LC system (Agilent Technologies, Santa Clara, CA, USA). The chromatography run was conducted as follows: Column temperature was maintained at 10°C and the separation was realised by reverse phase separation using a flow rate of 0.4 mL/min with a Scherzo SM-C18 column 3 µm, 3.0×150mm (Imtakt Corp, JAPAN) The gradient started at 100% mobile phase A (5 mM ammonium acetate in water) with a 5 min gradient to 100% B (200 mM ammonium acetate in 80% water / 20% ACN) at a flow rate of 0.4 ml/min. This was followed by a 5 min hold time at 100% mobile phase B and a subsequent re-equilibration time (6 min) before next injection.

The mass spectrometer is equipped with an electrospray ionization (ESI) source and samples were analyzed in positive mode. Multiple reaction monitoring (MRM) transitions were optimized on standards for each metabolite quantitated. Transitions for quantifier and qualifier ions were as follows: AICAR (259.1 → 127.0 and 110.0, 82.1, 55.1), IMP (349.0 → 147 and 110.0), and AMP (324.0 → 112.1 and 324.0 → 95.1). Gas temperature and flow were set at 350°C and 10 l/min respectively, nebulizer pressure was set at 40 psi and capillary voltage was set at 3500V. Relative concentrations were determined from external calibration curves prepared in water and compared to sample area under the curve. Note that no corrections were made for ion suppression or enhancement. Data were analyzed using MassHunter Quant (Agilent Technologies b, Santa Clara, CA, USA).

3.9 SUPPLEMENTAL FIGURE AND TABLE

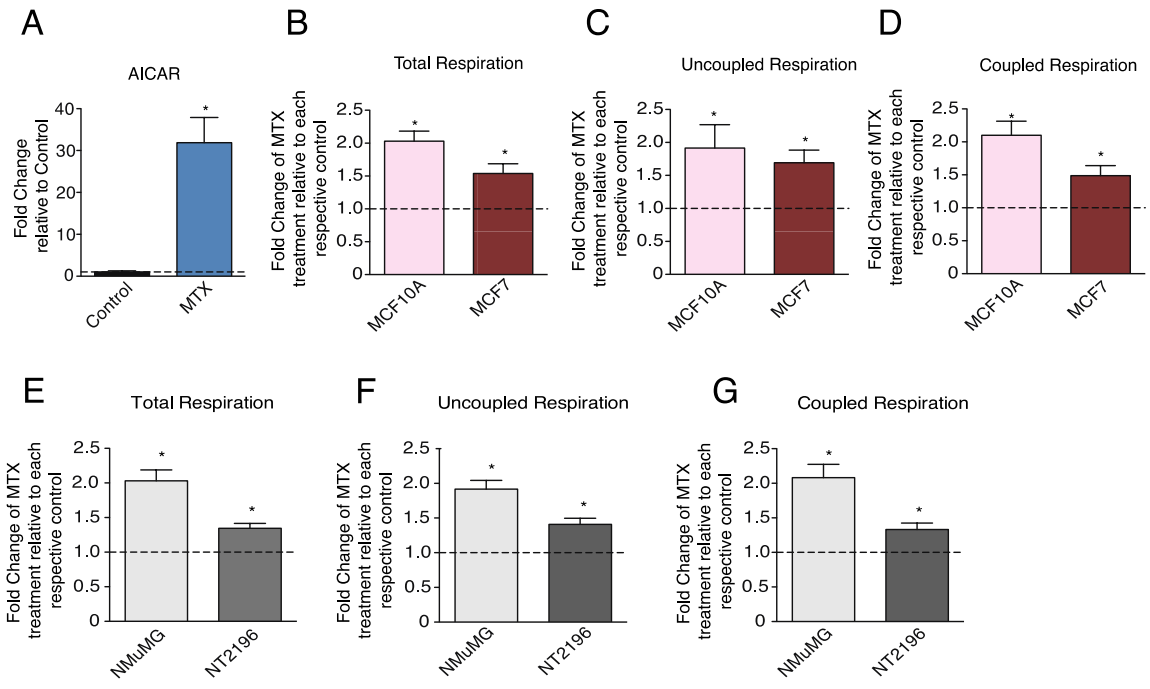

Figure S3.1: Methotrexate induces AICAR and increases cellular respiration

(A) Analysis of AICAR levels following treatment with 0.02μM MTX (blue) or control (black) for 72 hours in MEF cells, normalized to control treatment (dashed line) (n=3).

(B-D) Total, uncoupled, and coupled respiration of MCF10A cells treated with MTX (pink) and MCF7 cells treated with MTX (maroon) compared to each respective control (dashed line) (n=9-10).

(E-G) Total, uncoupled, and coupled respiration of NMuMG cells treated with MTX (light grey) and MCF7 cells treated with MTX (dark grey) compared to each respective control (dashed line) (n=4). Data are presented as means + SEM, *$p<0.05$, Student's t test.

Table S1: List of Human and Mouse Primers used for qRT-PCR				
Human Primers				
Gene Symbol	Gene Name	Forward Primer	Reverse Primer	Reference
PPARGC1A	peroxisome proliferator-activated receptor gamma coactivator 1 alpha	CCTGTGATGCTTTTGCTGCTCTTG	AAACTATCAAAATCCAGAGAGTCA	(Eichner et al., 2010)
ESRRA	estrogen-related receptor alpha	GCTGCCCTGCTGCAACTAGTG	GCCGCCGCTCAGCACCCCCTC	(Eichner et al., 2010)
MTHFD1	methylenetetrahydrofolate dehydrogenase 1, methenyltetrahydrofolate cyclohydrolase, formyltetrahydrofolate synthetase	TTGTTGGCCCAGAAGGGTTT	CTGACAGTGGCAACAAGCAC	(Audet-Walsh et al., 2016)
MTHFD1L	methylenetetrahydrofolate dehydrogenase (NADP+ dependent) 1 like	AGGTGTCAACCTAGATGGAAAGA	GCTTTGAAGCTGGCGTGTTT	(Audet-Walsh et al., 2016)
MTHFD2	methylenetetrahydrofolate dehydrogenase (NADP+ dependent) 2, methenyltetrahydrofolate cyclohydrolase	TTCTGGAAGGAAACTGGCCC	TTCTCGCCAACCAGGATCAC	(Audet-Walsh et al., 2016)
Pum1	pumilio RNA-binding family member 1	ACGGATTCGAGGCCACGTCC	CATTAATTACCTGCTGGTCTGAAGGA	(Audet-Walsh et al., 2016)
TBP	TATA box binding protein	TGCCACGCCAGCTTCGGAGA	ACCGCAGCAAACCGCTTGGG	(Audet-Walsh et al., 2016)
Mouse Primers				
Gene Symbol	Gene Name	Forward Primer	Reverse Primer	Reference
Mthfd1	methylenetetrahydrofolate dehydrogenase (NADP+ dependent), methenyltetrahydrofolate cyclohydrolase, formyltetrahydrofolate synthase	AGAACCAGGTAACTCGGATG	TGGCTTTGATCCCAATCTCT	(This study)
Mthfd1l	methylenetetrahydrofolate dehydrogenase (NADP+ dependent) 1-like	TCATCCAAAGTCAGGTCTCG	AGTGGTTCTTTCGTGGTCTT	(This study)
Mthfd2	methylenetetrahydrofolate dehydrogenase (NAD+ dependent), methenyltetrahydrofolate cyclohydrolase	TTTCCTTGTTGTCTGCGTTG	AACGGCTTCATTTCGCAC	(This study)
Tbp	TATA box binding protein	ACCTTATGCTCAGGGCTTGG	GCCATAAGGCATCATTGGAC	(Klimcakova, et al. 2012)

Table S3.1: Primers for qRT-PCR

3.10 AUTHOR CONTRIBUTIONS

Conceptualization and design: D.J.P., G.B., D.A., R.G.J., J.St-P.; Development of methodology: D.J.P., G.B., D.A.; Acquisition of data: D.J.P, E.M., D.R., G.B., D.A.; Analysis and interpretation of data: D.J.P, G.B., D.A. Writing of the manuscript: D.J.P., D.A., J.St-P. Study supervision: J.St-P.

3.11 ACKNOWLEDGEMENTS

We would like to thank staff scientists at the Goodman Cancer Research Centre (GCRC) Metabolomics Core Facility (McGill University) for guidance with metabolomics studies. The

Metabolomics Core Facility is funded by the Dr. John R and Clara M. Fraser Memorial Trust, the Terry Fox Foundation (TFF Oncometabolism Team Grant # 242122), the Québec Breast Cancer Foundation, and McGill University. This work was supported by grants from Terry Fox Research Institute and Québec Breast Cancer Foundation (TFF-242122 to J.S.-P.). We acknowledge salary support from Fonds de Recherche du Québec-Santé (FRQS) and the McGill Integrated Cancer Research Training Program (MICRTP) to D.J.P.

3.12 REFERENCES

1 Deberardinis, R. J., Sayed, N., Ditsworth, D. & Thompson, C. B. Brick by brick: metabolism and tumor cell growth. *Curr Opin Genet Dev* **18**, 54-61, doi:10.1016/j.gde.2008.02.003 (2008).

2 Locasale, J. W. Serine, glycine and one-carbon units: cancer metabolism in full circle. *Nature reviews. Cancer* **13**, 572-583, doi:10.1038/nrc3557 (2013).

3 DeBerardinis, R. J. Serine metabolism: some tumors take the road less traveled. *Cell metabolism* **14**, 285-286, doi:10.1016/j.cmet.2011.08.004 (2011).

4 Ducker, G. S. & Rabinowitz, J. D. One-Carbon Metabolism in Health and Disease. *Cell metabolism* **25**, 27-42, doi:10.1016/j.cmet.2016.08.009 (2017).

5 Nilsson, R. *et al.* Metabolic enzyme expression highlights a key role for MTHFD2 and the mitochondrial folate pathway in cancer. *Nature communications* **5**, 3128, doi:10.1038/ncomms4128 (2014).

6 Locasale, J. W. *et al.* Phosphoglycerate dehydrogenase diverts glycolytic flux and contributes to oncogenesis. *Nat Genet* **43**, 869-874, doi:10.1038/ng.890 (2011).

7 Possemato, R. *et al.* Functional genomics reveal that the serine synthesis pathway is essential in breast cancer. *Nature* **476**, 346-350, doi:10.1038/nature10350 (2011).

8 Jain, M. *et al.* Metabolite profiling identifies a key role for glycine in rapid cancer cell proliferation. *Science (New York, N.Y.)* **336**, 1040-1044, doi:10.1126/science.1218595 (2012).

9 Lee, G. Y. *et al.* Comparative oncogenomics identifies PSMB4 and SHMT2 as potential cancer driver genes. *Cancer research* **74**, 3114-3126, doi:10.1158/0008-5472.CAN-13-2683 (2014).

10 Kim, D. *et al.* SHMT2 drives glioma cell survival in ischaemia but imposes a dependence on glycine clearance. *Nature* **520**, 363-367, doi:10.1038/nature14363 (2015).

11 Koseki, J. *et al.* Enzymes of the one-carbon folate metabolism as anticancer targets predicted by survival rate analysis. *Sci Rep* **8**, 303, doi:10.1038/s41598-017-18456-x (2018).

12 Ducker, G. S. *et al.* Reversal of Cytosolic One-Carbon Flux Compensates for Loss of the Mitochondrial Folate Pathway. *Cell metabolism* **23**, 1140-1153, doi:10.1016/j.cmet.2016.04.016 (2016).

13 Farber, S. & Diamond, L. K. Temporary remissions in acute leukemia in children produced by folic acid antagonist, 4-aminopteroyl-glutamic acid. *N Engl J Med* **238**, 787-793, doi:10.1056/NEJM194806032382301 (1948).

14 Chabner, B. A. & Roberts, T. G., Jr. Timeline: Chemotherapy and the war on cancer. *Nature reviews. Cancer* **5**, 65-72, doi:10.1038/nrc1529 (2005).

15 Hertz, R., Li, M. C. & Spencer, D. B. Effect of methotrexate therapy upon choriocarcinoma and chorioadenoma. *Proc Soc Exp Biol Med* **93**, 361-366 (1956).

16 Munzone, E., Curigliano, G., Burstein, H. J., Winer, E. P. & Goldhirsch, A. CMF revisited in the 21st century. *Annals of oncology : official journal of the European Society for Medical Oncology / ESMO* **23**, 305-311, doi:10.1093/annonc/mdr309 (2012).

17 Hitchings, G. H. & Burchall, J. J. Inhibition of folate biosynthesis and function as a basis for chemotherapy. *Adv Enzymol Relat Areas Mol Biol* **27**, 417-468 (1965).

18 Chabner, B. A. *et al.* Polyglutamation of methotrexate. Is methotrexate a prodrug? *The Journal of clinical investigation* **76**, 907-912, doi:10.1172/JCI112088 (1985).

19 Howard, S. C., McCormick, J., Pui, C. H., Buddington, R. K. & Harvey, R. D. Preventing and Managing Toxicities of High-Dose Methotrexate. *Oncologist* **21**, 1471-1482, doi:10.1634/theoncologist.2015-0164 (2016).

20 Tennant, D. A., Duran, R. V. & Gottlieb, E. Targeting metabolic transformation for cancer therapy. *Nature reviews. Cancer* **10**, 267-277, doi:10.1038/nrc2817 (2010).

21 Audet-Walsh, É. *et al.* The PGC-1α/ERRα Axis Represses One-Carbon Metabolism and Promotes Sensitivity to Anti-folate Therapy in Breast Cancer. *Cell Reports* **14**, 920-931, doi:https://doi.org/10.1016/j.celrep.2015.12.086 (2016).

22 Yan, M. *et al.* The tumor suppressor folliculin regulates AMPK-dependent metabolic transformation. *The Journal of clinical investigation* **124**, 2640-2650, doi:10.1172/jci71749 (2014).

23 Hardie, D. G. AMPK: a target for drugs and natural products with effects on both diabetes and cancer. *Diabetes* **62**, 2164-2172, doi:10.2337/db13-0368 (2013).

24 Jager, S., Handschin, C., St-Pierre, J. & Spiegelman, B. M. AMP-activated protein kinase (AMPK) action in skeletal muscle via direct phosphorylation of PGC-1alpha. *Proceedings of the National Academy of Sciences of the United States of America* **104**, 12017-12022, doi:10.1073/pnas.0705070104 (2007).

25 Chaube, B. *et al.* AMPK maintains energy homeostasis and survival in cancer cells via regulating p38/PGC-1alpha-mediated mitochondrial biogenesis. *Cell Death Discov* **1**, 15063, doi:10.1038/cddiscovery.2015.63 (2015).

26 Mookerjee, S. A., Gerencser, A. A., Nicholls, D. G. & Brand, M. D. Quantifying intracellular rates of glycolytic and oxidative ATP production and consumption using extracellular flux measurements. *The Journal of biological chemistry* **292**, 7189-7207, doi:10.1074/jbc.M116.774471 (2017).

27 Shuvalov, O. *et al.* One-carbon metabolism and nucleotide biosynthesis as attractive targets for anticancer therapy. *Oncotarget* **8**, 23955-23977, doi:10.18632/oncotarget.15053 (2017).

28 Faubert, B., Vincent, E. E., Poffenberger, M. C. & Jones, R. G. The AMP-activated protein kinase (AMPK) and cancer: Many faces of a metabolic regulator. *Cancer Letters* **356**, 165-170, doi:https://doi.org/10.1016/j.canlet.2014.01.018 (2015).

29 Faubert, B. *et al.* AMPK is a negative regulator of the Warburg effect and suppresses tumor growth in vivo. *Cell metabolism* **17**, 113-124, doi:10.1016/j.cmet.2012.12.001 (2013).

30 Hadad, S. M., Fleming, S. & Thompson, A. M. Targeting AMPK: a new therapeutic opportunity in breast cancer. *Critical reviews in oncology/hematology* **67**, 1-7, doi:10.1016/j.critrevonc.2008.01.007 (2008).

31 Ursini-Siegel, J. *et al.* Elevated expression of DecR1 impairs ErbB2/Neu-induced mammary tumor development. *Molecular and cellular biology* **27**, 6361-6371, doi:10.1128/mcb.00686-07 (2007).

32 Vazquez, A., Tedeschi, P. M. & Bertino, J. R. Overexpression of the mitochondrial folate and glycine-serine pathway: a new determinant of methotrexate selectivity in tumors. *Cancer research* **73**, 478-482, doi:10.1158/0008-5472.CAN-12-3709 (2013).

33 Zakikhani, M., Dowling, R., Fantus, I. G., Sonenberg, N. & Pollak, M. Metformin is an AMP kinase-dependent growth inhibitor for breast cancer cells. *Cancer research* **66**, 10269-10273, doi:10.1158/0008-5472.CAN-06-1500 (2006).

34 Zakikhani, M., Dowling, R. J., Sonenberg, N. & Pollak, M. N. The effects of adiponectin and metformin on prostate and colon neoplasia involve activation of AMP-activated protein kinase. *Cancer Prev Res (Phila)* **1**, 369-375, doi:10.1158/1940-6207.CAPR-08-0081 (2008).

35 Corominas-Faja, B. *et al.* Metabolomic fingerprint reveals that metformin impairs one-carbon metabolism in a manner similar to the antifolate class of chemotherapy drugs. *Aging (Albany NY)* **4**, 480-498, doi:10.18632/aging.100472 (2012).

36 Cronstein, B. N., Naime, D. & Ostad, E. The antiinflammatory mechanism of methotrexate. Increased adenosine release at inflamed sites diminishes leukocyte accumulation in an in vivo model of inflammation. *The Journal of clinical investigation* **92**, 2675-2682, doi:10.1172/JCI116884 (1993).

37 Pirkmajer, S. *et al.* Methotrexate promotes glucose uptake and lipid oxidation in skeletal muscle via AMPK activation. *Diabetes* **64**, 360-369, doi:10.2337/db14-0508 (2015).

38 Fodor, T. *et al.* Combined Treatment of MCF-7 Cells with AICAR and Methotrexate, Arrests Cell Cycle and Reverses Warburg Metabolism through AMP-Activated Protein Kinase (AMPK) and FOXO1. *PLoS One* **11**, e0150232, doi:10.1371/journal.pone.0150232 (2016).

39 Beckers, A. *et al.* Methotrexate enhances the antianabolic and antiproliferative effects of 5-aminoimidazole-4-carboxamide riboside. *Mol Cancer Ther* **5**, 2211-2217, doi:10.1158/1535-7163.MCT-06-0001 (2006).

40 Tedeschi, P. M. *et al.* Quantification of folate metabolism using transient metabolic flux analysis. *Cancer & metabolism* **3**, 6, doi:10.1186/s40170-015-0132-6 (2015).

41 Elango, T., Dayalan, H., Gnanaraj, P., Malligarjunan, H. & Subramanian, S. Impact of methotrexate on oxidative stress and apoptosis markers in psoriatic patients. *Clin Exp Med* **14**, 431-437, doi:10.1007/s10238-013-0252-7 (2014).

42 Dixon, R. *et al.* AICA-riboside: safety, tolerance, and pharmacokinetics of a novel adenosine-regulating agent. *J Clin Pharmacol* **31**, 342-347 (1991).

43 Mallik, R. & Chowdhury, T. A. Metformin in cancer. *Diabetes Res Clin Pract*, doi:10.1016/j.diabres.2018.05.023 (2018).

44 Griss, T. *et al.* Metformin Antagonizes Cancer Cell Proliferation by Suppressing Mitochondrial-Dependent Biosynthesis. *PLoS Biology* **13**, e1002309, doi:10.1371/journal.pbio.1002309 (2015).

45 Andrzejewski, S., Gravel, S.-P., Pollak, M. & St-Pierre, J. Metformin directly acts on mitochondria to alter cellular bioenergetics. *Cancer & metabolism* **2**, 12-12, doi:10.1186/2049-3002-2-12 (2014).

46 Fantin, V. R., St-Pierre, J. & Leder, P. Attenuation of LDH-A expression uncovers a link between glycolysis, mitochondrial physiology, and tumor maintenance. *Cancer cell* **9**, 425-434, doi:10.1016/j.ccr.2006.04.023 (2006).

CHAPTER 4:

Perturbations of cancer cell metabolism by the anti-diabetic drug canagliflozin

David J. Papadopoli[1,2], Oro Uchenunu[3,4], Laura Hulea[3,4] , Ivan Topisirovic[2,3,4,5] , Michael Pollak[3,4,5,*], and Julie St-Pierre[2,6,7*]

[1]Goodman Cancer Centre, 1160 Avenue des Pins, Montréal, QC, Canada. H3A 1A3

[2]Department of Biochemistry, McGill University, 3655 Promenade Sir William Osler, Montreal, QC, Canada, H3G 1Y6

[3]Lady Davis Institute for Medical Research, 3755 Chemin de la Côte-Sainte-Catherine, Montréal, QC, Canada, H3T 1E2

[4]Department of Medicine, Division of Experimental Medicine, McGill University, 1001 Decarie Blvd, Montreal, QC, Canada, H4A 3J1

[5]Gerald Bronfman Department of Oncology, McGill University, 5100 Maisonneuve Blvd West, Montréal, QC, Canada, H4A 3T2

[6]Departments of Biochemistry, Microbiology and Immunology, University of Ottawa, 451 Smyth Road, Ottawa, ON, Canada, K1H 8M5

[7]Ottawa Institute of Systems Biology, University of Ottawa, 451 Smyth Road, Ottawa, ON, Canada, K1H 8M5

* Corresponding authors: julie.st-pierre@uottawa.ca (J.St-P), michael.pollak@mcgill.ca (M.P.)

4.1 OBJECTIVES OF THIS CHAPTER:

1) Elucidate if SGLT2 inhibitors have antineoplastic effects
2) Uncover if SGLT2 inhibitors modulate bioenergetics and the electron transport chain
3) Determine how SGLT2 inhibitors affect the metabolome of cancer cells

4.2 SUMMARY:

Metabolic perturbations are a hallmark of cancer cells. For instance, high rates of glucose uptake and glycolysis are common in neoplasia. However, pharmacological efforts to inhibit glucose utilization for cancer treatment have not been successful. Recent evidence suggests that in addition to classical glucose transporters (e.g. GLUT1), sodium-glucose transporters (SGLTs) are expressed by cancers. We therefore investigated the possibility that SGLT inhibitors (used in treatment of type 2 diabetes) might constrain neoplastic growth by inhibiting glucose uptake by cancer cells. Using HER2+ breast cancer cells, which are characterized by a high rate of aerobic glycolysis, we show that the SGLT2 inhibitor canagliflozin inhibits proliferation. Unexpectedly, antiproliferative effects of canagliflozin were not affected by glucose availability, indicating that inhibition of glucose uptake does not account for the anti-proliferative effects. Metabolic studies using cells and isolated mitochondria revealed that canagliflozin reduces oxygen consumption by perturbing complex II-dependent mitochondrial respiration. Furthermore, we demonstrate that canagliflozin directly inhibits glutamate dehydrogenase to reduce anaplerotic flux of glutamine through the citric acid cycle and causes accumulation of glutamate in extracellular media. Thus, the anti-proliferative effect of canagliflozin is linked to inhibition of glutamine metabolism that fuels respiration, which represents an entirely unanticipated mechanism of antineoplastic action.

4.3 INTRODUCTION:

Inhibitors of sodium-coupled glucose co-transporter 2 (SGLT2) including dapagliflozin, canagliflozin, and empagliflozin are widely used in the treatment of type 2 diabetes. They inhibit reabsorption of glucose in the kidney, which results in increased glucose excretion and reduction

in glucose blood levels (Chao and Henry, 2010). While SGLT2 inhibitors are widely used clinically, the molecular pharmacology and mechanism of action of these drugs at the classic site of action are incompletely described (Hummel et al., 2012). These drugs are all related to the natural product phlorizin and have similar effects on glucose reabsorption in the kidney, but have different potencies and structural features, including for example a distinct phenylthiophene moiety in the case of canagliflozin (Nomura et al., 2010).

Recent reports suggest that SGLT2 inhibitors may exhibit antineoplastic effects (Kaji et al., 2018; Obara et al., 2017; Okada et al., 2018; Scafoglio et al., 2015; Shiba et al., 2018; Villani et al., 2016; Wright et al., 2017), but there is no consensus with regards to the underlying mechanism. While there is evidence that some cancers express SGLT family transporters (Kepe et al., 2018; Scafoglio et al., 2015; Wright et al., 2017), GLUT-1 is a better characterized glucose transporter in neoplastic cells (Zhao and Keating, 2007). Thus, it is not clear if putative antiproliferative effects of SGLT inhibitors are in fact related to inhibition of glucose uptake by cancer cells or another mechanism.

We sought to investigate the metabolic effects of SGLT2 inhibitors in relation to their antiproliferative activity. We treated HER2-amplified breast cancer cells known to exhibit high glucose dependence with two SGLT2 inhibitors, canagliflozin and dapagliflozin. Unexpectedly, we found that canagliflozin, and to a lesser extent dapagliflozin, inhibit proliferation of HER2-amplified breast cancer cells in the presence or absence of glucose. This result indicates that inhibition of glucose uptake does not explain the antiproliferative effects of these drugs. Rather, the growth inhibition of canagliflozin was linked to significant perturbations in cellular metabolism, notably inhibition of glutamine metabolism and mitochondrial respiration.

4.4 RESULTS

4.4.1 Canagliflozin acts as a growth inhibitor in the absence of glucose

We used two human HER2+ breast cancer cell lines, SKBR3 and BT474, and one murine cell line expressing an activated form of ErbB2 (NT2197), which exhibit high rates of aerobic glycolysis (Chang et al., 2011; Deblois et al., 2009; Fantin et al., 2006) and glucose uptake to study the impact of the SGLT2 inhibitors canagliflozin and dapagliflozin on cancer cells. In glucose replete media, canagliflozin, and to a lesser extent dapagliflozin, inhibited the proliferation of both SKBR3 and BT474 cells (Fig. 4.1A, B). In NT2197 cells, the growth inhibition by dapagliflozin was modest, while that of canagliflozin was similar to that seen in the two human cell lines (Fig. 4.1C). To determine whether canagliflozin or dapagliflozin act by inhibiting glucose transport, we compared their effects on proliferation in media containing either glucose or galactose. Cells cultured in the presence of galactose are dependent on mitochondrial metabolism for proliferation. Accordingly, proliferation of highly glucose dependent SKBR3 and BT474 cells was reduced when the cells were maintained in galactose-substituted, glucose-free media (Fig. 4.1D). In the presence of glucose, 50 uM canagliflozin significantly reduced the proliferation of SKBR3 and BT474 cells, similar to the impact of 5 mM metformin (a drug that is used to treat type II diabetes that blocks mitochondrial complex I (Bridges et al., 2014), which is currently under investigation for repurposing as a cancer treatment (Pollak, 2014), while the impact of dapagliflozin was more modest (Fig. 4.1D). Unexpectedly, the impact of canagliflozin or dapagliflozin was similar in the presence or absence of glucose, indicating that the anti-proliferative effects of these SGLT2 inhibitors are unrelated to inhibition of glucose transport (Fig. 4.1D).

Cancer cells grown in galactose media and exposed to metformin are severely growth restricted (Fig. 4.1E) given that these cells are solely dependent on mitochondrial functions for their growth and that metformin inhibits mitochondrial respiration. Interestingly, canagliflozin, and to a small extent dapagliflozin, could potentiate the growth inhibition of metformin under these conditions, suggesting that canagliflozin may impact mitochondrial metabolism by a mechanism that is different than that of metformin (Fig. 4.1E).

4.4.2 Canagliflozin directly targets complex II-dependent respiration

Considering the unexpected finding that the anti-proliferative effects of canagliflozin and dapagliflozin are glucose independent in the SKBR3 cell line, and a prior report that canagliflozin inhibits respiratory complex I in cancer cells (Villani et al., 2016), we examined the effects of these drugs on cellular oxygen consumption and ATP production. Cellular respiration was significantly inhibited by canagliflozin, but not dapagliflozin, at low micromolar concentrations (Fig. 4.2A-D). This is reminiscent of the inhibition of mitochondrial respiration by metformin and other biguanides, which are known inhibitors of complex I of the electron transport chain (Andrzejewski et al., 2014b; Bridges et al., 2014). We next measured the effects of canagliflozin on bioenergetic capacity, by employing recently published algorithms to quantify ATP production from oxidative phosphorylation (J ATP ox) relative to ATP production from glycolysis (JATP glyc) (Mookerjee et al., 2017). Canagliflozin, but not dapagliflozin, markedly decreased J ATP ox while exerting an increase on J ATP glyc (Fig. 4.2B-D), which together resulted in a dramatic decrease in global bioenergetic capacity compared to controls (Fig. 2C). These data show that canagliflozin is a potent inhibitor of mitochondrial respiration and total ATP production.

To determine whether SGLT2 inhibitors can directly act on mitochondria, we tested the impact of canagliflozin and dapagliflozin on isolated mitochondria derived from murine skeletal muscle as previously described (Andrzejewski et al., 2014b). The quality and integrity of mitochondrial preparations were assessed by measuring the respiratory control ratio (RCR), which is calculated as the quotient of state 3 respiration rate (addition of ADP) on state 4 respiration (addition of oligomycin) (Brand and Nicholls, 2011). Mitochondrial suspensions required for testing the impact of compounds on mitochondrial functions should exhibit high RCR, which represents the gold standard of mitochondrial integrity. To determine the effect of canagliflozin and dapagliflozin on the electron transport chain, mitochondrial suspensions were incubated with complex I substrates (malate, pyruvate) or complex II substrate (succinate, in the presence of the complex I inhibitor rotenone). Canagliflozin and dapagliflozin failed to suppress complex I-dependent respiration, as they had no effect on states 2, 3, 4, or the maximal respiratory capacity (following FCCP treatment) of mitochondria respiring on complex I substrates (Fig. 4.2E-H). Rotenone and metformin, known inhibitors of complex I, were used as controls to show inhibition of complex I-dependent mitochondrial respiration (Fig. 4.2E-H). Strikingly, canagliflozin, but not dapagliflozin, significantly reduced state 3 and the maximal respiratory capacity of mitochondria respiring on complex II substrates (Fig. 4.2I-L). These actions of canagliflozin are similar to low dose of malonate, a known inhibitor of complex II, and differ from those of complex I inhibitors (Andrzejewski et al., 2014b). Overall, these data demonstrate that canagliflozin can directly inhibit complex II-dependent mitochondrial functions.

4.4.3 Canagliflozin decreases glutamine-mediated anaplerosis

Since we observed that canagliflozin reduces complex II-dependent mitochondrial respiration, we next carried out metabolite profiling of SKBR3 cancer cells. Canagliflozin decreased the levels of several citric acid cycle intermediates (citrate, cis-aconitate, alpha ketoglutarate and succinate), while dapagliflozin only modestly affected succinate levels (Fig. 4.3A). In addition, canagliflozin increased the levels of several amino acids (cysteine, glutamate, glutamine, histidine, leucine) and decreased the amounts of alanine, aspartate, and proline. In contrast, dapagliflozin had little effect on global amino acid levels. As amino acids can be used to fuel the citric acid cycle, we postulated that canagliflozin could be targeting this central metabolic pathway by modulating amino acid metabolism. More specifically, as cancer cells often take up glutamine as a means of fueling the citric acid cycle, and that HER2 + breast cancer cells exhibit glutamine dependency for growth (McGuirk et al., 2013), we hypothesized that canagliflozin inhibits glutamine-mediated anaplerosis. To test this, we employed stable isotope tracer analysis to follow the incorporation of labeled glutamine into the citric acid cycle. Treatment of SKBR3 cells with canagliflozin decreased the fraction of labeled alpha-ketoglutarate m+5, succinate m+4, fumarate m+4, malate m+4, and citrate m+4, thereby confirming that canagliflozin perturbs the entry of glutamine into the citric acid cycle (Fig. 4.3B). Unlike canagliflozin, the glutamine tracing upon dapagliflozin treatment was similar to controls. Together, these results demonstrate that canagliflozin perturbed the citric acid cycle and amino acids metabolome and inhibits glutamine anaplerosis.

4.4.4 Canagliflozin impairs glutamine-mediated respiration by inhibiting glutamate dehydrogenase

In order to determine whether blocking of glutamine-mediated anaplerosis contributes to the anti-respiratory effect of canagliflozin, SKBR3 cells were treated with canagliflozin in the presence or absence of glutamine. Canagliflozin decreased the respiration of cells in the presence of glutamine, but was unable to inhibit mitochondrial respiration in the absence of glutamine, suggesting that canagliflozin perturbs cellular respiration by impairing glutamine utilization (Fig. 4.4A). Accordingly, canagliflozin was proficient at inhibiting cell proliferation in the presence of glutamine, but unable to further inhibit proliferation already decreased in glutamine free media (Fig. 4.4B). In order to determine whether canagliflozin impairs glutamine uptake, we monitored its levels in media in cells treated with the drug relative to controls. Strikingly, we observed that canagliflozin treatment not only increases the consumption of glutamine, but also greatly increases the concentration of glutamate in the extracellular media (Fig. 4.4C). This suggests an impairment of glutamate utilization by cells. As glutamate dehydrogenase is the enzyme that directly links glutamate to the citric acid cycle, we carried out a cell-free assay to determine if canagliflozin inhibits the activity of this enzyme. Canagliflozin, but not dapagliflozin, decreased the activity of glutamate dehydrogenase by nearly 50% (Fig. 4.4D). Overall, these data show that canagliflozin inhibits glutamine metabolism by targeting glutamate dehydrogenase (Fig. 4.4E).

4.5 FIGURES

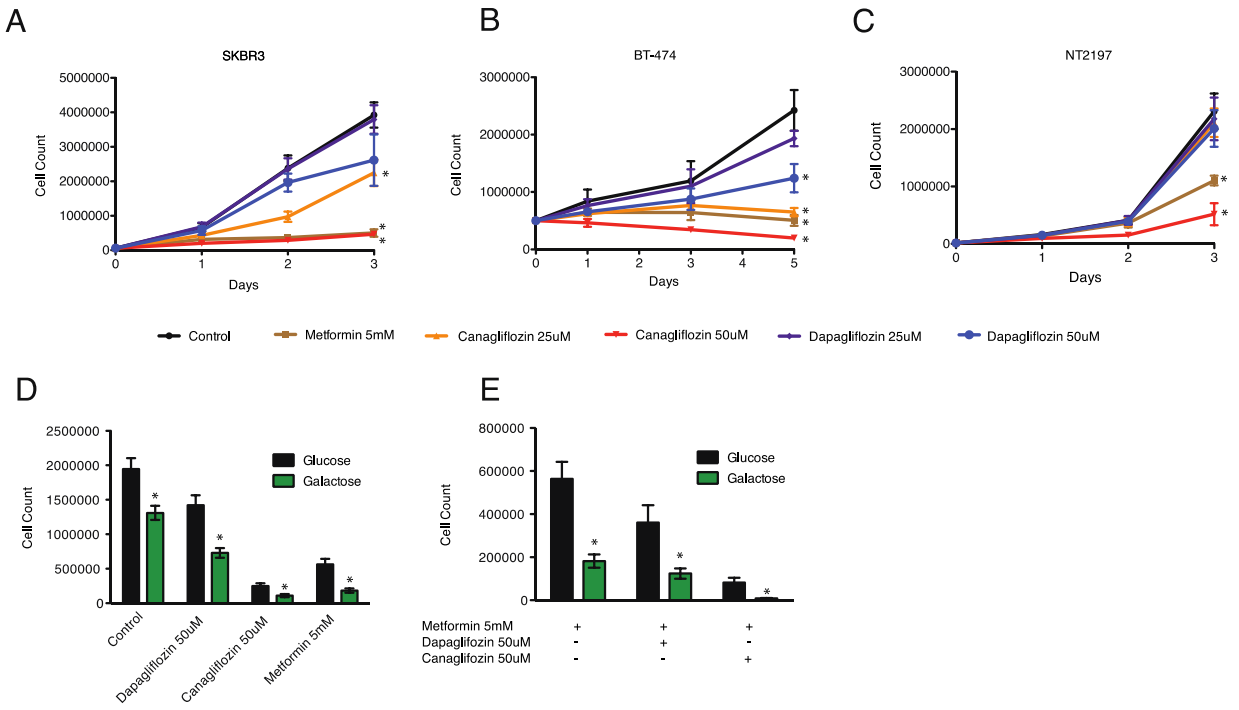

Figure 4.1: Canagliflozin inhibits cell proliferation

(A–C) Cell proliferation of SGLT2 inhibitors (canagliflozin, dapagliflozin) and metformin in SKBR3 cells (A) (n=4), BT474 cells (B) (n=4), and NT2197 cells (n=3).

(D) Cell proliferation of SKBR3 cells treated with SGLT2 inhibitors (canagliflozin, dapagliflozin), metformin, or control, and grown in media containing glucose (11mM) or galactose (11mM) (n=4).

(E) Cell proliferation of SKBR3 cells treated with canagliflozin or dapagliflozin in combination with metformin and grown in media containing glucose (11mM) or galactose (11mM) (n=4). All data are presented as means + SEM, $^{*}p < 0.05$, Student's *t* test.

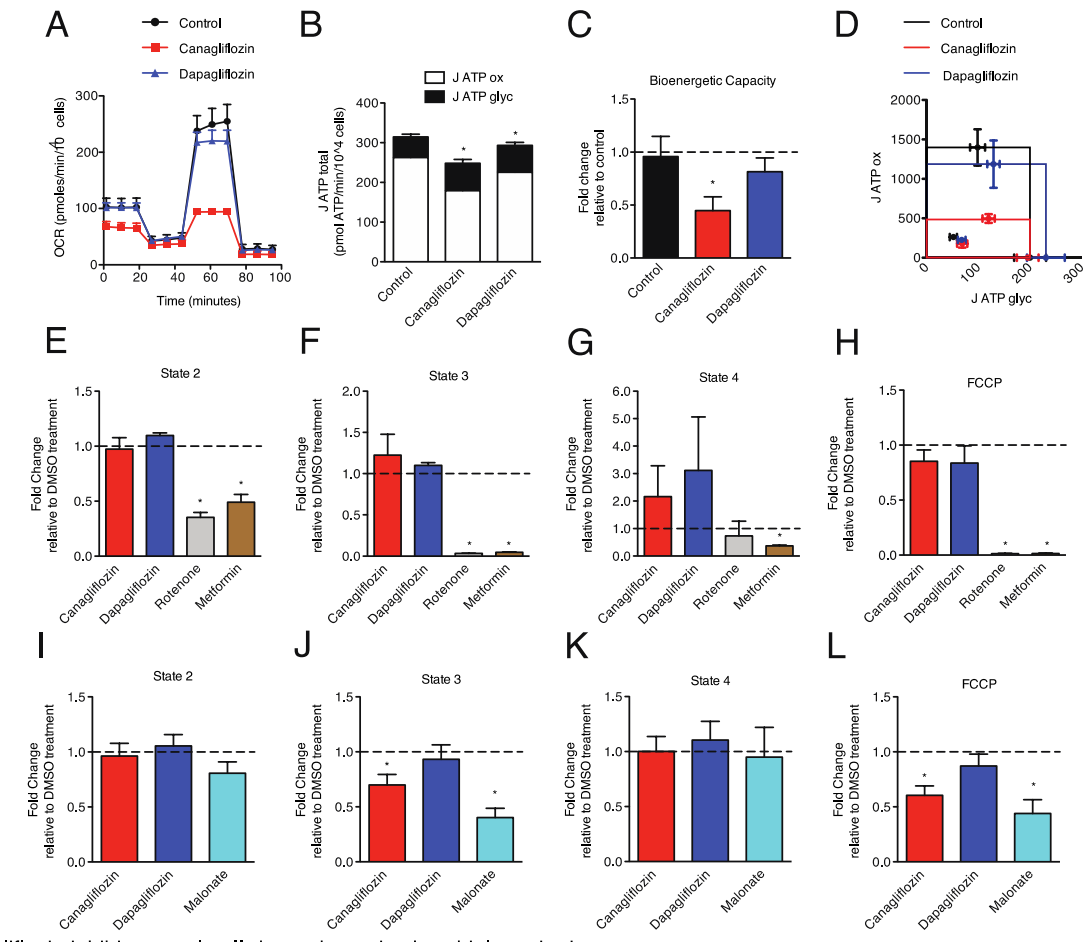

Figure 4.2: Canagliflozin inhibits complex II-dependent mitochondrial respiration

(A–D) Cellular bioenergetics upon treatment with canagliflozin (50µM) or dapagliflozin (50µM) for 24 hours. Oxygen consumption rates (OCR) (A), J ATP levels from glycolysis (J ATP glyc) and from OXPHOS (J ATP ox) (B), Bioenergetic capacity as a function of J ATP glyc and J ATP ox (C,D) were measured using Seahorse XF technology (n=3).

(E–H) Respiration of isolated mitochondria upon treatment with canagliflozin (50µM) or dapagliflozin (50µM) relative to control was measured using complex I substrates (malate, pyruvate) for states 2, 3, 4, and FCCP (n=3).

(I–L) Respiration of isolated mitochondria upon treatment with canagliflozin (50µM) or dapagliflozin (50µM) relative to control was measured using complex II substrates (succinate, rotenone) for states 2, 3, 4, and FCCP (n=5). All data are presented as means + SEM, $^{*}p < 0.05$, Student's *t* test.

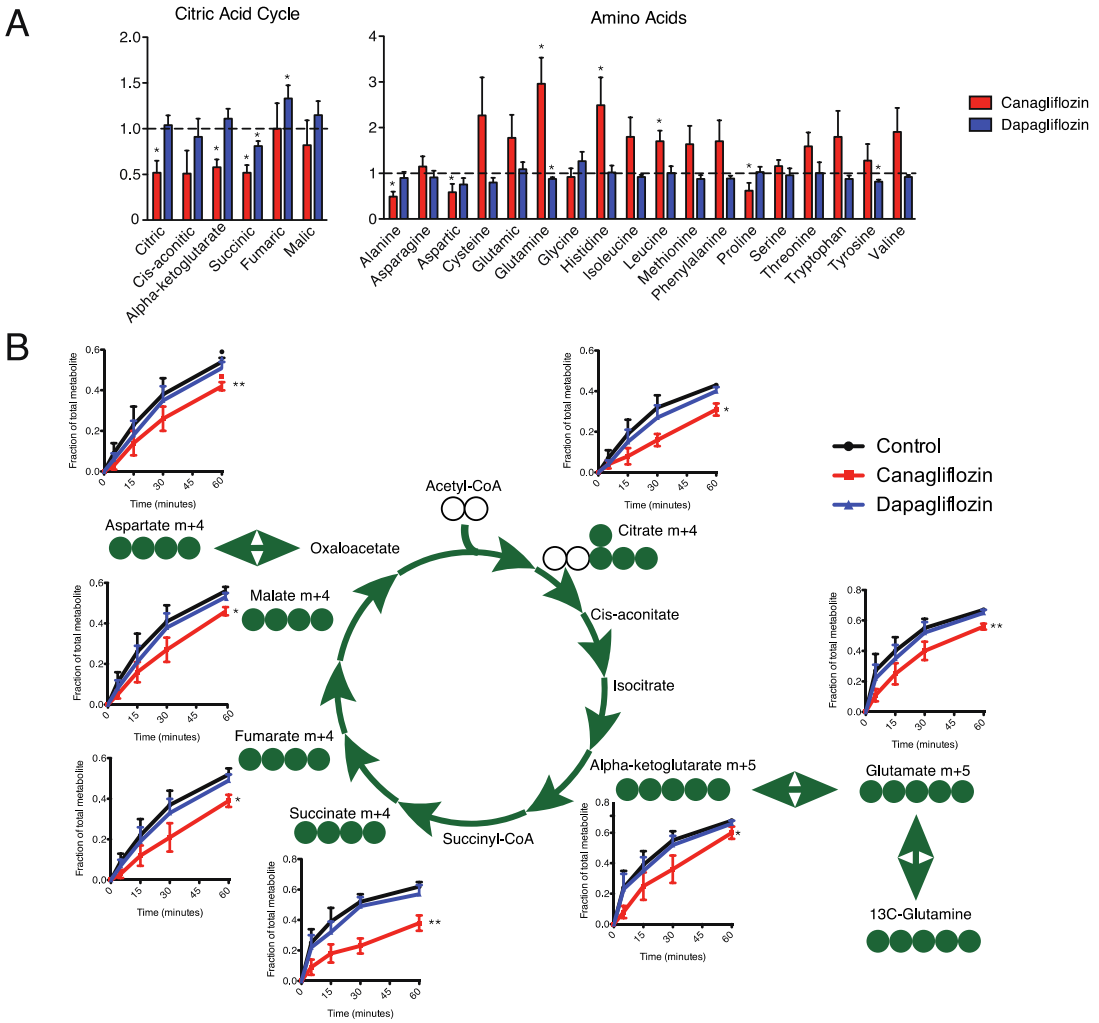

Figure 4.3: Canagliflozin perturbs glutamine metabolism through the citric acid cycle

(A) Intracellular steady-state metabolite levels in SKBR3 cells treated with canagliflozin (50μM), dapagliflozin (50μM), or control after 24 hours. Metabolites are intermediates of the citric acid cycle or amino acids (n=4-6).

(B) Diagram depicting tracing of 13C-labelled glutamine through the citric acid cycle in the forward direction. Line graphs indicate the fraction of total metabolite produced from the tracing of 13C glutamine in SKBR3 cells treated with canagliflozin (50μM), dapagliflozin (50μM) (n=4). All data are presented as means + SEM, *$p < 0.05$, Student's t test.

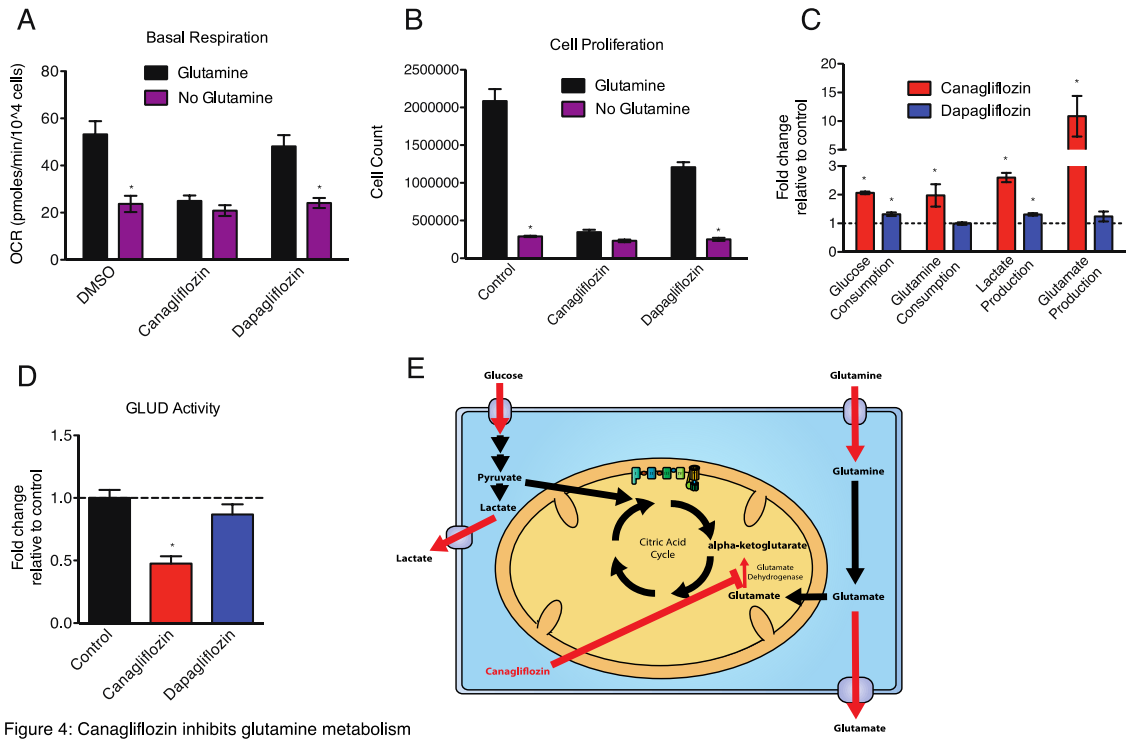

Figure 4: Canagliflozin inhibits glutamine metabolism

Figure 4.4: ***Canagliflozin inhibits glutamine metabolism***

(A) Respiration of SKBR3 cells treated with canagliflozin (50μM), dapagliflozin (50μM), or control in the presence or absence of glutamine (2mM) (n=4).

(B) Cell proliferation of SKBR3 cells treated with canagliflozin or control and grown in media containing glutamine (2mM) or no glutamine (0mM) after 72 hours (n=3).

(C) Extracellular metabolite levels in media containing SKBR3 cells treated with canagliflozin (50μM), dapagliflozin (50μM), or control after 24 hours (n=5).

(D) Glutamate dehydrogenase (GLUD1) activity assay in SKBR3 cells treated with canagliflozin (50μM), dapagliflozin (50μM) for 24 hours (n=3).

(E) Schematic of the major metabolic changes induced by canagliflozin treatment in cancer cells. All data are presented as means + SEM, $^{*}p < 0.05$, Student's *t* test.

4.6 DISCUSSION

We describe canagliflozin-induced metabolic changes associated with inhibition of proliferation in HER2+ breast cancer cells by this compound. The pattern of alterations included accumulation of glutamate, which suggested decreased flux through glutamate dehydrogenase as one plausible possibility. This was supported by a direct cell-free enzyme activity assay which indicated that canagliflozin, but not dapagliflozin, inhibits this enzymatic activity. We cannot exclude the possibility than in some contexts SGLT2 inhibitors have antineoplastic activity related to inhibition of SGLT2-mediated glucose transport by cancer cells, as reported by others (Kaji et al., 2018), but our results, including antiproliferative effects on transformed cells grown in media without glucose, point to SGLT2-independent actions of canagliflozin.

While our manuscript was being prepared, another laboratory investigating the basis for the nephrotoxicity occasionally encountered with canagliflozin therapy also observed inhibition of glutamate dehydrogenase, but this was in a human renal proximal tubule epithelial cell model system (Secker et al., 2018), rather than transformed cells. Nevertheless, our data taken together with that report provide strong evidence for an effect of canagliflozin on glutamate dehydrogenase, rather than the classic SGLT2 target.

Prior studies have explored targeting glutamine utilization as a metabolic strategy to reduce neoplastic proliferation (Cluntun et al., 2017; Hensley et al., 2013; Luengo et al., 2017), particularly for the subset of neoplasms that exhibit ‘glutamine addiction’ (Altman et al., 2016; Dejure and Eilers, 2017). Most research in this area involved development of glutaminase inhibitors, and on the basis of favorable preclinical data, clinical trials have been initiated (e.g. ClinicalTrials.gov identifier: NCT020718620). There has been no attempt to therapeutically

target glutamate dehydrogenase, and previously described inhibitors of this enzyme lack specificity (Whitelaw and Robinson, 2013).

High expression of glutamate dehydrogenase has been identified as a marker of poor cancer prognosis (26) and is associated with neoplastic cell survival under metabolic stress (27). Furthermore, this enzyme has been shown to regulate redox homeostasis in a manner that favours neoplastic proliferation (28). Our results may have particular implications for cancers that have mutations in isocitrate dehydrogenase (which converts isocitrate to alpha ketoglutarate in the TCA cycle). The mutated enzyme produces the oncometabolite D-2-hydroxyglutarate from alpha-ketoglutarate, and may create an exploitable dependency on glutamate dehydrogenase to provide alpha ketoglutarate (Chen et al., 2014; Waitkus et al., 2018; Zhao et al., 2009).

Apart from its glutamate dehydrogenase inhibitory activity, prior reports (Secker et al., 2018; Villani et al., 2016), concluded that canagliflozin inhibits oxidative phosphorylation at complex I. Our data confirm inhibition of oxidative phosphorylation, but demonstrate that, at least in our model, this occurs at complex 2-dependent mitochondrial respiration. The inhibition of complex I presented in the paper of Villani and colleagues (Villani et al., 2016) may be explained by the fact that they used malate and glutamate as substrates to test complex I functions, and that canagliflozin inhibits glutamate dehydrogenase (19, this paper). It is also important to highlight that although we report inhibition of complex II in the presence of canagliflozin, this inhibition is evident in very active mitochondrial states (state 3 and in the presence of FCCP), which may not be physiologically relevant. Indeed, canagliflozin does not inhibit mitochondrial respiration under basal conditions (states 2 and 4). Hence, glutamate dehydrogenase may be the more physiologically important target underlying the anti-

proliferative effect of canagliflozin as we observed inhibition of glutamine metabolism under normal growth conditions.

Separate laboratory models have suggested the hypothesis that metformin, another commonly used agent used in the treatment of type 2 diabetes known to inhibit respiratory complex I, might be 'repurposed' for cancer treatment (Pollak, 2012). However, initial clinical trials have been disappointing (Kordes et al., 2015), and it is unclear if the drug can be dosed clinically in a manner that would lead to adequate concentration at the site of action. This precedent suggests caution is needed in proposing 'repurposing' of canagliflozin for indications in oncology. Nevertheless, it is of interest in the context of our observation that canagliflozin is active at ~50 uM *in vitro*, that mice tolerated an oral dose of 100 mg/Kg, which achieved a peak serum level greater than this (Mamidi et al., 2014). Chronic dosing in humans of 100 mg/day and 300 mg/day achieves serum levels of 2.5 and 7.6μM respectively (Product monograph INVOKANA, Janssen Inc). If the relationship between administered oral dose and serum level is linear, a crude estimate would be that a dose of 2000mg/day would be required to achieve serum levels in the 50μM range. Human doses higher than those that achieve maximal renal glucose excretion have not been studied clinically, so safety data are not available. Further preclinical studies are required to determine if clinical trials to evaluate the safety of high dose canagliflozin are justified.

4.7 CONCLUSION

This work elucidates the metabolic consequences of the SGLT2 inhibitor canagliflozin in cancer cells. Firstly, canagliflozin portrays antineoplastic effects even in the absence of glucose, suggesting the possibilities of alternate mechanisms. Secondly, canagliflozin inhibits

bioenergetic processes and inhibits complex-II mediated respiration, but not complex I. Lastly, canagliflozin inhibits glutamine-mediated anaplerosis through modulation of glutamate dehydrogenase. Thus, the antiproliferative functions of canagliflozin are linked to perturbation of glutamine metabolism.

4.8 EXPERIMENTAL PROCEDURES

4.8.1 Cell lines, animals, and reagents: SKBR3 and BT474 cell lines were purchased from ATCC. SKBR3 cells were grown in RPMI media (11mM glucose, 2mM glutamine) supplemented with 10% FBS and 1% gentamycin, while BT-474 cells were grown in DMEM media (25mM glucose, 4mM glutamine, 1mM sodium pyruvate) supplemented with 10% FBS and 1% penicillin/streptomycin. NT2197 cells are immortalized NMuMG mouse mammary epithethial cells that were transformed with an activated variant of Neu (rat form of ErbB2), which has been previously described in (35) and grown in DMEM media (25mM glucose, 4mM glutamine, 1mM sodium pyruvate) supplemented with 10% FBS, 1% penicillin/streptomycin, 10ug/ml insulin, 20mM HEPES, pH 7.5, and 2mM glutamine, to obtain a final glutamine concentration of 6mM. Wild-type male C57BL/6J mice were purchased from the Jackson Laboratory (Bar Harbour, ME, USA). Mice were sacrificed with approval from the McGill University Animal Care Committee. Canagliflozin and Dapagliflozin were purchased from ADOOQ Bioscience. All other reagents were purchased from Sigma unless otherwise stated.

4.8.2 Cell proliferation: Cell proliferation was quantified using an automated TC10 cell counter (Bio-Rad) and viability was determined using trypan blue exclusion assay. For nutrient

deprivation experiments, cells were grown in either standard culture media, glutamine-free media, or galactose media (standard glucose-free media supplemented with galactose).

4.8.3 Seahorse Respirometry: Oxygen Consumption Rate (OCR) and Extracellular Acidification Rate (ECAR) were measured using Seahorse XF technology (Seahorse Bioscience) according to the manufacturer's protocol. Briefly, cells were seeded 50,000 cells per well in 250µl of culture media and incubated overnight at 37°C. Cells were washed twice and incubated in 525µl of XF media, containing 11mM glucose, 2mM glutamine (for SKBR3 cells) or 25mM glucose, 4mM glutamine, 1mM sodium pyruvate (for BT-474 cells) for 1 hour at 37°C in a CO_2-free incubator. Measurements for OCR and ECAR were conducted in an XF24 Seahorse instrument and values were normalized to cell counts. Cellular mitochondrial respiration and glycolytic activity were quantified according to algorithms introduced in Mookerjee et al. (19)

4.8.4 Mitochondrial Isolation and Respirometry: Mitochondrial suspensions were derived from skeletal muscle as previously described (18). The RCR (respiratory control ratio) was used to evaluate the integrity of mitochondrial preparations, in which only samples with RCR values of at least 3 in controls were used (18). Respiration of mitochondrial suspensions were performed using a Digital Model 10 Clark-type Electrode (Rank Brothers, Cambridge, UK) and incubated in KHEB assay buffer as previously described (18).

4.8.5 Metabolic Assays: Glucose and glutamine consumption, as well as lactate and glutamate production were measured from extracellular media using the Nova BioProfile Analyzer 400 (Nova Biomedical) and normalized to cell number as previously described (18).

4.8.6 Glutamate dehydrogenase assay: Glutamate dehydrogenase enzymatic activity was assessed using an assay kit according to the manufacturer's instructions (Sigma). Briefly, $1x10^6$

cells were homogenized and 25µl of the homogenates of each condition was used. Samples were processed in 96-well dishes and absorbance at 450nm was taken every hour up until 8 hours.

4.8.7 Stable isotope tracing experiments and metabolite quantification: All metabolomics extractions and analyses were performed as previously described (21). Briefly, cells were treated with DMSO, canagliflozin, or dapagliflozin for 24 hours. For stable isotope tracer experiments, cells were incubated with media containing 2mM unlabeled glutamine for 2 hours, then changed to 2mM labeled ([U-^{13}C])-glutamine media (Cambridge Isotope Laboratories, MA, USA; CLM-1822; L-glutamine ([U-^{13}C]), 99%). The tracing of labeled glutamine into citric acid intermediates and amino acids was performed at 5, 15, 30, and 60 minutes. Subsequently for both steady state and tracing experiments, cells were washed three times in cold saline solution (0.9g/L NaCl) and quenched in 600µl 80% methanol. The lysates are subsequently sonicated at 4°C for 10 minutes, 30 seconds on and 30 seconds off, on high setting and centrifuged at (4°C at 14000g) for 10 minutes. An internal standard (750ng myristic acid-D_{27}) is added to the supernatants, which are then dried overnight at 4°C in a cold speedvac (Labconco). The following day, pellets were dissolved in 30µl of methoxyamine hydrochloride (10mg/ml diluted in pyridine, Sigma-Aldrich) with three rounds of sonication (30 sec) and vortexing (30 sec), then centrifuged for 10 minutes. Samples are incubated at 70°C for 30 minutes then derivatised with 70µl of N-tert-butyldimethylsilyl-N-methyltrifluoroacetamide (MTBSTFA) at 70°C for 1 hour. Samples were injected (1µl) into an Agilent 5975C GC/MS (Aglient, CA, USA) configured for Selected Ion Monitoring (SIM) as described in (21, 36). Mass isotopomer distribution analyses were performed using MassHunter software (Aglient, CA, USA). Metabolites were normalized by the internal standard and cell number. For tracing experiments, isotopic distributions were corrected for naturally occurring isotopes using an in-house algorithm as performed in (21).

4.9 AUTHOR CONTRIBUTIONS

Conceptualization and design: D.J.P., M.P., J.St-P., Development of methodology: D.J.P., M.P., J.St-P., Acquisition of data: D.J.P, O.U., L.H., Analysis and interpretation of data: D.J.P., I.T., M.P., J.St-P., Writing of the manuscript: D.J.P., M.P., J.St-P., Study supervision: D.J.P., I.T., M.P., J.St-P.

4.10 ACKNOWLEDGEMENTS

We would like to thank staff scientists at the Goodman Cancer Research Centre (GCRC) Metabolomics Core Facility (McGill University) for guidance with metabolomics studies. The Metabolomics Core Facility is funded by the Dr. John R and Clara M. Fraser Memorial Trust, the Terry Fox Foundation (TFF Oncometabolism Team Grant # 242122), the Québec Breast Cancer Foundation, and McGill University. This work was supported by grants from Terry Fox Research Institute and Québec Breast Cancer Foundation (TFF-242122 and TFF-116128 to I.T., M.P. and J.S.-P.). We acknowledge salary support from Fonds de Recherche du Québec-Santé (FRQS) and the McGill Integrated Cancer Research Training Program (MICRTP) to D.J.P.

4.11 REFERENCES

1. Chao EC, Henry RR. SGLT2 inhibition--a novel strategy for diabetes treatment. Nature reviews Drug Discovery. 2010;9(7):551-9.

2. Hummel CS, Lu C, Liu J, Ghezzi C, Hirayama BA, Loo DD, Kepe V, Barrio JR, Wright EM. Structural selectivity of human SGLT inhibitors. American Journal of Physiology Cell Physiology. 2012;302(2):C373-82.

3. Nomura S, Sakamaki S, Hongu M, Kawanishi E, Koga Y, Sakamoto T, Yamamoto Y, Ueta K, Kimata H, Nakayama K, Tsuda-Tsukimoto M. Discovery of canagliflozin, a novel C-glucoside with thiophene ring, as sodium-dependent glucose cotransporter 2

inhibitor for the treatment of type 2 diabetes mellitus. Journal of Medicinal Chemistry. 2010;53(17):6355-60.

4. Kaji K, Nishimura N, Seki K, Sato S, Saikawa S, Nakanishi K, Furukawa M, Kawaratani H, Kitade M, Moriya K, Namisaki T, Yoshiji H. Sodium glucose cotransporter 2 inhibitor canagliflozin attenuates liver cancer cell growth and angiogenic activity by inhibiting glucose uptake. International Journal of Cancer. 2018;142(8):1712-22.

5. Wright EM, Ghezzi C, Loo DDF. Novel and Unexpected Functions of SGLTs. Physiology (Bethesda, Md). 2017;32(6):435-43.

6. Obara K, Shirakami Y, Maruta A, Ideta T, Miyazaki T, Kochi T, Sakai H, Tanaka T, Seishima M, Shimizu M. Preventive effects of the sodium glucose cotransporter 2 inhibitor tofogliflozin on diethylnitrosamine-induced liver tumorigenesis in obese and diabetic mice. Oncotarget. 2017;8(35):58353-63.

7. Villani LA, Smith BK, Marcinko K, Ford RJ, Broadfield LA, Green AE, Houde VP, Muti P, Tsakiridis T, Steinberg GR. The diabetes medication Canagliflozin reduces cancer cell 18
proliferation by inhibiting mitochondrial complex-I supported respiration. Molecular Metabolism. 2016;5(10):1048-56.

8. Scafoglio C, Hirayama BA, Kepe V, Liu J, Ghezzi C, Satyamurthy N, Moatamed NA, Huang J, Koepsell H, Barrio JR, Wright EM. Functional expression of sodium-glucose transporters in cancer. Proceedings of the National Academy of Sciences of the United States of America. 2015;112(30):E4111-9.

9. Shiba K, Tsuchiya K, Komiya C, Miyachi Y, Mori K, Shimazu N, Yamaguchi S, Ogasawara N, Katoh M, Itoh M, Suganami T, Ogawa Y. Canagliflozin, an SGLT2 inhibitor, attenuates the development of hepatocellular carcinoma in a mouse model of human NASH. Scientific Reports. 2018;8(1):2362.

10. Okada J, Matsumoto S, Kaira K, Saito T, Yamada E, Yokoo H, Katoh R, Kusano M, Okada S, Yamada M. Sodium Glucose Cotransporter 2 Inhibition Combined With Cetuximab Significantly Reduced Tumor Size and Carcinoembryonic Antigen Level in Colon Cancer Metastatic to Liver. Clinical Colorectal Cancer. 2018;17(1):e45-e8.

11. Kepe V, Scafoglio C, Liu J, Yong WH, Bergsneider M, Huang SC, Barrio JR, Wright EM. Positron emission tomography of sodium glucose cotransport activity in high grade astrocytomas. Journal of Neuro-Oncology. 2018.
12. Zhao FQ, Keating AF. Functional properties and genomics of glucose transporters. Current Genomics. 2007;8(2):113-28.

13. Chang CY, Kazmin D, Jasper JS, Kunder R, Zuercher WJ, McDonnell DP. The metabolic regulator ERRalpha, a downstream target of HER2/IGF-1R, as a therapeutic target in breast cancer. Cancer Cell. 2011;20(4):500-10

14. Deblois G, Hall JA, Perry MC, Laganiere J, Ghahremani M, Park M, Hallett M, Giguère V. Genome-wide identification of direct target genes implicates estrogen-related receptor alpha as a determinant of breast cancer heterogeneity. Cancer Research. 2009;69(15):6149-57.

15. Fantin VR, St-Pierre J, Leder P. Attenuation of LDH-A expression uncovers a link between glycolysis, mitochondrial physiology, and tumor maintenance. Cancer Cell. 2006;9(6):425-34.

16. Bridges HR, Jones AJ, Pollak MN, Hirst J. Effects of metformin and other biguanides on oxidative phosphorylation in mitochondria. The Biochemical Journal. 2014;462(3):475-87.

17. Pollak M. Overcoming Drug Development Bottlenecks With Repurposing: Repurposing biguanides to target energy metabolism for cancer treatment. Nature Medicine. 2014;20(6):591-3.

18. Andrzejewski S, Gravel SP, Pollak M, St-Pierre J. Metformin directly acts on mitochondria to alter cellular bioenergetics. Cancer & Metabolism. 2014;2:12.

19. Mookerjee SA, Gerencser AA, Nicholls DG, Brand MD. Quantifying intracellular rates of glycolytic and oxidative ATP production and consumption using extracellular flux measurements. The Journal of Biological Chemistry. 2017;292(17):7189-207.

20. Brand MD, Nicholls DG. Assessing mitochondrial dysfunction in cells. The Biochemical Journal. 2011;435(2):297-312.

21. McGuirk S, Gravel SP, Deblois G, Papadopoli DJ, Faubert B, Wegner A, Hiller K, Avizonis D, Akavia UD, Jones RG, Giguère V, St-Pierre J. PGC-1alpha supports glutamine metabolism in breast cancer. Cancer & Metabolism. 2013;1(1):22.
20

22. Secker PF, Beneke S, Schlichenmaier N, Delp J, Gutbier S, Leist M, Dietrich DR. Canagliflozin mediated dual inhibition of mitochondrial glutamate dehydrogenase and complex I: an off-target adverse effect. Cell Death & Disease. 2018;9(2):226.

23. Luengo A, Gui DY, Vander Heiden MG. Targeting Metabolism for Cancer Therapy. Cell Chemical Biology. 2017;24(9):1161-80.

24. Cluntun AA, Lukey MJ, Cerione RA, Locasale JW. Glutamine Metabolism in Cancer: Understanding the Heterogeneity. Trends in Cancer. 2017;3(3):169-80.

25. Hensley CT, Wasti AT, DeBerardinis RJ. Glutamine and cancer: cell biology, physiology, and clinical opportunities. The Journal of Clinical Investigation. 2013;123(9):3678-84.

26. Dejure FR, Eilers M. MYC and tumor metabolism: chicken and egg. The EMBO Journal. 2017;36(23):3409-20.

27. Altman BJ, Stine ZE, Dang CV. From Krebs to clinic: glutamine metabolism to cancer therapy. Nature Reviews Cancer. 2016;16(12):773.

28. Whitelaw BS, Robinson MB. Inhibitors of glutamate dehydrogenase block sodiumdependent glutamate uptake in rat brain membranes. Frontiers in Endocrinology. 2013;4:123.

29. Waitkus MS, Pirozzi CJ, Moure CJ, Diplas BH, Hansen LJ, Carpenter AB, Yang R, Wang Z, Ingram BO, Karoly ED, Mohney RP, Spasojevic I, McLendon RE, Friedman HS, He Y, Bigner DD, Yan H. Adaptive Evolution of the GDH2 Allosteric Domain Promotes Gliomagenesis by Resolving IDH1(R132H)-Induced Metabolic Liabilities. Cancer Research. 2018;78(1):36-50.
21

30. Chen R, Nishimura MC, Kharbanda S, Peale F, Deng Y, Daemen A, Forrest WF, Kwong M, Hedehus M, Hatzivassiliou G, Friedman LS, Phillips HS. Hominoid-specific enzyme GLUD2 promotes growth of IDH1R132H glioma. Proceedings of the National Academy of Sciences of the United States of America. 2014;111(39):14217-22.

31. Zhao S, Lin Y, Xu W, Jiang W, Zha Z, Wang P, Yu W, Li Z, Gong L, Peng Y, Ding J, Lei Q, Guan KL, Xiong Y. Glioma-derived mutations in IDH1 dominantly inhibit IDH1 catalytic activity and induce HIF-1alpha. Science (New York, NY). 2009;324(5924):261-5.

32. Pollak MN. Investigating metformin for cancer prevention and treatment: the end of the beginning. Cancer Discovery. 2012;2(9):778-90.

33. Kordes S, Pollak MN, Zwinderman AH, Mathot RA, Weterman MJ, Beeker A, Punt CJ, Richel DJ, Wilmink JW. Metformin in patients with advanced pancreatic cancer: a double-blind, randomised, placebo-controlled phase 2 trial. The Lancet Oncology. 2015;16(7):839-47.

34. Mamidi RN, Cuyckens F, Chen J, Scheers E, Kalamaridis D, Lin R, Silva J, Sha S, Evans DC, Kelley MF, Devineni D, Johnson MD, Lim HK. Metabolism and excretion of canagliflozin in mice, rats, dogs, and humans. Drug Metabolism and Disposition: the Biological Fate of Chemicals. 2014;42(5):903-16.

35. Ursini-Siegel J, Rajput AB, Lu H, Sanguin-Gendreau V, Zuo D, Papavasiliou V, et al. Elevated expression of DecR1 impairs ErbB2/Neu-induced mammary tumor development. Mol Cell Biol 2007; 27:6361-71

36. Mamer O, Gravel SP, Choiniere L, Chenard V, St-Pierre J, Avizonis D. The complete

targeted profile of the organic acid intermediates of the citric acid cycle using a single stable isotope dilution analysis, sodium borodeuteride reduction and select ion monitoring GC/MS. Metabolomics 2013;9;1019-30

37. Ursini-Siegel, J. et al. ShcA signalling is essential for tumour progression in mouse models of human breast cancer. EMBO J 27, 910-920, doi:emboj200822 [pii] 10.1038/emboj.2008.22 (2008).

CHAPTER 5: DISCUSSION

5.1 PGC-1α/ERRα AS EFFECTORS OF AMPK SIGNALLING IN CANCER

AMPK governs metabolic processes to facilitate cellular adaptation to energetic stress. Indeed, PGC-1α acts as an important effector of AMPK-mediated mitochondrial metabolism and biogenesis (Jager et al. 2007). In cancer, AMPK/PGC-1α signalling improves mitochondrial functions to promote androgen-receptor positive prostate cancer (Tennakoon et al. 2014), FLCN-null renal cancer (Yan et al. 2014), and lung cancer (Chaube B. et al. 2015). In addition, several other AMPK/PGC-1α functions that may be beneficial for cancer cells include stimulation of glucose uptake (Jager et al. 2007), ROS detoxification (Rabinowitz et al. 2017), fatty acid oxidation (Lee et al., 2006), and autophagy (Shi et al., 2015).

This thesis describes the impact of AMPK activation on ERRα interaction with the genome. The activation of AMPK not only increases the binding of ERRα to nuclear encoded mitochondrial genes, but also to the promoters of genes involved in one-carbon metabolism. Ultimately, this work adds another node to the plethora of metabolic functions controlled by the PGC-1α/ERRα signalling, especially under conditions wherein AMPK is activated. As one-carbon metabolism drives nucleotide biosynthesis, the inhibition of one-carbon metabolism supports the anti-anabolic role of AMPK. Another key anabolic process controlled by AMPK is the inhibition of protein synthesis through the suppression of mTOR (Inoki et al., 2012). Recently, the mTOR/ATF4 axis has been shown to activate the expression of genes involved in mitochondrial one-carbon metabolism, serine biosynthesis, and purine biosynthesis (Ben-Sahra et al. 2016). Thus, AMPK holds a pivotal position in repressing one-carbon metabolism by activating PGC-1α/ERRα axis and perhaps also by the repression of the mTOR/ATF4 axis.

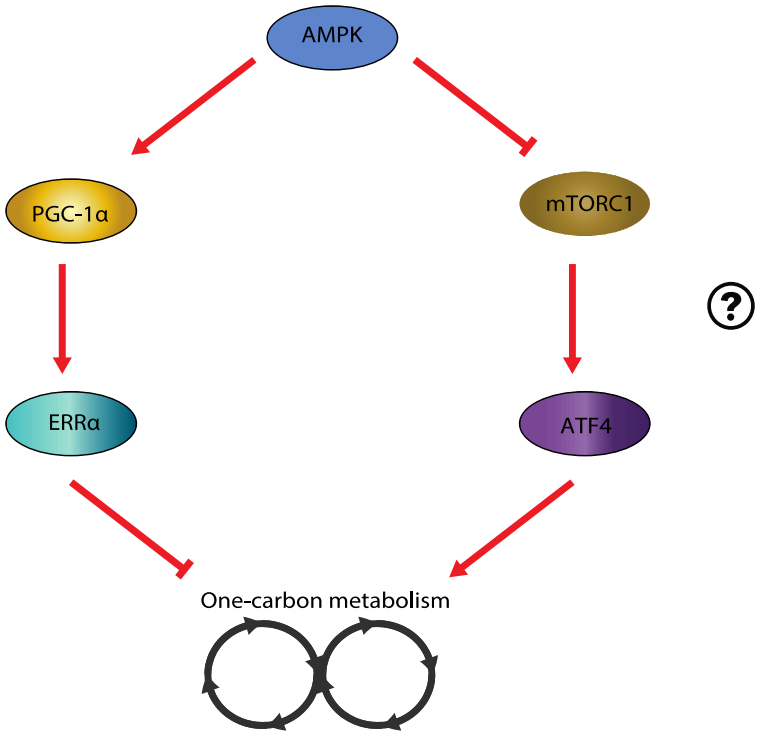

Figure 5.1 AMPK signalling mechanisms that are thought to inhibit one-carbon metabolism. Activation of PGC-1α/ERRα pathway inhibits the expression of the *MTHFD* genes of one-carbon metabolism, thereby decreasing its activity. The mTOR/ATF4 axis activates the expression of one-carbon metabolism genes, and mTORC1 is inhibited by AMPK. Future work will be needed to confirm if AMPK can impact one-carbon metabolism by modulating mTORC1/ATF4 activity.

Mitochondria host both bioenergetic and biosynthetic functions, and the ETC plays an important role in supporting mitochondrial-dependent anabolic processes. For example, dihydroorotate dehydrogenase (DHODH) of pyrimidine biosynthesis, is found in the inner mitochondrial membrane and couples the oxidation of dihydroorotate to orotate with the

reduction of ubiquinone to ubiquinol of the ETC. Suppression of DHODH impairs the function of complex III (Khutornenko et al., 2010) (Fang et al., 2013). In fact, uridine needs to be added to culture media of ρ0 cells (cells lacking mitochondrial DNA), exemplifying the importance of the ETC in supporting cell growth (Grassian et al., 2014) (Mullen et al., 2014). As one-carbon metabolism is also localized in mitochondria, recent reports have also observed the role of the ETC in supporting mitochondrial one-carbon metabolism. Respiratory chain impairment, as observed in mitochondrial disease, leads to a decrease in serine catabolism (Bao et al., 2016), while loss of SHMT2 decreases OXPHOS and translation of mitochondrial-encoded RNAs (Morscher et al., 2018). In addition, glycine is also used for heme biosynthesis, which is needed to build cytochromes of the electron transport chain (di Salvo et al., 2013). Finally, mTOR signalling upregulates mitochondrial activity by promoting the expression of nuclear-encoded mitochondrial genes at the level of translation (Morita et al. 2013). Thus, mitochondria link their biosynthetic processes to its bioenergetic capabilities.

Given their bioenergetic and biosynthetic functions, mitochondria are critical for responding to the needs of the cell. The AMPK/PGC-1α/ERRα axis coordinates the fine-tuning of gene programs to preserve energy homeostasis, which typically involves the upregulation of cellular bioenergetics and the inhibition of anabolic processes. One of the advantages of this signalling axis is that it targets both cytosolic and mitochondrial one-carbon metabolism pathways. Seeing that loss of mitochondrial one-carbon metabolism renders cells dependent on cytoplasmic pathway (Ducker et al. 2016), the inhibition of both one-carbon metabolic pathways by AMPK/PGC-1/ERR signalling can prevent compensation by one pathway over the other.

5.2. STRATEGIES FOR TARGETING ONE-CARBON METABOLISM IN CANCER

5.2.1 Improving methotrexate response

In this thesis, the impact of MTX treatment on AMPK/PGC-1α/ERRα signalling was observed. MTX induces AICAR, which can activate AMPK given its close similarity to AMP, an allosteric activator of AMPK. Indeed, AICAR is used as a pharmacological agent to activate AMPK in many *in vitro* studies (Fodor et al. 2016), (Beckers et al. 2006) (Tedeschi et al. 2015) (Pirkmajer et al. 2015). The intracellular concentration of AICAR represents a non-canonical method of activating AMPK. Other non-canonical ways of AMPK activation have also been described, including F6P induction in lysozymes (Zhang et al. 2017) and the accumulation of cellular ROS (Rabinowitz et al. 2017). The presence of non-canonical activators supports the notion that AMPK acts not only as a sensor of energetic stress due to adenylate charge, but rather as a global modulator of metabolic stress response.

MTX can cause several metabolic changes through AMPK. MTX-mediated AMPK activation increases glucose uptake (Pirkmajer et al. 2015 Diabetes) and inhibits protein synthesis (Tedeschi et al. 2015 Cancer & Metabolism). It is shown in this thesis that MTX increases bioenergetic capacity, mostly due to an increase in oxidative metabolism. As a result, MTX treatment rewires the metabolism of cancer cells towards an anti-Warburg phenotype where catabolic pathways such as cellular respiration are activated and anabolic pathways such as one-carbon metabolism and protein synthesis are inhibited. Indeed, the shift towards OXPHOS has been observed in several chemotherapy treatments in AML (Farge et al., 2017) and liver metastasis from colon cancer cells (Vellinga et al., 2015). The oxidative shift may provide a bioenergetic advantage for cells to cope with the energetic stress induced by

chemotherapy. In fact, OXPHOS has been found to be increased in chemo-resistant cancers (Wolf, 2014), underlining the importance of OXPHOS for maintaining cell survival in face of chemotherapeutic stress.

Given that MTX targets AMPK, combining MTX treated cells with AMPK activators is a strategy that could enhance the antiproliferative effects of MTX. As shown in this work, the combination of phenformin and MTX had a stronger impact on proliferation than either drug alone. In addition, enhancing AMPK as a strategy to improve MTX response had been observed using the combination of MTX with AICAR *in vitro* (Beckers et al. 2006) (Fodor T. et al. 2016). However, AICAR has poor bioavailability *in vivo* (Dixon et al., 1991), suggesting that pairing up MTX with an AMPK activator with greater bioavailability, such as phenformin, may help improve the antineoplastic effect of MTX *in vivo*.

Another factor that can improve methotrexate response is the addition of histidine. It was recently shown that high expression of histidine catabolism genes, a pathway that also consumes THF, is correlated with increased methotrexate sensitivity (Kanarek et al., 2018). The addition of histidine alone decreases the cellular pool of THF, a cofactor required for one-carbon reactions (Kanarek et al. 2018). Thus, upregulating the activity of histidine catabolism competes with one-carbon metabolism for THF availability, and improves the response of methotrexate, which blocks THF synthesis through inhibition of DHFR.

Furthermore, another factor contributing to methotrexate sensitivity is the drug's bioavailability. Natural folates and MTX are retained inside cells through polyglutamylation by the enzyme folylpolyglutamate synthetase (*FPGS*). Considering that this process involves the addition of glutamate groups, this reaction is evidently dependent on the availability of

glutamate. PGC-1α/ERRα signalling control glutamine metabolism in cells including the glutamine synthetase (*GLS1*) reaction that converts glutamine to glutamate, as well as several transaminase reactions that use or produce glutamate (McGuirk et al. 2013). Given the control of glutamine metabolism, the PGC-1α/ERRα axis act as determinants of glutamate availability. Whether the PGC-1α/ERRα axis impacts polyglutamylation is unknown and warrants further study.

5.2.2 Improving 5-FU treatment

Although PGC-1α/ERRα can inhibit the purine biosynthesis pathway, the axis is known to affect pyrimidine catabolism as well. PGC-1α/ERRα activate uridine phosphorylase (UPP), an enzyme that breaks down uridine to uracil and ribose -1-phosphate (Kong et al., 2009). Although uracil is the principal substrate of UPP, the enzyme can also incorporate 5-flurouracil (5-FU), an antifolate that inhibits the conversion of uracil into thymidine (Yan et al., 2006). Incorporation of 5-flurouracil into 5'-deoxy-5-flurouridine (5'-DFUR) acts as an uracil mimic and prevents the synthesis of thymidine, thereby inhibiting DNA synthesis (Yan et al. 2006). Given its control of UPP1, overexpression of PGC-1α sensitises breast cancer and colon cancer cells to 5-FU in vitro (Kong et al. 2009). Whether PGC-1α/ERRα can improve 5-FU response in vivo is still unclear.

5.2.3 Novel inhibitors of one-carbon metabolism

Increased one-carbon metabolism is emerging as metabolic characteristic of cancer cells. As a result, there is resurging interest in developing novel inhibitors that specifically target key regulatory enzymes of this pathway. The initial discovery of *de novo* serine biosynthesis in cancer had emerged in 1986 (Snell and Weber, 1986), but it wasn't until 2011 when the genomic amplification of *PHGDH* was observed in breast cancer (Possemato et al. 2011) and melanoma

(Locasale et al. 2011) that sparked interest in targeting serine metabolism in cancer. Novel inhibitors of PHGDH have been developed and confirmed using in vitro and in vivo models. The Cantley lab demonstrated that the inhibitor CBR-5884 is toxic to cells that overexpress *PHGDH*, with little effect on cells with low *PHGDH* expression (Mullarky et al., 2016a; Mullarky et al., 2016b). Removal of serine intensifies the antiproliferative effect of CBR-5884, while knockdown of *PHGDH* phenocopies the effects of CBR-5884 (Mullarky et al. 2016a) (Mullarky et al. 2016b). In addition, the PHGDH inhibitors NCT-502 and NCT-503 reduce the production of glucose-derived serine and the incorporation of one-carbon units into nucleotide formation, resulting in suppressed growth of cells in vitro and tumours in vivo (Pacold et al., 2016). Another key step of serine metabolism is the SHMT-mediated conversion of serine to glycine. Dual inhibitors of SHMT1 and SHMT2 have been reported to effective at blocking B-cell lymphoma cells which are defective at importing glycine (Ducker et al. 2017) and limits the proliferation of T cells, which are dependent on serine metabolism (Ma et al., 2017). Considering that serine biosynthesis has even been linked to BRAF resistance in melanoma (Ross et al., 2017), targeting serine metabolism using novel inhibitors may provide a clinical benefit.

Furthermore, novel inhibitors of the folate cycle have also been discovered. Recently, the natural product carolactin derived from the myxobacterium *Sorangium cellusoum* has been shown to inhibit both MTHFD1 and MTHFD2 in numerous cancer cell lines, including over 80% inhibition in HCT-116 cells, leading to decreased cellular proliferation (Fu et al., 2017). In addition, the MTHFD2 inhibitor, LY345899, was also designed as a means of specifically targeting MTHFD2, an isoform mostly restricted to embryonic and transformed cells (Gustafsson et al., 2017). It is still unclear to date whether these inhibitors have any effect on tumour growth *in vivo*.

Given the resurgence of one-carbon metabolism research, the development of novel inhibitors of this pathway has also resurfaced. It remains to be determined whether the combination of these novel inhibitors can produce a more potent effect on cancer cells than traditional antifolates such as MTX or 5-FU, as many of these novel inhibitors target isoforms that are highly expressed in cancer cells but have little or no expression in non-proliferative cells. Thus, these novel inhibitors have the opportunity of providing antiproliferative effects with greater specificity to cancer cells, compared to traditional antifolates. Perhaps, seeing that AMPK/PGC-1α/ERRα signalling can inhibit several reactions of one-carbon metabolism, the combination of novel inhibitors with activators of this transcriptional axis may also provide a therapeutic advantage.

5.3 SGLT2 INHIBITORS AND CANCER

The emergence of evidence supporting the antineoplastic effects of antidiabetic drugs has been explored extensively in the past decade. Epidemiological studies have shown a reduced risk of cancer in antidiabetic patients, which were taking metformin (Evans et al. 2005) (Libby et al. 2009) (Landman et al. 2010) (Decensi et al. 2010). Metabolic effects of metformin may be in part explained via activation of AMPK signalling (Shaw RJ et al. 2005) (Dowling RJ et al. 2007), and inhibition of complex I (Andrzejewski et al. 2014) (Wheaton et al. 2014). However, the emergence of clinical trials using metformin as a potential anti-neoplastic agent have shown disappointing results (He and Wondisford, 2015). One explanation is that the dose used in vitro studies may be too high to achieve antineoplastic response in patients (He and Wondisford, 2015).

The SGLT class of therapeutics has emerged as a metformin-alternative treatment strategy for type II diabetes (T2D). The inhibition of glucose reabsorption in the kidney by SGLT2 inhibitors, coupled with the anti-gluconeogenic response of metformin has had promising results for the treatment of diabetes (Zhang et al., 2014b). However, it was recently shown that SGLT2 inhibitors canagliflozin and dapagliflozin may have antineoplastic effects, but the mechanisms driving these anti-cancer effects are still elusive (Scafoglio et al. 2015) (Hawley et al. 2016) (Villiani et al. 2016). Canagliflozin and dapagliflozin appear to reduce growth of tumors expressing SGLT2 including colorectal cancer (Saito et al. 2015). However, it is been shown that canagliflozin still has antineoplastic effects even in the absence of glucose. This suggests that the antineoplastic action of canagliflozin may stem from its glucose-independent actions. Recently, it has been suggested that canagliflozin targets the electron transport chain (Hawley et al. 2016) (Villiani et al. 2016). Conversely, as shown in this thesis, both canagliflozin and dapagliflozin have no effect on complex I-mediated respiration. However, canagliflozin affects complex II-mediated respiration to an intensity that is comparable to malonate, a well established complex II inhibitor. Furthermore, canagliflozin can inhibits glutamate dehydrogenase, which provides further evidence that canagliflozin modulates the CAC (Secker et al. 2018).

Glutamine metabolism has been studied extensively for treatment in cancer (Luengo et al. 2017) (Cluntuin et al. 2017) (Hensley et al. 2017). After glucose, glutamine is considered the most important metabolite for fuelling tumour growth (DeBerardinins and Cheng, 2010). Most of the attention regarding targeting glutamine metabolism has been centred on glutamine synthetase (GLS), which converts glutamine to glutamate (Mates et al., 2018). The expression of glutamate dehydrogenase is increased in cancer, has been linked to poor prognosis (Dejure et al. 2017) and

is required for cells to survive under metabolic stress (Altman et al. 2016). Myc-amplified cancers have a high dependency on glutamine and are more susceptible to glutamine deprivation (Altman et al. 2016). As a result, given that canagliflozin perturbs glutamine metabolism, the antineoplastic effects of canagliflozin may be more potent in Myc-amplified cancers. In addition, tumours that harbour *IDH* mutations may also be particularly sensitive to canagliflozin, as these tumours are more reliant on glutamate dehydrogenase to produce α-ketoglutarate (Dang et al. 2009).

Thus, SGLT2 inhibitors such as canagliflozin also portray antineoplastic effects, although the mechanisms have only begun to be elucidated. SGLT2 inhibitors also have a high safety prolife, with mild side effects, such as bacterial urinary tract infections (UTI), which can be treated easily with antibiotics (Kufel et al., 2017). Given that metabolism is now a well-established determinant for both diabetes and cancer, it remains to be seen if other metabolic drugs can be repurposed as potential cancer therapeutics.

5.4 METABOLIC THERAPEUTICS AS ADJUNCT THERAPY FOR ONCOLOGICAL INDICATIONS

From Otto Warburg's initial discovery of aerobic glycolysis to the present-day resurgence of cancer metabolism research, it has become apparent that dysregulated metabolism is an emerging hallmark of cancer (Hanahan and Weinberg, 2011). Many chemotherapeutic agents, such as MTX, have metabolic consequences on cancer cells that affect their ability to survive and proliferate. In addition, metabolic drugs such as biguanides and SGLT2 inhibitors portray metabolic effects that can may be exploitable for treating cancer.

As aforementioned, one possible therapeutic avenue is the combination of biguanides and methotrexate. Biguanides activate AMPK/PGC-1α/ERRα-mediated repression of one-carbon metabolism (Audet-Walsh et al. 2016), which can improve MTX response in vitro, as shown in this work. Although metformin has a good safety profile, phenformin can cause lactic acidosis in patients, which is what led to its removal from the clinic in the US and Canada (Rosand et al., 1997), but is still used in several European countries and China (Salpeter et al., 2006). Nevertheless, the use of phenformin is still safer in comparison to the heavy toxicity posed by chemotherapeutic agents for treating cancer (Miskimins et al., 2014).

Furthermore, the combination of canagliflozin and metformin is used to treat diabetes (Zhang et al. 2014b). Given that both drugs have reported antineoplastic properties, their combination may have an additive effect on cancer treatment. Firstly, as metformin inhibits complex I, and we have shown evidence that canagliflozin can inhibit complex II, the combination of both drugs may produce a potent inhibition of OXPHOS. Secondly, it has been shown that metformin can further attenuate proliferation under glutamine deprivation, whereas increasing glutamine can protect against metformin treatment (Fendt et al. 2013). Given that we have shown evidence that canagliflozin inhibits glutamate dehydrogenase, the combination of canagliflozin and metformin may provide a stronger antiproliferative response.

Lastly, the perturbation of glutamate dehydrogenase by canagliflozin causes an increase in glutamate. Given that the availability of glutamate is required for the retention of MTX inside cells, it is tempting to speculate that canagliflozin may promote the polyglutamylation of MTX, thereby boosting its antineoplastic activity.

In conclusion, deciphering the underpinnings of cancer metabolism coupled to the development or repurposing of metabolic drugs can serve as an effective strategy to inhibit cancer progression. Future work will include the use of cutting-edge metabolomics and bioenergetics techniques to expose metabolic vulnerabilities that can be targeted pharmacologically to treat cancer.

REFERENCES:

Accioly, M.T., Pacheco, P., Maya-Monteiro, C.M., Carrossini, N., Robbs, B.K., Oliveira, S.S., Kaufmann, C., Morgado-Diaz, J.A., Bozza, P.T., and Viola, J.P. (2008). Lipid bodies are reservoirs of cyclooxygenase-2 and sites of prostaglandin-E2 synthesis in colon cancer cells. Cancer research *68*, 1732-1740.

Adamovich, Y., Shlomai, A., Tsvetkov, P., Umansky, K.B., Reuven, N., Estall, J.L., Spiegelman, B.M., and Shaul, Y. (2013). The protein level of PGC-1alpha, a key metabolic regulator, is controlled by NADH-NQO1. Molecular and cellular biology *33*, 2603-2613.

Agilent Technologies Ltd. (2017) Aglient Seahorse XF Cell Mito Stress Test Kit. Accessed August 28, 2018 https://www.agilent.com/cs/library/usermanuals/public/XF_Cell_Mito_Stress_Test_Kit_User_Guide.pdf

Al-Khallaf, H. (2017). Isocitrate dehydrogenases in physiology and cancer: biochemical and molecular insight. Cell Biosci *7*, 37.

Alaynick, W.A., Kondo, R.P., Xie, W., He, W., Dufour, C.R., Downes, M., Jonker, J.W., Giles, W., Naviaux, R.K., Giguère, V., et al. (2007). ERRgamma directs and maintains the transition to oxidative metabolism in the postnatal heart. Cell metabolism *6*, 13-24.

Alessi, D.R., Sakamoto, K., and Bayascas, J.R. (2006). LKB1-dependent signalling pathways. Annu Rev Biochem *75*, 137-163.

Altman, B.J., Stine, Z.E., and Dang, C.V. (2016). From Krebs to clinic: glutamine metabolism to cancer therapy. Nature reviews. Cancer *16*, 773.

Ancey, P.B., Contat, C., and Meylan, E. (2018). Glucose transporters in cancer - from tumor cells to the tumor microenvironment. FEBS J.

Andersson, U., and Scarpulla, R.C. (2001). Pgc-1-related coactivator, a novel, serum-inducible coactivator of nuclear respiratory factor 1-dependent transcription in mammalian cells. Molecular and cellular biology *21*, 3738-3749.

Andrzejewski, S., Gravel, S.-P., Pollak, M., and St-Pierre, J. (2014a). Metformin directly acts on mitochondria to alter cellular bioenergetics. Cancer & metabolism *2*, 12-12.

Andrzejewski, S., Gravel, S.P., Pollak, M., and St-Pierre, J. (2014b). Metformin directly acts on mitochondria to alter cellular bioenergetics. Cancer & metabolism *2*, 12.

Andrzejewski, S., Klimcakova, E., Johnson, R.M., Tabaries, S., Annis, M.G., McGuirk, S., Northey, J.J., Chenard, V., Sriram, U., Papadopoli, D.J., et al. (2017). PGC-1alpha Promotes

Breast Cancer Metastasis and Confers Bioenergetic Flexibility against Metabolic Drugs. Cell metabolism *26*, 778-787 e775.

Anisimov, V.N., Berstein, L.M., Egormin, P.A., Piskunova, T.S., Popovich, I.G., Zabezhinski, M.A., Kovalenko, I.G., Poroshina, T.E., Semenchenko, A.V., Provinciali, M., et al. (2005). Effect of metformin on life span and on the development of spontaneous mammary tumors in HER-2/neu transgenic mice. Exp Gerontol *40*, 685-693.

Antico Arciuch, V.G., Russo, M.A., Kang, K.S., and Di Cristofano, A. (2013). Inhibition of AMPK and Krebs cycle gene expression drives metabolic remodeling of Pten-deficient preneoplastic thyroid cells. Cancer research *73*, 5459-5472.

Appling, D.R., Anthony-Cahill, S.J., and Mathews, C.K. (2019). Biochemistry : concepts and connections. (New York: Pearson).

Arany, Z., Foo, S.Y., Ma, Y., Ruas, J.L., Bommi-Reddy, A., Girnun, G., Cooper, M., Laznik, D., Chinsomboon, J., Rangwala, S.M., et al. (2008). HIF-independent regulation of VEGF and angiogenesis by the transcriptional coactivator PGC-1alpha. Nature *451*, 1008-1012.

Arany, Z., Lebrasseur, N., Morris, C., Smith, E., Yang, W., Ma, Y., Chin, S., and Spiegelman, B.M. (2007). The transcriptional coactivator PGC-1beta drives the formation of oxidative type IIX fibers in skeletal muscle. Cell metabolism *5*, 35-46.

Ariazi, E.A., Clark, G.M., and Mertz, J.E. (2002). Estrogen-related receptor alpha and estrogen-related receptor gamma associate with unfavorable and favorable biomarkers, respectively, in human breast cancer. Cancer research *62*, 6510-6518.

Atsumi, T., Chesney, J., Metz, C., Leng, L., Donnelly, S., Makita, Z., Mitchell, R., and Bucala, R. (2002). High expression of inducible 6-phosphofructo-2-kinase/fructose-2,6-bisphosphatase (iPFK-2; PFKFB3) in human cancers. Cancer research *62*, 5881-5887.

Audet-Walsh, É., Papadopoli, D.J., Gravel, S.-P., Yee, T., Bridon, G., Caron, M., Bourque, G., Giguère, V., and St-Pierre, J. (2016). The PGC-1α/ERRα Axis Represses One-Carbon Metabolism and Promotes Sensitivity to Anti-folate Therapy in Breast Cancer. Cell Reports *14*, 920-931.

Austin, S., and St-Pierre, J. (2012). PGC1alpha and mitochondrial metabolism--emerging concepts and relevance in ageing and neurodegenerative disorders. J Cell Sci *125*, 4963-4971.

Ba, Y., Zhang, C.N., Zhang, Y., and Zhang, C.Y. (2008). [Down-regulation of PGC-1alpha expression in human hepatocellular carcinoma]. Zhonghua Zhong Liu Za Zhi *30*, 593-597.

Bailey, C.J. (1993). Metformin--an update. Gen Pharmacol *24*, 1299-1309.

Bao, X.R., Ong, S.E., Goldberger, O., Peng, J., Sharma, R., Thompson, D.A., Vafai, S.B., Cox, A.G., Marutani, E., Ichinose, F., et al. (2016). Mitochondrial dysfunction remodels one-carbon metabolism in human cells. Elife *5*.

Barry, J.B., and Giguère, V. (2005). Epidermal growth factor-induced signalling in breast cancer cells results in selective target gene activation by orphan nuclear receptor estrogen-related receptor alpha. Cancer research *65*, 6120-6129.

Bays, H. (2013). Sodium Glucose Co-transporter Type 2 (SGLT2) Inhibitors: Targeting the Kidney to Improve Glycemic Control in Diabetes Mellitus. Diabetes Ther *4*, 195-220.

Beckers, A., Organe, S., Timmermans, L., Vanderhoydonc, F., Deboel, L., Derua, R., Waelkens, E., Brusselmans, K., Verhoeven, G., and Swinnen, J.V. (2006). Methotrexate enhances the antianabolic and antiproliferative effects of 5-aminoimidazole-4-carboxamide riboside. Mol Cancer Ther *5*, 2211-2217.

Bell, J.L., and Baron, D.N. (1968). Subcellular distribution of the isoenzymes of NADP isocitrate dehydrogenase in rat liver and heart. Enzymol Biol Clin (Basel) *9*, 393-399.

Ben Sahra, I., Laurent, K., Loubat, A., Giorgetti-Peraldi, S., Colosetti, P., Auberger, P., Tanti, J.F., Le Marchand-Brustel, Y., and Bost, F. (2008). The antidiabetic drug metformin exerts an antitumoral effect in vitro and in vivo through a decrease of cyclin D1 level. Oncogene *27*, 3576-3586.

Ben-Haim, S., and Ell, P. (2009). 18F-FDG PET and PET/CT in the evaluation of cancer treatment response. J Nucl Med *50*, 88-99.

Ben-Sahra, I., Howell, J.J., Asara, J.M., and Manning, B.D. (2013). Stimulation of de novo pyrimidine synthesis by growth signalling through mTOR and S6K1. Science (New York, N.Y.) *339*, 1323-1328.

Ben-Sahra, I., Hoxhaj, G., Ricoult, S.J.H., Asara, J.M., and Manning, B.D. (2016). mTORC1 induces purine synthesis through control of the mitochondrial tetrahydrofolate cycle. Science (New York, N.Y.) *351*, 728-733.

Bensaad, K., Tsuruta, A., Selak, M.A., Vidal, M.N., Nakano, K., Bartrons, R., Gottlieb, E., and Vousden, K.H. (2006). TIGAR, a p53-inducible regulator of glycolysis and apoptosis. Cell *126*, 107-120.

Berg, J.M., Tymoczko, J.L., Stryer, L., and Stryer, L. (2007). Biochemistry. (New York: W. H. Freeman).

Bhalla, K., Hwang, B.J., Dewi, R.E., Ou, L., Twaddel, W., Fang, H.B., Vafai, S.B., Vazquez, F., Puigserver, P., Boros, L., et al. (2011). PGC1alpha promotes tumor growth by inducing gene expression programs supporting lipogenesis. Cancer research *71*, 6888-6898.

Bhutia, Y.D., and Ganapathy, V. (2016). Glutamine transporters in mammalian cells and their functions in physiology and cancer. Biochim Biophys Acta *1863*, 2531-2539.

Bookout, A.L., Jeong, Y., Downes, M., Yu, R.T., Evans, R.M., and Mangelsdorf, D.J. (2006). Anatomical profiling of nuclear receptor expression reveals a hierarchical transcriptional network. Cell *126*, 789-799.

Bouchoucha, M., Uzzan, B., and Cohen, R. (2011). Metformin and digestive disorders. Diabetes Metab *37*, 90-96.

Brahimi-Horn, M.C., Chiche, J., and Pouyssegur, J. (2007). Hypoxia and cancer. J Mol Med (Berl) *85*, 1301-1307.

Brand, M.D., and Nicholls, D.G. (2011). Assessing mitochondrial dysfunction in cells. The Biochemical journal *435*, 297-312.

Bridges, H.R., Jones, A.J., Pollak, M.N., and Hirst, J. (2014). Effects of metformin and other biguanides on oxidative phosphorylation in mitochondria. The Biochemical journal *462*, 475-487.

Brugarolas, J.B., Vazquez, F., Reddy, A., Sellers, W.R., and Kaelin, W.G., Jr. (2003). TSC2 regulates VEGF through mTOR-dependent and -independent pathways. Cancer cell *4*, 147-158.

Buescher, J.M., Antoniewicz, M.R., Boros, L.G., Burgess, S.C., Brunengraber, H., Clish, C.B., DeBerardinis, R.J., Feron, O., Frezza, C., Ghesquiere, B., et al. (2015). A roadmap for interpreting (13)C metabolite labeling patterns from cells. Curr Opin Biotechnol *34*, 189-201.

Buzzai, M., Jones, R.G., Amaravadi, R.K., Lum, J.J., DeBerardinis, R.J., Zhao, F., Viollet, B., and Thompson, C.B. (2007). Systemic treatment with the antidiabetic drug metformin selectively impairs p53-deficient tumor cell growth. Cancer research *67*, 6745-6752.

Cai, Y., Wang, J., Zhang, L., Wu, D., Yu, D., Tian, X., Liu, J., Jiang, X., Shen, Y., Zhang, L., et al. (2015). Expressions of fatty acid synthase and HER2 are correlated with poor prognosis of ovarian cancer. Med Oncol *32*, 391.

Canadian Cancer Statistics Advisory Committee. (2018) Canadian Cancer Statistics 2018. Toronto, ON: Canadian Cancer Society. Available at: cancer.ca/Canadian-Cancer-Statistics-2018-EN (accessed Aug. 28, 2018).

Cangoz, S., Chang, Y.Y., Chempakaseril, S.J., Guduru, R.C., Huynh, L.M., John, J.S., John, S.T., Joseph, M.E., Judge, R., Kimmey, R., et al. (2013). The kidney as a new target for antidiabetic drugs: SGLT2 inhibitors. J Clin Pharm Ther *38*, 350-359.

Canto, C., Gerhart-Hines, Z., Feige, J.N., Lagouge, M., Noriega, L., Milne, J.C., Elliott, P.J., Puigserver, P., and Auwerx, J. (2009). AMPK regulates energy expenditure by modulating NAD+ metabolism and SIRT1 activity. Nature *458*, 1056-1060.

Cantrell, L.A., Zhou, C., Mendivil, A., Malloy, K.M., Gehrig, P.A., and Bae-Jump, V.L. (2010). Metformin is a potent inhibitor of endometrial cancer cell proliferation--implications for a novel treatment strategy. Gynecol Oncol *116*, 92-98.

Cao, W., Collins, Q.F., Becker, T.C., Robidoux, J., Lupo, E.G., Jr., Xiong, Y., Daniel, K.W., Floering, L., and Collins, S. (2005). p38 Mitogen-activated protein kinase plays a stimulatory role in hepatic gluconeogenesis. The Journal of biological chemistry *280*, 42731-42737.

Castro-Vega, L.J., Buffet, A., De Cubas, A.A., Cascon, A., Menara, M., Khalifa, E., Amar, L., Azriel, S., Bourdeau, I., Chabre, O., et al. (2014). Germline mutations in FH confer predisposition to malignant pheochromocytomas and paragangliomas. Hum Mol Genet *23*, 2440-2446.

Cavallini, A., Notarnicola, M., Giannini, R., Montemurro, S., Lorusso, D., Visconti, A., Minervini, F., and Caruso, M.G. (2005). Oestrogen receptor-related receptor alpha (ERRalpha) and oestrogen receptors (ERalpha and ERbeta) exhibit different gene expression in human colorectal tumour progression. Eur J Cancer *41*, 1487-1494.

Cervera, A.M., Apostolova, N., Crespo, F.L., Mata, M., and McCreath, K.J. (2008). Cells silenced for SDHB expression display characteristic features of the tumor phenotype. Cancer research *68*, 4058-4067.

Chabner, B.A., Allegra, C.J., Curt, G.A., Clendeninn, N.J., Baram, J., Koizumi, S., Drake, J.C., and Jolivet, J. (1985). Polyglutamation of methotrexate. Is methotrexate a prodrug? The Journal of clinical investigation *76*, 907-912.

Chabner, B.A., and Roberts, T.G., Jr. (2005). Timeline: Chemotherapy and the war on cancer. Nature reviews. Cancer *5*, 65-72.

Chajes, V., Cambot, M., Moreau, K., Lenoir, G.M., and Joulin, V. (2006). Acetyl-CoA carboxylase alpha is essential to breast cancer cell survival. Cancer research *66*, 5287-5294.

Chang, C.Y., Kazmin, D., Jasper, J.S., Kunder, R., Zuercher, W.J., and McDonnell, D.P. (2011). The metabolic regulator ERRalpha, a downstream target of HER2/IGF-1R, as a therapeutic target in breast cancer. Cancer cell *20*, 500-510.

Chao, E.C., and Henry, R.R. (2010). SGLT2 inhibition--a novel strategy for diabetes treatment. Nature reviews. Drug discovery *9*, 551-559.

Charest-Marcotte, A., Dufour, C.R., Wilson, B.J., Tremblay, A.M., Eichner, L.J., Arlow, D.H., Mootha, V.K., and Giguère, V. (2010). The homeobox protein Prox1 is a negative modulator of ERR{alpha}/PGC-1{alpha} bioenergetic functions. Genes & development *24*, 537-542.

Chaube, B., Malvi, P., Singh, S.V., Mohammad, N., Viollet, B., and Bhat, M.K. (2015). AMPK maintains energy homeostasis and survival in cancer cells via regulating p38/PGC-1alpha-mediated mitochondrial biogenesis. Cell Death Discov *1*, 15063.

Chaveroux, C., Eichner, L.J., Dufour, C.R., Shatnawi, A., Khoutorsky, A., Bourque, G., Sonenberg, N., and Giguère, V. (2013). Molecular and genetic crosstalks between mTOR and ERRalpha are key determinants of rapamycin-induced nonalcoholic fatty liver. Cell metabolism *17*, 586-598.

Chen, C.Y., Chen, J., He, L., and Stiles, B.L. (2018). PTEN: Tumor Suppressor and Metabolic Regulator. Front Endocrinol (Lausanne) *9*, 338.

Chen, R., Nishimura, M.C., Kharbanda, S., Peale, F., Deng, Y., Daemen, A., Forrest, W.F., Kwong, M., Hedehus, M., Hatzivassiliou, G., et al. (2014). Hominoid-specific enzyme GLUD2 promotes growth of IDH1R132H glioma. Proceedings of the National Academy of Sciences of the United States of America *111*, 14217-14222.

Cheng, C., Geng, F., Cheng, X., and Guo, D. (2018). Lipid metabolism reprogramming and its potential targets in cancer. Cancer Commun (Lond) *38*, 27.

Cheung, C.P., Yu, S., Wong, K.B., Chan, L.W., Lai, F.M., Wang, X., Suetsugi, M., Chen, S., and Chan, F.L. (2005). Expression and functional study of estrogen receptor-related receptors in human prostatic cells and tissues. J Clin Endocrinol Metab *90*, 1830-1844.

Cho, E.S., Cha, Y.H., Kim, H.S., Kim, N.H., and Yook, J.I. (2018). The Pentose Phosphate Pathway as a Potential Target for Cancer Therapy. Biomol Ther (Seoul) *26*, 29-38.

Christofk, H.R., Vander Heiden, M.G., Wu, N., Asara, J.M., and Cantley, L.C. (2008). Pyruvate kinase M2 is a phosphotyrosine-binding protein. Nature *452*, 181-186.

Clem, B.F., O'Neal, J., Tapolsky, G., Clem, A.L., Imbert-Fernandez, Y., Kerr, D.A., 2nd, Klarer, A.C., Redman, R., Miller, D.M., Trent, J.O., et al. (2013). Targeting 6-phosphofructo-2-kinase (PFKFB3) as a therapeutic strategy against cancer. Mol Cancer Ther *12*, 1461-1470.

ClinicalTrials.gov. Bethesda (MD): National Library of Medicine (US). Metformin and Cancer. Accessed on August 28, 2018 https://clinicaltrials.gov/ct2/results?cond=metformin+and+cancer&term=&cntry=&state=&city=&dist=

Cluntun, A.A., Lukey, M.J., Cerione, R.A., and Locasale, J.W. (2017). Glutamine Metabolism in Cancer: Understanding the Heterogeneity. Trends in cancer *3*, 169-180.

Cockman, M.E., Masson, N., Mole, D.R., Jaakkola, P., Chang, G.W., Clifford, S.C., Maher, E.R., Pugh, C.W., Ratcliffe, P.J., and Maxwell, P.H. (2000). Hypoxia inducible factor-alpha

binding and ubiquitylation by the von Hippel-Lindau tumor suppressor protein. The Journal of biological chemistry *275*, 25733-25741.

Compagno, M., Lim, W.K., Grunn, A., Nandula, S.V., Brahmachary, M., Shen, Q., Bertoni, F., Ponzoni, M., Scandurra, M., Califano, A., et al. (2009). Mutations of multiple genes cause deregulation of NF-kappaB in diffuse large B-cell lymphoma. Nature *459*, 717-721.

Cool, B., Zinker, B., Chiou, W., Kifle, L., Cao, N., Perham, M., Dickinson, R., Adler, A., Gagne, G., Iyengar, R., et al. (2006). Identification and characterization of a small molecule AMPK activator that treats key components of type 2 diabetes and the metabolic syndrome. Cell metabolism *3*, 403-416.

Cormio, A., Guerra, F., Cormio, G., Pesce, V., Fracasso, F., Loizzi, V., Cantatore, P., Selvaggi, L., and Gadaleta, M.N. (2009). The PGC-1alpha-dependent pathway of mitochondrial biogenesis is upregulated in type I endometrial cancer. Biochem Biophys Res Commun *390*, 1182-1185.

Corominas-Faja, B., Quirantes-Pine, R., Oliveras-Ferraros, C., Vazquez-Martin, A., Cufi, S., Martin-Castillo, B., Micol, V., Joven, J., Segura-Carretero, A., and Menendez, J.A. (2012). Metabolomic fingerprint reveals that metformin impairs one-carbon metabolism in a manner similar to the antifolate class of chemotherapy drugs. Aging (Albany NY) *4*, 480-498.

Costello, L.C., and Franklin, R.B. (2016). A comprehensive review of the role of zinc in normal prostate function and metabolism; and its implications in prostate cancer. Arch Biochem Biophys *611*, 100-112.

Courtnay, R., Ngo, D.C., Malik, N., Ververis, K., Tortorella, S.M., and Karagiannis, T.C. (2015). Cancer metabolism and the Warburg effect: the role of HIF-1 and PI3K. Mol Biol Rep *42*, 841-851.

Cronstein, B.N., Naime, D., and Ostad, E. (1993). The antiinflammatory mechanism of methotrexate. Increased adenosine release at inflamed sites diminishes leukocyte accumulation in an in vivo model of inflammation. The Journal of clinical investigation *92*, 2675-2682.

Csibi, A., Fendt, S.M., Li, C., Poulogiannis, G., Choo, A.Y., Chapski, D.J., Jeong, S.M., Dempsey, J.M., Parkhitko, A., Morrison, T., et al. (2013). The mTORC1 pathway stimulates glutamine metabolism and cell proliferation by repressing SIRT4. Cell *153*, 840-854.

Cunningham, J.T., Moreno, M.V., Lodi, A., Ronen, S.M., and Ruggero, D. (2014). Protein and nucleotide biosynthesis are coupled by a single rate-limiting enzyme, PRPS2, to drive cancer. Cell *157*, 1088-1103.

D'Errico, I., Lo Sasso, G., Salvatore, L., Murzilli, S., Martelli, N., Cristofaro, M., Latorre, D., Villani, G., and Moschetta, A. (2011a). Bax is necessary for PGC1alpha pro-apoptotic effect in colorectal cancer cells. Cell Cycle *10*, 2937-2945.

D'Errico, I., Salvatore, L., Murzilli, S., Lo Sasso, G., Latorre, D., Martelli, N., Egorova, A.V., Polishuck, R., Madeyski-Bengtson, K., Lelliott, C., et al. (2011b). Peroxisome proliferator-activated receptor-gamma coactivator 1-alpha (PGC1alpha) is a metabolic regulator of intestinal epithelial cell fate. Proceedings of the National Academy of Sciences of the United States of America *108*, 6603-6608.

Dang, C.V. (2010). Glutaminolysis: supplying carbon or nitrogen or both for cancer cells? Cell Cycle *9*, 3884-3886.

Dang, L., White, D.W., Gross, S., Bennett, B.D., Bittinger, M.A., Driggers, E.M., Fantin, V.R., Jang, H.G., Jin, S., Keenan, M.C., et al. (2009). Cancer-associated IDH1 mutations produce 2-hydroxyglutarate. Nature *462*, 739-744.

Davies, S.P., Sim, A.T., and Hardie, D.G. (1990). Location and function of three sites phosphorylated on rat acetyl-CoA carboxylase by the AMP-activated protein kinase. European journal of biochemistry / FEBS *187*, 183-190.

DeBerardinis, R.J. (2011). Serine metabolism: some tumors take the road less traveled. Cell metabolism *14*, 285-286.

DeBerardinis, R.J., and Cheng, T. (2010). Q's next: the diverse functions of glutamine in metabolism, cell biology and cancer. Oncogene *29*, 313-324.

Deberardinis, R.J., Sayed, N., Ditsworth, D., and Thompson, C.B. (2008). Brick by brick: metabolism and tumor cell growth. Curr Opin Genet Dev *18*, 54-61.

Deblois, G., Hall, J.A., Perry, M.C., Laganiere, J., Ghahremani, M., Park, M., Hallett, M., and Giguère, V. (2009). Genome-wide identification of direct target genes implicates estrogen-related receptor alpha as a determinant of breast cancer heterogeneity. Cancer research *69*, 6149-6157.

Deblois, G., Smith, H.W., Tam, I.S., Gravel, S.P., Caron, M., Savage, P., Labbe, D.P., Begin, L.R., Tremblay, M.L., Park, M., et al. (2016). ERRalpha mediates metabolic adaptations driving lapatinib resistance in breast cancer. Nature communications *7*, 12156.

Decensi, A., Puntoni, M., Goodwin, P., Cazzaniga, M., Gennari, A., Bonanni, B., and Gandini, S. (2010). Metformin and cancer risk in diabetic patients: a systematic review and meta-analysis. Cancer Prev Res (Phila) *3*, 1451-1461.

DeFronzo, R.A., Barzilai, N., and Simonson, D.C. (1991). Mechanism of metformin action in obese and lean noninsulin-dependent diabetic subjects. J Clin Endocrinol Metab *73*, 1294-1301.

DeFronzo, R.A., Chilton, R., Norton, L., Clarke, G., Ryder, R.E., and Abdul-Ghani, M. (2016). Revitalization of pioglitazone: the optimum agent to be combined with a sodium-glucose co-transporter-2 inhibitor. Diabetes Obes Metab *18*, 454-462.

Dejure, F.R., and Eilers, M. (2017). MYC and tumor metabolism: chicken and egg. EMBO J *36*, 3409-3420.

Di Pietro, E., Sirois, J., Tremblay, M.L., and MacKenzie, R.E. (2002). Mitochondrial NAD-dependent methylenetetrahydrofolate dehydrogenase-methenyltetrahydrofolate cyclohydrolase is essential for embryonic development. Molecular and cellular biology *22*, 4158-4166.

Di Pietro, E., Wang, X.L., and MacKenzie, R.E. (2004). The expression of mitochondrial methylenetetrahydrofolate dehydrogenase-cyclohydrolase supports a role in rapid cell growth. Biochim Biophys Acta *1674*, 78-84.

di Salvo, M.L., Contestabile, R., Paiardini, A., and Maras, B. (2013). Glycine consumption and mitochondrial serine hydroxymethyltransferase in cancer cells: the heme connection. Med Hypotheses *80*, 633-636.

Dicker, A.P., Waltham, M.C., Volkenandt, M., Schweitzer, B.I., Otter, G.M., Schmid, F.A., Sirotnak, F.M., and Bertino, J.R. (1993). Methotrexate resistance in an in vivo mouse tumor due to a non-active-site dihydrofolate reductase mutation. Proceedings of the National Academy of Sciences of the United States of America *90*, 11797-11801.

Dittrich, A., Gautrey, H., Browell, D., and Tyson-Capper, A. (2014). The HER2 Signalling Network in Breast Cancer--Like a Spider in its Web. J Mammary Gland Biol Neoplasia *19*, 253-270.

Dixon, R., Gourzis, J., McDermott, D., Fujitaki, J., Dewland, P., and Gruber, H. (1991). AICA-riboside: safety, tolerance, and pharmacokinetics of a novel adenosine-regulating agent. J Clin Pharmacol *31*, 342-347.

Dodd, K.M., Yang, J., Shen, M.H., Sampson, J.R., and Tee, A.R. (2015). mTORC1 drives HIF-1alpha and VEGF-A signalling via multiple mechanisms involving 4E-BP1, S6K1 and STAT3. Oncogene *34*, 2239-2250.

Dowling, R.J., Zakikhani, M., Fantus, I.G., Pollak, M., and Sonenberg, N. (2007). Metformin inhibits mammalian target of rapamycin-dependent translation initiation in breast cancer cells. Cancer research *67*, 10804-10812.

Ducker, G.S., Chen, L., Morscher, R.J., Ghergurovich, J.M., Esposito, M., Teng, X., Kang, Y., and Rabinowitz, J.D. (2016). Reversal of Cytosolic One-Carbon Flux Compensates for Loss of the Mitochondrial Folate Pathway. Cell metabolism *23*, 1140-1153.

Ducker, G.S., and Rabinowitz, J.D. (2017). One-Carbon Metabolism in Health and Disease. Cell metabolism *25*, 27-42.

Dufour, C.R., Levasseur, M.P., Pham, N.H., Eichner, L.J., Wilson, B.J., Charest-Marcotte, A., Duguay, D., Poirier-Heon, J.F., Cermakian, N., and Giguère, V. (2011). Genomic convergence among ERRalpha, PROX1, and BMAL1 in the control of metabolic clock outputs. PLoS Genet *7*, e1002143.

Dufour, C.R., Wilson, B.J., Huss, J.M., Kelly, D.P., Alaynick, W.A., Downes, M., Evans, R.M., Blanchette, M., and Giguère, V. (2007). Genome-wide orchestration of cardiac functions by the orphan nuclear receptors ERRalpha and gamma. Cell metabolism *5*, 345-356.

Duvel, K., Yecies, J.L., Menon, S., Raman, P., Lipovsky, A.I., Souza, A.L., Triantafellow, E., Ma, Q., Gorski, R., Cleaver, S., et al. (2010). Activation of a metabolic gene regulatory network downstream of mTOR complex 1. Mol Cell *39*, 171-183.

Edmunds, L.R., Sharma, L., Kang, A., Lu, J., Vockley, J., Basu, S., Uppala, R., Goetzman, E.S., Beck, M.E., Scott, D., et al. (2014). c-Myc programs fatty acid metabolism and dictates acetyl-CoA abundance and fate. The Journal of biological chemistry *289*, 25382-25392.

Egan, D.F., Shackelford, D.B., Mihaylova, M.M., Gelino, S., Kohnz, R.A., Mair, W., Vasquez, D.S., Joshi, A., Gwinn, D.M., Taylor, R., et al. (2011). Phosphorylation of ULK1 (hATG1) by AMP-activated protein kinase connects energy sensing to mitophagy. Science (New York, N.Y.) *331*, 456-461.

Eichner, L.J., Perry, M.C., Dufour, C.R., Bertos, N., Park, M., St-Pierre, J., and Giguère, V. (2010). miR-378(*) mediates metabolic shift in breast cancer cells via the PGC-1beta/ERRgamma transcriptional pathway. Cell metabolism *12*, 352-361.

El-Masry, O.S., Brown, B.L., and Dobson, P.R. (2012). Effects of activation of AMPK on human breast cancer cell lines with different genetic backgrounds. Oncol Lett *3*, 224-228.
Elango, T., Dayalan, H., Gnanaraj, P., Malligarjunan, H., and Subramanian, S. (2014). Impact of methotrexate on oxidative stress and apoptosis markers in psoriatic patients. Clin Exp Med *14*, 431-437.

Elstrom, R.L., Bauer, D.E., Buzzai, M., Karnauskas, R., Harris, M.H., Plas, D.R., Zhuang, H., Cinalli, R.M., Alavi, A., Rudin, C.M., et al. (2004). Akt stimulates aerobic glycolysis in cancer cells. Cancer research *64*, 3892-3899.

Eroles, P., Bosch, A., Perez-Fidalgo, J.A., and Lluch, A. (2012). Molecular biology in breast cancer: intrinsic subtypes and signalling pathways. Cancer Treat Rev *38*, 698-707.
Estrella, V., Chen, T., Lloyd, M., Wojtkowiak, J., Cornnell, H.H., Ibrahim-Hashim, A., Bailey, K., Balagurunathan, Y., Rothberg, J.M., Sloane, B.F., et al. (2013). Acidity generated by the tumor microenvironment drives local invasion. Cancer research *73*, 1524-1535.

Evans, J.M., Donnelly, L.A., Emslie-Smith, A.M., Alessi, D.R., and Morris, A.D. (2005). Metformin and reduced risk of cancer in diabetic patients. BMJ *330*, 1304-1305.
Fan, J., Ye, J., Kamphorst, J.J., Shlomi, T., Thompson, C.B., and Rabinowitz, J.D. (2014). Quantitative flux analysis reveals folate-dependent NADPH production. Nature *510*, 298-302.

Fang, J., Uchiumi, T., Yagi, M., Matsumoto, S., Amamoto, R., Takazaki, S., Yamaza, H., Nonaka, K., and Kang, D. (2013). Dihydro-orotate dehydrogenase is physically associated with the respiratory complex and its loss leads to mitochondrial dysfunction. Biosci Rep *33*, e00021.

Fantin, V.R., St-Pierre, J., and Leder, P. (2006). Attenuation of LDH-A expression uncovers a link between glycolysis, mitochondrial physiology, and tumor maintenance. Cancer cell *9*, 425-434.

Farber, S., Cutler, E.C., Hawkins, J.W., Harrison, J.H., Peirce, E.C., 2nd, and Lenz, G.G. (1947). The Action of Pteroylglutamic Conjugates on Man. Science (New York, N.Y.) *106*, 619-621.

Farber, S., and Diamond, L.K. (1948). Temporary remissions in acute leukemia in children produced by folic acid antagonist, 4-aminopteroyl-glutamic acid. N Engl J Med *238*, 787-793.
Farge, T., Saland, E., de Toni, F., Aroua, N., Hosseini, M., Perry, R., Bosc, C., Sugita, M., Stuani, L., Fraisse, M., et al. (2017). Chemotherapy-Resistant Human Acute Myeloid Leukemia Cells Are Not Enriched for Leukemic Stem Cells but Require Oxidative Metabolism. Cancer Discov *7*, 716-735.

Faubert, B., Boily, G., Izreig, S., Griss, T., Samborska, B., Dong, Z., Dupuy, F., Chambers, C., Fuerth, B.J., Viollet, B., et al. (2013). AMPK is a negative regulator of the Warburg effect and suppresses tumor growth in vivo. Cell metabolism *17*, 113-124.

Faubert, B., Li, K.Y., Cai, L., Hensley, C.T., Kim, J., Zacharias, L.G., Yang, C., Do, Q.N., Doucette, S., Burguete, D., et al. (2017). Lactate Metabolism in Human Lung Tumors. Cell *171*, 358-371 e359.

Faubert, B., Vincent, E.E., Poffenberger, M.C., and Jones, R.G. (2015). The AMP-activated protein kinase (AMPK) and cancer: Many faces of a metabolic regulator. Cancer Letters *356*, 165-170.

Feilchenfeldt, J., Brundler, M.A., Soravia, C., Totsch, M., and Meier, C.A. (2004). Peroxisome proliferator-activated receptors (PPARs) and associated transcription factors in colon cancer: reduced expression of PPARgamma-coactivator 1 (PGC-1). Cancer Lett *203*, 25-33.

Fendt, S.M., Bell, E.L., Keibler, M.A., Davidson, S.M., Wirth, G.J., Fiske, B., Mayers, J.R., Schwab, M., Bellinger, G., Csibi, A., et al. (2013). Metformin decreases glucose oxidation and increases the dependency of prostate cancer cells on reductive glutamine metabolism. Cancer research *73*, 4429-4438.

Fernandez-Marcos, P.J., and Auwerx, J. (2011). Regulation of PGC-1alpha, a nodal regulator of mitochondrial biogenesis. Am J Clin Nutr *93*, 884S-890.

Fieuw, A., Kumps, C., Schramm, A., Pattyn, F., Menten, B., Antonacci, F., Sudmant, P., Schulte, J.H., Van Roy, N., Vergult, S., et al. (2012). Identification of a novel recurrent 1q42.2-1qter deletion in high risk MYCN single copy 11q deleted neuroblastomas. Int J Cancer *130*, 2599-2606.

Figueroa, M.E., Abdel-Wahab, O., Lu, C., Ward, P.S., Patel, J., Shih, A., Li, Y., Bhagwat, N., Vasanthakumar, A., Fernandez, H.F., et al. (2010). Leukemic IDH1 and IDH2 mutations result in

a hypermethylation phenotype, disrupt TET2 function, and impair hematopoietic differentiation. Cancer cell *18*, 553-567.

Filipp, F.V., Scott, D.A., Ronai, Z.A., Osterman, A.L., and Smith, J.W. (2012). Reverse TCA cycle flux through isocitrate dehydrogenases 1 and 2 is required for lipogenesis in hypoxic melanoma cells. Pigment Cell Melanoma Res *25*, 375-383.

Fodor, T., Szanto, M., Abdul-Rahman, O., Nagy, L., Der, A., Kiss, B., and Bai, P. (2016). Combined Treatment of MCF-7 Cells with AICAR and Methotrexate, Arrests Cell Cycle and Reverses Warburg Metabolism through AMP-Activated Protein Kinase (AMPK) and FOXO1. PLoS One *11*, e0150232.

Fogarty, S., and Hardie, D.G. (2010). Development of protein kinase activators: AMPK as a target in metabolic disorders and cancer. Biochim Biophys Acta *1804*, 581-591.
Foretz, M., Guigas, B., Bertrand, L., Pollak, M., and Viollet, B. (2014). Metformin: from mechanisms of action to therapies. Cell metabolism *20*, 953-966.

Fradet, A., Sorel, H., Bouazza, L., Goehrig, D., Depalle, B., Bellahcene, A., Castronovo, V., Follet, H., Descotes, F., Aubin, J.E., et al. (2011). Dual function of ERRalpha in breast cancer and bone metastasis formation: implication of VEGF and osteoprotegerin. Cancer research *71*, 5728-5738.

Fridman, A., Saha, A., Chan, A., Casteel, D.E., Pilz, R.B., and Boss, G.R. (2013). Cell cycle regulation of purine synthesis by phosphoribosyl pyrophosphate and inorganic phosphate. Biochem J *454*, 91-99.

Frigo, D.E., Howe, M.K., Wittmann, B.M., Brunner, A.M., Cushman, I., Wang, Q., Brown, M., Means, A.R., and McDonnell, D.P. (2011). CaM kinase kinase beta-mediated activation of the growth regulatory kinase AMPK is required for androgen-dependent migration of prostate cancer cells. Cancer research *71*, 528-537.

Fu, C., Sikandar, A., Donner, J., Zaburannyi, N., Herrmann, J., Reck, M., Wagner-Dobler, I., Koehnke, J., and Muller, R. (2017). The natural product carolacton inhibits folate-dependent C1 metabolism by targeting FolD/MTHFD. Nature communications *8*, 1529.

Fujimoto, J., Alam, S.M., Jahan, I., Sato, E., Sakaguchi, H., and Tamaya, T. (2007). Clinical implication of estrogen-related receptor (ERR) expression in ovarian cancers. J Steroid Biochem Mol Biol *104*, 301-304.

Ganapathy, V., Thangaraju, M., and Prasad, P.D. (2009). Nutrient transporters in cancer: relevance to Warburg hypothesis and beyond. Pharmacol Ther *121*, 29-40.

Garavito, M.F., Narvaez-Ortiz, H.Y., and Zimmermann, B.H. (2015). Pyrimidine Metabolism: Dynamic and Versatile Pathways in Pathogens and Cellular Development. J Genet Genomics *42*, 195-205.

Garraway, L.A., Widlund, H.R., Rubin, M.A., Getz, G., Berger, A.J., Ramaswamy, S., Beroukhim, R., Milner, D.A., Granter, S.R., Du, J., et al. (2005). Integrative genomic analyses identify MITF as a lineage survival oncogene amplified in malignant melanoma. Nature *436*, 117-122.

Gaude, E., and Frezza, C. (2016). Tissue-specific and convergent metabolic transformation of cancer correlates with metastatic potential and patient survival. Nature communications *7*, 13041.

Genestier, L., Paillot, R., Quemeneur, L., Izeradjene, K., and Revillard, J.P. (2000). Mechanisms of action of methotrexate. Immunopharmacology *47*, 247-257.

Giguère, V. (2008). Transcriptional control of energy homeostasis by the estrogen-related receptors. Endocrine reviews *29*, 677-696.

Giguère, V., Yang, N., Segui, P., and Evans, R.M. (1988). Identification of a new class of steroid hormone receptors. Nature *331*, 91-94.

Godlewski, J., Nowicki, M.O., Bronisz, A., Nuovo, G., Palatini, J., De Lay, M., Van Brocklyn, J., Ostrowski, M.C., Chiocca, E.A., and Lawler, S.E. (2010). MicroRNA-451 regulates LKB1/AMPK signalling and allows adaptation to metabolic stress in glioma cells. Mol Cell *37*, 620-632.

Goetzman, E.S., and Prochownik, E.V. (2018). The Role for Myc in Coordinating Glycolysis, Oxidative Phosphorylation, Glutaminolysis, and Fatty Acid Metabolism in Normal and Neoplastic Tissues. Front Endocrinol (Lausanne) *9*, 129.

Government of Canada (2016) Summary Safety Review - SGLT2 Inhibitors (canagliflozin, dapagliflozin, empagliflozin) - Assessing the Risk of the Body Producing High Levels of Acids in the Blood (diabetic ketoacidosis) Accessed August 28, 2018. https://www.canada.ca/en/health-canada/services/drugs-health-products/medeffect-canada/safety-reviews/summary-safety-review-sglt2-inhibitors-canagliflozin-dapagliflozin-empagliflozin.html

Gnaiger E. (2014) Mitochondrial Pathways and Respiratory Control: An Introduction to OXPHOS Analysis. OROBOROS MiPNET Publications. 4th Edition Accessed on August 28, 2018 www.bioblast.at/index.php/Gnaiger_2014_MitoPathways

Grassian, A.R., Parker, S.J., Davidson, S.M., Divakaruni, A.S., Green, C.R., Zhang, X., Slocum, K.L., Pu, M., Lin, F., Vickers, C., et al. (2014). IDH1 mutations alter citric acid cycle metabolism and increase dependence on oxidative mitochondrial metabolism. Cancer research *74*, 3317-3331.

Gravel, S.P. (2018). Deciphering the Dichotomous Effects of PGC-1alpha on Tumorigenesis and Metastasis. Front Oncol *8*, 75.

Grimm, F., Fets, L., and Anastasiou, D. (2016). Gas Chromatography Coupled to Mass Spectrometry (GC-MS) to Study Metabolism in Cultured Cells. Adv Exp Med Biol *899*, 59-88.

Griss, T., Vincent, E.E., Egnatchik, R., Chen, J., Ma, E.H., Faubert, B., Viollet, B., DeBerardinis, R.J., and Jones, R.G. (2015). Metformin Antagonizes Cancer Cell Proliferation by Suppressing Mitochondrial-Dependent Biosynthesis. PLoS Biology *13*, e1002309.

Guo, D., Prins, R.M., Dang, J., Kuga, D., Iwanami, A., Soto, H., Lin, K.Y., Huang, T.T., Akhavan, D., Hock, M.B., et al. (2009). EGFR signalling through an Akt-SREBP-1-dependent, rapamycin-resistant pathway sensitizes glioblastomas to antilipogenic therapy. Sci Signal *2*, ra82.

Guo, Z., Zhao, M., Howard, E.W., Zhao, Q., Parris, A.B., Ma, Z., and Yang, X. (2017). Phenformin inhibits growth and epithelial-mesenchymal transition of ErbB2-overexpressing breast cancer cells through targeting the IGF1R pathway. Oncotarget *8*, 60342-60357.

Guppy, M., Greiner, E., and Brand, K. (1993). The role of the Crabtree effect and an endogenous fuel in the energy metabolism of resting and proliferating thymocytes. European journal of biochemistry / FEBS *212*, 95-99.

Gustafsson, R., Jemth, A.S., Gustafsson, N.M., Farnegardh, K., Loseva, O., Wiita, E., Bonagas, N., Dahllund, L., Llona-Minguez, S., Haggblad, M., et al. (2017). Crystal Structure of the Emerging Cancer Target MTHFD2 in Complex with a Substrate-Based Inhibitor. Cancer research *77*, 937-948.

Gwinn, D.M., Shackelford, D.B., Egan, D.F., Mihaylova, M.M., Mery, A., Vasquez, D.S., Turk, B.E., and Shaw, R.J. (2008). AMPK phosphorylation of raptor mediates a metabolic checkpoint. Mol Cell *30*, 214-226.

Hadad, S.M., Fleming, S., and Thompson, A.M. (2008). Targeting AMPK: a new therapeutic opportunity in breast cancer. Critical reviews in oncology/hematology *67*, 1-7.
Hadad, S.M., Hardie, D.G., Appleyard, V., and Thompson, A.M. (2014). Effects of metformin on breast cancer cell proliferation, the AMPK pathway and the cell cycle. Clin Transl Oncol *16*, 746-752.

Hainaut, P., and Pfeifer, G.P. (2016). Somatic TP53 Mutations in the Era of Genome Sequencing. Cold Spring Harb Perspect Med *6*.

Hanahan, D., and Weinberg, R.A. (2000). The hallmarks of cancer. Cell *100*, 57-70.

Hanahan, D., and Weinberg, R.A. (2011). Hallmarks of cancer: the next generation. Cell *144*, 646-674.

Handschin, C., and Spiegelman, B.M. (2006). Peroxisome proliferator-activated receptor gamma coactivator 1 coactivators, energy homeostasis, and metabolism. Endocrine reviews *27*, 728-735.

Hao, H.X., Khalimonchuk, O., Schraders, M., Dephoure, N., Bayley, J.P., Kunst, H., Devilee, P., Cremers, C.W., Schiffman, J.D., Bentz, B.G., et al. (2009). SDH5, a gene required for flavination of succinate dehydrogenase, is mutated in paraganglioma. Science (New York, N.Y.) *325*, 1139-1142.

Haq, R., Shoag, J., Andreu-Perez, P., Yokoyama, S., Edelman, H., Rowe, G.C., Frederick, D.T., Hurley, A.D., Nellore, A., Kung, A.L., et al. (2013). Oncogenic BRAF regulates oxidative metabolism via PGC1alpha and MITF. Cancer cell *23*, 302-315.

Hara, K., Maruki, Y., Long, X., Yoshino, K., Oshiro, N., Hidayat, S., Tokunaga, C., Avruch, J., and Yonezawa, K. (2002). Raptor, a binding partner of target of rapamycin (TOR), mediates TOR action. Cell *110*, 177-189.

Hardie, D.G. (2013a). AMPK: a target for drugs and natural products with effects on both diabetes and cancer. Diabetes *62*, 2164-2172.

Hardie, D.G. (2013b). The LKB1-AMPK pathway-friend or foe in cancer? Cancer cell *23*, 131-132.

Hardie, D.G. (2018). Keeping the home fires burning: AMP-activated protein kinase. J R Soc Interface *15*.

Hardie, D.G., Carling, D., and Gamblin, S.J. (2011). AMP-activated protein kinase: also regulated by ADP? Trends Biochem Sci *36*, 470-477.

Hardie, D.G., Ross, F.A., and Hawley, S.A. (2012). AMPK: a nutrient and energy sensor that maintains energy homeostasis. Nature reviews. Molecular cell biology *13*, 251-262.

Hawley Simon, A.S. (2016). The Na+/Glucose Cotransporter Inhibitor Canagliflozin Activates AMPK by Inhibiting Mitochondrial Function and Increasing Cellular AMP Levels. Diabetes *65*, 2784-2794.

He, L., and Wondisford, F.E. (2015). Metformin action: concentrations matter. Cell metabolism *21*, 159-162.

Heck, S., Rom, J., Thewes, V., Becker, N., Blume, B., Sinn, H.P., Deuschle, U., Sohn, C., Schneeweiss, A., and Lichter, P. (2009). Estrogen-related receptor alpha expression and function is associated with the transcriptional coregulator AIB1 in breast carcinoma. Cancer research *69*, 5186-5193.

Heckman-Stoddard, B.M., DeCensi, A., Sahasrabuddhe, V.V., and Ford, L.G. (2017). Repurposing metformin for the prevention of cancer and cancer recurrence. Diabetologia *60*, 1639-1647.

Hemminki, A. (1999). The molecular basis and clinical aspects of Peutz-Jeghers syndrome. Cell Mol Life Sci *55*, 735-750.

Hensley, C.T., Wasti, A.T., and DeBerardinis, R.J. (2013). Glutamine and cancer: cell biology, physiology, and clinical opportunities. The Journal of clinical investigation *123*, 3678-3684.

Hertz, R., Li, M.C., and Spencer, D.B. (1956). Effect of methotrexate therapy upon choriocarcinoma and chorioadenoma. Proc Soc Exp Biol Med *93*, 361-366.

Hitchings, G.H., and Burchall, J.J. (1965). Inhibition of folate biosynthesis and function as a basis for chemotherapy. Adv Enzymol Relat Areas Mol Biol *27*, 417-468.

Horard, B., Rayet, B., Triqueneaux, G., Laudet, V., Delaunay, F., and Vanacker, J.M. (2004). Expression of the orphan nuclear receptor ERRalpha is under circadian regulation in estrogen-responsive tissues. J Mol Endocrinol *33*, 87-97.

Howard, S.C., McCormick, J., Pui, C.H., Buddington, R.K., and Harvey, R.D. (2016). Preventing and Managing Toxicities of High-Dose Methotrexate. Oncologist *21*, 1471-1482.
Hsu, P.P., and Sabatini, D.M. (2008). Cancer cell metabolism: Warburg and beyond. Cell *134*, 703-707.

Hu, W., Zhang, C., Wu, R., Sun, Y., Levine, A., and Feng, Z. (2010). Glutaminase 2, a novel p53 target gene regulating energy metabolism and antioxidant function. Proceedings of the National Academy of Sciences of the United States of America *107*, 7455-7460.

Huang, F., Ni, M., Chalishazar, M.D., Huffman, K.E., Kim, J., Cai, L., Shi, X., Cai, F., Zacharias, L.G., Ireland, A.S., et al. (2018). Inosine Monophosphate Dehydrogenase Dependence in a Subset of Small Cell Lung Cancers. Cell metabolism.
Huang, X., Wullschleger, S., Shpiro, N., McGuire, V.A., Sakamoto, K., Woods, Y.L., McBurnie, W., Fleming, S., and Alessi, D.R. (2008). Important role of the LKB1-AMPK pathway in suppressing tumorigenesis in PTEN-deficient mice. Biochem J *412*, 211-221.

Huennekens, F.M. (1994). The methotrexate story: a paradigm for development of cancer chemotherapeutic agents. Adv Enzyme Regul *34*, 397-419.

Hummel, C.S., Lu, C., Liu, J., Ghezzi, C., Hirayama, B.A., Loo, D.D., Kepe, V., Barrio, J.R., and Wright, E.M. (2012). Structural selectivity of human SGLT inhibitors. American journal of physiology. Cell physiology *302*, C373-382.

Huss, J.M., Kopp, R.P., and Kelly, D.P. (2002). Peroxisome proliferator-activated receptor coactivator-1alpha (PGC-1alpha) coactivates the cardiac-enriched nuclear receptors estrogen-related receptor-alpha and -gamma. Identification of novel leucine-rich interaction motif within PGC-1alpha. The Journal of biological chemistry *277*, 40265-40274.

Ichida, M., Nemoto, S., and Finkel, T. (2002). Identification of a specific molecular repressor of the peroxisome proliferator-activated receptor gamma Coactivator-1 alpha (PGC-1alpha). The Journal of biological chemistry *277*, 50991-50995.

Ijichi, N., Shigekawa, T., Ikeda, K., Horie-Inoue, K., Fujimura, T., Tsuda, H., Osaki, A., Saeki, T., and Inoue, S. (2011). Estrogen-related receptor gamma modulates cell proliferation and estrogen signalling in breast cancer. J Steroid Biochem Mol Biol *123*, 1-7.

Inoki, K., Kim, J., and Guan, K.L. (2012). AMPK and mTOR in cellular energy homeostasis and drug targets. Annu Rev Pharmacol Toxicol *52*, 381-400.

Inoki, K., Li, Y., Zhu, T., Wu, J., and Guan, K.L. (2002). TSC2 is phosphorylated and inhibited by Akt and suppresses mTOR signalling. Nat Cell Biol *4*, 648-657.

Inoki, K., Zhu, T., and Guan, K.L. (2003). TSC2 mediates cellular energy response to control cell growth and survival. Cell *115*, 577-590.

Isaacs, J.S., Jung, Y.J., Mole, D.R., Lee, S., Torres-Cabala, C., Chung, Y.L., Merino, M., Trepel, J., Zbar, B., Toro, J., et al. (2005). HIF overexpression correlates with biallelic loss of fumarate hydratase in renal cancer: novel role of fumarate in regulation of HIF stability. Cancer cell *8*, 143-153.

Ishikawa, N., Oguri, T., Isobe, T., Fujitaka, K., and Kohno, N. (2001). SGLT gene expression in primary lung cancers and their metastatic lesions. Jpn J Cancer Res *92*, 874-879.

Israelsen, W.J., and Vander Heiden, M.G. (2015). Pyruvate kinase: Function, regulation and role in cancer. Semin Cell Dev Biol *43*, 43-51.

Jackson, A.L., Sun, W., Kilgore, J., Guo, H., Fang, Z., Yin, Y., Jones, H.M., Gilliam, T.P., Zhou, C., and Bae-Jump, V.L. (2017). Phenformin has anti-tumorigenic effects in human ovarian cancer cells and in an orthotopic mouse model of serous ovarian cancer. Oncotarget *8*, 100113-100127.

Jager, S., Handschin, C., St-Pierre, J., and Spiegelman, B.M. (2007). AMP-activated protein kinase (AMPK) action in skeletal muscle via direct phosphorylation of PGC-1alpha. Proceedings of the National Academy of Sciences of the United States of America *104*, 12017-12022.

Jain, M., Nilsson, R., Sharma, S., Madhusudhan, N., Kitami, T., Souza, A.L., Kafri, R., Kirschner, M.W., Clish, C.B., and Mootha, V.K. (2012). Metabolite profiling identifies a key role for glycine in rapid cancer cell proliferation. Science (New York, N.Y.) *336*, 1040-1044.

Janeway, K.A., Kim, S.Y., Lodish, M., Nose, V., Rustin, P., Gaal, J., Dahia, P.L., Liegl, B., Ball, E.R., Raygada, M., et al. (2011). Defects in succinate dehydrogenase in gastrointestinal stromal tumors lacking KIT and PDGFRA mutations. Proceedings of the National Academy of Sciences of the United States of America *108*, 314-318.

Jarzabek, K., Koda, M., Kozlowski, L., Sulkowski, S., Kottler, M.L., and Wolczynski, S. (2009). The significance of the expression of ERRalpha as a potential biomarker in breast cancer. J Steroid Biochem Mol Biol *113*, 127-133.

Jeon, S.M., Chandel, N.S., and Hay, N. (2012). AMPK regulates NADPH homeostasis to promote tumour cell survival during energy stress. Nature *485*, 661-665.

Jeon, S.M., and Hay, N. (2012). The dark face of AMPK as an essential tumor promoter. Cell Logist *2*, 197-202.

Jiang, W.G., Douglas-Jones, A., and Mansel, R.E. (2003). Expression of peroxisome-proliferator activated receptor-gamma (PPARgamma) and the PPARgamma co-activator, PGC-1, in human breast cancer correlates with clinical outcomes. Int J Cancer *106*, 752-757.

Jones, R.G., Plas, D.R., Kubek, S., Buzzai, M., Mu, J., Xu, Y., Birnbaum, M.J., and Thompson, C.B. (2005). AMP-activated protein kinase induces a p53-dependent metabolic checkpoint. Mol Cell *18*, 283-293.

Jones, R.G., and Thompson, C.B. (2009). Tumor suppressors and cell metabolism: a recipe for cancer growth. Genes & development *23*, 537-548.

Kaji, K., Nishimura, N., Seki, K., Sato, S., Saikawa, S., Nakanishi, K., Furukawa, M., Kawaratani, H., Kitade, M., Moriya, K., et al. (2018). Sodium glucose cotransporter 2 inhibitor canagliflozin attenuates liver cancer cell growth and angiogenic activity by inhibiting glucose uptake. International journal of cancer *142*, 1712-1722.

Kalender, A., Selvaraj, A., Kim, S.Y., Gulati, P., Brule, S., Viollet, B., Kemp, B.E., Bardeesy, N., Dennis, P., Schlager, J.J., et al. (2010). Metformin, independent of AMPK, inhibits mTORC1 in a rag GTPase-dependent manner. Cell metabolism *11*, 390-401.

Kamei, Y., Ohizumi, H., Fujitani, Y., Nemoto, T., Tanaka, T., Takahashi, N., Kawada, T., Miyoshi, M., Ezaki, O., and Kakizuka, A. (2003). PPARgamma coactivator 1beta/ERR ligand 1 is an ERR protein ligand, whose expression induces a high-energy expenditure and antagonizes obesity. Proceedings of the National Academy of Sciences of the United States of America *100*, 12378-12383.

Kanarek, N., Keys, H.R., Cantor, J.R., Lewis, C.A., Chan, S.H., Kunchok, T., Abu-Remaileh, M., Freinkman, E., Schweitzer, L.D., and Sabatini, D.M. (2018). Histidine catabolism is a major determinant of methotrexate sensitivity. Nature *559*, 632-636.

Kawauchi, K., Araki, K., Tobiume, K., and Tanaka, N. (2008). p53 regulates glucose metabolism through an IKK-NF-kappaB pathway and inhibits cell transformation. Nat Cell Biol *10*, 611-618.

Kepe, V., Scafoglio, C., Liu, J., Yong, W.H., Bergsneider, M., Huang, S.C., Barrio, J.R., and Wright, E.M. (2018). Positron emission tomography of sodium glucose cotransport activity in high grade astrocytomas. Journal of neuro-oncology.

Kessler, R., Bleichert, F., Warnke, J.P., and Eschrich, K. (2008). 6-Phosphofructo-2-kinase/fructose-2,6-bisphosphatase (PFKFB3) is up-regulated in high-grade astrocytomas. J Neurooncol *86*, 257-264.

Khutornenko, A.A., Roudko, V.V., Chernyak, B.V., Vartapetian, A.B., Chumakov, P.M., and Evstafieva, A.G. (2010). Pyrimidine biosynthesis links mitochondrial respiration to the p53 pathway. Proceedings of the National Academy of Sciences of the United States of America *107*, 12828-12833.

Kim, D., Fiske, B.P., Birsoy, K., Freinkman, E., Kami, K., Possemato, R.L., Chudnovsky, Y., Pacold, M.E., Chen, W.W., Cantor, J.R., et al. (2015). SHMT2 drives glioma cell survival in ischaemia but imposes a dependence on glycine clearance. Nature *520*, 363-367.
Kim, H., and Park, Y.J. (2018). Links between Serine Biosynthesis Pathway and Epigenetics in Cancer Metabolism. Clin Nutr Res *7*, 153-160.

Kim, J., Kundu, M., Viollet, B., and Guan, K.L. (2011). AMPK and mTOR regulate autophagy through direct phosphorylation of Ulk1. Nat Cell Biol *13*, 132-141.
Kim, J.W., Tchernyshyov, I., Semenza, G.L., and Dang, C.V. (2006). HIF-1-mediated expression of pyruvate dehydrogenase kinase: a metabolic switch required for cellular adaptation to hypoxia. Cell metabolism *3*, 177-185.

Kim, S., Kim, D.H., Jung, W.H., and Koo, J.S. (2013). Succinate dehydrogenase expression in breast cancer. Springerplus *2*, 299.

Kleinsmith, L.J. (2006). Principles of cancer biology. (San Francisco: Pearson Benjamin Cummings).

Klomp, J.A., Petillo, D., Niemi, N.M., Dykema, K.J., Chen, J., Yang, X.J., Saaf, A., Zickert, P., Aly, M., Bergerheim, U., et al. (2010). Birt-Hogg-Dube renal tumors are genetically distinct from other renal neoplasias and are associated with up-regulation of mitochondrial gene expression. BMC Med Genomics *3*, 59.

Koepsell, H. (2017). The Na(+)-D-glucose cotransporters SGLT1 and SGLT2 are targets for the treatment of diabetes and cancer. Pharmacol Ther *170*, 148-165.

Kong, X., Fan, H., Liu, X., Wang, R., Liang, J., Gupta, N., Chen, Y., Fang, F., and Chang, Y. (2009). Peroxisome proliferator-activated receptor gamma coactivator-1alpha enhances antiproliferative activity of 5'-deoxy-5-fluorouridine in cancer cells through induction of uridine phosphorylase. Mol Pharmacol *76*, 854-860.

Kordes, S., Pollak, M.N., Zwinderman, A.H., Mathot, R.A., Weterman, M.J., Beeker, A., Punt, C.J., Richel, D.J., and Wilmink, J.W. (2015). Metformin in patients with advanced pancreatic cancer: a double-blind, randomised, placebo-controlled phase 2 trial. The Lancet. Oncology *16*, 839-847.

Koseki, J., Konno, M., Asai, A., Colvin, H., Kawamoto, K., Nishida, N., Sakai, D., Kudo, T., Satoh, T., Doki, Y., et al. (2018). Enzymes of the one-carbon folate metabolism as anticancer targets predicted by survival rate analysis. Sci Rep *8*, 303.
Kressler, D., Schreiber, S.N., Knutti, D., and Kralli, A. (2002). The PGC-1-related protein PERC is a selective coactivator of estrogen receptor alpha. The Journal of biological chemistry *277*, 13918-13925.

Kufel, W.D., Scrimenti, A., and Steele, J.M. (2017). A Case of Septic Shock Due to Serratia marcescens Pyelonephritis and Bacteremia in a Patient Receiving Empagliflozin. J Pharm Pract *30*, 672-675.

Labuschagne, C.F., Zani, F., and Vousden, K.H. (2018). Control of metabolism by p53 - Cancer and beyond. Biochim Biophys Acta.

Laganiere, J., Tremblay, G.B., Dufour, C.R., Giroux, S., Rousseau, F., and Giguère, V. (2004). A polymorphic autoregulatory hormone response element in the human estrogen-related receptor alpha (ERRalpha) promoter dictates peroxisome proliferator-activated receptor gamma coactivator-1alpha control of ERRalpha expression. The Journal of biological chemistry *279*, 18504-18510.

LaGory, E.L., Wu, C., Taniguchi, C.M., Ding, C.C., Chi, J.T., von Eyben, R., Scott, D.A., Richardson, A.D., and Giaccia, A.J. (2015). Suppression of PGC-1alpha Is Critical for Reprogramming Oxidative Metabolism in Renal Cell Carcinoma. Cell Rep *12*, 116-127.
Landman, G.W., Kleefstra, N., van Hateren, K.J., Groenier, K.H., Gans, R.O., and Bilo, H.J. (2010). Metformin associated with lower cancer mortality in type 2 diabetes: ZODIAC-16. Diabetes Care *33*, 322-326.

Lane, A.N., and Fan, T.W. (2015). Regulation of mammalian nucleotide metabolism and biosynthesis. Nucleic Acids Res *43*, 2466-2485.

Lao-On, U., Attwood, P.V., and Jitrapakdee, S. (2018). Roles of pyruvate carboxylase in human diseases: from diabetes to cancers and infection. J Mol Med (Berl) *96*, 237-247.

Laplante, M., and Sabatini, D.M. (2012). mTOR signalling in growth control and disease. Cell *149*, 274-293.

Lavalle-Gonzalez, F.J., Januszewicz, A., Davidson, J., Tong, C., Qiu, R., Canovatchel, W., and Meininger, G. (2013). Efficacy and safety of canagliflozin compared with placebo and sitagliptin in patients with type 2 diabetes on background metformin monotherapy: a randomised trial. Diabetologia *56*, 2582-2592.

LeBleu, V.S., O'Connell, J.T., Gonzalez Herrera, K.N., Wikman, H., Pantel, K., Haigis, M.C., de Carvalho, F.M., Damascena, A., Domingos Chinen, L.T., Rocha, R.M., et al. (2014). PGC-1alpha mediates mitochondrial biogenesis and oxidative phosphorylation in cancer cells to promote metastasis. Nat Cell Biol *16*, 992-1003, 1001-1015.

Lee, C.W., Wong, L.L., Tse, E.Y., Liu, H.F., Leong, V.Y., Lee, J.M., Hardie, D.G., Ng, I.O., and Ching, Y.P. (2012). AMPK promotes p53 acetylation via phosphorylation and inactivation of SIRT1 in liver cancer cells. Cancer research *72*, 4394-4404.

Lee, G.Y., Haverty, P.M., Li, L., Kljavin, N.M., Bourgon, R., Lee, J., Stern, H., Modrusan, Z., Seshagiri, S., Zhang, Z., et al. (2014). Comparative oncogenomics identifies PSMB4 and SHMT2 as potential cancer driver genes. Cancer research *74*, 3114-3126.

Lee, W.J., Kim, M., Park, H.S., Kim, H.S., Jeon, M.J., Oh, K.S., Koh, E.H., Won, J.C., Kim, M.S., Oh, G.T., et al. (2006). AMPK activation increases fatty acid oxidation in skeletal muscle by activating PPARalpha and PGC-1. Biochem Biophys Res Commun *340*, 291-295.

Lehtinen, L., Ketola, K., Makela, R., Mpindi, J.P., Viitala, M., Kallioniemi, O., and Iljin, K. (2013). High-throughput RNAi screening for novel modulators of vimentin expression identifies MTHFD2 as a regulator of breast cancer cell migration and invasion. Oncotarget *4*, 48-63.

Lemmon, M.A. (2009). Ligand-induced ErbB receptor dimerization. Exp Cell Res *315*, 638-648.

Lerin, C., Rodgers, J.T., Kalume, D.E., Kim, S.H., Pandey, A., and Puigserver, P. (2006). GCN5 acetyltransferase complex controls glucose metabolism through transcriptional repression of PGC-1alpha. Cell metabolism *3*, 429-438.

Li, X., Monks, B., Ge, Q., and Birnbaum, M.J. (2007). Akt/PKB regulates hepatic metabolism by directly inhibiting PGC-1alpha transcription coactivator. Nature *447*, 1012-1016.

Li, Y., Holmes, W.B., Appling, D.R., and RajBhandary, U.L. (2000). Initiation of protein synthesis in Saccharomyces cerevisiae mitochondria without formylation of the initiator tRNA. J Bacteriol *182*, 2886-2892.

Li, Y., Xu, S., Li, J., Zheng, L., Feng, M., Wang, X., Han, K., Pi, H., Li, M., Huang, X., et al. (2016). SIRT1 facilitates hepatocellular carcinoma metastasis by promoting PGC-1alpha-mediated mitochondrial biogenesis. Oncotarget *7*, 29255-29274.

Liang, J., Shao, S.H., Xu, Z.X., Hennessy, B., Ding, Z., Larrea, M., Kondo, S., Dumont, D.J., Gutterman, J.U., Walker, C.L., et al. (2007). The energy sensing LKB1-AMPK pathway regulates p27(kip1) phosphorylation mediating the decision to enter autophagy or apoptosis. Nat Cell Biol *9*, 218-224.

Liang, J., Yang, Q., Zhu, M.J., Jin, Y., and Du, M. (2013). AMP-activated protein kinase (AMPK) alpha2 subunit mediates glycolysis in postmortem skeletal muscle. Meat Sci *95*, 536-541.

Libby, G., Donnelly, L.A., Donnan, P.T., Alessi, D.R., Morris, A.D., and Evans, J.M. (2009). New users of metformin are at low risk of incident cancer: a cohort study among people with type 2 diabetes. Diabetes Care *32*, 1620-1625.

Lin, H.W., and Tseng, C.H. (2014). A Review on the Relationship between SGLT2 Inhibitors and Cancer. Int J Endocrinol *2014*, 719578.

Lin, J., Puigserver, P., Donovan, J., Tarr, P., and Spiegelman, B.M. (2002). Peroxisome proliferator-activated receptor gamma coactivator 1beta (PGC-1beta), a novel PGC-1-related transcription coactivator associated with host cell factor. The Journal of biological chemistry *277*, 1645-1648.

Lin, J., Tarr, P.T., Yang, R., Rhee, J., Puigserver, P., Newgard, C.B., and Spiegelman, B.M. (2003). PGC-1beta in the regulation of hepatic glucose and energy metabolism. The Journal of biological chemistry *278*, 30843-30848.

Lin, J., Yang, R., Tarr, P.T., Wu, P.H., Handschin, C., Li, S., Yang, W., Pei, L., Uldry, M., Tontonoz, P., et al. (2005). Hyperlipidemic effects of dietary saturated fats mediated through PGC-1beta coactivation of SREBP. Cell *120*, 261-273.

Liu, X., Romero, I.L., Litchfield, L.M., Lengyel, E., and Locasale, J.W. (2016). Metformin Targets Central Carbon Metabolism and Reveals Mitochondrial Requirements in Human Cancers. Cell metabolism *24*, 728-739.

Locasale, J.W. (2013). Serine, glycine and one-carbon units: cancer metabolism in full circle. Nature reviews. Cancer *13*, 572-583.

Locasale, J.W., Grassian, A.R., Melman, T., Lyssiotis, C.A., Mattaini, K.R., Bass, A.J., Heffron, G., Metallo, C.M., Muranen, T., Sharfi, H., et al. (2011). Phosphoglycerate dehydrogenase diverts glycolytic flux and contributes to oncogenesis. Nat Genet *43*, 869-874.
Long, Q.Q., Yi, Y.X., Qiu, J., Xu, C.J., and Huang, P.L. (2014). Fatty acid synthase (FASN) levels in serum of colorectal cancer patients: correlation with clinical outcomes. Tumour Biol *35*, 3855-3859.

Longley, D.B., Harkin, D.P., and Johnston, P.G. (2003). 5-fluorouracil: mechanisms of action and clinical strategies. Nature reviews. Cancer *3*, 330-338.

Longo, L., Vanegas, O.C., Patel, M., Rosti, V., Li, H., Waka, J., Merghoub, T., Pandolfi, P.P., Notaro, R., Manova, K., et al. (2002). Maternally transmitted severe glucose 6-phosphate dehydrogenase deficiency is an embryonic lethal. EMBO J *21*, 4229-4239.

Losman, J.A., Looper, R.E., Koivunen, P., Lee, S., Schneider, R.K., McMahon, C., Cowley, G.S., Root, D.E., Ebert, B.L., and Kaelin, W.G., Jr. (2013). (R)-2-hydroxyglutarate is sufficient to promote leukemogenesis and its effects are reversible. Science (New York, N.Y.) *339*, 1621-1625.

Lu, C., Venneti, S., Akalin, A., Fang, F., Ward, P.S., Dematteo, R.G., Intlekofer, A.M., Chen, C., Ye, J., Hameed, M., et al. (2013). Induction of sarcomas by mutant IDH2. Genes & development *27*, 1986-1998.

Lu, W., Bennett, B.D., and Rabinowitz, J.D. (2008). Analytical strategies for LC-MS-based targeted metabolomics. J Chromatogr B Analyt Technol Biomed Life Sci *871*, 236-242.
Lucon, D.R., Rocha Cde, S., Craveiro, R.B., Dilloo, D., Cardinalli, I.A., Cavalcanti, D.P., Aguiar Sdos, S., Maurer-Morelli, C., and Yunes, J.A. (2013). Downregulation of 14q32 microRNAs in Primary Human Desmoplastic Medulloblastoma. Front Oncol *3*, 254.

Luengo, A., Gui, D.Y., and Vander Heiden, M.G. (2017). Targeting Metabolism for Cancer Therapy. Cell chemical biology *24*, 1161-1180.

Luo, C., Widlund, H.R., and Puigserver, P. (2016). PGC-1 Coactivators: Shepherding the Mitochondrial Biogenesis of Tumors. Trends Cancer *2*, 619-631.

Lustig, Y., Ruas, J.L., Estall, J.L., Lo, J.C., Devarakonda, S., Laznik, D., Choi, J.H., Ono, H., Olsen, J.V., and Spiegelman, B.M. (2011). Separation of the gluconeogenic and mitochondrial functions of PGC-1{alpha} through S6 kinase. Genes & development *25*, 1232-1244.
Ma, E.H., Bantug, G., Griss, T., Condotta, S., Johnson, R.M., Samborska, B., Mainolfi, N., Suri, V., Guak, H., Balmer, M.L., et al. (2017). Serine Is an Essential Metabolite for Effector T Cell Expansion. Cell metabolism *25*, 482.

Madiraju, A.K., Erion, D.M., Rahimi, Y., Zhang, X.M., Braddock, D.T., Albright, R.A., Prigaro, B.J., Wood, J.L., Bhanot, S., MacDonald, M.J., et al. (2014). Metformin suppresses gluconeogenesis by inhibiting mitochondrial glycerophosphate dehydrogenase. Nature *510*, 542-546.

Mallik, R., and Chowdhury, T.A. (2018). Metformin in cancer. Diabetes Res Clin Pract.
Mamidi, R.N., Cuyckens, F., Chen, J., Scheers, E., Kalamaridis, D., Lin, R., Silva, J., Sha, S., Evans, D.C., Kelley, M.F., et al. (2014). Metabolism and excretion of canagliflozin in mice, rats, dogs, and humans. Drug metabolism and disposition: the biological fate of chemicals *42*, 903-916.

Mannava, S., Grachtchouk, V., Wheeler, L.J., Im, M., Zhuang, D., Slavina, E.G., Mathews, C.K., Shewach, D.S., and Nikiforov, M.A. (2008). Direct role of nucleotide metabolism in C-MYC-dependent proliferation of melanoma cells. Cell Cycle *7*, 2392-2400.

Marsin, A.S., Bouzin, C., Bertrand, L., and Hue, L. (2002). The stimulation of glycolysis by hypoxia in activated monocytes is mediated by AMP-activated protein kinase and inducible 6-phosphofructo-2-kinase. The Journal of biological chemistry *277*, 30778-30783.

Mates, J.M., Campos-Sandoval, J.A., and Marquez, J. (2018). Glutaminase isoenzymes in the metabolic therapy of cancer. Biochim Biophys Acta.

Matoba, S., Kang, J.G., Patino, W.D., Wragg, A., Boehm, M., Gavrilova, O., Hurley, P.J., Bunz, F., and Hwang, P.M. (2006). p53 regulates mitochondrial respiration. Science (New York, N.Y.) *312*, 1650-1653.

McGuirk, S., Gravel, S.P., Deblois, G., Papadopoli, D.J., Faubert, B., Wegner, A., Hiller, K., Avizonis, D., Akavia, U.D., Jones, R.G., et al. (2013). PGC-1alpha supports glutamine metabolism in breast cancer. Cancer & metabolism *1*, 22.

Menendez, J.A. (2010). Fine-tuning the lipogenic/lipolytic balance to optimize the metabolic requirements of cancer cell growth: molecular mechanisms and therapeutic perspectives. Biochim Biophys Acta *1801*, 381-391.

Merrill, G.F., Kurth, E.J., Hardie, D.G., and Winder, W.W. (1997). AICA riboside increases AMP-activated protein kinase, fatty acid oxidation, and glucose uptake in rat muscle. Am J Physiol *273*, E1107-1112.

Metallo, C.M., Gameiro, P.A., Bell, E.L., Mattaini, K.R., Yang, J., Hiller, K., Jewell, C.M., Johnson, Z.R., Irvine, D.J., Guarente, L., et al. (2011). Reductive glutamine metabolism by IDH1 mediates lipogenesis under hypoxia. Nature *481*, 380-384.

Michael, L.F., Wu, Z., Cheatham, R.B., Puigserver, P., Adelmant, G., Lehman, J.J., Kelly, D.P., and Spiegelman, B.M. (2001). Restoration of insulin-sensitive glucose transporter (GLUT4) gene expression in muscle cells by the transcriptional coactivator PGC-1. Proceedings of the National Academy of Sciences of the United States of America *98*, 3820-3825.

Migita, T., Narita, T., Nomura, K., Miyagi, E., Inazuka, F., Matsuura, M., Ushijima, M., Mashima, T., Seimiya, H., Satoh, Y., et al. (2008). ATP citrate lyase: activation and therapeutic implications in non-small cell lung cancer. Cancer research *68*, 8547-8554.

Minchenko, A., Leshchinsky, I., Opentanova, I., Sang, N., Srinivas, V., Armstead, V., and Caro, J. (2002). Hypoxia-inducible factor-1-mediated expression of the 6-phosphofructo-2-kinase/fructose-2,6-bisphosphatase-3 (PFKFB3) gene. Its possible role in the Warburg effect. The Journal of biological chemistry *277*, 6183-6187.

Miskimins, W.K., Ahn, H.J., Kim, J.Y., Ryu, S., Jung, Y.S., and Choi, J.Y. (2014). Synergistic anti-cancer effect of phenformin and oxamate. PLoS One *9*, e85576.
Mitchell, P. (1961). Coupling of phosphorylation to electron and hydrogen transfer by a chemi-osmotic type of mechanism. Nature *191*, 144-148.

Miyo, M., Konno, M., Colvin, H., Nishida, N., Koseki, J., Kawamoto, K., Tsunekuni, K., Nishimura, J., Hata, T., Takemasa, I., et al. (2017). The importance of mitochondrial folate enzymes in human colorectal cancer. Oncol Rep *37*, 417-425.

Mookerjee, S.A., Gerencser, A.A., Nicholls, D.G., and Brand, M.D. (2017). Quantifying intracellular rates of glycolytic and oxidative ATP production and consumption using extracellular flux measurements. The Journal of biological chemistry *292*, 7189-7207.

Mootha, V.K., Handschin, C., Arlow, D., Xie, X., St Pierre, J., Sihag, S., Yang, W., Altshuler, D., Puigserver, P., Patterson, N., et al. (2004). Erralpha and Gabpa/b specify PGC-1alpha-dependent oxidative phosphorylation gene expression that is altered in diabetic muscle.

Proceedings of the National Academy of Sciences of the United States of America *101*, 6570-6575.

Mootha, V.K., Lindgren, C.M., Eriksson, K.F., Subramanian, A., Sihag, S., Lehar, J., Puigserver, P., Carlsson, E., Ridderstrale, M., Laurila, E., et al. (2003). PGC-1alpha-responsive genes involved in oxidative phosphorylation are coordinately downregulated in human diabetes. Nat Genet *34*, 267-273.

Morita, M., Gravel, S.P., Chenard, V., Sikstrom, K., Zheng, L., Alain, T., Gandin, V., Avizonis, D., Arguello, M., Zakaria, C., et al. (2013). mTORC1 controls mitochondrial activity and biogenesis through 4E-BP-dependent translational regulation. Cell metabolism *18*, 698-711.
Morita, M., Gravel, S.P., Hulea, L., Larsson, O., Pollak, M., St-Pierre, J., and Topisirovic, I. (2015). mTOR coordinates protein synthesis, mitochondrial activity and proliferation. Cell Cycle *14*, 473-480.

Morrish, F., and Hockenbery, D. (2014). MYC and mitochondrial biogenesis. Cold Spring Harb Perspect Med *4*.

Morrish, F., Noonan, J., Perez-Olsen, C., Gafken, P.R., Fitzgibbon, M., Kelleher, J., VanGilst, M., and Hockenbery, D. (2010). Myc-dependent mitochondrial generation of acetyl-CoA contributes to fatty acid biosynthesis and histone acetylation during cell cycle entry. The Journal of biological chemistry *285*, 36267-36274.

Morscher, R.J., Ducker, G.S., Li, S.H., Mayer, J.A., Gitai, Z., Sperl, W., and Rabinowitz, J.D. (2018). Mitochondrial translation requires folate-dependent tRNA methylation. Nature *554*, 128-132.

Mullarky, E., Lairson, L.L., Cantley, L.C., and Lyssiotis, C.A. (2016a). A novel small-molecule inhibitor of 3-phosphoglycerate dehydrogenase. Mol Cell Oncol *3*, e1164280.

Mullarky, E., Lucki, N.C., Beheshti Zavareh, R., Anglin, J.L., Gomes, A.P., Nicolay, B.N., Wong, J.C., Christen, S., Takahashi, H., Singh, P.K., et al. (2016b). Identification of a small molecule inhibitor of 3-phosphoglycerate dehydrogenase to target serine biosynthesis in cancers. Proceedings of the National Academy of Sciences of the United States of America *113*, 1778-1783.

Mullen, A.R., Hu, Z., Shi, X., Jiang, L., Boroughs, L.K., Kovacs, Z., Boriack, R., Rakheja, D., Sullivan, L.B., Linehan, W.M., et al. (2014). Oxidation of alpha-ketoglutarate is required for reductive carboxylation in cancer cells with mitochondrial defects. Cell Rep *7*, 1679-1690.

Munzone, E., Curigliano, G., Burstein, H.J., Winer, E.P., and Goldhirsch, A. (2012). CMF revisited in the 21st century. Annals of oncology : official journal of the European Society for Medical Oncology / ESMO *23*, 305-311.

Nauck, M.A., Del Prato, S., Meier, J.J., Duran-Garcia, S., Rohwedder, K., Elze, M., and Parikh, S.J. (2011). Dapagliflozin versus glipizide as add-on therapy in patients with type 2 diabetes who have inadequate glycemic control with metformin: a randomized, 52-week, double-blind, active-controlled noninferiority trial. Diabetes Care *34*, 2015-2022.

Newman, A.C., and Maddocks, O.D.K. (2017). One-carbon metabolism in cancer. Br J Cancer *116*, 1499-1504.

Nicklin, P., Bergman, P., Zhang, B., Triantafellow, E., Wang, H., Nyfeler, B., Yang, H., Hild, M., Kung, C., Wilson, C., et al. (2009). Bidirectional transport of amino acids regulates mTOR and autophagy. Cell *136*, 521-534.

Nilsson, R., Jain, M., Madhusudhan, N., Sheppard, N.G., Strittmatter, L., Kampf, C., Huang, J., Asplund, A., and Mootha, V.K. (2014). Metabolic enzyme expression highlights a key role for MTHFD2 and the mitochondrial folate pathway in cancer. Nature communications *5*, 3128.

Nomura, S., Sakamaki, S., Hongu, M., Kawanishi, E., Koga, Y., Sakamoto, T., Yamamoto, Y., Ueta, K., Kimata, H., Nakayama, K., et al. (2010). Discovery of canagliflozin, a novel C-glucoside with thiophene ring, as sodium-dependent glucose cotransporter 2 inhibitor for the treatment of type 2 diabetes mellitus. Journal of medicinal chemistry *53*, 6355-6360.

Obara, K., Shirakami, Y., Maruta, A., Ideta, T., Miyazaki, T., Kochi, T., Sakai, H., Tanaka, T., Seishima, M., and Shimizu, M. (2017). Preventive effects of the sodium glucose cotransporter 2 inhibitor tofogliflozin on diethylnitrosamine-induced liver tumorigenesis in obese and diabetic mice. Oncotarget *8*, 58353-58363.

Okada, J., Matsumoto, S., Kaira, K., Saito, T., Yamada, E., Yokoo, H., Katoh, R., Kusano, M., Okada, S., and Yamada, M. (2018). Sodium Glucose Cotransporter 2 Inhibition Combined With Cetuximab Significantly Reduced Tumor Size and Carcinoembryonic Antigen Level in Colon Cancer Metastatic to Liver. Clinical colorectal cancer *17*, e45-e48.

Olson, B.L., Hock, M.B., Ekholm-Reed, S., Wohlschlegel, J.A., Dev, K.K., Kralli, A., and Reed, S.I. (2008). SCFCdc4 acts antagonistically to the PGC-1alpha transcriptional coactivator by targeting it for ubiquitin-mediated proteolysis. Genes & development *22*, 252-264.

Osthus, R.C., Shim, H., Kim, S., Li, Q., Reddy, R., Mukherjee, M., Xu, Y., Wonsey, D., Lee, L.A., and Dang, C.V. (2000). Deregulation of glucose transporter 1 and glycolytic gene expression by c-Myc. The Journal of biological chemistry *275*, 21797-21800.

Owen, M.R., Doran, E., and Halestrap, A.P. (2000). Evidence that metformin exerts its anti-diabetic effects through inhibition of complex 1 of the mitochondrial respiratory chain. Biochem J *348 Pt 3*, 607-614.

Pacold, M.E., Brimacombe, K.R., Chan, S.H., Rohde, J.M., Lewis, C.A., Swier, L.J., Possemato, R., Chen, W.W., Sullivan, L.B., Fiske, B.P., et al. (2016). A PHGDH inhibitor reveals coordination of serine synthesis and one-carbon unit fate. Nat Chem Biol *12*, 452-458.

Park, H.U., Suy, S., Danner, M., Dailey, V., Zhang, Y., Li, H., Hyduke, D.R., Collins, B.T., Gagnon, G., Kallakury, B., et al. (2009). AMP-activated protein kinase promotes human prostate cancer cell growth and survival. Mol Cancer Ther *8*, 733-741.

Parsons, D.W., Jones, S., Zhang, X., Lin, J.C., Leary, R.J., Angenendt, P., Mankoo, P., Carter, H., Siu, I.M., Gallia, G.L., et al. (2008). An integrated genomic analysis of human glioblastoma multiforme. Science (New York, N.Y.) *321*, 1807-1812.

Patra, K.C., Wang, Q., Bhaskar, P.T., Miller, L., Wang, Z., Wheaton, W., Chandel, N., Laakso, M., Muller, W.J., Allen, E.L., et al. (2013). Hexokinase 2 is required for tumor initiation and maintenance and its systemic deletion is therapeutic in mouse models of cancer. Cancer cell *24*, 213-228.

Pearce, H.L., Safa, A.R., Bach, N.J., Winter, M.A., Cirtain, M.C., and Beck, W.T. (1989). Essential features of the P-glycoprotein pharmacophore as defined by a series of reserpine analogs that modulate multidrug resistance. Proceedings of the National Academy of Sciences of the United States of America *86*, 5128-5132.

Pikman, Y., Puissant, A., Alexe, G., Furman, A., Chen, L.M., Frumm, S.M., Ross, L., Fenouille, N., Bassil, C.F., Lewis, C.A., et al. (2016). Targeting MTHFD2 in acute myeloid leukemia. J Exp Med *213*, 1285-1306.

Pirkmajer, S., Kulkarni, S.S., Tom, R.Z., Ross, F.A., Hawley, S.A., Hardie, D.G., Zierath, J.R., and Chibalin, A.V. (2015). Methotrexate promotes glucose uptake and lipid oxidation in skeletal muscle via AMPK activation. Diabetes *64*, 360-369.

Plas, D.R., and Thompson, C.B. (2005). Akt-dependent transformation: there is more to growth than just surviving. Oncogene *24*, 7435-7442.

Pollak, M. (2014). Overcoming Drug Development Bottlenecks With Repurposing: Repurposing biguanides to target energy metabolism for cancer treatment. Nature medicine *20*, 591-593.

Pollak, M.N. (2012). Investigating metformin for cancer prevention and treatment: the end of the beginning. Cancer discovery *2*, 778-790.

Possemato, R., Marks, K.M., Shaul, Y.D., Pacold, M.E., Kim, D., Birsoy, K., Sethumadhavan, S., Woo, H.K., Jang, H.G., Jha, A.K., et al. (2011). Functional genomics reveal that the serine synthesis pathway is essential in breast cancer. Nature *476*, 346-350.

Pourdehnad, M., Truitt, M.L., Siddiqi, I.N., Ducker, G.S., Shokat, K.M., and Ruggero, D. (2013). Myc and mTOR converge on a common node in protein synthesis control that confers synthetic lethality in Myc-driven cancers. Proceedings of the National Academy of Sciences of the United States of America *110*, 11988-11993.

Pu, H., Zhang, Q., Zhao, C., Shi, L., Wang, Y., Wang, J., and Zhang, M. (2015). Overexpression of G6PD is associated with high risks of recurrent metastasis and poor progression-free survival in primary breast carcinoma. World J Surg Oncol *13*, 323.

Puigserver, P., Rhee, J., Lin, J., Wu, Z., Yoon, J.C., Zhang, C.Y., Krauss, S., Mootha, V.K., Lowell, B.B., and Spiegelman, B.M. (2001). Cytokine stimulation of energy expenditure through p38 MAP kinase activation of PPARgamma coactivator-1. Mol Cell *8*, 971-982.

Puigserver, P., Wu, Z., Park, C.W., Graves, R., Wright, M., and Spiegelman, B.M. (1998). A cold-inducible coactivator of nuclear receptors linked to adaptive thermogenesis. Cell *92*, 829-839.

Rabinovitch, R.C., Samborska, B., Faubert, B., Ma, E.H., Gravel, S.P., Andrzejewski, S., Raissi, T.C., Pause, A., St-Pierre, J., and Jones, R.G. (2017). AMPK Maintains Cellular Metabolic Homeostasis through Regulation of Mitochondrial Reactive Oxygen Species. Cell Rep *21*, 1-9.

Rajeshkumar, N.V., Yabuuchi, S., Pai, S.G., De Oliveira, E., Kamphorst, J.J., Rabinowitz, J.D., Tejero, H., Al-Shahrour, F., Hidalgo, M., Maitra, A., et al. (2017). Treatment of Pancreatic Cancer Patient-Derived Xenograft Panel with Metabolic Inhibitors Reveals Efficacy of Phenformin. Clin Cancer Res *23*, 5639-5647.

Rank Brothers LTD. (2002) The Rank Brothers Oxygen Electrode Opertaing Manual (1) 1-4. Accessed August 28, 2018. http://www.rankbrothers.co.uk/download/OxygenElectrode.pdf

Rehman, G., Shehzad, A., Khan, A.L., and Hamayun, M. (2014). Role of AMP-activated protein kinase in cancer therapy. Arch Pharm (Weinheim) *347*, 457-468.

Ricketts, C., Woodward, E.R., Killick, P., Morris, M.R., Astuti, D., Latif, F., and Maher, E.R. (2008). Germline SDHB mutations and familial renal cell carcinoma. J Natl Cancer Inst *100*, 1260-1262.

Rieg, T., Masuda, T., Gerasimova, M., Mayoux, E., Platt, K., Powell, D.R., Thomson, S.C., Koepsell, H., and Vallon, V. (2014). Increase in SGLT1-mediated transport explains renal glucose reabsorption during genetic and pharmacological SGLT2 inhibition in euglycemia. Am J Physiol Renal Physiol *306*, F188-193.

Rodgers, J.T., Lerin, C., Haas, W., Gygi, S.P., Spiegelman, B.M., and Puigserver, P. (2005). Nutrient control of glucose homeostasis through a complex of PGC-1alpha and SIRT1. Nature *434*, 113-118.

Romero-Garcia, S., Lopez-Gonzalez, J.S., Baez-Viveros, J.L., Aguilar-Cazares, D., and Prado-Garcia, H. (2011). Tumor cell metabolism: an integral view. Cancer Biol Ther *12*, 939-948.
Rosand, J., Friedberg, J.W., and Yang, J.M. (1997). Fatal phenformin-associated lactic acidosis. Ann Intern Med *127*, 170.

Rosenwasser, R.F., Sultan, S., Sutton, D., Choksi, R., and Epstein, B.J. (2013). SGLT-2 inhibitors and their potential in the treatment of diabetes. Diabetes Metab Syndr Obes *6*, 453-467.

Ross, F.A., MacKintosh, C., and Hardie, D.G. (2016). AMP-activated protein kinase: a cellular energy sensor that comes in 12 flavours. FEBS J *283*, 2987-3001.

Ross, K.C., Andrews, A.J., Marion, C.D., Yen, T.J., and Bhattacharjee, V. (2017). Identification of the Serine Biosynthesis Pathway as a Critical Component of BRAF Inhibitor Resistance of Melanoma, Pancreatic, and Non-Small Cell Lung Cancer Cells. Mol Cancer Ther *16*, 1596-1609.

Roux, P.P., and Topisirovic, I. (2012). Regulation of mRNA translation by signalling pathways. Cold Spring Harb Perspect Biol *4*.

Rytinki, M.M., and Palvimo, J.J. (2009). SUMOylation attenuates the function of PGC-1alpha. The Journal of biological chemistry *284*, 26184-26193.

Saito Tsugumichi, T. (2015). Effect of dapagliflozin on colon cancer cell [Rapid Communication]. Endocrine Journal *62*, 1133-1137.

Salpeter, S., Greyber, E., Pasternak, G., and Salpeter, E. (2006). Risk of fatal and nonfatal lactic acidosis with metformin use in type 2 diabetes mellitus. Cochrane Database Syst Rev, CD002967.

Samanta, D., and Semenza, G.L. (2018). Metabolic adaptation of cancer and immune cells mediated by hypoxia-inducible factors. Biochim Biophys Acta.

Sanchez-Cespedes, M., Parrella, P., Esteller, M., Nomoto, S., Trink, B., Engles, J.M., Westra, W.H., Herman, J.G., and Sidransky, D. (2002). Inactivation of LKB1/STK11 is a common event in adenocarcinomas of the lung. Cancer research *62*, 3659-3662.

Sarbassov, D.D., Ali, S.M., Kim, D.H., Guertin, D.A., Latek, R.R., Erdjument-Bromage, H., Tempst, P., and Sabatini, D.M. (2004). Rictor, a novel binding partner of mTOR, defines a rapamycin-insensitive and raptor-independent pathway that regulates the cytoskeleton. Curr Biol *14*, 1296-1302.

Scafoglio, C., Hirayama, B.A., Kepe, V., Liu, J., Ghezzi, C., Satyamurthy, N., Moatamed, N.A., Huang, J., Koepsell, H., Barrio, J.R., et al. (2015). Functional expression of sodium-glucose transporters in cancer. Proceedings of the National Academy of Sciences of the United States of America *112*, E4111-4119.

Schafer, Z.T., Grassian, A.R., Song, L., Jiang, Z., Gerhart-Hines, Z., Irie, H.Y., Gao, S., Puigserver, P., and Brugge, J.S. (2009). Antioxidant and oncogene rescue of metabolic defects caused by loss of matrix attachment. Nature *461*, 109-113.

Schreiber, S.N., Knutti, D., Brogli, K., Uhlmann, T., and Kralli, A. (2003). The transcriptional coactivator PGC-1 regulates the expression and activity of the orphan nuclear receptor estrogen-related receptor alpha (ERRalpha). The Journal of biological chemistry *278*, 9013-9018.
Sciacovelli, M., and Frezza, C. (2016). Oncometabolites: Unconventional triggers of oncogenic signalling cascades. Free Radic Biol Med *100*, 175-181.

Sciacovelli, M., and Frezza, C. (2017). Metabolic reprogramming and epithelial-to-mesenchymal transition in cancer. FEBS J *284*, 3132-3144.

Secker, P.F., Beneke, S., Schlichenmaier, N., Delp, J., Gutbier, S., Leist, M., and Dietrich, D.R. (2018). Canagliflozin mediated dual inhibition of mitochondrial glutamate dehydrogenase and complex I: an off-target adverse effect. Cell death & disease *9*, 226.

Selak, M.A., Armour, S.M., MacKenzie, E.D., Boulahbel, H., Watson, D.G., Mansfield, K.D., Pan, Y., Simon, M.C., Thompson, C.B., and Gottlieb, E. (2005). Succinate links TCA cycle dysfunction to oncogenesis by inhibiting HIF-alpha prolyl hydroxylase. Cancer cell *7*, 77-85.
Semenza, G.L. (2011). Hypoxia-inducible factor 1: regulator of mitochondrial metabolism and mediator of ischemic preconditioning. Biochim Biophys Acta *1813*, 1263-1268.

Shackelford, D.B., Abt, E., Gerken, L., Vasquez, D.S., Seki, A., Leblanc, M., Wei, L., Fishbein, M.C., Czernin, J., Mischel, P.S., et al. (2013). LKB1 inactivation dictates therapeutic response of non-small cell lung cancer to the metabolism drug phenformin. Cancer cell *23*, 143-158.

Shah, U.S., Dhir, R., Gollin, S.M., Chandran, U.R., Lewis, D., Acquafondata, M., and Pflug, B.R. (2006). Fatty acid synthase gene overexpression and copy number gain in prostate adenocarcinoma. Hum Pathol *37*, 401-409.

Shaw, R.J., Kosmatka, M., Bardeesy, N., Hurley, R.L., Witters, L.A., DePinho, R.A., and Cantley, L.C. (2004). The tumor suppressor LKB1 kinase directly activates AMP-activated kinase and regulates apoptosis in response to energy stress. Proceedings of the National Academy of Sciences of the United States of America *101*, 3329-3335.

Shi, L., Zhang, T., Zhou, Y., Zeng, X., Ran, L., Zhang, Q., Zhu, J., and Mi, M. (2015). Dihydromyricetin improves skeletal muscle insulin sensitivity by inducing autophagy via the AMPK-PGC-1alpha-Sirt3 signalling pathway. Endocrine *50*, 378-389.
Shiba, K., Tsuchiya, K., Komiya, C., Miyachi, Y., Mori, K., Shimazu, N., Yamaguchi, S., Ogasawara, N., Katoh, M., Itoh, M., et al. (2018). Canagliflozin, an SGLT2 inhibitor, attenuates the development of hepatocellular carcinoma in a mouse model of human NASH. Scientific reports *8*, 2362.

Shim, E.H., Livi, C.B., Rakheja, D., Tan, J., Benson, D., Parekh, V., Kho, E.Y., Ghosh, A.P., Kirkman, R., Velu, S., et al. (2014). L-2-Hydroxyglutarate: an epigenetic modifier and putative oncometabolite in renal cancer. Cancer Discov *4*, 1290-1298.

Shiota, M., Yokomizo, A., Tada, Y., Inokuchi, J., Tatsugami, K., Kuroiwa, K., Uchiumi, T., Fujimoto, N., Seki, N., and Naito, S. (2010). Peroxisome proliferator-activated receptor gamma coactivator-1alpha interacts with the androgen receptor (AR) and promotes prostate cancer cell growth by activating the AR. Mol Endocrinol *24*, 114-127.

Shroff, E.H., Eberlin, L.S., Dang, V.M., Gouw, A.M., Gabay, M., Adam, S.J., Bellovin, D.I., Tran, P.T., Philbrick, W.M., Garcia-Ocana, A., et al. (2015). MYC oncogene overexpression drives renal cell carcinoma in a mouse model through glutamine metabolism. Proceedings of the National Academy of Sciences of the United States of America *112*, 6539-6544.

Shuvalov, O., Petukhov, A., Daks, A., Fedorova, O., Vasileva, E., and Barlev, N.A. (2017). One-carbon metabolism and nucleotide biosynthesis as attractive targets for anticancer therapy. Oncotarget *8*, 23955-23977.

Sigoillot, F.D., Berkowski, J.A., Sigoillot, S.M., Kotsis, D.H., and Guy, H.I. (2003). Cell cycle-dependent regulation of pyrimidine biosynthesis. The Journal of biological chemistry *278*, 3403-3409.

Snell, K., and Weber, G. (1986). Enzymic imbalance in serine metabolism in rat hepatomas. Biochem J *233*, 617-620.

Song, C.W., Lee, H., Dings, R.P., Williams, B., Powers, J., Santos, T.D., Choi, B.H., and Park, H.J. (2012). Metformin kills and radiosensitizes cancer cells and preferentially kills cancer stem cells. Sci Rep *2*, 362.

Sonoda, J., Laganiere, J., Mehl, I.R., Barish, G.D., Chong, L.W., Li, X., Scheffler, I.E., Mock, D.C., Bataille, A.R., Robert, F., et al. (2007). Nuclear receptor ERR alpha and coactivator PGC-1 beta are effectors of IFN-gamma-induced host defense. Genes & development *21*, 1909-1920.

Sonveaux, P., Vegran, F., Schroeder, T., Wergin, M.C., Verrax, J., Rabbani, Z.N., De Saedeleer, C.J., Kennedy, K.M., Diepart, C., Jordan, B.F., et al. (2008). Targeting lactate-fueled respiration selectively kills hypoxic tumor cells in mice. The Journal of clinical investigation *118*, 3930-3942.

Sorich, M.J., Pottier, N., Pei, D., Yang, W., Kager, L., Stocco, G., Cheng, C., Panetta, J.C., Pui, C.H., Relling, M.V., et al. (2008). In vivo response to methotrexate forecasts outcome of acute lymphoblastic leukemia and has a distinct gene expression profile. PLoS Med *5*, e83.

Spears, C.P., Shahinian, A.H., Moran, R.G., Heidelberger, C., and Corbett, T.H. (1982). In vivo kinetics of thymidylate synthetase inhibition of 5-fluorouracil-sensitive and -resistant murine colon adenocarcinomas. Cancer research *42*, 450-456.

Sradhanjali, S., and Reddy, M.M. (2018). Inhibition of Pyruvate Dehydrogenase Kinase as a Therapeutic Strategy against Cancer. Curr Top Med Chem *18*, 444-453.

St-Pierre, J., Drori, S., Uldry, M., Silvaggi, J.M., Rhee, J., Jager, S., Handschin, C., Zheng, K., Lin, J., Yang, W., et al. (2006). Suppression of reactive oxygen species and neurodegeneration by the PGC-1 transcriptional coactivators. Cell *127*, 397-408.

St-Pierre, J., Lin, J., Krauss, S., Tarr, P.T., Yang, R., Newgard, C.B., and Spiegelman, B.M. (2003). Bioenergetic analysis of peroxisome proliferator-activated receptor gamma coactivators 1alpha and 1beta (PGC-1alpha and PGC-1beta) in muscle cells. The Journal of biological chemistry *278*, 26597-26603.

Stearman, R.S., Dwyer-Nield, L., Zerbe, L., Blaine, S.A., Chan, Z., Bunn, P.A., Jr., Johnson, G.L., Hirsch, F.R., Merrick, D.T., Franklin, W.A., et al. (2005). Analysis of orthologous gene expression between human pulmonary adenocarcinoma and a carcinogen-induced murine model. Am J Pathol *167*, 1763-1775.

Stein, R.A., and McDonnell, D.P. (2006). Estrogen-related receptor alpha as a therapeutic target in cancer. Endocr Relat Cancer *13 Suppl 1*, S25-32.

Sullivan, L.B., Gui, D.Y., and Heiden, M.G.V. (2016). Altered metabolite levels in cancer: implications for tumour biology and cancer therapy. Nature reviews. Cancer *16*, 680-693.
Sun, P.M., Wei, L.H., Sehouli, J., Denkert, C., Zhao, D., Gao, M., Sun, X.L., and Litchtenegger, W. (2005). [Role of estrogen receptor-related receptors alpha, beta and gamma in ovarian cancer cells]. Zhonghua Fu Chan Ke Za Zhi *40*, 544-548.

Suwa, M., Egashira, T., Nakano, H., Sasaki, H., and Kumagai, S. (2006). Metformin increases the PGC-1alpha protein and oxidative enzyme activities possibly via AMPK phosphorylation in skeletal muscle in vivo. J Appl Physiol (1985) *101*, 1685-1692.

Suzuki, S., Tanaka, T., Poyurovsky, M.V., Nagano, H., Mayama, T., Ohkubo, S., Lokshin, M., Hosokawa, H., Nakayama, T., Suzuki, Y., et al. (2010). Phosphate-activated glutaminase (GLS2), a p53-inducible regulator of glutamine metabolism and reactive oxygen species. Proceedings of the National Academy of Sciences of the United States of America *107*, 7461-7466.

Swinnen, J.V., Beckers, A., Brusselmans, K., Organe, S., Segers, J., Timmermans, L., Vanderhoydonc, F., Deboel, L., Derua, R., Waelkens, E., et al. (2005). Mimicry of a cellular low energy status blocks tumor cell anabolism and suppresses the malignant phenotype. Cancer research *65*, 2441-2448.

Swinnen, J.V., Brusselmans, K., and Verhoeven, G. (2006). Increased lipogenesis in cancer cells: new players, novel targets. Curr Opin Clin Nutr Metab Care *9*, 358-365.

Tabata, M., Rodgers, J.T., Hall, J.A., Lee, Y., Jedrychowski, M.P., Gygi, S.P., and Puigserver, P. (2014). Cdc2-like kinase 2 suppresses hepatic fatty acid oxidation and ketogenesis through disruption of the PGC-1alpha and MED1 complex. Diabetes *63*, 1519-1532.

Tedeschi, P.M., Johnson-Farley, N., Lin, H., Shelton, L.M., Ooga, T., Mackay, G., Van Den Broek, N., Bertino, J.R., and Vazquez, A. (2015). Quantification of folate metabolism using transient metabolic flux analysis. Cancer & metabolism *3*, 6.

Tennakoon, J.B., Shi, Y., Han, J.J., Tsouko, E., White, M.A., Burns, A.R., Zhang, A., Xia, X., Ilkayeva, O.R., Xin, L., et al. (2014). Androgens regulate prostate cancer cell growth via an AMPK-PGC-1alpha-mediated metabolic switch. Oncogene *33*, 5251-5261.

Tennant, D.A., Duran, R.V., and Gottlieb, E. (2010). Targeting metabolic transformation for cancer therapy. Nature reviews. Cancer *10*, 267-277.

Teyssier, C., Ma, H., Emter, R., Kralli, A., and Stallcup, M.R. (2005). Activation of nuclear receptor coactivator PGC-1alpha by arginine methylation. Genes & development *19*, 1466-1473.

Theodoropoulou, S., Kolovou, P.E., Morizane, Y., Kayama, M., Nicolaou, F., Miller, J.W., Gragoudas, E., Ksander, B.R., and Vavvas, D.G. (2010). Retinoblastoma cells are inhibited by aminoimidazole carboxamide ribonucleotide (AICAR) partially through activation of AMP-dependent kinase. FASEB J *24*, 2620-2630.

Thorpe, L.M., Yuzugullu, H., and Zhao, J.J. (2015). PI3K in cancer: divergent roles of isoforms, modes of activation and therapeutic targeting. Nature reviews. Cancer *15*, 7-24.

Tibbetts, A.S., and Appling, D.R. (2010). Compartmentalization of Mammalian folate-mediated one-carbon metabolism. Annu Rev Nutr *30*, 57-81.

Tiraby, C., Hazen, B.C., Gantner, M.L., and Kralli, A. (2011). Estrogen-related receptor gamma promotes mesenchymal-to-epithelial transition and suppresses breast tumor growth. Cancer research *71*, 2518-2528.

Tomlinson, I.P., Alam, N.A., Rowan, A.J., Barclay, E., Jaeger, E.E., Kelsell, D., Leigh, I., Gorman, P., Lamlum, H., Rahman, S., et al. (2002). Germline mutations in FH predispose to dominantly inherited uterine fibroids, skin leiomyomata and papillary renal cell cancer. Nat Genet *30*, 406-410.

Tong, Y., Chen, X., Fei, X., Lin, L., Wu, J., Huang, O., He, J., Zhu, L., Chen, W., Li, Y., et al. (2018). Can breast cancer patients with HER2 dual-equivocal tumours be managed as HER2-negative disease? Eur J Cancer *89*, 9-18.

Torrano, V., Valcarcel-Jimenez, L., Cortazar, A.R., Liu, X., Urosevic, J., Castillo-Martin, M., Fernandez-Ruiz, S., Morciano, G., Caro-Maldonado, A., Guiu, M., et al. (2016). The metabolic co-regulator PGC1alpha suppresses prostate cancer metastasis. Nat Cell Biol *18*, 645-656.
Tremblay, A.M., and Giguère, V. (2007). The NR3B subgroup: an ovERRview. Nucl Recept Signal *5*, e009.

Trousil, S., Chen, S., Mu, C., Shaw, F.M., Yao, Z., Ran, Y., Shakuntala, T., Merghoub, T., Manstein, D., Rosen, N., et al. (2017). Phenformin Enhances the Efficacy of ERK Inhibition in NF1-Mutant Melanoma. J Invest Dermatol *137*, 1135-1143.

Turcan, S., Rohle, D., Goenka, A., Walsh, L.A., Fang, F., Yilmaz, E., Campos, C., Fabius, A.W., Lu, C., Ward, P.S., et al. (2012). IDH1 mutation is sufficient to establish the glioma hypermethylator phenotype. Nature *483*, 479-483.

Ursini-Siegel, J., Rajput, A.B., Lu, H., Sanguin-Gendreau, V., Zuo, D., Papavasiliou, V., Lavoie, C., Turpin, J., Cianflone, K., Huntsman, D.G., et al. (2007). Elevated expression of DecR1 impairs ErbB2/Neu-induced mammary tumor development. Molecular and cellular biology *27*, 6361-6371.

Vander Heiden, M.G., Cantley, L.C., and Thompson, C.B. (2009). Understanding the Warburg effect: the metabolic requirements of cell proliferation. Science (New York, N.Y.) *324*, 1029-1033.

Vazquez, F., Lim, J.H., Chim, H., Bhalla, K., Girnun, G., Pierce, K., Clish, C.B., Granter, S.R., Widlund, H.R., Spiegelman, B.M., et al. (2013). PGC1alpha expression defines a subset of human melanoma tumors with increased mitochondrial capacity and resistance to oxidative stress. Cancer cell *23*, 287-301.

Veiga, S.R., Ge, X., Mercer, C.A., Hernandez-Alvarez, M.I., Thomas, H.E., Hernandez-Losa, J., Ramon, Y.C.S., Zorzano, A., Thomas, G., and Kozma, S.C. (2018). Phenformin-Induced Mitochondrial Dysfunction Sensitizes Hepatocellular Carcinoma for Dual Inhibition of mTOR. Clin Cancer Res *24*, 3767-3780.

Vellinga, T.T., Borovski, T., de Boer, V.C., Fatrai, S., van Schelven, S., Trumpi, K., Verheem, A., Snoeren, N., Emmink, B.L., Koster, J., et al. (2015). SIRT1/PGC1alpha-Dependent Increase in Oxidative Phosphorylation Supports Chemotherapy Resistance of Colon Cancer. Clin Cancer Res *21*, 2870-2879.

Vercauteren, K., Gleyzer, N., and Scarpulla, R.C. (2009). Short hairpin RNA-mediated silencing of PRC (PGC-1-related coactivator) results in a severe respiratory chain deficiency associated with the proliferation of aberrant mitochondria. The Journal of biological chemistry *284*, 2307-2319.

Villani, L.A., Smith, B.K., Marcinko, K., Ford, R.J., Broadfield, L.A., Green, A.E., Houde, V.P., Muti, P., Tsakiridis, T., and Steinberg, G.R. (2016). The diabetes medication Canagliflozin reduces cancer cell proliferation by inhibiting mitochondrial complex-I supported respiration. Molecular metabolism *5*, 1048-1056.

Vivanco, I., and Sawyers, C.L. (2002). The phosphatidylinositol 3-Kinase AKT pathway in human cancer. Nature reviews. Cancer *2*, 489-501.

Waitkus, M.S., Pirozzi, C.J., Moure, C.J., Diplas, B.H., Hansen, L.J., Carpenter, A.B., Yang, R., Wang, Z., Ingram, B.O., Karoly, E.D., et al. (2018). Adaptive Evolution of the GDH2 Allosteric Domain Promotes Gliomagenesis by Resolving IDH1(R132H)-Induced Metabolic Liabilities. Cancer research *78*, 36-50.

Warburg, O. (1956). On the origin of cancer cells. Science (New York, N.Y.) *123*, 309-314.
Ward, P.S., and Thompson, C.B. (2012). Metabolic reprogramming: a cancer hallmark even warburg did not anticipate. Cancer cell *21*, 297-308.
Watkins, G., Douglas-Jones, A., Mansel, R.E., and Jiang, W.G. (2004). The localisation and reduction of nuclear staining of PPARgamma and PGC-1 in human breast cancer. Oncol Rep *12*, 483-488.

Wheaton, W.W., Weinberg, S.E., Hamanaka, R.B., Soberanes, S., Sullivan, L.B., Anso, E., Glasauer, A., Dufour, E., Mutlu, G.M., Budigner, G.R.S., et al. (2014). Metformin inhibits mitochondrial complex I of cancer cells to reduce tumorigenesis. eLife *3*, e02242.

Whitelaw, B.S., and Robinson, M.B. (2013). Inhibitors of glutamate dehydrogenase block sodium-dependent glutamate uptake in rat brain membranes. Frontiers in endocrinology *4*, 123.

Wingo, S.N., Gallardo, T.D., Akbay, E.A., Liang, M.C., Contreras, C.M., Boren, T., Shimamura, T., Miller, D.S., Sharpless, N.E., Bardeesy, N., et al. (2009). Somatic LKB1 mutations promote cervical cancer progression. PLoS One *4*, e5137.

Wise, D.R., DeBerardinis, R.J., Mancuso, A., Sayed, N., Zhang, X.Y., Pfeiffer, H.K., Nissim, I., Daikhin, E., Yudkoff, M., McMahon, S.B., et al. (2008). Myc regulates a transcriptional program that stimulates mitochondrial glutaminolysis and leads to glutamine addiction. Proceedings of the National Academy of Sciences of the United States of America *105*, 18782-18787.

Witkiewicz, A.K., Nguyen, K.H., Dasgupta, A., Kennedy, E.P., Yeo, C.J., Lisanti, M.P., and Brody, J.R. (2008). Co-expression of fatty acid synthase and caveolin-1 in pancreatic ductal adenocarcinoma: implications for tumor progression and clinical outcome. Cell Cycle *7*, 3021-3025.

Wolf, D.A. (2014). Is reliance on mitochondrial respiration a "chink in the armor" of therapy-resistant cancer? Cancer cell *26*, 788-795.

Wong, B.W., Kuchnio, A., Bruning, U., and Carmeliet, P. (2013). Emerging novel functions of the oxygen-sensing prolyl hydroxylase domain enzymes. Trends Biochem Sci *38*, 3-11.

Wong, S.C., Proefke, S.A., Bhushan, A., and Matherly, L.H. (1995). Isolation of human cDNAs that restore methotrexate sensitivity and reduced folate carrier activity in methotrexate transport-defective Chinese hamster ovary cells. The Journal of biological chemistry *270*, 17468-17475.

Woo, C.C., Kaur, K., Chan, W.X., Teo, X.Q., and Lee, T.H.P. (2018). Inhibiting Glycine Decarboxylase Suppresses Pyruvate-to-Lactate Metabolism in Lung Cancer Cells. Front Oncol *8*, 196.

Wright, E.M., Ghezzi, C., and Loo, D.D.F. (2017). Novel and Unexpected Functions of SGLTs. Physiology (Bethesda, Md.) *32*, 435-443.

Wu, N., Gu, C., Gu, H., Hu, H., Han, Y., and Li, Q. (2011). Metformin induces apoptosis of lung cancer cells through activating JNK/p38 MAPK pathway and GADD153. Neoplasma *58*, 482-490.

Wu, Z., Puigserver, P., Andersson, U., Zhang, C., Adelmant, G., Mootha, V., Troy, A., Cinti, S., Lowell, B., Scarpulla, R.C., et al. (1999). Mechanisms controlling mitochondrial biogenesis and respiration through the thermogenic coactivator PGC-1. Cell *98*, 115-124.

Xiao, M., Yang, H., Xu, W., Ma, S., Lin, H., Zhu, H., Liu, L., Liu, Y., Yang, C., Xu, Y., et al. (2012). Inhibition of alpha-KG-dependent histone and DNA demethylases by fumarate and succinate that are accumulated in mutations of FH and SDH tumor suppressors. Genes & development *26*, 1326-1338.

Yan, M., Gingras, M.C., Dunlop, E.A., Nouet, Y., Dupuy, F., Jalali, Z., Possik, E., Coull, B.J., Kharitidi, D., Dydensborg, A.B., et al. (2014). The tumor suppressor folliculin regulates AMPK-dependent metabolic transformation. The Journal of clinical investigation *124*, 2640-2650.

Yan, R., Wan, L., Pizzorno, G., and Cao, D. (2006). Uridine phosphorylase in breast cancer: a new prognostic factor? Front Biosci *11*, 2759-2766.

Yang, J., Craddock, L., Hong, S., and Liu, Z.M. (2009). AMP-activated protein kinase suppresses LXR-dependent sterol regulatory element-binding protein-1c transcription in rat hepatoma McA-RH7777 cells. J Cell Biochem *106*, 414-426.

Ye, J., Fan, J., Venneti, S., Wan, Y.W., Pawel, B.R., Zhang, J., Finley, L.W., Lu, C., Lindsten, T., Cross, J.R., et al. (2014). Serine catabolism regulates mitochondrial redox control during hypoxia. Cancer Discov *4*, 1406-1417.

Ye, J., Mancuso, A., Tong, X., Ward, P.S., Fan, J., Rabinowitz, J.D., and Thompson, C.B. (2012). Pyruvate kinase M2 promotes de novo serine synthesis to sustain mTORC1 activity and cell proliferation. Proceedings of the National Academy of Sciences of the United States of America *109*, 6904-6909.

Zakikhani, M., Dowling, R., Fantus, I.G., Sonenberg, N., and Pollak, M. (2006). Metformin is an AMP kinase-dependent growth inhibitor for breast cancer cells. Cancer research *66*, 10269-10273.

Zakikhani, M., Dowling, R.J., Sonenberg, N., and Pollak, M.N. (2008). The effects of adiponectin and metformin on prostate and colon neoplasia involve activation of AMP-activated protein kinase. Cancer Prev Res (Phila) *1*, 369-375.

Zaugg, K., Yao, Y., Reilly, P.T., Kannan, K., Kiarash, R., Mason, J., Huang, P., Sawyer, S.K., Fuerth, B., Faubert, B., et al. (2011). Carnitine palmitoyltransferase 1C promotes cell survival and tumor growth under conditions of metabolic stress. Genes & development *25*, 1041-1051.

Zhang, C., Zhang, Z., Zhu, Y., and Qin, S. (2014a). Glucose-6-phosphate dehydrogenase: a biomarker and potential therapeutic target for cancer. Anticancer Agents Med Chem *14*, 280-289.

Zhang, C.S., Hawley, S.A., Zong, Y., Li, M., Wang, Z., Gray, A., Ma, T., Cui, J., Feng, J.W., Zhu, M., et al. (2017). Fructose-1,6-bisphosphate and aldolase mediate glucose sensing by AMPK. Nature *548*, 112-116.

Zhang, J., and Zhang, Q. (2018). VHL and Hypoxia Signalling: Beyond HIF in Cancer. Biomedicines *6*.

Zhang, Q., Dou, J., and Lu, J. (2014b). Combinational therapy with metformin and sodium-glucose cotransporter inhibitors in management of type 2 diabetes: systematic review and meta-analyses. Diabetes Res Clin Pract *105*, 313-321.

Zhang, Y., Ba, Y., Liu, C., Sun, G., Ding, L., Gao, S., Hao, J., Yu, Z., Zhang, J., Zen, K., et al. (2007). PGC-1alpha induces apoptosis in human epithelial ovarian cancer cells through a PPARgamma-dependent pathway. Cell Res *17*, 363-373.

Zhao, F.Q., and Keating, A.F. (2007). Functional properties and genomics of glucose transporters. Current genomics *8*, 113-128.

Zhao, S., Lin, Y., Xu, W., Jiang, W., Zha, Z., Wang, P., Yu, W., Li, Z., Gong, L., Peng, Y., et al. (2009). Glioma-derived mutations in IDH1 dominantly inhibit IDH1 catalytic activity and induce HIF-1alpha. Science (New York, N.Y.) *324*, 261-265.

Zheng, B., Jeong, J.H., Asara, J.M., Yuan, Y.Y., Granter, S.R., Chin, L., and Cantley, L.C. (2009). Oncogenic B-RAF negatively regulates the tumor suppressor LKB1 to promote melanoma cell proliferation. Mol Cell *33*, 237-247.

Zhu, Y., Soto, J., Anderson, B., Riehle, C., Zhang, Y.C., Wende, A.R., Jones, D., McClain, D.A., and Abel, E.D. (2013). Regulation of fatty acid metabolism by mTOR in adult murine hearts occurs independently of changes in PGC-1alpha. Am J Physiol Heart Circ Physiol *305*, H41-51.